

**EXPERIMENTAL AND COMPUTATIONAL MODELING OF MOLECULAR
PRODUCTS FROM THE THERMAL DEGRADATION OF TOBACCO,
MARIJUANA AND KHAT**

By

Omare Micah Omari

**A Thesis Submitted in Partial Fulfillment of the Requirements for the Award of
the Degree of Doctor of Philosophy in Analytical Chemistry**

Moi University

2021

DECLARATION

DECLARATION BY STUDENT

This thesis is my original work and has not been presented for examination towards the award of a degree in any institution.

.....

.....

Omara Micah Omari

Date

PHD/ACH/8/18

DECLARATION BY SUPERVISORS

This thesis has been submitted for examination with our approval as University supervisors

.....

.....

Dr. Jackson Cherutoi.

Date

Department of chemistry and biochemistry

Moi University

.....

.....

Prof. Joshua Kibet

Date

Department of Chemistry

Egerton University

.....

.....

Prof. Fredrick Kengara

Date

School of pure and applied sciences

Department of physical and biological sciences

Bomet University College

DEDICATION

It is my sincere gratitude and heartfelt regard that I bestow this work to my mother, Mrs. Rebecca Lavine Omare. Your never-ending encouragement and moral support have given me power to achieve this undertaking. May God bless you. To my late dad, I know you wished me for the best in life, continue resting in peace.

ACKNOWLEDGEMENT

I express my heartfelt appreciations to my supervisors Prof. Joshua Kibet of Egerton University, Professor Fredrick Kengara of Bomet University College and Dr. Jackson Cherutoi of Moi University for granting me the chance to be their student under this research project and guaranteeing that all was done correct. I am truthfully honored to have been under their supervision. My mom, brothers, sisters and friends are really recognized for their prayers, financial and moral support during the course of this study. I am forever grateful to the African Centre of Excellence II in phytochemicals, textile and renewable energy (ACE II PTRE) of Moi University for the financial support offered to me towards the success of this research. I thank Egerton University especially the department of chemistry for allowing me to use some their facilities during sample preparation. The University of KwaZulu-Natal is sincerely appreciated for the role they played in thermal, elemental and chromatographic analyses of samples.

ABSTRACT

The economic burden caused by death due to lung cancer and other respiratory diseases is attributed in part to tobacco use – presently linked to approximately 8 million deaths per year worldwide. Notably, 80% of these deaths occur in low and middle income countries making tobacco epidemic a major global public health concern. Biomass pyrolysis remains an important chemical process in the thermochemical conversion of biomass materials to produce high density reaction products such as bio-oil, and molecular products that are hazardous and of interest to public health and the environment. This work investigated the compounds that are released from the pyrolysis of tobacco, marijuana and khat, and their ternary mixtures; explored the elemental composition of thermal char; and performed geometry optimization of hazardous molecular products released in the entire pyrolysis temperature range of 200-700 °C, at increments of 50 °C. Research license, NACOSTI/21/11/11440, was obtained prior to sampling and analysis. A quartz tubular reactor was designed for the pyrolysis of the biomass components at 1 atm. in nitrogen at a residence time of 2 s – under conditions representative of cigarette smoking and municipal waste incineration characteristics. The pyrolysate was characterized using a Gas chromatograph hyphenated to a mass selective detector. Geometry optimization and reactivity coefficients of selected molecular products were performed under the density functional theory formalism at B3LYP level of theory coupled to 6-31++G (d,p) basis set using Gaussian '9 computational suite of programs. Elemental composition of thermal char was done using an elemental analyzer; thermal analysis explored using thermogravimetric analysis and differential scanning calorimetry (DSC). It was noted that the thermal degradation of khat is accompanied by the evolution of phenolic compounds such as *p*-cresol, catechol, hydroquinone and other substituted methoxy phenols at temperatures between 300 °C and 500 °C. Marijuana pyrolysis led to the evolution of molecular compounds such as phytol, phytocannabinoids, cannabidiol (CBD), tetrahydrocannabinol (THC), Δ -9-tetrahydrocannabivarin, cannabigerol, and 2,6-dimethylhydroquinone. Pyrolysis of marijuana-khat mixture showed a decrease in the concentration of phytocannabinoids such as cannabichromene, cannabicooumarone, Δ -9-tetrahydrocannabivarin, cannabigerol, and cannabinol, while the equimassic mixture of tobacco and khat pyrolysis yielded nicotine, nicotyrine and cotinine at concentrations lower by 4.34%, 5.63% and 1.60%, respectively. TGA results revealed that the thermal decomposition of khat, marijuana and tobacco biomass is accompanied by weight loss of 4.52%, 81.37% and 5.22% in the first, second and third stages, respectively in the temperature range of 200 °C to 500 °C. DSC results showed that most of the khat-tobacco biomass pyrolysis occurred in the exothermic zone with peak temperatures of 350 °C and 477 °C, and final temperature of 682 °C. Elemental analysis of khat thermal char at 400 °C found C and O content at 37.08% and 43.73%, respectively. The computational details revealed the optimization step number for THC, CBD, cathinone and cathine to be 68, 40, 64 and 22 at energies of 968.73, 968.41, 231.52 and 480.65 hartrees correspondingly and found THC as the most unstable compound. This study has demonstrated that molecular toxins are produced in higher concentrations at pyrolysis temperatures of 350 °C to 550 °C with a possible reduction of their release on co-pyrolysis of equimassic mixtures of tobacco, khat and marijuana. The study recommends heightened research on the use of khat-tobacco mixtures in cigarettes to reduce the evolution of toxic molecular products.

TABLE OF CONTENTS

DECLARATION	ii
DEDICATION	iii
ACKNOWLEDGEMENT	iv
ABSTRACT.....	v
TABLE OF CONTENTS.....	vi
LIST OF TABLES	x
LIST OF FIGURES	xi
ACRONYMS	xiii
CHAPTER ONE	1
INTRODUCTION.....	1
1.1 Background of the Study	1
1.2 Statement of the Problem.....	6
1.3 Objectives of the Study.....	7
1.3.1 General objective.....	7
1.3.2 Specific objectives.....	7
1.4 Hypotheses	8
1.5 Justification of Study	8
1.6 Significance of Study	9
CHAPTER TWO	11
LITERATURE REVIEW	11
2.1 Cigarette Smoking and Cigarette Smoke	11
2.2 Tobacco, Marijuana and Khat Cigarette Smoke, and their Toxicological Implications	12
2.2.1 Tobacco cigarette smoke	13
2.2.2 Chemical Products of Tobacco Smoke	20
2.2.3 Consequences of tobacco use.....	23
2.3 Marijuana Smoke	25
2.3.1 Ways and techniques of consuming marijuana	27
2.3.2 Chemical products from marijuana smoke and their cancer potency	30
2.3.3 Harms and health impacts resulting from Cannabis.....	32
2.4 Catha edulis.....	34
2.4.1 Trends and methods through which khat is consumed	36

2.4.2 Emerging chemical compounds from khat and their carcinogenicity	38
2.4.3 Harms and health impacts arising from consumption of khat.....	41
2.5 Effect of free radicals on human health	42
2.5.1 Polycyclic hydrocarbons	44
2.5.2 Heterocyclic hydrocarbons in cigarette smoke	45
2.5.3 N-Nitrosamines	46
2.5.4 Heterocyclic aromatic amines	47
2.5.6 Other organic compounds in cigarette smoke	48
2.6 Computational modeling.....	49
2.6.1 The Density Functional Theory.....	52
2.6.2 The Hohenberg-Kohn Theorem	53
2.6.3 The Kohn-Sham equations	55
2.6.4 Basis sets	56
2.6.5 Polarized basis sets.....	57
2.6.6 Diffuse basis set	58
2.6.7 Understanding predictions for properties of molecules using computational modelling.....	58
2.7 Elemental characterization of thermal char	59
2.8 Thermogravimetric analysis and differential scanning calorimetry	59
CHAPTER THREE.....	61
MATERIALS AND METHODS	61
3.1 Sample Collection and Preparation.....	61
3.2 Pyrolysis of Biomass Components	61
3.3 The Reactor Design and Assembly.....	62
3.4 Sample Introduction to the Reactor for Fractional Pyrolysis and Co-Pyrolysis....	63
3.5 GC-MS Characterization of Molecular Products.....	64
3.6 Computational Methodology	65
3.7 Elemental Characterization of Thermal Char Using Elemental Analyzer	65
3.8 Thermogravimetric analysis and differential scanning calorimetry of khat-tobacco biomass.....	66
3.9 Data Analysis	66
CHAPTER FOUR.....	68
RESULTS AND DISCUSSION	68

4.1 Phenolic reaction products released from the thermal degradation of <i>Catha edulis</i>	68
4.1.1 Decomposition profile of khat.....	73
4.1.2 Elemental analysis of khat, tobacco and marijuana and their binary mixtures char	74
4.1.3 Health implications of phenolic compounds in khat.....	78
4.1.4 Molecular modelling of phenolic compounds and selected khat alkaloids generated from khat pyrolysis	81
4.1.5 Molecular geometries for phenolic and selected alkaloid compounds and their corresponding potential energy surfaces	85
4.1.6 Geometry optimization of phenolic compounds and selected alkaloids of khat	87
4.1.7 Molecular orbitals and Electronic properties for phenols and selected khat alkaloids.....	90
4.2 Molecular products released from thermal degradation of Marijuana.....	96
4.2.1 Molecular geometries of cannabinoid derivatives generated from marijuana pyrolysis	101
4.2.2 Molecular orbitals and electronic properties of selected phytocannabinoids	103
4.2.3 Electron density and contour maps of selected phytocannabinoids	105
4.3 Molecular products released from thermal degradation of Marijuana-Khat biomass	106
4.3.1 Effects of Khat on concentration of Marijuana pyrolysis products	107
4.3.2 The unique variations in yields of phytocannabinoids from the pyrolysis of marijuana in khat regime	109
4.4 Molecular products released from thermal degradation of Tobacco–khat biomass	112
4.4.1 Synergetic effects of khat on concentration of molecular products released during tobacco pyrolysis in khat regime	116
4.4.2 Synergetic effects of khat on concentration of molecular products released during tobacco pyrolysis in Marijuana	118
4.4.3 Synergetic effects of khat on the concentration of molecular products released during the co-pyrolysis of tobacco, khat and marijuana	120
4.5 Thermogravimetric analysis and differential scanning calorimetry results	123
4.6 Rejection or acceptance of hypotheses	126

CHAPTER FIVE	128
CONCLUSION AND RECOMMENDATION	128
5.1 Conclusion	128
5.2 Recommendation	131
REFERENCES	133
APPENDICES	157
Appendix 1: Sample GC-MS data for marijuana	157
Appendix 2: Sample GC-MS data for khat	160
Appendix 3: Sample GC-MS data for tobacco-khat	163
Appendix 4: Sample GC-MS data for tobacco-khat	166
Appendix 5: Sample GC-MS data for marijuana-khat.....	170
Appendix 6: Sample GC-MS data for Tobacco-marijuana-khat.....	173
Appendix 8: Gaussian raw geometric data for benzenyl radical at 673 °C.....	176
Appendix 9: Benzenyl bond parameter for output structure	182
Appendix 10: Gaussian raw geometric data for CBD at 623 °C.....	183
Appendix 11: THC bond parameter for output structure	200
Appendix 12: Rights to use information of published work in thesis by oalib journal	201
Appendix 13: Rights to use information of published work in thesis by journal of public health	203
Appendix 14: Rights to use information of published work in thesis by JANSET	204
Appendix 15: Research license	205

LIST OF TABLES

Table 2.1: Some carcinogenic chemical compounds reported present in tobacco as classified by IARC	21
Table 2.2: Cannabis consumption methods and popularity	29
Table 2.3: Carcinogenic chemical compounds reported present in cannabis	31
Table 2.4: Khat consumption techniques and popularity trends	37
Table 2.5: Concentrations of polycyclic hydrocarbons in mainstream cigarette smoke	45
Table 2.6: Concentrations of heterocyclic hydrocarbon components in mainstream cigarette smoke	46
Table 2.7: Concentrations of N-Nitrosamine in mainstream cigarette smoke.....	47
Table 2.8: Concentrations of heterocyclic aromatic amines in mainstream cigarette smoke	48
Table 2.9: Concentration levels of aldehydes, phenolic compounds, volatile hydrocarbons and nitro-hydrocarbons	49
Table 4.1: Intensities of products generated from khat pyrolysis at selected temperatures	69
Table 4.2: Elemental composition of khat char	75
Table 4.3: Paired samples statistics for elemental compounds in char.....	77
Table 4.4: Paired samples t-test for char.....	78
Table 4.5: Paired samples statistics for the molecular compounds generated from Marijuana and Marijuana-khat mixture pyrolysis.....	109
Table 4.6: Paired samples t-test	109
Table 4.7: Chemical formula and structure of some toxic/ carcinogenic components identified from pyrolysis of khat-tobacco binary mixture	115
Table 4.8: Paired samples statistics for tobacco and tobacco khat pyrolysis.....	118
Table 4.9: Paired samples t-test for tobacco and tobacco khat pyrolysis	118
Table 4.10: Paired samples statistics for molecular products generated from the pyrolysis of tobacco and tobacco marijuana pyrolysis	122
Table 4.11: Paired samples t-test	123

LIST OF FIGURES

Figure 1.1: Tobacco leaves, khat fresh leaves and marijuana leaves.....	2
Figure 2.1: Tobacco specific nitrosamines	19
Figure 2.2: Marijuana phytocannabinoids	26
Figure 2.3: Major khat alkaloids	35
Figure 2.4: Phenylalkylamine alkaloids of khat.....	39
Figure 2.5: Phenylpentylamine and catheduline alkaloids from khat.....	40
Figure 2.6: Biological systems affected by khat chewing and health effects associated with khat chewing.	42
Figure 3.1: Reactor assembly.....	62
Figure 4.1: Overlay GC-MS chromatogram for phenolic compounds released from khat pyrolysis	68
Figure 4.2: Phenolic and methoxy phenol compounds distribution from khat biomass pyrolysis	70
Figure 4.3: Nitrogen containing compound released from khat pyrolysis.....	72
Figure 4.4: Furans and furfurals and ketones from khat biomass pyrolysis	73
Figure 4.5: Khat percentage weight loss at various pyrolysis temperatures.....	74
Figure 4.6: Elemental distribution in biomass materials and their binary mixtures ...	76
Figure 4.7: Energy change plots for the formation of radicals from phenolic compounds.....	82
Figure 4.8: Input and optimized geometries and geometric parameters for hydroquinone, <i>p</i> -cresol and phenol	86
Figure 4.9: Cathinone optimized structure and its optimization steps plot.....	87
Figure 4.10: Cathine optimized structure and its optimization steps plot	87
Figure 4.11: Benzenyl radical optimized structure and its optimization steps plot	89
Figure 4.12: 3-aminobutyryl-2-one radical optimized structure and optimization steps plot.....	89
Figure 4.13: HOMO and LUMO energies for hydroquinone, phenol and <i>p</i> -cresol....	90
Figure 4.14: HOMO and LUMO structures for cathinone and cathine molecules	91
Figure 4.15: HOMO and LUMO structures for benzenyl and 3-aminobutyryl-2-one radicals.....	93
Figure 4.16: Contour maps for phenol, <i>p</i> -cresol and hydroquinone	95
Figure 4.17: HOMO and LUMO contour maps for cathinone and cathine	95

Figure 4.18: GC-MS chromatogram of products from marijuana pyrolysis at 500 °C	96
Figure 4.19: Terpenes and cannabinoids released from marijuana pyrolysis.....	97
Figure 4.20: Coumaranone and phthalate from marijuana pyrolysis.....	101
Figure 4.21: CBD input structure and optimized structure.....	102
Figure 4.22: CBD and THC optimization plots.....	103
Figure 4.23: CBD HOMO and LUMO.....	104
Figure 4.24: THC HOMO and LUMO.....	104
Figure 4.25: CBD and THC electrostatic potential.....	105
Figure 4.26: CBD and THC contour maps.....	106
Figure 4.27: GC-MS chromatogram of products from marijuana-khat pyrolysis	107
Figure 4.28: Comparison of GC-MS intensities of the molecular products released from the pyrolysis of equimassic mixture of khat and marijuana and pure marijuana.....	108
Figure 4.29: GC-MS chromatogram of products from tobacco pyrolysis in khat regime at 500 °C.....	113
Figure 4.30: High and low concentration pyrolysis product from khat-tobacco binary mixture.....	114
Figure 4.31: GC-MS chromatogram of products from tobacco pyrolysis at 500 °C	116
Figure 4.32: Comparison in concentration of molecular products released during pure tobacco pyrolysis and tobacco pyrolysis in khat regime at 500 °C.....	117
Figure 4.33: GC-MS chromatogram of products released from tobacco-marijuana mixture pyrolysis at 500 °C.....	119
Figure 4.34: Level of intensities of the compounds released in marijuana pyrolysis to a racemic mixture of marijuana and tobacco.....	120
Figure 4.35: GC-MS chromatogram of products released from tobacco-marijuana- khat mixture pyrolysis at 700 °C.....	121
Figure 4.36: Comparison in intensity of molecular compounds released from tobacco-marijuana-khat racemic mixture with pure tobacco.	122
Figure 4.37: Tobacco-khat binary mixture weight loss at a heating rate of 5 °C/min	124
Figure 4.38: DSC curve for tobacco-khat binary mixture pyrolysis.....	125

ACRONYMS

B3LYP	Becke-3Parameter-Lee-Yang-Parr correlation function
CB1	Cannabinoid type I receptor
CB2	Cannabinoid type II receptor
CBCA	Cannabichromenic acid
CBD	Cannabidiol
CBN	Cannabinol
CNS	Central nervous system
DFT	Density functional theory
DNA	Deoxyribose nucleic acid
DSC	Differential scanning calorimetry
EI	Electron impact
EPFR	Environmental persistent free radicals
FCTC	Framework convention on tobacco control
FDA	Food and drug administration
GC-MS	Gas chromatography-mass spectrometry
GTO	Gaussian type orbital
HAA	Heterocyclic aromatic amines
HIV	Human immunodeficiency virus
HCN	Hydrogen cyanide
HOMO	Highest occupied molecular orbital
IARC	International agency for research on cancer
IQ	Intelligence quotient
Log P	Logarithm of octanol-water partition coefficient
LUMO	Lowest unoccupied molecular orbital

MO	molecular orbital
MSD	Mass selective detector
NAB	N-nitrosoanabasine
NAT	N-nitrosoanatabine
NIDA	National institute on drug abuse
NIST	National institute of science and technology
NNK	4-methyl-N-nitrosamino-1-(3-pyridyl)-1-butanone
NNN	N-nitrosornicotine
PAHs	Polycyclic aromatic hydrocarbons
PCDFs	Polychlorinated dibenzo-furans
TGA	Thermogravimetric analysis
THC	Tetrahydrocannabinol
THCA	Tetrahydrocannabinolic acid
USA	United States of America
Wt	Weight

CHAPTER ONE

INTRODUCTION

1.1 Background of the Study

Tobacco, marijuana and khat (*Catha edulis*) are notorious substances abused among the rural and urban communities in Kenya with consumption patterns replicated in both developing and industrialized nation states (Vellios et al., 2018). It is estimated by the National Institute on Drug Abuse (NIDA) of the United States of America that cost of tobacco ill use, alcohol and proscribed drugs to be an expensive task in terms of criminality, lost human efficiency and health care which is projected to consume about \$740 billion in cost (NIDA, 2020c). Currently, across the globe, there is a steady escalation in the amount of consumed narcotic substances such as *Nicotiana tabacum* (tobacco), *cannabis sativa* (marijuana) and *Catha edulis* (khat) as reported within the last decade (Mishra et al., 2016; O'Connor et al., 2020). As a result, there is mounting interest in scientific research on a range of toxic smoke compounds produced during the tobacco smoking and other drug substances including marijuana and *Catha edulis* (Sawicka et al., 2020; WHO, 2008). Accordingly, the increasing trends in drug consumption have precipitated serious concern on how the concentration levels of harmful molecular products released during smoking can be reduced (Fuster et al., 2011).

Tobacco biomass has been identified to be a complex plant material which consists of cellulose (fiber), pectin, lignin, in addition to a variety of supplementary elemental components whose exact composition is determined by the tobacco assortment and growing environments (Wang et al., 2021). Repeated consumption of tobacco merchandises has been associated to cardiovascular diseases such as emphysema,

cancers, oxidative stress and reproductive health infections and thus cigarette smoking has been identified as a hazardous cause for degenerative diseases including lung cancer besides cancer of other respiratory organs by several scientific and epidemiological evidences (Ghosh et al., 2012). The World Health Organization (WHO) has remained on the front position on educating the general public all over the world on the threats posed by tobacco consumption that constitutes part of the foundation of the Framework Convention on Tobacco Control (FCTC) guidelines (WHO, 2019). Tobacco, marijuana and khat can be used in various forms such as cigarettes, smokeless tobacco and water pipes (shisha) which is a common method in developing countries (Baumung et al., 2016). Figure 1.1 a, b and c present fresh leaves of tobacco, khat and marijuana, respectively.



Figure 1.1: Tobacco leaves (a), khat fresh leaves (b) and marijuana leaves (c) (Global Force Reggae, 2017; Laura et al., 2019)

An individual can be exposed to cigarette smoke directly if he is a smoker and indirectly inhale it from cigarette contaminated environment as a passive smoker (second hand smoker) thereby subjects both smokers and non-smokers to the detrimental effects associated with cigarette smoking. Burning cigarettes are the major sources of cigarette smoke which may comprise of tobacco, marijuana or khat. Cigarette smoking is the major method through which the psychoactive components

find entry into the human biological system. During cigarette smoking, smoke containing venomous, genotoxic and carcinogenic organic and inorganic composites is generated (Soliman, 2018).

Accordingly, cigarette smoking has been identified as the principal origin of malignancy and mutagenesis and the determining factor is mainly how long the period in which cigarette is smoked, in addition to the amount of hand-rolled cigarettes smoked which quicken up the threat of histologic forms of lung cancer; squamous cell, small cell, large cell carcinoma and adenocarcinoma (Babalik et al., 2018; WHO, 2019). As a result of these preventable disease occurrences, tobacco smoking has been linked to mortalities of about eight million each year, whereby almost 80% of these deaths are being reported to occur in low class and middle class income economies. The WHO (2019) estimates that about 1,200,000 of these deaths are individuals who don't smoke but get exposure to some second hand cigarette smoke making tobacco use a major epidemic facing the world. Besides the dominant and toxic nicotine, other agents of these tobacco induced ailments include lethal and cancer-causing chemicals of the nitrosamine types, aldehydes, polonium-210 and benzo[a]pyrene, which are known to biologically accumulate in the human body system in the course of cigarette smoking to cause disease (Edwards et al., 2017; Morgan et al., 2017; O'Connor et al., 2020). The toxicity of the molecular compounds resulting from the degradation of tobacco during heating has become a subject of health and environmental concern. Conniving ways and means that can effectively lessen these contaminants present in tobacco will be an effective approach and solution in curtailing mortality and morbidity in the midst of the individuals that are addicted to cigarette smoking (Abrams et al., 2018). With respect to this study, the use of heat not burn approaches have been deliberated for consumption of

tobacco products. These practices comprise insertion of tobacco biomass material and some products into a tobacco heating system where the biomass materials are intensely heated at temperatures lower than the cigarette burning temperatures as unlike the traditional method that involves directly burning the tobacco filled cigarette (Lachenmeier et al., 2018).

Efforts geared towards safe cigarette smoking have led to the design of electronic cigarettes (e-cigarettes) assumed to be a harmless way for tobacco smoking and as such, e-cigarette popularity has shown a tremendous increase in the last decade (Hajek et al., 2019). In an ideal world, electronic cigarettes usually assist by mainly acting as an alternative for replacing nicotine and eventually boosts in the reducing of the craving for one to smoke and ultimately easily enabling the smokers to quit smoking cigarettes but on the contrary, extensive research analysis has established this to be untrue (Kindvall et al., 2019).

Electronic cigarettes therefore operate on the principle that, when an electronic liquid is heated, electronic vapors that take the form of vaporizers are produced with flavors and nicotine, that are then subsequently conveyed into the consumer (DeVito & Krishnan-Sarin, 2018). While the consumption of electronic cigarettes are assumed to be less toxic than the conventional cigarettes (Hilton et al., 2016), electronic cigarettes have been identified to be potential sources of human toxins that prompt toxicological processes, body tissue inflammation and sometimes extreme oxidative stress in cigarette smokers (Dasgupta & Klein, 2014) calling for further research on alternative nicotine reduction methods in cigarettes.

Additionally, marijuana authorization to be used in medical applications as anti-inflammatory, antioxidant, neuroprotective and anticonvulsant properties has

escalated in a number of countries and states in the world upon the belief that it comprises chemical compounds that have potency towards treating and management of a number of ailments and symptoms irrespective of the accompanying health threats (Koren & Cohen, 2020). In this regard, CBD has been established to have numerous properties that aid individuals struggling with nicotine addiction given that it reduces cravings for cigarettes and ease collective tobacco withdrawal symptoms such as anxiety, irritation, sleep disturbance and weight gain even though there is no known study recommending CBD as a nicotine replacement (Hindocha et al., 2016).

Therefore, this study aims at exploring the effects of marijuana on nicotine when smoked together in equimassic mixtures. Even though there is limited documented research that has exhaustively reported on khat smoking, and the toxicity of the generated products during smoking, this study seeks to report on the chemical compounds released from khat biomass pyrolysis and examine the synergetic effects of khat copyrolysis with tobacco biomass on the concentration of the toxic molecular products produced during tobacco burning.

Existing computer programs and methodologies can be efficiently useful for particular chemical problems in obtaining chemical and physical properties of molecules, liquids and solids thus making computational studies important in predicting the laboratory viability of synthesizing particular compounds. Additionally, computational studies can be employed in predicting the likelihood of unidentified molecules and investigating reaction mechanisms that cannot be readily elucidated by experimental procedures (Tchernook, 2016).

There is limited documented literature that explores the thermodynamic properties of molecular compounds evolved from marijuana, tobacco and khat smoke. To this

regard therefore, this study shall employ computational techniques in investigating the electronic properties and perform geometry optimization of selected molecular compounds generated from the pyrolysis of the biomass materials. Generally, the physical laws that govern the behavior of molecules in materials are governed by the Schrodinger wave equation (Jain & Shin, 2016)

$$H\Psi = E\Psi \quad 1.1$$

H is a representation of the Hamiltonian operator, Ψ the wave or eigen function and E the aggregate energy or eigen value of the equation of a given system. The wave function is used to describe the system and it takes into consideration the spatial locations of the electrons that are present in the electronic system as variables resulting to the derivation equation 1.2.

$$H\Psi(\vec{r}_1, \dots, \vec{r}_N) = E\Psi(\vec{r}_1, \dots, \vec{r}_N) \quad 1.2$$

In this case, \vec{r} is used to define the location of the electron in the available molecular space while Ψ is used to permit the state of the system to be construed.

1.2 Statement of the Problem

Even though a lot of scientific efforts have been initiated towards exploring and understanding the pyrolytic behaviour of tobacco, several complex and uncertain reaction processes involving the pyrolysis of marijuana and khat are scarcely documented in literature. Presently, biomass pyrolysis is regarded as the main critical chemical method employed in the production of reusable energy and investigating pyrolysis products that are hazardous to environmental and public health (Czajczyńska et al., 2017). Evidently, the co-pyrolytic characteristics and properties of biomass components are critical in gauging the toxicological nature and

unraveling information about the degradation pathways in tobacco, marijuana and khat burning. The chemistry of co-pyrolysis of biomass components is not only poorly understood but their mechanistic formation pathways remain to be debatable. More so, scientific efforts have been geared towards development of methods that can aid in reducing concentration levels of toxic molecular products present in cigarette smoke which have resulted to the design of e-cigarettes that are presumed to be less poisonous. For this reason therefore, co-pyrolysis experiments under conditions that simulate the burning tobacco cigarette with marijuana and khat in order to probe the thermodynamic, electronic, and mechanistic behaviour of these compounds over the whole range of smoking (200-700 °C) will be preferred. Furthermore, the investigation of molecular products and elemental speciation in thermal char from the pyrolysis of khat and marijuana has not received significant attention in literature. This study will explore the effects of co-pyrolytic experiments in suppressing the harmful molecular products commonly associated with grave diseases in biomass burning.

1.3 Objectives of the Study

1.3.1 General objective

The major objective of this study is to perform experimental and computational studies of toxic molecular products from the pyrolysis of equimassic mixture of tobacco, marijuana and khat.

1.3.2 Specific objectives

1. To determine the molecular products released from the pyrolysis of tobacco, marijuana, and khat and their ternary mixture.
2. To determine elemental composition of the thermal char from the pyrolysis of tobacco, marijuana and khat using elemental analyzer

3. To perform TGA and DSC analysis on tobacco, marijuana and khat biomasses
4. To perform geometry optimization and reactivity coefficients (band-gap energies) for selected molecular products from tobacco, marijuana and khat burning

1.4 Hypotheses

H₁: Molecular products from the individual pyrolysis of tobacco, marijuana and khat will not be different from those evolved during the co-pyrolysis of tobacco, marijuana and khat

H₂: Thermal char from the co-pyrolysis of tobacco and khat will not contain nitrogen as the major element.

H₃: The thermal degradation data obtained from the pyrolysis of khat and tobacco binary mixtures will not be similar to the data obtained from the co-pyrolysis of tobacco and khat using laboratory designed thermal reactor.

H₄: The optimized geometries of the selected molecular compounds cannot be generated

1.5 Justification of Study

The purpose of this research is to perform experimental and computational studies on molecular products released from the pyrolysis of tobacco, marijuana and *Catha edulis*. While tobacco, marijuana and khat development, composition, and toxicity has been identified as a rich area of study (Sharma & Hajaligol, 2003), experimental data in literature reporting on molecular compounds evolved from the pyrolysis of tobacco, marijuana and khat equimassic mixtures is scarce or absent and therefore the findings from this study shall be of great importance to researchers and scholars

interested in biomass pyrolysis. The broad topic of tobacco biomass has received more attention on scientific research in minimizing levels of nicotine released during tobacco burning and safe cigarette smoking (WHO, 2008). The results of this study may provide insight to cigarette manufacturers on methods of minimizing tobacco smoke toxicity during cigarette smoking. A number of smokers have opted on the concurrent use of tobacco, marijuana and khat cigarettes in order to quickly get their enhanced pleasurable effects within a short period of time without knowing their possible toxicological implications and therefore the study findings shall be of great benefits in informing both smokers and the general public on the dangers and benefits of smoking these biomass mixtures.

1.6 Significance of Study

This study aims at enlightening the general public on the pros and cons of smoking tobacco, khat and marijuana and their mixtures. The current trends in drug abuse involve the concurrent use of the three drug substances (khat, tobacco and marijuana) or in mixed forms with the aim of the users to get their induced effects of “getting high” within the shortest time possible without much concern on the possible toxic precursors evolved during use. The recent past has been met with a rise in the number of debates among many nations in regard to the legalization and consumption of marijuana leading to increased concerns on the ethical questions vis-à-vis health care givers, patients and authorities. This work seeks to explore and contribute more information on the possible health implications associated with marijuana use in form of cigarettes.

The tobacco industry has focused on ways of minimizing the concentration levels of the toxic carcinogenic effluents released and ingested by smokers during cigarette smoking leading to the design of e-cigarettes that are presumed to be less toxic but

proven to be carcinogenic. As a result, the advocating for the use of additives in order to lower concentration levels of these toxins. This study seeks to investigate the effects of khat and marijuana on the concentration level of nicotine shading light on their possible use as alternative additives. Studies that report on marijuana, khat and tobacco copyrolysis are limited and therefore this work shall be one of a kind to have experimentally reported on the possible environmental and health effects associated with their use.

CHAPTER TWO

LITERATURE REVIEW

2.1 Cigarette Smoking and Cigarette Smoke

The consumption of cigarettes through smoking is explicitly proven to be a risk aspect that influences the genesis of several generative ailments that includes cancers of the lung, cardiac and human circulatory system infections by a number of systematic, scientific and epidemiological evidences (Kibet et al., 2014). Accordingly, cigarette smoking is well-known to be the principal cause of preventable and premature deaths resulting from chronic obstructive pulmonary disease and cardiovascular disorders (Eaton et al., 2018; Omare, 2015). Cigarette smoke can be regarded as a multifarious mixture of chemicals that consist of carbon (II) oxide, hydrogen cyanide (HCN) and oxides of nitrogen, mostly gases, with some volatile chemical compounds such as formaldehyde, acrolein, benzene and a number of N-nitrosamines forming the liquid vapor fraction of the smoke aerosol (Lal, 2013). In this regard, it is perceived as an aerosol that constitutes the solid-liquid droplets in the gaseous state resulting from complex and corresponding burning, pyrolysis, pyrosynthesis, distillation, sublimation and condensation processes (Baker, 2006).

The submicron concrete elements forming the precipitate of cigarette smoke comprise of nicotine, phenols, polyaromatic hydrocarbons (PAHs) and some tobacco specific nitroso-amines in case of tobacco cigarettes (Yershova et al., 2016). Accordingly, cigarette smoke generally comprises of lethal, genotoxic and cancer-causing organic and inorganic complexes which have adverse effects on human health. Matt et al. (2017) reported that repeated human contact with cigarette smoke is a prospective in inducing multiple, highly diverse effects on human health with

certain physical-chemical cigarette smoke properties likely to participate in disease initiation processes.

Generally, a burning cigarette can be described as a multifarious system in which multiple chemical and physical reactions take place at the binary distinct sections which constitutes the combustion zone and the pyrolysis distillation zone (Baker, 2006). The reactions that occur at the combustion zone include combustion reactions where oxygen reacts with carbonized tobacco, marijuana or khat to produce simple gases and release the heat that sustains the burning of the cigarette. Once the smoker makes a puff, in case of tobacco cigarettes, the temperatures rises up to around 650 – 950 ° C at the edge of the burning region and the temperatures at that moment reduce rapidly to ambient temperatures at the cooler pyrolysis area where the bulk of chemicals in smoke are generated (CDCP, 2010a; Omare, 2015). The rapidly cooling super-saturated vapour contracts into aerosol units that form the cigarette smoke which has been demonstrated by a significant number of scientific research to consist of genotoxic toxins that have the potential to attack the lungs thus resulting to the cancerous effects (Ivashynka et al., 2019). The distribution of molecular compounds in various cigarette matrices is influenced by the nature of plant biomass that has been used in the cigarette.

2.2 Tobacco, Marijuana and Khat Cigarette Smoke, and their Toxicological Implications

Studies by various scientists on cigarette smoking and cigarette smoke have reported serious health impacts in the midst of the cigarette smoking community, and even second hand smokers. A research survey conducted by Ivashynka et al. (2019) reconnoitered on the precipitated effects of smoking cigarettes and found out that it can lead to augmented heart rate and an equivalent upsurge in blood pressure.

Additionally, mothers who smoke have been linked to reduced acumen in exam performance, poor academic achievements, short term working remembrance, hyperactivity and attention deficit disorders (Kristjansson et al., 2018a). In agreement to Mallock et al. (2018), cigarette smoke is extremely toxic because of the formation of deadly products of pyrolysis in the course of burning.

2.2.1 Tobacco cigarette smoke

Traditionally, the methods by which tobacco biomass can be used are either through smoking tobacco in form of cigars or thorough smokeless tobacco techniques. When tobacco is used as smoked, it is rolled into tobacco cigarettes which usually give off smoke effluent which has greatly been associated to be the cause of lung linked fatalities as demonstrated by a good number of scientific works which have reported and identified the compounds released from burning cigarettes to be biologically injurious (Jha, 2020; WHO, 2019). The class of some of the smoked tobacco merchandises include but not restricted to steaming water pipes (Shihadeh et al., 2015), rolled cigarettes, electronically heated cigarettes (Parker, 2019), bidis and krekets (Mishra et al., 2016). Otherwise, in the event tobacco biomass is ingested in other ways and means apart from smoking, it forms the types of smokeless tobacco products such as slackly chewed tobacco leaves, snus, naswar, gutka snuffs, and tobacco paste (Hajek et al., 2019; Khan et al., 2019; Kindvall et al., 2019; Mathews & Krishnan, 2019; Mohapatra, 2019; Pillitteri et al., 2020).

Scientific investigations on tobacco products that are smokeless have revealed more than 20 elemental compounds which have been identified to be precursors for cancer, for instance, N-nitrosamine acids, , polycyclic aromatic hydrocarbons, volatile N-nitrosamines tobacco-specific nitrosamines and aldehydes (Warnakulasuriya & Straif, 2018). In preparation of tobacco loose leaves for chewing air cured tobacco

leaves are crushed into pieces and flavouring agent added to make its taste better (Griscik & Miller, 2019; Stepanov et al., 2014). Fire and air cured black tobacco leaves form moist snuf (snus) whereas dry snuf is made of fermented and fire treated fine particles (Kindvall et al., 2019; McAdam et al., 2013). Ostensibly, the key inspiring reason that drives a person to consume most of these products comprising of tobacco is nicotine; an alkaloid of tobacco which constitutes of approximately 95% of tobacco compounds (Frandsen et al., 2017; Ji et al., 2017; McKinney & Vansickel, 2016). When tobacco gains entry into the human biotic system in form of smoke, various compounds constituting the smoke are taken in by the smoker (Tsai et al., 2018) which are originators for reproductive and progressive diseases including cancer and severe respiratory infections (Ferrante & Conti, 2017).

The chemistry of the smoke arising from burning tobacco has been extensively investigated by various researchers and reported over 7,000 compounds to be present in the tobacco smoke out of which roughly more than 70 of the chemicals constituents have been acknowledged as cancer-causing by IARC (Etemadi et al., 2019; Hecht, 2018). In the course of tobacco combustion reactions, some compounds including formaldehyde, carbon monoxide, benzene, polycyclic aromatic hydrocarbons (PAHs) and hydrogen cyanide are produced (Morgan et al., 2017; Nlemedim, 2017; Warnakulasuriya & Straif, 2018). Eventually, incomplete combustion reactions/ processes end up taking place within the core of the burning cigar which subsequently result to the formation of the hazardous PAHs (Abdel-Shafy & Mansour, 2016).

Tobacco smoke compounds have been identified as carcinogenic, tumor promoters and inflammatory agents (Kapar et al., 2018). Incomplete thermogenic degradation

and pyrolysis of tobacco cigarettes produces harmful components such as acetaldehyde, aggravating cancer-causing unstable organic compounds, benzo[a]pyrene, carcinogenic polycyclic aromatic hydrocarbons and carbon (II) oxide (Auer et al., 2017). According to the WHO (2019), these compounds have been highly linked to one out of ten deaths caused by tobacco use around the world. Some studies have suggested that tobacco use has remained the leading preventable cause of death in the world (Bauld et al., 2017). Rodgman and Perfetti (2013) in their book on the chemical components of tobacco and tobacco smoke found similar compounds.

Genotoxic cancer-causing agents that are extant in cigarette smoke influence deleterious mutagenic effects and therefore human disclosure to these mixture of chemical pollutants in cigarette smoke devises serious penalties especially in form of lung disease mortality (Anderson & Chan, 2016). An understanding of the mechanisms of how cigarette smoke can initiate disease can provide an insight on how disease can be prevented among cigarette smokers. Kaur et al. (2018), analyzed the toxicological mechanisms of cigarette smoke and found that use of flavouring agents causes lung toxicity as a result of induced oxidative stress and DNA damage. However, these research findings did not address the effects of flavouring agents in nicotine concentration levels.

Nicotine reduction in cigarettes is regarded as the safest way that can decrease nicotine dependence thereby contributing to reduction in cigarette smoking (Benowitz & Henningfield, 2018). This has been enhanced by introducing the use of e-cigarettes which are considered less toxic (Langley, 2019). Nonetheless, Carlsen et al. (2018) in their work on the toxicity of e-cigarettes have noted adverse health

effects that are ascribed to nicotine and the vapours impinging on the lungs, airways and the cardiovascular system. E-cigarettes are intended to be electrically powered to allow the user to inhale or vap an aerosolized liquid (Parker, 2019). The US Food and Drug Administration (FDA) has provided a regulatory plan that explores the lowering of nicotine concentration levels in cigarettes but scientific evidence has raised concern over the possibility of cigarette smokers to smoke more cigarettes as compensatory effect for more nicotine uptake (Abrams et al., 2018; Apelberg et al., 2018).

Tobacco effluent commonly contains poisonous, mutagenic and cancer-causing abilities given that they are enormously dissolve in body fats (Baali & Yahyaoui, 2019) and consequently suddenly adsorbed from the digestive tract in living organisms (Abdel-Shafy & Mansour, 2016; Hussain et al., 2018; Rengarajan et al., 2015). PAHs are fast dispersed in human body cells and tissues and get deposited into body lipids where they attach to DNA cells and as a result initiate a sequence of disruptive body effects which normally ends up as malignant tumor precursors (Abdel-Shafy & Mansour, 2016). For these reason therefore, PAHs are recorded amongst the extremely human well-being threatening chemical compounds which have a high potency as cancer causal agents (Rengarajan et al., 2015). Additionally, PAHs have been testified to effect other numerous toxicological effects in human being as well as enlargement of the human liver that is characterized by cell oedema and blockage of the tissues that offer a connection between the liver and some blood veins and arteries, decreased body weight, intoxication of both male and female genital system, retardation of fetus development, learning and lowered Intelligence Quotients, oocyte damaging and kidney cells infection (Abdel-Shafy & Mansour, 2016; O'Brien et al., 2016).

A number of chemical compounds such as tobacco specific nitrosamines (TSNAs) and the main nicotine alkaloid come about as expected in tobacco and are produced when tobacco is smoked (Edwards et al., 2017; Konstantinou et al., 2018; Lee et al., 2016). The main alkaloid, nicotine which is primarily present in tobacco biomass generally subsists in two classifications; protonated nicotine and non-protonated nicotine which are reliant on pH (El-Hellani et al., 2015). The non-protonated nicotine is free of a base and therefore regarded as the most addictive form of nicotine which is highly bioavailable and is easily absorbed into the blood system where it ends up causing gratifying psychoactive effects (O'Connor et al., 2020). Systematically, TSNAs have been identified to be the major cancer triggering agents that are present in both smoked and smokeless tobacco (Shi & Yang, 2017). Four principle TSNA chemicals; N-nitrosornicotine (NNN), 4-methyl-N-nitrosamino-1-(3-pyridyl)-1-butanone (NNK), N-nitrosoanatabine (NAT) and N-nitrosoanabasine (NAB), indicated in Figure 2.1, have been determined to be present in tobacco (de Godoy Lusso et al., 2019; Edwards et al., 2017). Out of these four, IARC has identified NNN and NNK as the main cancer instigating agents in tobacco (Singhavi et al., 2018; Xue et al., 2014). When secondary and tertiary amines react with nitrile, nitrosamines are yielded with over 70 of these nitrosamines having been confirmed scientifically as carcinogenic (Gunduz et al., 2016). Nitrosation of secondary amines process is known to be a very rapid reaction in which the hydrogen attached to the nitrogen is substituted by the $-NO$ group in significantly high yields (Spahr et al., 2017).

Accordingly, Lee et al. (2016) have classified tertiary amines nitrosation as a slow reaction. Consequently, nitrosation of nornicotine, anabasine and anatabine, which are secondary amines usually leads to the creation of the tobacco specific

nitrosamines NNN, NAB and NAT (Cai et al., 2016; de Godoy Lusso et al., 2019; Edwards et al., 2017). These TSNA form part of the chief alkaloids present in tobacco (Jonnie, 2018). On the other hand, the yield of NNN is as a result of nitrosation of tertiary amines of nicotine which collectively with nicotine-derived NNK have been acknowledged to be robust carcinogens that have the ability to induce malignant and nonmalignant tumors in organisms depending on the route by which they are administered or ingested (De Flora et al., 2016; de Godoy Lusso et al., 2019; Gunduz et al., 2016). Low levels of TSNA have been detected in fresh tobacco leaves although these concentration levels intensify in the course of tobacco curing (Edwards et al., 2017; Jun et al., 2017).

Therefore, when an individual smokes cigarettes N-Nitrosamines manage to enter into his/ her body system via the mainstream smoke from cigarette and side stream cigarette smoke inhalation (Auer et al., 2017; Hang et al., 2018). Consequently, equally individuals who are perceived to be actively involved in smoking and those that are passively involved in smoking are both vulnerable to these nitrosamines which form from uptake of alkaloids and nitrogen oxides or nitriles (Hecht, 2016; Hecht et al., 2016). Further cancer causes in tobacco smokers include ingestion of benzo(a)pyrene (BaP), polonium -210, and cadmium (Kurgat et al., 2015; Omare, 2015). IARC has consequently classified BaP as group 2A cancer triggering agents since it is t a dangerous chemical dominantly found in tobacco smoke (IARC, 2019; Vu et al., 2015).

Electronic cigarettes have been introduced into tobacco cigarette market on the assumption that it can be safer way to smoke since they are presumed to deliver little concentrations levels of nicotine (Carlsen et al., 2018). Differing to this suggestion,

systematic investigation on the threats posed by e-cigarettes has shown that e-cigarettes are more poisonous and possess potential carcinogenic substances which are formed in the course of consumption of e-cigarettes (Armendáriz-Castillo et al., 2019). A good number of these compounds which get released from e-cigarettes have been stated to cause genetic mutations which result in the development of malignant cells and eventually cancerous cells (Stephen, 2018).

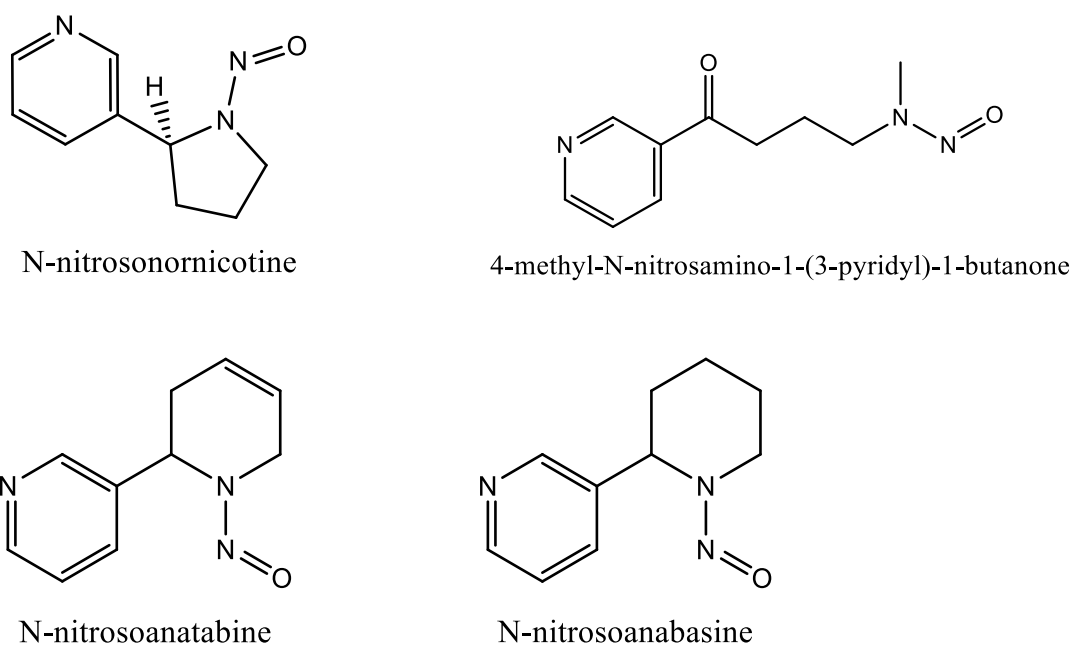


Figure 2.1: Tobacco specific nitrosamines (CDCP, 2010b)

In view of that, Drazen et al (2019), have emphasized that there is a higher possibility of an e-cigarette consumer getting nicotine addiction due to elevated concentration levels of nicotine as a result of numerous vaping than regular smokers, thereby exposing the consumer to severe health risks associated with smoking (Drazen et al., 2019). Therefore, it can be pointed out that the growing rates of e-cigarette use amongst the youths is due to the extremely addictive characteristics of nicotine which has been credited to its potential to cause a public health crisis

amongst the youths who are the major consumers of the e-cigarette product according to scientific surveys (Kuo et al., 2019).

2.2.2 Chemical Products of Tobacco Smoke

Various studies, scientifically conducted, have documented the chemical composition of tobacco smoke with substantial efforts put in to the identification of the presence of known and suspected carcinogens that can provide a link between cigarette smoking and its related adverse effects (Armendáriz-Castillo et al., 2019; McAdam et al., 2018). Moreover, the active chemical species largely present in cigarette smoke consist of hydroxyl radicals, hydrogen peroxide and superoxide anion radicals which are commonly produced throughout the pyrolysis processes (Assaf et al., 2016). Consequently environmentally persistent free radicals are a subject of great interest in exploration with more attention being emphasized on the formation mechanisms and their associated effects on human health. Free radicals have a vital influence on damaging the respiratory system by majorly initiating chronic and cardiopulmonary dysfunction due to the fact that they are reactive oxygen species which are well-established to be precursors for oxidative stress (Panth et al., 2016).

Further, heterocyclic hydrocarbons have been reported to be dominantly present in cigarette smoke (Anderson & Chan, 2016; Roemer et al., 2016). During the thermal degradation of biomass, furan, (C_4H_4O), belonging to a group of dioxins (polychlorinated dibenzo-furans, PCDFs) that are notoriously very toxic organic compound are produced. Furan has been categorized as endocrine disrupting biochemical particularly because of its higher ability to change animal physiology by disturbing hormonal levels (Ferreira et al., 2019).

Table 2.1: Some carcinogenic chemical compounds reported present in tobacco as classified by IARC (Bjurlin et al., 2020; IARC, 2019)

Chemical compounds	Carcinogenicity	Reference
carbon monoxide,	Group 1	(International Agency for Research on Cancer, 2013; Lawin et al., 2017)
benzene,	Group 1	(Loomis et al., 2017)
formaldehyde	Group 1	(d'Ettoire et al., 2017; Pires et al., 2018)
polycyclic aromatic hydrocarbons (PAHs)	Group 1, Group 2A and group 2B	(International Agency for Research on Cancer, 2010; Santonicola et al., 2017)
hydrogen cyanide	Not listed	
lead,	Group 2B	(Bjurlin et al., 2020)
tobacco specific nitrosamines (TSNAs)	Group 1	(Bjurlin et al., 2020)
nicotine	Not listed	
benzo(a)pyrene (BaP)	Group 1	(Santonicola et al., 2017)
polonium -210	Group 1	(Stanfill, 2020)
cadmium	Group 1	(Stanfill, 2020)
heterocyclic aromatic amines	Group 2A	(Bjurlin et al., 2020)
Aldehydes	Group 2B	
phenolic compounds	Not listed	
volatile hydrocarbons	Group 1	(IARC, 2019)
nitro hydrocarbons	Not listed	
toluene	Group 2A	(Prueitt et al., 2017; Warden et al., 2018)
furans,	Group 2A	(Hang et al., 2018; IARC, 2019)
2-methylfuran	Group 2B	(Prueitt et al., 2017)

In the course of organ growth, if an animal gets subjected to these endocrine disrupting compounds, the chemical effects permanent mutilation to the hormonal profiles. Therefore, these chemical compounds of furans induce overwhelming organizational effects on the evolving fetus if exposed to cigarette smoking during the pregnancy period (Rehman, Ullah, et al., 2019). Heterocyclic aromatic

compounds are known to be produced during the conventional numerous chemical reactions which involve creatinine, free amino acids and sugars (Barzegar et al., 2019; Zamora & Hidalgo, 2020).

Accordingly, a study carried out on heterocyclic aromatic compounds by Roemer et al. (2016) has revealed that these class of chemical compounds contribute to bacterial mutagenicity. Precisely, heterocyclic aromatic hydrocarbons are stimulated metabolically by N-hydroxylation which forms the intermediary ion, arylnitrenium, and they have been testified to influence DNA impairment and toxicity (Chen, 2020; Roemer et al., 2016; Yu et al., 2018). Other chemical compounds that have been reported present in cigarette smoke at significant levels include aldehydes, phenolic compounds, volatile hydrocarbons and nitro hydrocarbons (Bjurlin et al., 2020).

Further, a survey conducted by Sapkota and Wyatt (2015) came up with findings that showed that aldehydes actually go through biochemical reactions that involve nucleophilic targets in tissues, lipids and proteins and subsequently form stable and unstable adducts. As a result, pathological damages in human beings are started in the lungs where variations in cellular functions together with impaired proteins, nucleic acids and lipids occur and in so doing vascular diseases are propagated (Phaniendra et al., 2015). In the recent past, efforts have been geared towards exploring better methods and ways by which these toxins resulting from tobacco smoking can be reduced or their development in the course of cigarette burning prevented due to the witnessed unwillingness in the smoking people to abandon smoking, and the resistance of tobacco processing and manufacturing companies to implement technologies that would lower harm as a consequence of cigarette consumption (Lee et al., 2016).

2.2.3 Consequences of tobacco use

Agreeing to the study by Mallock, cigarette smoke can be considered to be extremely poisonous given that poisonous pyrolysis products are generated in the course of burning (Mallock et al., 2018). Further, a study survey conducted by Ivashynka exploring on the effects induced by cigarette smoking came up with findings that showed that smoking of cigarettes led to augmented heart beat rate and a corresponding intensification in blood pressure (Ivashynka et al., 2019). Further, smoking in mothers has been linked with a decline in performance of intelligence test, poor cognitive achievements, impaired memory, hyperactivity and weak attention span (Kristjansson et al., 2018b). Markedly, from other conducted studies, getting old in humans has been associated to recurring inhalation of smoke from cigarettes both in passive and active smokers (MacNee et al., 2014). Therefore, smoking increases an individual's biological age to about 55 years particularly in womenfolk (Skjodt et al., 2018). Successively, cigarette substance smoking speeds up the normal ageing process of the smoker's skin contributing to wrinkles in addition to damage of skin's appealing worthiness and beauty (Clatici et al., 2017). These effects are likely to occur to a smoker within a duration of approximately ten years or less keeping in mind that the more the number of cigarettes a person smokes, and the lengthier the smoking period, the more skin wrinkles one is likely to suffer (Fatani et al., 2020; Osman, O. F. et al., 2017). Worthwhile to note, earlier skin impairment as a consequence of smoking can be displayed on the smoker however it is challenging for an individual to note them (Clatici et al., 2017). Likewise, facial wrinkles in human beings can be intensely expected on or after cigarette smoking and these can be accredited fundamentally to nicotine uptake which effects dilation of blood vessels on the outermost skin deposit and by this

means damaging blood flow to the skin (Benowitz & Burbank, 2016; Osman, O. F. et al., 2017). As a result, the skin is therefore depleted of oxygen and nutrients as well as vitamin A (Clatici et al., 2017). More so, fibers like collagen and elastin which are responsible for skin strength and elasticity get damaged by a further 7,000 chemical compounds present in tobacco smoke thereby initiating skin sagging and untimely wrinkles and drawn appearances (Skjodt et al., 2018).

Further, scientific research has laid down evidence that the manifestation of prolonged coughs and tuberculosis incidences are as a result of cigarette smoking suggesting that high tobacco ingesting rates and exposure to second hand tobacco smoke intensifies the threats of tuberculosis and eventually fatality (Bisallah¹ et al., 2018). As such, coughs can be used as the first indicators in cigarette smokers for the diagnosis of respiratory infection (Ashok et al., 2017). The arising injurious effects resulting from cigarette smoking are significantly magnified in HIV infected persons who keep on to smoke even after the disease is under control as a consequence of medication (Popova et al., 2018). Reasonably, these individuals lose their years of life expectancy to cigarette smoking than the illness itself given that other than the associated adverse health effects of smoking, cigarette smoking subjects the HIV-positive persons to the dangers of hosting serious HIV related comorbidities and premature deaths (Giles et al., 2018).

Addiction to nicotine among smokers is a severe community health hazard in the entire world owing to the genetic aspects that add to disease susceptibility resulting in brain disorders that are harmful to the individual smokers and the general public at large (Ji et al., 2017). Chromosomal problems arise as a result of concealing risk genes for dependence to a myriad of chemical compounds present in cigarette smoke (Li &

Burmeister, 2009). According to studies performed on innumerable addiction phenotypes, a likelihood for linkage regions on chromosome 11 influence towards addictive phenotypes has been made (Bevilacqua & Goldman, 2009). Characteristic smoking hence has been related to chromosome 11q14 and the smoking behaviour associated with the chromosome 11q12 (Li, 2018). A study conducted by Hassan found out that tobacco ingredients can damage significantly the chromosomes in the sperms or change the morphological variations of the sperm, reduce the sperm concentration, sperm mobility and semen bulk thus distressing the male fertility capability (Hassan et al., 2019).

2.3 Marijuana Smoke

Scientific evidence has shown that there is a close similarity in chemical composition concerning second hand marijuana and tobacco smoke with major variances being element concentrations and variations (Holitzki et al., 2017). *Cannabis sativa* is the main source of marijuana which finds the name from the dried tobacco like prepared plant leaves and flowers (Fitzgerald et al., 2013). According to Atakan (2012), marijuana is a multifarious plant that comprises of dissimilar compounds that have diverse effects on individuals. Presently, more than five hundred chemical compounds have been acknowledged to be available in cannabis with over sixty cannabinoids which spawn further two thousand chemical compounds in cannabis smoke via a sequence of pyrolysis reactions (Archie & Cucullo, 2019; Borgan et al., 2019). Regardless of the chief psychoactive alkaloid in marijuana, other cannabinoids like cannabidiol (CBD), delta-8-tetracannabinol (d-8-THC) and cannabinol, designated as **2**, **3** and **4** in Figure 2.2, add to its pharmacological effects (Kögel et al., 2018).

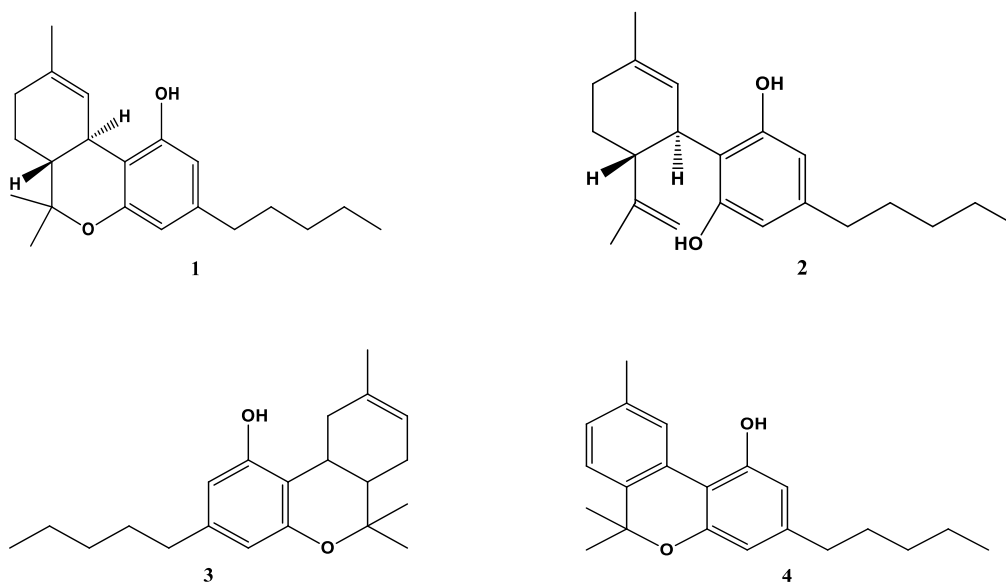


Figure 2.2: Marijuana phytocannabinoids

In the course of marijuana smoking, these chemical compounds gain their way into the smokers' body system where they produce a chain of disturbing effects in several organs including the pulmonary, respiratory and the central nervous systems (Archie & Cucullo, 2019). However, insignificant death cases arising from marijuana consumption have been reported amongst consumers, but still it's augmented unlawful trading in black markets and consumption patterns triggers anxieties on its prospective as a hazardous substance on human healthiness and more particularly its role as an agent of cancer advancement. Nonetheless, cannabis smoking has been documented as a risk factor for a pulmonary function and respiratory difficulties by a number of systematic and epidemiological studies (Ribeiro & Ind, 2016).

THC introduction to users' biosystem prompts numerous of effects characterized by changes in memory, movement, mood, perception and cognition and in certain circumstances augmented dopamine discharge that eventually yields euphoric feelings and anxiolytic effects (Cohen et al., 2017). CBD constitutes nearly forty percent of the marijuana extracts from the *Cannabis sativa* plant and is

predominantly found in seeds, stalks and flowers of cannabis plant and offers antipsychotic and alerting properties when used and this forms the foundation for its pharmaco-therapeutic properties (NIDA, 2019). Therefore, because of these variations in carcinogenic compounds concentration in marijuana, it is probable that it can produce more lung cancer as opposed to tobacco which is the primary contributing factor to lung cancer. Moreover, marijuana use has been associated with harmful effects such as high risk of mental illness and negative brain development in teenagers (Volkow et al., 2014). Tashkin (2013), evaluated the effects of cannabis smoking on the lungs and came up with findings showing that continued marijuana smoking results to lung cancer and that of the upper aero digestive tract system. It has also been proven scientifically that short-term exposure to second hand smoke from marijuana is likely to cause severe vascular endothelial dysfunction (Wang et al., 2016).

2.3.1 Ways and techniques of consuming marijuana

The effects brought about on consumers by marijuana as soon as it gains entry into the user's body system are largely dependent on the technique by which it is delivered. Currently, about three main marijuana delivery methods are in existence; namely, inhalation, oral and topical. These techniques have been commonly applied for the consumption of marijuana in diverse occasions with each one of the technique entailing different designed methods that offer distinctive purposes and outcomes (Williams, 2014). Smoking and vaporization are the supreme customary prehistoric inhalation approaches that are frequently used and it comprises the use of hand pipes, water pipes, paper rolls (joints or blunts), hooker in addition to shisha (Baldwin, 2020).

Likewise, vaporization method incorporates the usage of vaporizers that gradually heat up marijuana herbs to high temperatures that are sufficient enough to extract THC, CBD and additional cannabinoids but then again excessively low to speed up the discharge of injurious contaminants such as benzene and toluene as well as odor, which are produced and in so doing apparently, depressing the accompanying health hazards during the course of the cannabis smoking period (Romano & Hazekamp, 2019). This method is extensively used and varies from the customary smoking routine, owing to the fact that it does not encompass combustion. Accordingly, vaporization technique can be deliberated as harmless since it reduces exposure to the possibly detrimental cannabis smoke emissions which may well be carcinogenic and lethal to the well-being of both active and passive smokers (Romano & Hazekamp, 2018). Consumption of marijuana in form of vapor take into account the use of vape pens, dab rigs and desktop vaporizers such as volcano medic vaporizer.

Vaporized and smoked THC when compared, they portray comparable pharmacokinetic profiles, though on the contrary, vaporizers yield greater levels of THC concentrations equated to smoked marijuana which results to higher THC concentrations levels in blood, drug effects, mouth dryness and dry irritated eyes when similar amounts are smoked and vaped (Spindle et al., 2020). Oral approaches comprise of methods which administer marijuana via the mouth and they include edibles and tinctures. Precisely, cannabis edibles comprises drinks, foods and lozenges which have THC infused on them while tinctures consist of liquid marijuana extracts consumed by insertion of about 3-4 droplets underneath the tongue and gets instantaneously absorbed into the human biological system (Franklin et al., 2019). Subsequently, cannabis products are categorized as liquors, which can either be butane, hash oil or distillate, soft solids that could be wax or budder, and

hard solids such as shatter and crumble. A collection of cannabis consumption techniques and their popularity is listed in Table 2.2.

Table 2.2: Cannabis consumption methods and popularity

Method of intake	Designed Techniques	Popularity percentage	Trend in the last decade	Ref.
smoking	Blunt: cannabis rolled into a cigar removed of tobacco	40%	increase	(Williams, 2014)
	Joint: cannabis rolled in paper and smoked	30%	Increase	(NIDA, 2020b)
	Pipe: cannabis smoked in a glass pipe	40%	increase	(NIDA, 2020b)
ingestion	drinks	60%	Increase	(Franklin et al., 2019)
ingestion	food	60%	Increase	(Franklin et al., 2019)
ingestion	lozenges	60%	increase	
vaporizing techniques	Bong: burned cannabis bubbled through water	13%	Increase	(NIDA, 2020b)
	Hookah: cannabis mixed with flavored tobacco and smoke bubbled through water	25%	Increase	(Baldwin, 2020)
	Dabbing: cannabis products chemically dissolved in solvent vapors	25%	increase	(Baldwin, 2020)
	G-pen: Cannabis concentrated into wax, oil, or hash and vaporized through e-cigarette	26%	increase	(Spindle et al., 2020)
skin and mucosal surface absorption	creams	18%	Increase	(Williams, 2014)
	patches	13%	increase	(Bruni et al., 2018)
	sprays	16%	Increase	(Bruni et al., 2018)

2.3.2 Chemical products from marijuana smoke and their cancer potency

Numerous scientific investigative studies have comprehensively recognized the elemental composition of cannabis smoke and clearly noted that there is a close relationship in chemical composition amid second hand marijuana, and tobacco smoke with chief variances being component concentrations discrepancy with ordinarily comparable chemicals such as nitric oxides and aldehydes which have been demonstrated to cause damaging health effects (Holitzki et al., 2017). There is considerably little scientific exploration that has researched on the chemical characterization of marijuana cigarette smoke but then a record of the accessible readings have concentrated on defining cannabinoids in cannabis smoke and have testified that cannabis contains many toxins, irritants and carcinogens normally found to be present in tobacco smoke (Graves et al., 2020).

Specifically, when cannabis is smoked, it discharges more tar together with a considerably greater concentrations of cancer-causing agents such as benzo[a]pyrene as likened to tobacco smoke, and therefore it has been categorized as a secondary carcinogen which possesses nearly fifty to seventy percent more dangerous polycyclic aromatic hydrocarbons (PAHs) including benzo[a]anthracene, benzene and phenols in together with deadly fumes and reactive oxygen species that are 20 times higher in concentration than they are in tobacco (Ghasemiesfe et al., 2019). Conspicuously, these differences in concentration levels of the carcinogenic chemical compounds in cannabis heighten its likelihood of triggering lung cancer just in similar ways tobacco does, which has been accredited as the principal source of lung malignant cells in innumerable investigative studies (Graves et al., 2020). A variety of venomous molecular compounds sequestered from cannabis and their groupings are displayed in Table 2.3.

Table 2.3: Carcinogenic chemical compounds reported present in cannabis

Chemical compounds	carcinogenicity	Ref.
carbon monoxide	Not listed	(IARC, 2019)
benzene	Group 1	(IARC, 2019)
formaldehyde	Group 1	(Svenberg et al., 2013)
polycyclic aromatic hydrocarbons (PAHs)	Group 1, Group 2A and group 2B	(Abdel-Shafy & Mansour, 2016)
hydrogen cyanide	Not listed	(IARC, 2019)
benzo(a)pyrene (BaP)	Group 1	(Nakajima & Yagishita, 2018)
heterocyclic aromatic amines	Not listed	(Dong et al., 2020)
aldehydes	Group 1	(Tan et al., 2017)
phenolic compounds	Not listed	(IARC, 2019)
volatile hydrocarbons,	Group 2A	(IARC, 2019)
toluene	Group 3	(IARC, 2019)
furan	Group 2B	(IARC, 2019)
2-methylfuran	Not listed	(IARC, 2019)
isobutylene	Group 1A	(NCBI, 2020a)
ter-penes and terpenoids	Group 2B	(Coddington, 2017)
tetrahydrocannabinol	Not listed	(WHO, 2018)
cannabidiol	Group 2B	(Russo et al., 2019)

Nonetheless, it can be acknowledged that smoking of cannabis is a major causative agent of respiratory infections and cancers comparable to those instigated by tobacco smoking, but on the other hand, there is insignificant works validating that cannabis or marijuana smoking can be the foundation for the initiation of malignant cells in humans (Callaghan et al., 2017). Moreover, it has been proposed that cannabis smoke consist of particulate matter that is injurious and cancer-causing when inhaled

since it comprises potent compounds such as volatile organics and aromatic amines (Graves et al., 2020).

2.3.3 Harms and health impacts resulting from Cannabis

Individuals who smoke marijuana are inspired by the desire to achieve the psychotropic effects characterized by the enjoyable sensation, euphoria and relaxation which leads to the production of psychotic symptoms, cognitive changes, panic reactions and anxiety that have been informed to induce severe side effects on consumers (Radhakrishnan et al., 2014). Epidemiological confirmation has associated lung infection, augmented respiratory and cardiovascular symptoms, chronic bronchitis and chronic obstreperous ailment and emphysema to cannabis smoking (National Academies of Sciences Engineering and Medicine, 2017). In some illustrations, marijuana consumption can effect variation and occasionally loss in memory characterized by slackened reaction time, hindered information dispensation, un-coordinated motor reactions and performance, and attention deficit that consequently lead to mood disorder syndrome, psychosis and schizophrenia (Cohen et al., 2019). Consequently, an evaluation on the effects of cannabis smoking on the lungs established that continued marijuana smoking can cause lung malignant cells and cancers of the upper aero digestive tract system (Byers, 2017). Furthermore, even short-lived contact to second hand cannabis smoke results to severe vascular endothelial dysfunction (Wang et al., 2016). Nonetheless, deficiency of temperate intellectual governance as a result of the injurious effects induced by cannabis amongst intoxicated motorists has been stated to intensify the risk of road mishaps (Hartman & Huestis, 2013). The manifestation of these happenings is assumed given that when an individual consumes marijuana joint, he or she has four times more chances of getting exposed to carbon monoxide and five

times more tar deposition than when they consume single tobacco cigarette owing to more profound inhalation and lengthier holding sniff times and absence of cannabis cigarette filters (National Academies of Sciences Engineering and Medicine, 2017). Accordingly, psychiatric syndromes amid cannabis smokers have been linked with severe and long-lasting smoking (NIDA, 2020a). Therefore, early marijuana consumers are expected to experience a lack in psychological performance described by leisureliness in data processing, forgetfulness and depressed thoughtfulness which unpleasantly distresses their learning capabilities (Cohen et al., 2019). In addition, expectant females who become exposed to cannabis stand more probable to have deteriorated visualization and dexterousness, and may give labor to off springs that are likely to have abnormal behaviors (Archie & Cucullo, 2019).

As soon as the manifestation of marijuana is sensed in the CNS of human beings, it stimulates the production of dopamine and endogenous opioids which impedes the discharge of acetylcholine accountable for pharmacological alterations in the brain resulting to a reduction of glutamatergic synaptic transmission which induces brain operative aberrations amongst the marijuana smoking populations (Bloomfield et al., 2016). Inhibitory functions are offered by endocannabinoid system receptors, CB1 and CB2, whereby CB1 receptor enhances the manufacture of cyclic adenosine monophosphate pathway the moment a signal is received from adenylyl cyclase inhibitor while CB2 receptor plays a significant role in hindering inflammatory activity and tissue impairment (Archie & Cucullo, 2019). As a result, brain structural aberration has been witnessed in chronic marijuana smokers with supplementary effects executed on the grey and white matter density (Cohen et al., 2019). Furthermore, inconstant brain activity amid marijuana users has been noted and compared with non-smokers and in this case, better brain stimulation is observed

in the prefrontal region of smokers while hypo-activation is prominent alongside the left superior parietal cortex due to high concentrations of the two cannabinoids, THC and CBD. THC changes the hippocampal capacity and neurochemistry while CBD shields against toxic variants (Beale et al., 2018).

Nevertheless, cerebral stroke, which has been identified to be the leading cause of fatalities in humans has been linked with cannabis consumption according to a number of preclinical surveys and scientific case reports (Wolff & Jouanjus, 2017). neurological stroke and Alzheimer's disease have been scientifically demonstrated to exclusively be consequences of human introduction to reactive oxygen species such as peroxy nitrite, hydrogen peroxide, epoxides and oxidative stress pathways which are capable of inducing tissue and cellular mutilation, disorders which are essentially stimulated by cannabis smoking (Archie & Cucullo, 2019). As a result, THC has been regarded as an impending agent of oxidative stress and a threat in the commencement of ischemic stroke (Wolff Valérie et al., 2011). Reactive oxidative stress chemical compounds can be spawned by incineration reactions that transpire in the course of cannabis smoking.

2.4 Catha edulis

Khat comprises of the leaves and shoots that are obtained from the shrub, *Catha edulis* which is nurtured, cultivated and habitually chewed by millions of the inhabitants of East African and Arabian Peninsula due to its stimulating effects that are prompted by the amphetamine like alkaloids, Cathinone and Cathine indicated as 1 and 2 respectively in Figure 2.3, once they gain entry into the human brain (Abebe et al., 2015).

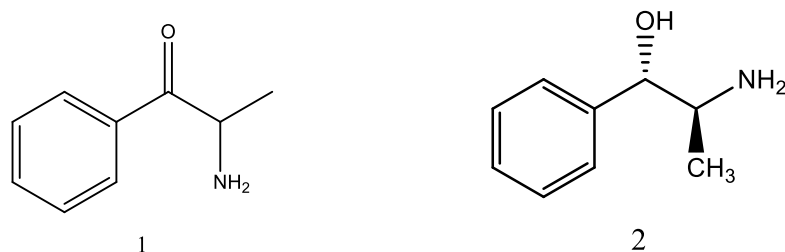


Figure 2.3: Major khat alkaloids

This plant substance finds additional forenames like miraa, qat/ khat, chat, havigat, qaadka, muhulo, mairungu, kijiti, veve, gomba, African salad, tschat, and Abyssinian tea, all dependent on the nation state in which it is cultivated or sold (EMCDDA, 2015; SAPTA, 2012). Even though categorized under class C drug substance by the world health organization, khat cultivation, possession and consumption is permitted in Kenya and most of the East African countries while certain countries such as Bangladesh, California, Canada, South Africa and some other states of the United States of America (USA), have prohibited its usage and possession (DWAF, 2013; Law Tech Publishing Group, 2016; Mahmud, 2019). Therefore, *Catha edulis* and its principle chemical compounds, cathinone and cathine, have been patented as regulated ingredients by the Controlled Substances Act and the Drug Enforcement Administration in schedule I and IV respectively (DEA, 2019).

The chewing of *Catha edulis* is a renowned social tradition and a recreational activity which is practiced in a variety of social amenities by equally young and old men and women in the cultivating countries (SAPTA, 2012). A person is driven and addicted to chew khat because of its high content in the psychoactive ingredient, cathinone, that acts symphathomimetically on the CNS, and directly impacts on both the central dopaminergic and peripheral noradrenergic presynaptic spots, in order to yield insignificant euphoric, enjoyment, hysterical behaviors, hyperactivity, illusions, and

a soothing effect within a period of thirty minutes commencing from the time it is consumed (Haydock, 2012; SAPTA, 2012). In addition, cathine too adds to the stimulation of CNS characteristics even though it has been reported to be less effective in garden-fresh khat shrubberies by a number of studies (Glennon, 2014).

2.4.1 Trends and methods through which khat is consumed

The levels of stimulation and the psycho-effects prompted on khat users are significantly determined by the techniques through which it is consumed due to differences in concentration intensities of the key khat alkaloids which are determined by the freshness of the leaves, shoots and twigs of the *Catha edulis* shrub. For instance, cathinone and cathine are found in higher concentrations in fresh leaves compared to dry leaves which are considered less potent and less addictive (Dhabbah, 2020; Laura et al., 2019). There exist a number of oral techniques by which this drug substance can be consumed. The customary method by which khat is consumed is through chewing which involves chewing fresh leaves, twigs, and shoots of the *Catha edulis* shrub, that are held in reserve in the cheek and further, munched intermittently and spasmodically so as to release the active drug components in form of a juice which that is extracted by enzyme action and subsequently dissolved in saliva, swallowed and absorbed through the buccal mucosa and gastro-intestinal tract (Feng et al., 2017; Mihretu et al., 2017; Orlie et al., 2018). In the course of khat mastication, individuals occasionally drink water to counter mouth dehydration, or a sip of soda or a pinch of sugar to improve on its bitter taste (Al- Maweri et al., 2018; Gudata et al., 2019). In some cases, the *Catha edulis* dried material is made into tea or a chewable paste (MedicineNet, 2020).

Nonetheless, khat leaves can be smoked by crushing dried leaves which are then rolled into cigarettes or grinded into powder and sprinkled on or in food (Ademe et

al., 2020; Laura et al., 2019; MedicineNet, 2020; SAPTA, 2012). The technique used for khat consumption is determined by the cultural practices of the community, a person's social status, economy, political and spiritual lives (Gudata et al., 2019). Capsules that are designed with synthetic cathinones in white and brown amorphous and crystalline powders consisting of mephedrone, methylone, naphyrone, butylone, methcathinone, pyrovalerone, 4-fluoromethcathinone, 3,4-methylenedioxypropylone, and methedrone ingredients, have been used in illicit market together with tablets even though they are less common techniques (EMCDDA, 2020; Worku, 2018).

Table 2.4: Khat consumption techniques and popularity trends

Method of intake	Designed technique	Popularity percentage	Trend in the last 1 decade	Reference
chewing	Fresh twigs and leaves chewed for mucosal absorption	80%	increasing	(Al- Maweri et al., 2018; Feng et al., 2017)
smoking	Dried khat leaves rolled into smoked cigars	30%	increasing	(Laura et al., 2019; SAPTA, 2012)
khat tea	Dried and grinded khat leaves packed into sachets that are added into hot water for drinking.	27%	increasing	(SAPTA, 2012)
khat paste	Dried khat leaves made into chewable paste	31%	increasing	(SAPTA, 2012)
khat food powder	Dried khat leaves are finely grinded into powder sprinkled onto food during eating	23%	increasing	(Laura et al., 2019)
Capsules/ tablets	Bombing; cathinone derivative powder rolled into cigar paper and swallowed. Keying; insufflation of 8keys per gram of cathinone derivative by key dipping into powder.	not known	increasing	(Dunne et al., 2015; EMCDDA, 2020; Prosser & Nelson, 2012; Wolff V. et al., 2018; Worku, 2018)

The sole reason for consumers to use khat is due to the exciting effects contributed largely by cathinone and cathine ingredients, but unstable cathinone decomposes into

cathine once the fresh khat leaves get exposed to oxygen after harvest during withering or when dry and therefore, khat leaves are commonly chewed when fresh in order to offer maximum potency (Drugs.com, 2019). Accordingly, the other techniques listed in table 2.4 have minimal but increasing popularity in their application given that the effects of stimulation require more amounts of the drug to be taken or longer time periods to be exhibited in the consumer due to lowered levels of cathinone, the chief khat stimulant that usually induces its psycho-stimulating activity in 1 to 3 hours after chewing onset.

Regardless of these assumptions, capsules and tablets which encompass synthetic cathinones have gained an increasing popularity and widespread availability and are sold as “bath salts” or “plant food” commonly in internet website markets and drug suppliers and consumed by ingestion or nasal insufflation (Prosser & Nelson, 2012). Bombing and keying form the basic techniques by which synthetic cathinones are consumed whereby bombing as a technique, involves wrapping a fine cathinone derivative powder, usually comprising of mephedrone, in a cigarette paper which is then swallowed, while keying encompasses the act of dipping a key into finely grinded khat powder which is then insufflated (Dunne et al., 2015; Prosser & Nelson, 2012).

2.4.2 Emerging chemical compounds from khat and their carcinogenicity

The phytochemicals dominantly present in khat includes amino acids, carbohydrates, flavonoids, glycosides, niacin, sterols, tannins, terpenoids, thiamin, vitamins C, riboflavin, noncyclic nitrogen containing compounds, and approximately 62 alkaloids (Al- Maweri et al., 2018; Atlabachew et al., 2014; Jerah et al., 2017). The stimulating activity of khat is mainly contributed by alkaloids of the group,

phenylalkylamines, which constitutes cathinone [*S*-(-)-cathinone], and two cathine diastereomers [*1S*, *2S*-(+)-norpseudoephedrine] and norephedrine, [*1R*, *2S*-(-)-norephedrine as indicated in figure 2.4 respectively. The *S*-(-)-cathinone enantiomer is the only one that has been reported to be present in khat and has a structural stereochemistry resembling that of *S*-(+)-amphetamine but differ in their pharmacology (Atlabachew et al., 2017). Cathinone instability leads to its disintegration resulting to the development of ‘dimer’ (3,6-dimethyl-2,5-diphenylpyrazine) in the course of withering and drying processes of khat (Drugs.com, 2019). Further about 62 cathedulins which are mainly euonyminol polyesters ensuing from poly hydroxylation of sesquiterpenes have been reported to be present in khat leaves (Gashawa & Getachew, 2014).

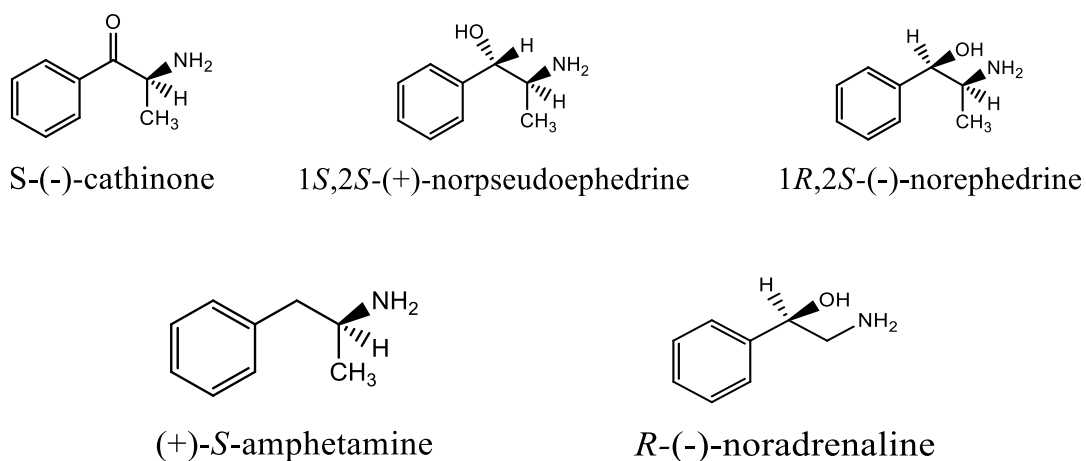


Figure 2.4: Phenylalkylamine alkaloids of khat

More other phenylalkylamine alkaloids such as merucathinone, merucathine and pseudomerucathine, illustrated in Figure 2.5, with less stimulation effect have been reported in khat leaves (Jerah et al., 2017).

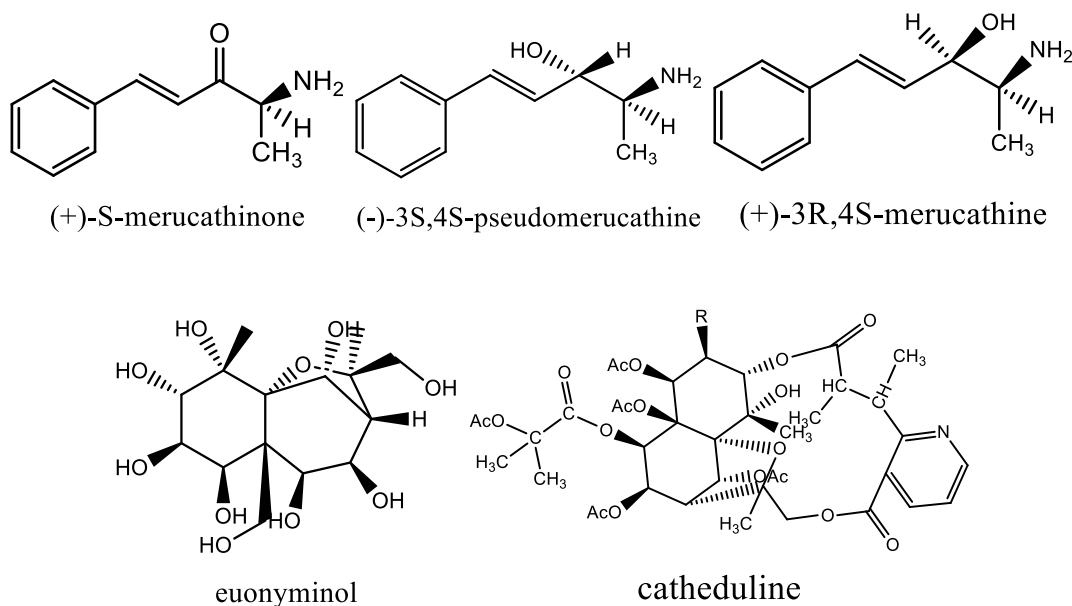


Figure 2.5: Phenylpentylamine and catheduline alkaloids from khat

Even though the mutagenic and the cancer-causing potentials of these phenylalkylamines and alkaloids present in khat are have not been surveyed exhaustively, a few of experimental and epidemiological studies have established on the teratogenic, mutagenic, and clastogenic activities of cathinone in human cells, regardless of a limitation in the literature documentation on the plant component accountable for its genotoxicity (Leon et al., 2017). For instance, Hassan et al (2020) have revealed that prolonged khat chewing stimulates cancer-causing processes in human being by starting endogenous oxidative impairment on the DNA cells (Hassan et al., 2020) and manifestation of oesophageal and stomach casinomas in khat chewers which have been accredited to khat leaves capability to undergo nitrosilation in the gut, producing nitrosamines (Nigussie et al., 2013). In addition, khat is has been reported to be highly concentrated with tannins, compounds which have been extremely linked to oesophageal cell carcinoma, oral malignancy (Leon et al., 2017).

2.4.3 Harms and health impacts arising from consumption of khat

Chronic khat chewing has been associated with a number of health problems and effects on the human biotic systems such as the respiratory, cardiovascular, hepatobiliary, genitourinary, endocrine and digestive systems by many scientific and epidemiological analyses (Lu et al., 2017; Orlien et al., 2018). These systems that are characterized by khat chewing effects which includes metabolic and weight related complications, cancers of the aero digestive system as well as oral cancer ischemic heart disease, neuropsychological disease, liver problems, endocrine and sexual disorder and hypertension (Girma et al., 2015; Hassan et al., 2020; Orlien et al., 2018). For instance severe effects such as arrhythmias, cerebral hemorrhage, hypertension, myocardial infection, pulmonary edema, tachycardia, palpitations and vasoconstriction are expressed in the bronchitis in the respiratory system, cardiovascular system, chronic gastritis, dry mouth, dental caries, duodenal ulcers, hemorrhoids, periodontal disease, polydipsia, tachypnea and upper gastro-intestinal malignancy in the gastro intestinal system, fibrosis and cirrhosis in the hepatobiliary system in addition to urinary retention, spermatorrhea, spermatozoa malfunctions, impotence and libido change which affect the genitourinary system of chronic khat consumers (Leon et al., 2017; Muema, 2015; Nigussie et al., 2013). Further, salivary glands infection, plasma cell gingivitis, teeth attrition and discoloration, temporomandibular joint disorder, and keratotic white lesions including mucosal lesions are other health issues that have been reported to occur as a result of prolonged khat chewing (Al- Maweri et al., 2018). Figure 2.6 gives a summary of the biological systems and effects associated with khat consumption.

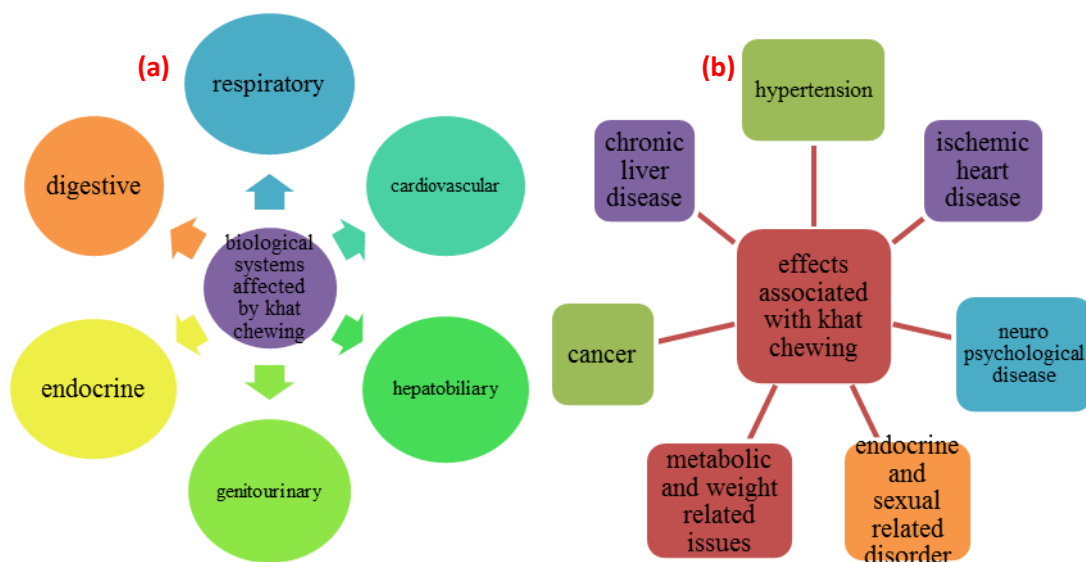


Figure 2.6: Biological systems affected by khat chewing(a) and health effects associated with khat chewing (b) (Alshagga et al., 2016; Girma et al., 2015; Hassan et al., 2020; Lu et al., 2017; Lukandu et al., 2015).

Regardless of all these highlighted toxicological impacts of khat, a number of studies have reported on khat application as medicine for the management of diabetes, muscle strength, depression, obesity, male infertility and cancer. Precisely, a study conducted by Lu et al (2017) demonstrated the cytotoxic effects of khat extracts on breast cancer and came up with findings showing that khat suppresses breast cancer by inducing apoptosis of breast cancer cells (Lu et al., 2017).

2.5 Effect of free radicals on human health

A study conducted by Assaf et al. (2016), has vividly pointed out that environmentally persistent free radicals remain to be a subject of great interest in research with more focus being emphasized on the mechanisms leading to their formation and their related effects on human health. Accordingly, these free radicals are noted to have a major contribution to the damaging of the respiratory system by majorly causing chronic and cardiopulmonary dysfunction due to the fact that they are reactive oxygen species which are under oxidative stress (Panth et al., 2016).

Some of this active chemical species that are predominantly present in cigarette smoke include hydroxyl radicals, hydrogen peroxide and superoxide anion radicals generated during the pyrolysis processes (Assaf et al., 2016). Hatzinikolaou et al. (2006) have reported benzene, toluene, furan, 2-methylfuran and isobutylene as some of the components of gas phase cigarette smoke. These compounds have been identified to be potential leads in initiating lung cancer even though much information has not been documented in literature in regard to their cancer causing mechanisms. Tentatively, lung cancer is the dominant malignance caused by smoking and over 1 million deaths reported in the world have been linked to cigarette smoking (U.S Department of Health and Human Services, 2006).

The determinant factor on cigarette smoking as a causative agent of cancer is the extent of smoking and the number of cigarettes smoked that exposes the smoker to the risk of histologic types of lung cancer such as squamous cell carcinoma, small cell carcinoma, adenocarcinoma (bronchiolar-alveolar carcinoma) and large cell carcinoma (Babalik et al., 2018). The most common of these cancers caused by smoking is adenocarcinoma (Coleman et al., 2018). Cigarette smoking has also been identified as the major cause of transitional cell carcinomas of the bladder, ureter and renal pelvis and can possibly increase the risks of sinonasal and nasopharyngeal cancer (Arora et al., 2018).

Among the many cancers in humans, oropharyngeal and hypopharyngeal cancer are also certain types of the cancers which have been reported to be induced by continued cigarette smoking (Liao et al., 2018). In addition, cancer of the liver is among the human cancers that can be caused and boosted by cigarette smoking (Bray et al., 2018). All these cancers are as a result of the carcinogenic agents present in cigarette smoke which includes polycyclic hydrocarbons, heterocyclic compounds,

N-Nitrosamines, Aromatic amines, Heterocyclic aromatic amines, Aldehydes, Phenolic compounds, Volatile hydrocarbons, Nitro-hydrocarbons, Miscellaneous organic compounds and Metals and inorganic compounds. These components are proven carcinogenic by experiments on animals. Therefore, the IARC has categorized these compounds as either group 2B, which are possibly carcinogenic to human beings, group 2A which are probably carcinogenic to humans or group 1 which are carcinogenic to humans (WHO, 2019).

2.5.1 Polycyclic hydrocarbons

Abdel-Shafy and Mansour (2016), have described polycyclic aromatic hydrocarbons (PAHs) as ever-present environmental pollutants which are produced during biomass pyrolysis under limited supply of air. PAHs can also be emitted from anthropogenic activities such as residential heating, coal gasification and petroleum refineries and motor vehicle exhaust. PAHs possess toxic, mutagenic and carcinogenic properties owing to the fact that they are known to be highly lipid soluble and therefore readily adsorbed from gastrointestinal tract in living organisms (Kim et al., 2013). PAHs are rapidly distributed in the body tissues and get deposited in the body fats where they attach or bind to the DNA cells and start to cause a series of disruptive effects that often end up as tumor initiators (Abdel-Shafy & Mansour, 2016). PAHs are listed as the ninth most threatening chemical compounds to humans having been identified as cancer causative agents (Rengarajan et al., 2015). Table 2.5 shows common PAHs present in cigarette smoke and reported concentration levels.

Table 2.5: Concentrations of polycyclic hydrocarbons in mainstream cigarette smoke

Carcinogen	Amounts in mainstream cigarette smoke	IARC monograph evaluation of carcinogenicity		
		In animals	In human	IARC group
Benz[a]anthracene	20–70 ng	Sufficient		2A
Benzo[b]fluoranthene	4–22 ng	Sufficient		2B
Benzo[j]fluoranthene	6–21 ng	Sufficient		2B
Benzo[k]fluoranthene	6–12 ng	Sufficient		2B
Benzo[a]pyrene	8.5–17.6 ng	Sufficient	limited	1
Dibenz[a,h]anthracene	4 ng	Sufficient		2A
Dibenzo[a,i]pyrene	1.7–3.2 ng	Sufficient		2B
Dibenzo[a,e]pyrene	Present	Sufficient		2B
Benz[a]anthracene	20–70 ng	Sufficient		2A

Tobacco smoke containing PAHs has been linked to lung cancer (Ifegwu & Anyakora, 2015). PAHs are not only carcinogenic but have also been confirmed to be potential causes of other numerous toxicological manifestations including decreased body weight, enlarged liver with cellular edema, and congestion of the liver parenchyma, reproductive toxicity, intrauterine growth retardation, learning and IQ deficits, destruction of oocytes, and inflammation of kidney cells (Osman, G. et al., 2017).

2.5.2 Heterocyclic hydrocarbons in cigarette smoke

During thermal degradation of biomass, furan, (C_4H_4O), which belongs to a group of organic compounds known as dioxins (polychlorinated dibenzo-furans, PCDFs), physically characterized as colorless toxic organic compound are produced (Rehman, Jahan, et al., 2019). Furan can be categorized as endocrine disrupting chemical compounds given that it has a potentially higher capacity to alter the animal

physiology by disrupting its hormonal levels (Ferreira et al., 2019). Some of the furans and heterocyclic hydrocarbons that have been detected and reported to be present in tobacco cigarette smoke are listed in table 2.6.

Table 2.6: Concentrations of heterocyclic hydrocarbon components in mainstream cigarette smoke

Carcinogen	Amounts in mainstream cigarette smoke	IARC monograph evaluation of carcinogenicity		
		In animals	In human	IARC group
Furan	20–40 µg	Sufficient		2B
Dibenz[a,h]acridine	ND-0.1 ng	Sufficient		2B
Dibenz[a,j]acridine	ND-10 ng	Sufficient		2B
Dibenzo[c,g]carbazole	ND-0.7 ng	Sufficient		2B
Benzo[b]furan	Present	Sufficient		2B

During organ development, if the organisms get exposed to endocrine disrupting chemicals, they cause irreversible changes in the hormonal profiles (Rehman, Jahan, et al., 2019). As a result, furans can have extremely devastating structural effects on the evolving fetus if it gets exposed to cigarette smoking by the mother.

2.5.3 N-Nitrosamines

By inhaling mainstream cigarette smoke, individual that are actively involved in smoking and those that are passive smokers both get exposed to nitrosamines which endogenously are known to form as a result of the uptake of alkaloids and nitrogen oxides or nitrile (Hecht, 2016). The main driving influence for an individual to smoke is nicotine, which is the major alkaloid in tobacco (McKinney & Vansickel, 2016). Other alkaloids such as nornicotine, anabasine and anatabine form part of the chief alkaloids in tobacco (Williams, 2012). Nitrosamines are known to form once secondary and tertiary amines react with nitrile leading to the yield nitrosamine in which over 70 of the nitrosamines have been confirmed scientifically to be

carcinogenic. Nitrosation of secondary amines is known to be a very rapid reaction whereby the hydrogen attached to the nitrogen is replaced by the –NO group in high yields (Spahr et al., 2017). Some of the N' nitrosoamines are listed in Table 2.7.

Table 2.7: Concentrations of N-Nitrosamine in mainstream cigarette smoke

Carcinogen	Amounts in mainstream cigarette smoke	IARC monograph evaluation of carcinogenicity		
		In animals	In human	IARC group
N-Nitrosodimethylamine	0.1–180 ng	Sufficient		2A
N-Nitrosoethylmethylamine	ND-13 ng	Sufficient		2B
N-Nitrosodiethylamine	ND-25 ng	Sufficient		2A
N-Nitrosopyrrolidine	1.5–110 ng	Sufficient		2B
N-Nitrosopiperidine	ND-9 ng	Sufficient		2B
N-Nitrosodiethanolamine	ND-36 ng	Sufficient		2B
N'-Nitrosornicotine	154–196 ng	Sufficient	Limited	1
4-(Methylnitrosamino)-1-(3-pyridyl)-1-butanone	110–133 ng	Sufficient	limited	1

On the other hand, the nitrosation process of these tertiary amines is confirmed to be a slow reaction. Therefore, the nitrosation of some of the secondary amines such as nornicotine, anabasine and anatabine usually lead to the production of tobacco specific nitrosamines such as N' nitrosoanabasine (NAB), N' Nitrosoanatabine (NAT) (Cai et al., 2016). Nitrosation of tertiary amine nicotine yields NNN and nicotine-derived nitrosoaminoketone (NNK) which has been identified to be a strong carcinogen. NNN and NNK are known to induce benign and malignant tumors in organisms by affecting specific organs depending on the route of administration (De Flora et al., 2016).

2.5.4 Heterocyclic aromatic amines

Roemer et al. (2016), conducted research on heterocyclic aromatic compounds and found out that these chemical compounds can contribute to bacterial mutagenicity

and a majority of these compounds are known to form as a result of milliard reactions that involve creatinine, free amino acids and sugars. Heterocyclic aromatic hydrocarbons usually undergo metabolic activation reactions by N-hydroxylation leading to the formation of an intermediate ion (arylnitrenium) which has been reported to cause DNA cells damaging and toxicity. Table 2.8 illustrates some of the HAA and their concentration levels in cigarette smoke.

Table 2.8: Concentrations of heterocyclic aromatic amines in mainstream cigarette smoke

Carcinogen	Amounts in mainstream cigarette smoke	IARC monograph evaluation of carcinogenicity		
		In animals	In human	IARC group
A- α -C	25–260 ng	Sufficient		2B
MeA- α -C	2–37 ng	Sufficient		2B
IQ	0.3 ng	Sufficient		2A
Trp-P-1	0.3–0.5 ng	Sufficient		2B
Trp-P-2	0.8–1.1 ng	Sufficient		2B
Glu-P-1	0.37–0.89 ng	Sufficient		2B
Glu-P-2	0.25–0.88 ng	Sufficient		2B
PhIP	11–23 ng	Sufficient		2B

2.5.6 Other organic compounds in cigarette smoke

Aldehydes, phenolic compounds, volatile hydrocarbons, nitro hydrocarbons are some of the chemical compounds which have been reported by (Hecht, 2016) to be dominantly present in cigarette smoke in innumerable concentration levels. Sapkota and Wyatt (2015) found out that aldehydes have the ability to react with human nucleophilic targets in body cells, lipids and body proteins resulting to the formation of stable and unstable adducts that causes disturbance to cellular functions and damage body proteins, nucleic acids and lipids thereby initiating pathological

conditions in the lungs and vascular disease. Table 2.9 displays the reported concentration levels of these compounds in cigarettes smoke.

Table 2.9: Concentration levels of aldehydes, phenolic compounds, volatile hydrocarbons and nitro-hydrocarbons

Carcinogen	Amounts in mainstream cigarette smoke	IARC monograph evaluation of carcinogenicity		
		In animals	In human	IARC group
Formaldehyde	10.3–25 μ	Sufficient	Sufficient	1
Acetaldehyde	770–864 μ g	Sufficient		2B
Catechol	59–81 μ g	Sufficient		2B
Caffeic acid	< 3 μ g	Sufficient		2B
1,3-Butadiene	20–40 μ g	Sufficient	limited	2A
Isoprene	450–1,000 μ g	Sufficient		2B
Benzene	12–50 μ g	Sufficient	Sufficient	1
Nitromethane	0.5–0.6 μ g	Sufficient		2B
2-Nitropropane	0.7–1.2 ng	Sufficient		2B
Nitrobenzene	25 μ g	Sufficient		2B
2-Toluidine	30–200 ng	Sufficient	Limited	2A
2,6-Dimethylaniline	4–50 ng	Sufficient		2B
2-Naphthylamine	1–22 ng	Sufficient	Sufficient	1
4-Aminobiphenyl	2–5 ng	Sufficient	Sufficient	1

2.6 Computational modeling

In the recent past, there has been a great documentation of literature that advocates for the use of computational chemistry which has made it probable for calculation of properties of minute chemical compounds and radicals by using computationally exhaustive methods such as ‘theoretical model chemistry’ which relies on the application of high level *ab initio* computations (Mebel et al., 1995). These techniques to a large extent have enhanced on essential and convenient understandings in the learning and study of molecules (Keith et al., 2021). Therefore, the application of computational modelling in chemistry is a useful technique that is

commonly applied in generating data that can give crucial information to the users. In many cases, the use of computational chemistry tools is established on quantum chemistry which describes the computationally determined arithmetical analyses founded on quantum mechanics (Keith et al., 2021). Computational modelling techniques are commonly preferred compared to experimental methods because of the level of quantitative accuracy which is dependent on its appropriateness in describing a given system and its capability to generate data sets that are well-controlled and comparatively accurate thermochemistry experiments on minor, secluded molecules (Curtiss et al., 2000; Keith et al., 2021).

Bartocci and Lió (2016), labeled computational modeling as a technique that includes the application of computers in mimicking and learning the behavior of multifaceted systems by assimilation of arithmetic, quantum mechanics and computer science. The use of computational modelling has aided in giving justifiable reasons to tentative interpretations of experiments and probable predictions of expected results from experiments making it a suitable alternative to scientists for investigative studies (Craig et al., 2020). A computational model encompasses numerous variables which describe the system under study by changing these variables either singly or in permutation with others and interpretations on the effects of these variations made on the conclusions during modeling. Computational chemistry aims at solving the ground state energy for a given system of atoms which constitutes the potential energy surface that can be defined as a hypersurface straddling $3N$ dimensions of an atomic system, with N representing the number of atoms within that system (Keith et al., 2021).

The attained results of the computer-generated prototypical group of molecules aid researchers in forecasting what transpires in the actual system under study in

response to the shifting circumstances (Harrison et al., 2018). Sokolowski and Banks (2011), in their book on principles of modeling and simulation, they have alleged that modeling can prompt up research given that it can permit scientists to carry out numerous replicated trials by means of computers in order to classify the real physical experiments that can simplify the research in finding out explanations to the research problem. Besides, computational modeling has been built around estimated solutions, some of which are more precise than any well-known experimental data and this technological advances are capable of identifying the structure and property connections that may give suggestions regarding atomic arrangement, stoichiometry's and arrangements that perhaps drive the assimilated data bases (Nyshadham et al., 2017). Jain and Shin (2016), have argued that the substantial laws that achieve the behavior of materials are summed up in the Schrödinger equation whose universal notation consists of the Hamiltonian H , the total energy of the system E and the wave function ψ which is the eigen function of the Hamiltonian that forms the basis of computational chemistry.

$$H\psi = E\psi \quad 2.9$$

Omnes (2018) have their explanation of wave mechanics emphasizing that the wave function articulates the system and it takes the location of electrons in the system as variables leading to the equation;

$$H\psi\left(\vec{r}_1, \dots, \vec{r}_N\right) = E\psi\left(\vec{r}_1, \dots, \vec{r}_N\right) \quad 2.10$$

While \vec{r} defines the position of electrons in space, ψ is used to determine the calculated system properties. The wave function can be orthogonal or orthonormal in space depending on the type of the wave function (Iserles & Webb, 2020). Therefore, equation 2.11 is considered.

$$\langle \psi_i / \psi_j \rangle = \delta_{ij} \begin{cases} 1 \text{ if } i = j \\ 0 \text{ if } i \neq j \end{cases} \quad 2.11$$

In many cases the Hamiltonian belongs to a specific system which consists of the nuclei and the electrons whose special positions can be given by their corresponding vectors R_A and r_i (Omnes, 2018). Karlström et al. (2003) in their work on program package for computational chemistry, they reason that entire field of computational chemistry is built in more or less of approximate solutions, some of which are extra accurate than any other known experimental data. Consequently, the quantum chemical computation of thermodynamics data can be developed beyond the level of simply reproducing experimental values (Tentscher et al., 2019) and the obtained data can be used in making significantly correct and precise predictions for molecules in which their experimental data are unknown (Deng et al., 2019).

2.6.1 The Density Functional Theory

Lejaeghere et al. (2016), performed reproducibility tests in density functional theory calculations of solids and illustrated the DFT as a ground state method that can be applied in calculating the properties of various electron systems from first principles. Accordingly, the DFT as a method successfully describes structural and electronic properties in several materials ranging from atoms to molecules (Kratzer & Neugebauer, 2019). Therefore, the DFT is the first tool in the first principles calculation that describes and predicts the properties of molecular systems (Parks et al., 2019).

Grossi et al. (2017) in their work on fermionic statistics in the strongly correlated limit of the Density Functional Theory, they found out that the DFT puts more focuses on describing the interacting systems of fermions through its density and not through wave function. As such, given that a number N of electrons in a solid that

obey the Pauli principle and are able to repulse one another through the Coulomb potential, then the basic variable of the system will depend only on three spatial coordinates x , y , and z – rather than $3N$ degrees of freedom (Parks et al., 2019; Sun et al., 2016). Therefore, in order to determine the properties of a molecule in its ground state, the knowledge of the DFT is very important.

2.6.2 The Hohenberg-Kohn Theorem

In mention to the study conducted by Lammert (2018) in search of the Hohenberg-Kohn theory they argue that it can be split into two; the first Hohenberg-Kohn theorem and the second Hohenberg-Kohn theorem. The first Hohenberg-Kohn theorem asserts that the density of any system determines all the ground state properties of the specified system (Medvedev et al., 2017; Nikolaou, 2021).

$$E = E[\rho] \tag{2.12}$$

where, ρ is the ground state density of the system?

According to Baer and Kronik (2018), the second Hohenberg-Kohn theorem can be employed to demonstration that there exists is a variational principle for the above energy density functional ρ . For instance, if ρ' is not the ground state density function of the described system, then;

$$E[\rho'] > E[\rho] \tag{2.13}$$

Therefore, if we deliberate on a system of N interacting electrons which are under an external potential $V(r)$ called a coulomb potential, then it can be assumed that the system has a non-degenerate ground state which has only one ground state charge density $n(r)$ which responds to a given $V(r)$ (Nordholm, 2021). Accordingly,

Bauman et al. (2019) have defined a system with many electrons Hamiltonian, $H = T + U + V$ and a ground state wave function ψ ; where T is the kinetic energy, U the electron-electron interaction, V the external potential; the charge density $n(r)$ as;

$$n(r) = N \int |\psi(r, r_2, r_3, \dots, r_N)|^2 dr_2 \dots dr_N \quad 2.14$$

If the system has a dissimilar Hamiltonian given by $H' = T + U + V'$, in this case V and V' do not differ by a constant, the ground state wave function can be assumed to have the ground state charge densities which are the same. According to (Bauman et al., 2019) the inequality below holds:

$$E' = \langle \psi' | H' | \psi' \rangle < \langle \psi | H' | \psi \rangle = \langle \psi | H + V' - V | \psi \rangle \quad 2.15$$

that is,

$$E' < E + \int (V(r) - V'(r)) n(r) dr \quad 2.16$$

ψ , and ψ' are taken to be different because they are Eigen states of different Hamiltonians and thus the inequality is strictly suggesting that no two different potentials can have the same charge density (Beckwith, 2021). From the first Hohenberg-Kohn theorem, the ground state E energy is uniquely calculated by the ground-state charge density. In mathematical terms, E is a function, $E[n(r)]$

$$E[n(r)] = \langle \psi | T + U + V | \psi \rangle = \langle \psi | T + U | \psi \rangle + \langle \psi | V | \psi \rangle = F[n(r)] + \int n(r) V(r) dr \quad 2.17$$

where; $F[n(r)]$, is a universal functional of the charge density $n(r)$ and not of, $V(r)$.

For this functional charge density, Savin (2017) further clarifies that a variational principle holds and therefore the ground state energy is minimized by the ground state charge density and the DFT reduces the N -body problem to the determination of a 3-dimensional function $n(r)$ which minimizes a functional $E[n(r)]$.

2.6.3 The Kohn-Sham equations

These Kohn-Sham equations are applied in mapping systems in which electrons are interacting to a secondary system comprising of non-interacting electrons which have similar ground state charge density, $n(r)$. In such a system of non-interacting electrons, as described by Hossain (2004) the ground state charge density can be denoted as a summation over one-electron orbitals (the KS orbitals), $\psi_i(r)$:

$$n(r) = 2 \sum_i |\psi_i(r)|^2 \quad 2.18$$

in this case; i , ranges from 1 to, $\frac{N}{2}$ if dual tenancy of the entire conditions is assumed and the KS orbitals are the answers of the Schrödinger equation given.

$$\left(-\frac{\hbar^2}{2m} \nabla^2 + V_{KS}(r) \right) \psi_i(r) = \varepsilon_i \psi_i(r) \quad 2.19$$

m , can be seen the electron mass conforming orthogonal freedoms:

$$\int \psi_i^*(r) \psi_j(r) dr = \delta_{ij} \quad 2.20$$

Agreeing to Capelle (2006) that the presence of an exceptional potential of $V_{KS}(r)$ with the $n(r)$ value as its ground state charge density which is significance to the Hohenberg and Kohn theorem which holds regardless of the arrangement of the electron-electron interaction U .

2.6.4 Basis sets

A basis set can be regarded as a numerical model that defines the orbitals within a given system, which gives approximations of the over-all electronic wave function, that is applied to carry out hypothetical calculations (Stein et al., 2019). Accordingly, quantum chemistry, describes a basis set as a conventional set of particle functions that are applied in build molecular orbitals (Varandas, 2021). Molecular orbitals can be regarded as singular electron function which can be categorized into two classes; Slater type orbitals (STO) and Gaussian type orbitals (GTO). Slater type orbitals are arithmetically characterized by the expression;

$$\phi_{abc}^{STO}(x, y, z) = N x^a y^b z^c e^{-\zeta r} \quad 2.21$$

In this case;

N is standardization constant

a, b, c regulates the angular momentum, $L = a + b + c$

ζ (zeta) regulates the breadth of the orbital whereby a bulky ζ value provides close-fitting functions and insignificant ζ value provides diffuse functions (Varandas, 2021). This scenario is applicable on H- atom-like, minimal for 1s orbital. Nonetheless these orbitals do not have radial nodes and are therefore none-pure

spherical harmonics. Gaussian Type Orbitals (GTO) is characterized by the subsequent equations;

$$\phi_{abc}^{STO}(x, y, z) = N x^a y^b z^c e^{-\zeta r^2} \quad 2.22$$

Similar to the STO, a, b, c regulates the angular momentum, $L = a + b + c$ where ζ regulates the width of orbital and the H-atom-like are not replication even for 1s. GTOs have been found to be much easier to calculate and are collectively used by the quantum chemists in finding molecular interaction solutions. The arithmetic involving finding solutions to the electronic structure basis sets incorporates the use of the Gaussian functions to generate the orbitals (Petruzielo et al., 2011). Accordingly, Gaussian computational code make available an extensive range of pre-defined basis sets which are categorized by the number and the types of basis functions which they encompass (Foresman & Frisch, 1996).

2.6.5 Polarized basis sets

This type of basis set eliminates the restriction of orbitals altering size devoid of varying shape. Polarized basis sets supplement orbitals which have angular momentum further than what is essential for the ground state in the description of every single atom in the ground state and in so doing permitting the atom to change shape (Binkley et al., 1980; Gianturco & Huo, 2013).

Polarized basis sets are represented as shown,

6-31G(*d*) or 6-31G* order.

where for (*d*) or * type; * -type are functions added to atoms with $Z > 2$ (heavy atoms). We also have; 6-31G(*d, p*) or 6-31G** where for (*d, p*) or ** type;

p -type functions are added to H atoms. d -type are functions added to atoms with $Z > 2$

In the formation of molecules, the atomic orbitals become distorted in their shape (polarization) (Gianturco & Huo, 2013).

2.6.6 Diffuse basis set

Diffuse basis sets are used to define anions, molecules which have lone pairs of electrons, excited states and transition states or electrons that are loosely held (Schaefer, 2012). Diffuse functions are large size s- and p- type functions which permit orbitals to reside in large space (Peterson et al., 1988; Schaefer, 2012). They are represented as shown.

$6-31+G(d)$ or $6-31++G(d)$

$6-31+G(d)$ is a basis set with an additional larger p-function for atoms with $Z > 2$.

$6-31++G(d)$ is a basis set with additional larger s-function for H-atoms.

2.6.7 Understanding predictions for properties of molecules using computational modelling

Computational modeling involves solving the electronic properties and structures of a given chemical compound and the obtained results describe the molecular energies and energy band (Vicent-Luna et al., 2021). The obtained data enables scientists to calculate the properties of the molecule which are based on the quantum mechanics such as thermodynamic energies, highest and lowest occupied molecular orbital energies, and band gaps, in addition to other numerous properties (Tkatchenko, 2020). Most of the properties of the molecule are well-defined by the orbital types

(Evers et al., 2020). The obtained information and acquired knowledge is crucial in developing valuable predictions in designing chemical compounds and molecules for a specific purpose (von Lilienfeld et al., 2020).

Additionally, a scientist is majorly focused on knowing how these molecules and chemical compounds behave in a set of system or environment within a set of conditions of temperature and pressure for varied periods of time for the selected set of probable degrees of freedom (Huang & von Lilienfeld, 2021). This is important to chemists given that by understanding the way these atomic or molecular energies and forces vary with time, it is possible to make predictions on thermal and pressure dependences and the spectroscopic properties (Keith et al., 2021).

2.7 Elemental characterization of thermal char

Elemental analysis involves the measurement of a variety of elements within a sample matrix (Goldstein et al., 2017). A variety of techniques have been used to analyse different element speciation in tobacco smoke and ash including mass spectrometry, X-ray fluorescence spectrometry (Theobaldo et al., 2018), atomic absorption (Omari et al., 2015), inductively coupled plasma techniques (Huang et al., 2018) and instrumental neutron activation analysis (Zinicovscaia et al., 2018). Elemental analysis can be quantitative which involves the determination of the atom % or weight % of each element present while qualitative analysis involves determining which elements are present in a given sample (Goldstein et al., 2017).

2.8 Thermogravimetric analysis and differential scanning calorimetry

Thermogravimetric analysis (TGA) is a common analytical technique that is employed in the determination of the thermal stability of a material and effectively report on the fraction of volatile chemical components through analysis the sample

weight change that the material undergoes as a result of decomposition, oxidation, volatile loss such as moisture when it is being heated at a set temperature range at a constant rate (Polini & Yang, 2017). This method reveals information regarding the thermal and oxidative stability, decomposition profile, moisture and volatile content and life expectancy of a given biomass material under pyrolysis (Sarfraz et al., 2020). Differential scanning calorimetry (DSC) as a thermo-analytical technique measures the amount of heat required to raise the temperature of a given sample (De Las Heras et al., 2021). It aims at measuring the change in heat flows for a given sample initiated by alterations in the sample temperature and therefore the enthalpy change pattern of the biomass material under analysis (Reza et al., 2020).

CHAPTER THREE

MATERIALS AND METHODS

3.1 Sample Collection and Preparation

The research license NACOSTI/21/11/11440 was issued by National Commission of Science, Technology and Innovation before the sample collection exercise commenced. Khat twigs that were ready for chewing were obtained from Muthuri farm of Meru county, Buuri subcounty, Naari location, Gimene sublocation, Michaka village and transferred to the laboratory. The fresh khat twigs were then dried in an oven at temperatures of 45 °C for 72 hours and used without any further treatment. Unprocessed tobacco dry leaves that were ready for human consumption were purchased from local vendors operating in Njoro town and transferred to the laboratory. Rolled Marijuana cigarette sticks were purchased from vendors operating in Njoro town and transferred to the laboratory. The raw marijuana substances were unpacked from the rolled cigarette sticks and used without any further treatment. The dry khat twigs, tobacco and marijuana substances were then reduced into 1 mm size particles using a grinding machine before pyrolysis.

3.2 Pyrolysis of Biomass Components

The co-pyrolysis system for the thermal degradation of organoleptic biomass materials under investigation was designed to aid in investigating the thermal characteristics of a wide range of organic compounds that were under varying physical conditions as described by (Kibet et al., 2017). The system allows the testing of pure organic compounds and mixtures comprising of gaseous, liquids, solids and polymeric composites and multiphase components. The system composed

of units that are critical for analyses of organic material: the reactor compartment and the temperature control console (Kibet et al., 2015).

3.3 The Reactor Design and Assembly

The pyrolysis reactor used for this study was designed in our lab and assembled as shown in Figure 3.1. It encompassed a set of components that included; the reactor compartment which housed the electrical heater and the reactor; temperature regulation unit which controlled the pyrolysis temperature to temperature gradient of 5 °C/min. A quartz tubular reactor that had a capacity of 49.96 mL was employed in the fractional pyrolysis of the dried biomass materials (khat, tobacco and marijuana), their racemic and their mixtures.

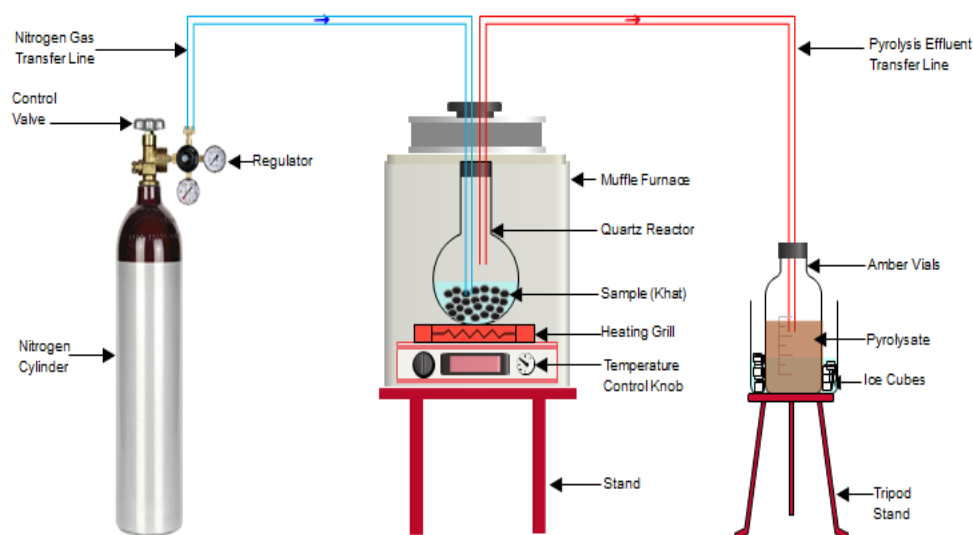


Figure 3.1: Reactor assembly (Kibet et al., 2018)

A 2 seconds residence time was selected for all temperature runs. The pyrolysis gas was set to flow through the reactor for a residence time of 2 seconds at flow rates that were calculated using equation 3.1 (Rubey & Carnes, 1985).

$$F_0 = \left(\frac{\pi r^2 L}{\tau_0} \right) \left(\frac{T_1}{T_0} \right) \times \left[1 + \frac{P_d}{P_0} \right]. \quad 3.1$$

where t_0 denotes the resident time and F_0 the pyrolysis gas flow rate, which was controlled by a digital mass flow meter that was able to deliver volume of up to 6000 mL/min of the gas into the reactor system. T_0 represents the temperature of the reactor before pyrolysis commenced, T_1 the temperature of the reactor at the end of the pyrolysis, L refers to the length of the reactor and r represents the inner radius of the reactor. P_d denotes the difference in pressure between the pressures inside the reactor while P_0 represents the inside reactor pressure before the pyrolysis commenced. Consequently, the selected rates of gas flow for the temperatures of 250, 500 and 700 °C were 2630.33 mL/min, 3887.66 mL/min and 4893.52 mL/min, respectively.

3.4 Sample Introduction to the Reactor for Fractional Pyrolysis and Co-Pyrolysis

The pyrolysis experiments involved pyrolysis of pure biomass materials which included khat, tobacco and marijuana samples. Copyrolysis of biomass materials, which included khat-tobacco, khat-marijuana and tobacco-marijuana biomasses, was carried out and their pyrolysate collected in top crimp vials filled with methanol solvent. Finally, a ternary mixture of the three biomass materials, khat-tobacco-marijuana, were mixed in equimassic ratios and pyrolysed and their pyrolysate collected in top crimp vials filled with methanol solvent. For each pyrolysis and copyrolysis experiment, about 30 ± 0.2 mg of the biomass samples were accurately weighed and placed inside the quartz tube and held in place by quartz reactor. For copyrolysis experiments, a 1:1 ratio of either khat-tobacco, khat-marijuana or marijuana-tobacco samples were mixed before introduction into the reactor. The copyrolysis of ternary mixture was conducted on a 1:1:1 ratio of tobacco- marijuana-khat mixture. The temperature control unit was then set to 200 °C and adjusted in

increment intervals of 50 °C up to maximum temperatures of 700 °C on the fractional pyrolysis mode. The effluent flowing from the reactor was then transmitted through a deactivated silica coated transfer line that was kept at a constant temperature of 270 °C to prevent condensation along the transfer line into 2 mL methanol in crimp top vials as a pyrolysate. The pyrolysate was analyzed using a Gas chromatograph hyphenated to a mass selective detector (MSD). The amounts of char that were yielded at every temperature was calculated by employing the method of difference that is described by Soi et al. (2015). The char samples obtained from pyrolysis of the biomass materials at the selected temperatures were then packed in crimp top vials and transferred for elemental analysis experiments.

3.5 GC-MS Characterization of Molecular Products

The GC-MS machine that was used for analysis of the pyrolysate was an Agilent instrument, model number 6890N which was equipped with a 5973N mass selective detector (MSD) that had an ion source electron impact (EI) of 70 eV. A column whose specifications were DB5-MS, (30 m × 0.25 mm × 0.25 µm) dimensions was used to isolate pyrolysate effluent. A GC injection was used to inject 1µL of the obtained liquid sample into the GC column which had its injection port set at temperature of 250 °C using nitrogen as the carrier gas. The temperature programming was at a rate of 25 °C/ min at 50 °C for 10 minutes and holding for 2 minutes at 250 °C followed by a heating rate of 10 °C/ min and holding for 10 minutes at 300 °C. The identified molecular compounds were run through NIST identification software and confirmed using ChemStation Agilent software in order to guarantee accurate reporting of the reaction products. To ensure the correct compounds were positively identified the retention times of pure compounds (standards) were determined and matched with those of the analytes. All the standard

reagents used were of analytical grade and were purchased from Sigma-Aldrich, South Africa and were used without subjecting them to any further chemical adjustments. To quantitatively determine the percentage yields of the molecular compounds in each pyrolysis and co-pyrolysis experiments, equation 3.2 described by (Jebet et al., 2017) was applied.

$$\text{percentage yield} = \frac{M_c}{M_o} \times 100 \quad 3.2$$

Where M_c is the mass of the produced compound and M_o is the original mass of all the compounds produced from the biomass under pyrolysis and co-pyrolysis.

3.6 Computational Methodology

All the performed theoretical calculations for the selected molecular compounds from the pyrolysis of biomass materials were executed by using Gaussian '09 computational program packages as described by (Kibet et al., 2018). The energies, thermodynamic properties, geometry optimizations and frequencies were computed using DFT quantum level of theory using 6-311G++ basis set under the Becke's three parameter Lee-Yang-Parr (B3LYP) hybrid function as illustrated by (El Foujji et al., 2020). The obtained optimized geometries and the molecular orbitals (MOs) of the molecular components were used in frequency calculations in order to determine their global energies and subsequently establish their global minima (Kibet, 2016).

3.7 Elemental Characterization of Thermal Char Using Elemental Analyzer

The char samples were collected from the thermal furnace after pyrolysis and vacuum dried for one hour. A homogeneous composition and structure of the char sample matrix was obtained by grinding the char to dust-sized particles. Ten (10) mg of the sample were then weighed into crimp top containers of 8 x 5 mm using the analytical micro-balance, rolled into little round ball shapes using forceps in order to

ensure flash combustion before delivery into the elemental analyzer instrument. The chemical elemental analysis (C, H, N, O, and S) of the samples was conducted in an eager 300 for EA112 elemental analyzer.

3.8 Thermogravimetric analysis and differential scanning calorimetry of khat-tobacco biomass

The samples were dried at 30 °C for 96 hours in an electrical oven until a constant mass was attained. The samples were then ground into smaller particle size ranging between 0.1 to 1.0 mm. The thermogravimetric measurements including sample thermal decomposition were carried out using simultaneous DSC-TGA (SDT) technique, which had the ability to measure both the heat flow and weight changes in tobacco-khat biomass as a function of temperature. A SDT Q600 instrument with a maximum temperature of 1500 °C was employed in this study. Twenty two (22) mg of tobacco-khat binary mixture samples were loaded into alumina sample cups, and subsequently subjected to a temperature increase from 150 °C to 700 °C at a rate of 5 °C/min to avoid secondary cracking reactions occurring above 700 °C. In order to ensure an inert atmosphere, ultrahigh purity argon (99.99%) was supplied to the TGA furnace at a flow rate of 40 mL/min. The pyrolysis experiments were replicated two times to ensure repeatability of the results.

3.9 Data Analysis

The data from GC-MS was obtained in chromatograms which were interpreted and presented. The computed enthalpies were analyzed using Igor computer software and the graphs of the various parameters such as enthalpy and temperature were then plotted. Statistical treatment of data was done using SPSS and data reported in tables. In order to inspect if the obtained sample means had statistical differences amongst

the obtained values, one sample t- test packaged under the SPSS suite of programs was performed.

CHAPTER FOUR

RESULTS AND DISCUSSION

4.1 Phenolic reaction products released from the thermal degradation of *Catha edulis*

During the pyrolysis of khat dried biomass materials under conditions that simulate the actual cigarette smoking, a number of pyrolysis products are generated throughout the whole pyrolysis temperatures. The principle products of this biomass pyrolysis under nitrogen environment include phenolic compounds such as p-cresol, catechol, hydroquinone and other substituted methoxy phenols including 3-phenoxy phenol and 3,4-dimethoxy phenol. It is important to note that at all the selected temperature range; the identified molecular substances were detected. Figure 4.1 shows the GC-MS spectrum for the compounds identified at temperatures of 200 °C and 700 °C.

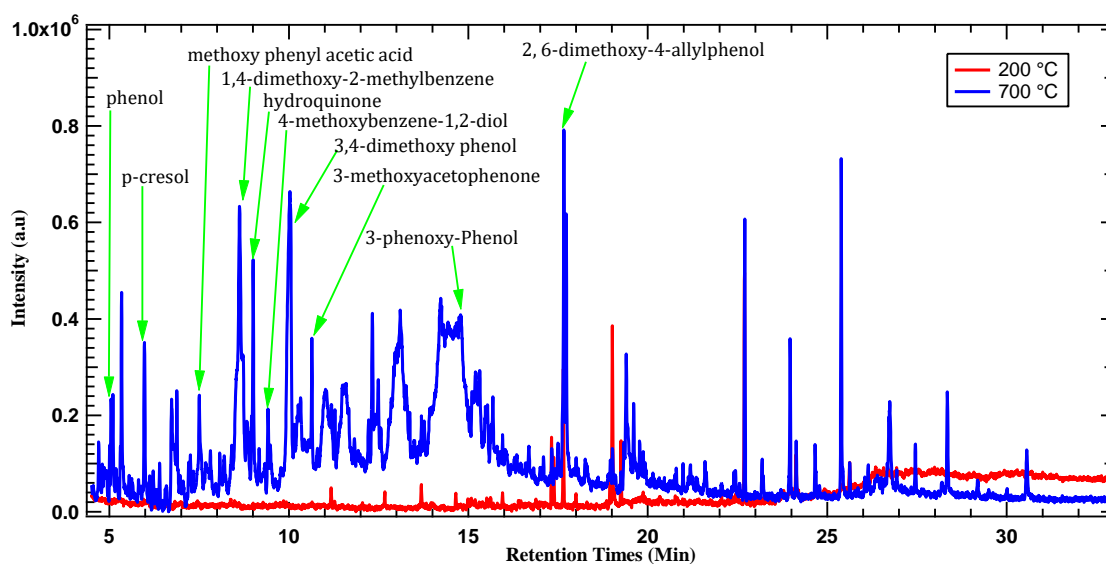


Figure 4.1: Overlay GC-MS chromatogram for phenolic compounds released from khat pyrolysis

Table 4.1: Intensities of products generated from khat pyrolysis at selected temperatures

Compound	Retention time	Intensities (GC Area counts)										
		200 °C	250°C	300°C	350°C	400°C	450°C	500°C	550°C	600°C	650°C	700°C
2,4,5-Trimethyloxazole	4.885	95432	176329	285981	312576	334673	985897	1294059	95687	76453	63215	48963
1-Methyl-1H-pyrazole-4-carbaldehyde	5.080	12541	17932	21766	28596	51177	982311	1505878	317211	154477	119153	17177
4-methoxypyridine-N-oxide	6.320	14746	17792	20352	276344	371220	543167	716079	153935	44856	40143	9052
N-Phenoxyacetamide	6.615	12004	19651	541013	135786	268032	469083	861692	237993	140023	73724	4186
1-methyl-2,5-Pyrrolidinedione	7.005	7810	22966	27810	28833	49382	317502	1778912	1011893	282062	38917	17170
1-(tetrahydro-2H-pyran-2-yl)-1H-Pyrazole-5-carboxaldehyde	7.080	11844	15520	25342	83980	137531	415467	962847	265631	44124	4152	3980
4,5-Diamino-6-hydroxypyrimidine	7.315	14335	15647	98148	113543	128502	563198	778792	465213	241191	98356	54321
3-(Pyridin-4-ylcarbamoyl)-acrylic acid	7.990	14848	19719	22437	37731	53467	78206	1105240	573806	181358	85870	46577
Indole	9.985	15659	30957	64431	117634	280659	347851	654983	947187	618633	479493	186233
2,5-Dimethylfuran	5.145	21410	25153	29248	29552	206543	1004327	1525038	1204450	452959	257293	58521
Mequinol	6.905	17316	20867	21531	21819	29371	1238321	3035141	1932316	539483	350904	101777
4-Methoxybenzene-1,2-diol	7.835	10976	15539	15616	18828	27864	494184	543598	519923	89361	14481	8193
3,4-dimethoxy-Phenol	10.69	15310	30592	42772	69530	242871	2121798	3111166	5098091	824968	250536	20147
2,6-Dimethoxy-4-allylphenol	15.01	14905	17477	31763	40722	476406	1320729	2257423	2603056	860708	125755	30109
3-phenoxy-Phenol	15.14	14567	20260	41551	46974	457452	1433084	3948431	9009342	1116108	148861	32732

The release of these pyrolysis products that were phenolic in nature exhibited a difference in concentrations at the various selected temperatures whereby highest concentrations were being achieved at the temperatures ranging between 400 °C – 600 °C as demonstrated in Figure 4.2 (a) and (b). Particularly, at extreme temperatures of approximately 700 °C, there were more phenolic compounds that were generated compared to low temperatures regions that started at around 200°C. Table 4.1 gives a summary of the molecular compounds that were detected from the pyrolysis of khat and their concentrations at various temperatures.

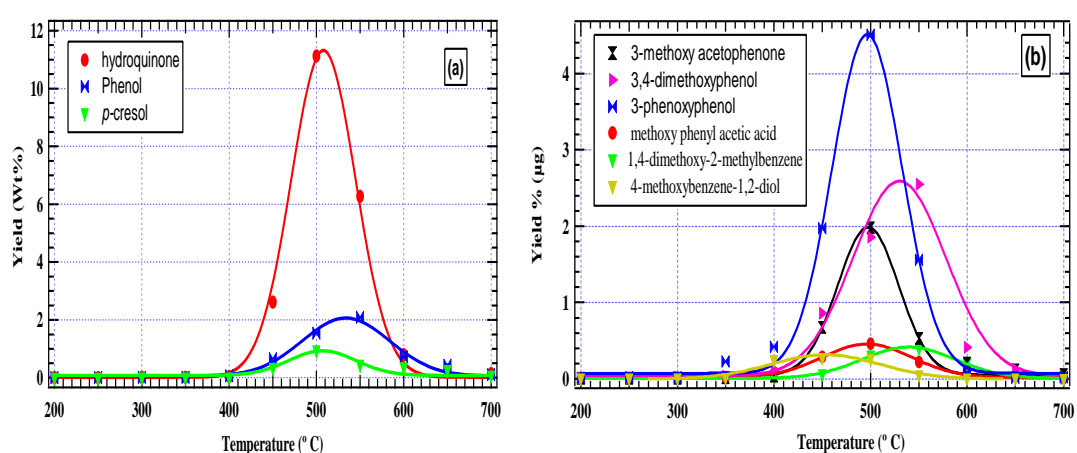


Figure 4.2: Phenolic (a) and (b) methoxy phenol compounds distribution from khat biomass pyrolysis

It is evident that most of the identified phenolic compounds achieved their high concentration release at temperature of around 450 °C and 600 °C as indicated in Figure 4.2 a, whereby compounds such as p-cresol, phenol and its analogous substituted molecular products such as 3-phenoxy phenol, 2, 6-dimethoxy-4-allylphenol and 3,4-dimethoxy phenol recorded the highest yields and consequently can be classified as high khat pyrolysis generated phenolic compounds. Similarly, hydroquinone had its highest produced concentration attained at temperatures of about 500 °C with approximated yields of 11.12 wt % and a overall yield of 21.32

wt % in the entire pyrolysis temperature range. This marked representation of nearly 40 % of the total phenol content reported in this study. The aggregate yield of phenol and *p*-cresol in the whole pyrolysis temperature range were 5.67 and 2.54 wt %, respectively. This proposes that during pyrolysis, the chief phenolic component in khat is hydroquinone, and is conceivably the supreme intoxicating chemical generated from khat smoking. The phenolic compounds that were identified in low yields at these peak temperatures included 4-methoxybenzene-1,2-diol, which was released at low concentrations throughout the entire pyrolysis temperature range as shown in Figure 4.2 b. At a temperature of 500, the yield of 4-methoxybenzene-1,2-diol was at 0.37 wt %.

On the other hand, methoxy phenol chemical compounds were reported in fairly high produces from temperatures of around 400 °C and achieved a maximum evolution at 500 °C before decreasing sharply at temperatures of 650 °C. For instance, compounds such as methoxy phenyl acetic acid and 1, 4-dimethoxy-2-methylbenzene at around 500 °C presented low yields of about 0.40 wt % while 3-phenoxy phenol depicted the highest yields of 4.82 wt % at the same temperature as illustrated in Figure 4.2b. 3,4-dimethoxyphenol achieved a yield of 6.0 wt % in the whole pyrolysis temperature range whereas 3-phenoxyphenol yield was about 3.6% in the entire temperature range. It is imperative to note from the khat pyrolysis experiments, that all stated phenolic compounds had their concentration profiles increasing with rise in temperature up to about temperatures between 400-600 °C before decreasing between 650 °C and 700 °C where it can be assumed that the oxygenated components are entirely decomposed.

In addition, a vast of nitrogen containing compounds, were generated in great intensities between the temperature range of 450 °C – 550 °C, which can be classified as either high pyrolysis or low pyrolysis generated products. Accordingly, it can be depicted from the graphical plots in Figure 4.3 that, high pyrolysis generated nitrogen containing compounds obtained from khat pyrolysis include 2, 4, 5-trimethyloxazole, 1-methyl-2,5-Pyrrolidinedione, 2- amino-1-naphthalenol and 3-(Pyridin-4-ylcarbamoyl)-acrylic acid whose maximum intensities were 2.1×10^6 , 1.8×10^6 , 1.7×10^6 and 1.66×10^6 area counts at temperatures of 480 °C, 510 °C, 500 °C and 485 °C respectively.

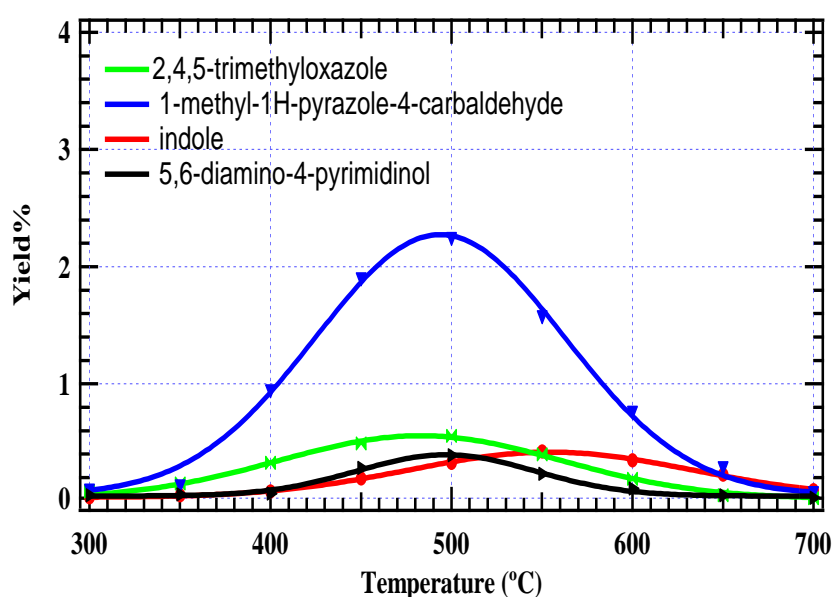


Figure 4.3: Nitrogen containing compound released from khat pyrolysis

On the other hand, low pyrolysis generated nitrogen containing compounds include 1-(tetrahydro-2H-pyran-2-yl)-1H-Pyrazole-5-carboxaldehyde, N-phenoxyacetamide, indole and 4-methoxypyridine-N-oxide whose maximum intensity peaks of showed at 500 °C, 480 °C, 500 °C, 550 °C and 450 °C respectively with area counts of 0.9×10^6 , 0.8×10^6 , 0.75×10^6 , 0.7×10^6 and 0.6×10^6 , which represents 8.17, 7.27, 6.81 and

5.45 wt % respectively. It is important to note that all the released nitrogen containing products exhibited ring aromatism which are known to disintegrate at high temperatures to yield hydrogen cyanide that is known to be a highly biosystem contaminant capable of initiating cell malignancy and carcinogenic (Drzeżdżon et al., 2018). Nonetheless, other chemical compounds such as furans and furfurals, and ketones were detected present in khat pyrolisate extracts in varying concentrations as shown in Figures 4.4 a and b respectively.

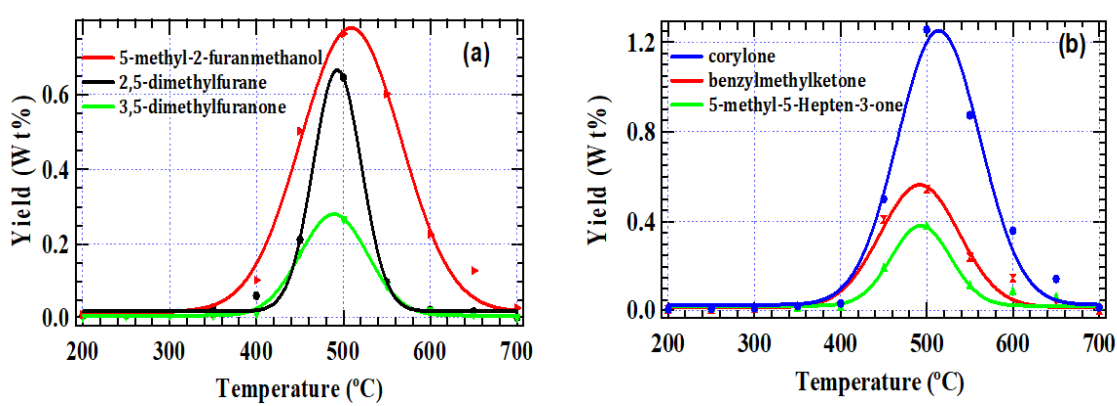


Figure 4.4: Furans and furfurals (a) ketones (b) from khat biomass pyrolysis

4.1.1 Decomposition profile of khat

Clearly from the khat pyrolysis experiments, it can be noted that all the reported compounds had their concentrations profiles increasing with a rise in temperature to a peak temperature before decreasing to minimum release concentrations at high temperatures where the biomass material is presumably totally decomposed. This can be demonstrated in percentage mass loss profiles at the selected pyrolysis temperature range in Figure 4.5.

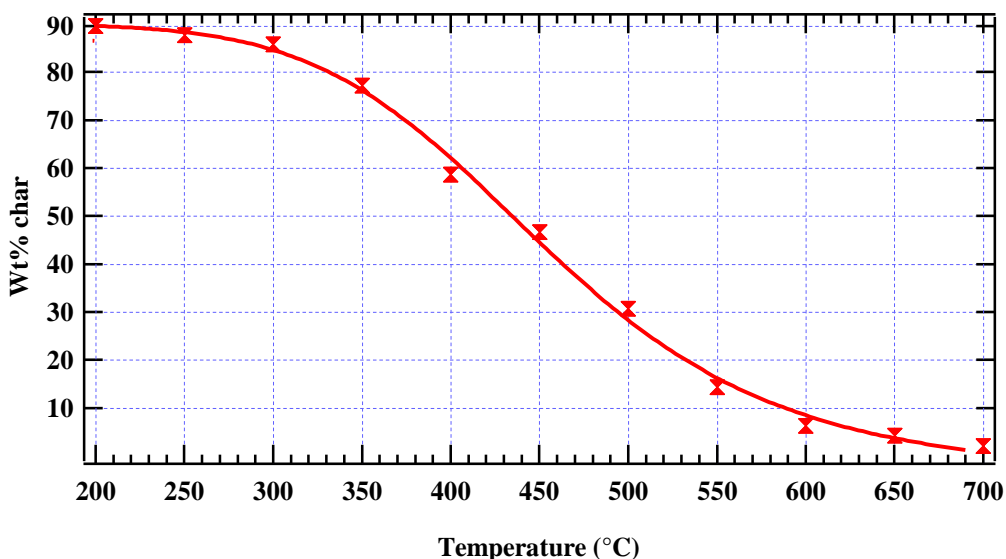


Figure 4.5: Khat percentage weight loss at various pyrolysis temperatures

It can be noted that the mass loss between temperatures of 200–350 ° C was nearly 12% while at temperatures ranging between 350-550 ° C the registered mass loss was about 65%. This matches with the zone where there is a high evolution of the pyrolysis products and is consistent with literature studies. The subsequent regime begins to occur from temperatures of about 550-700 ° C in the course of which a mass loss of about 11% is witnessed. At temperatures of nearly 650 ° C, the biomass material under pyrolysis is mainly carbon. Clearly from the obtained results, khat pyrolysis is supplemented by a loss in weight with temperature intensifications. The utmost loss in weight was attained at temperatures of around 500 °C. The core reason for such pyrolysis behaviour is largely due to the discharge of most pyrolysis products at this elevated temperature.

4.1.2 Elemental analysis of khat, tobacco and marijuana and their binary mixtures char

The elemental investigation on the char samples that were acquired from the pyrolysis of khat pointed out a disparity in the percentage composition of O, C, N, H

and S as presented in Table 4.2. Clearly, the carbon content in the char samples obtained from khat pyrolysis at a temperature 400 °C was found to be 37.08% while that of oxygen was considerably high (43.73%) which can be attributed to the existence of oxygenated organic constituents that includes esters, phenols, alkanolic acids and additional oxygenated chemical compounds that include aldehydes and ketones in khat. Hydrogen, nitrogen and sulphur were also reported in slightly lower concentrations as displayed in Table 4.2. These chemical components which have been reported in this study, particularly nitrogen and sulphur are chemical constituents that are well recognized as venomous chemical components that occur in some nitrogen containing organic compounds such as cathinone, pyridine, pyrrole and thiols, which stand as disreputable environmental pollutants and are potent in initiating grave health injury.

Table 4.2: Elemental composition of khat char

Element	Composition (%) in khat
C	37.08
N	1.47
H	5.519
O	43.732
S	0.144
Total	87.94%

A comparison of elemental composition in the char for tobacco, marijuana and khat with their binary mixture was as illustrated in Figure 4.6.

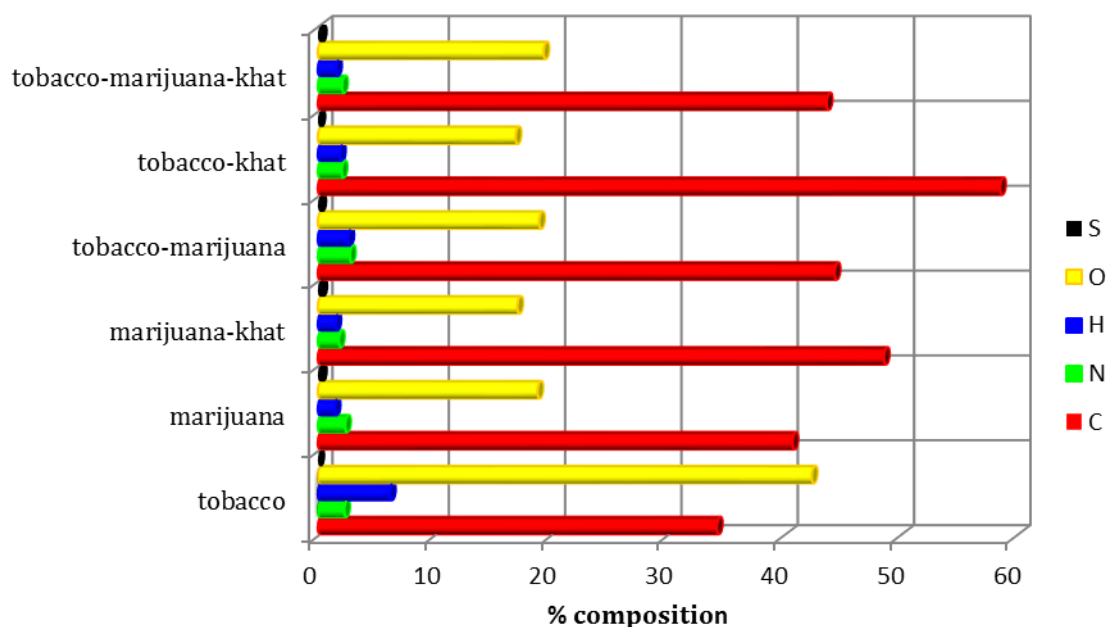


Figure 4.6: Elemental distribution in biomass materials and their binary mixtures

As it can be observed, char from tobacco, marijuana and their binary mixtures reported similar elements at different percentage composition. It is clear that carbon was the most abundant element detected in tobacco and marijuana, and marijuana-khat, tobacco-marijuana, tobacco-khat and tobacco-marijuana-khat mixtures at 34.3%, 40.81%, 48.66%, 44.43%, 58.65% and 43.74%, respectively. Tobacco-khat mixture reported the highest carbon content at 58.65%, which is relatively higher than that in khat. Of the pure biomass materials that were pyrolysed, marijuana displayed the highest percentages of C at 40.81% compared to tobacco and khat where C was reported at 34.30% and 37.08% respectively. This implies that a marijuana-khat combination during pyrolysis yields more carbonaceous products, and probably highly toxic.

The second most abundant element detected in char samples was O whose detection levels were 42.46%, 18.88%, 17.15%, 19.02% 17.00%, and 19.40% by weight in tobacco, marijuana, marijuana-khat, tobacco-marijuana, tobacco-khat, and tobacco-

marijuana-khat char mixtures respectively. The release of O can be associated with functional groups in biomass such as hydroxyls, phenols, ethers, carbonyls and carboxyls. Notably, the O levels in tobacco decreased by nearly 2 times when tobacco pyrolysis was conducted in marijuana and khat regime, an indication of less of these functional groups as a result of loss of H₂O during pyrolysis.

The elemental ratios of O:C in the char samples measures the density of the polar functional groups present in the biomass materials and for fresh chars, an index for the carbonizing degree, thus enabling one to understand the extent of post pyrolysis oxidation that transpires during environmental char aging and hence estimate their stability in soils (Bakshi et al., 2020; Crombie et al., 2013). Accordingly, a majority of char from organic samples exhibit O:C ratios ranging from 0.2-0.6, where by organic biomass char with O:C ratios approaching 0.6 are considered to be highly unstable (Spokas, 2010). In this regard, our results indicated the O:C ratios of 1.24, 0.46, 0.35, 0.29 and 0.44 for tobacco, marijuana, marijuana-khat, tobacco-khat and tobacco-marijuana-khat samples, respectively, depicting tobacco char as the most unstable and tobacco-khat char as the most stable. Other elements such as H, N and S were found to be present in the char samples in fairly low concentrations ranging between 1.5% to 6.2% for H, 1.80% - 2.80% for N, and 0.10% - 0.45% for S. Table 4.3 and Table 4.4 gives a comparison of the sample means.

Table 4.3: Paired samples statistics for elemental compounds in char

		Mean	N	Std. Deviation	Std. Error Mean
Pair 1	Tobacco	17.0738	5	19.78183	8.84670
	Tobacco-khat	15.9680	5	24.80830	11.09461

The mean elemental composition in tobacco char was 17.07 whereas the mean elemental composition in tobacco mixed with khat char was 15.96 respectively.

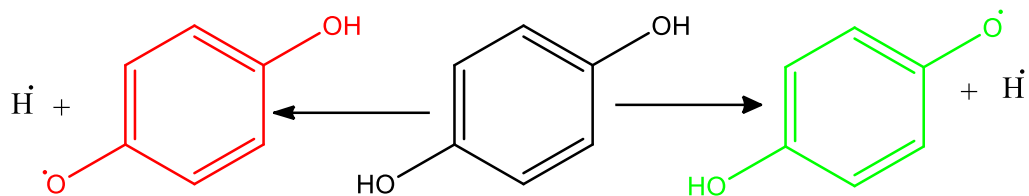
Table 4.4: Paired samples t-test for char

		Mean	Std. Deviation	Std. Error Mean	95% Confidence Interval of the Difference		t	Sig.	
					Lower	Upper			
					Difference				
Pair 1	tobacco – tobacco-khat	1.10580	17.70239	7.91675	-20.87462	23.08622	0.140	4	0.896

The mean difference in the concentrations of the elements present in thermal char generated from tobacco pyrolysis and tobacco mixed with khat pyrolysis was found to be 1.10 with a t value of 0.140. According to the obtained p value (0.896), the mean difference is not statistically significant which therefore implies that mixing tobacco with khat does not reduce the elemental compounds in char to significant levels.

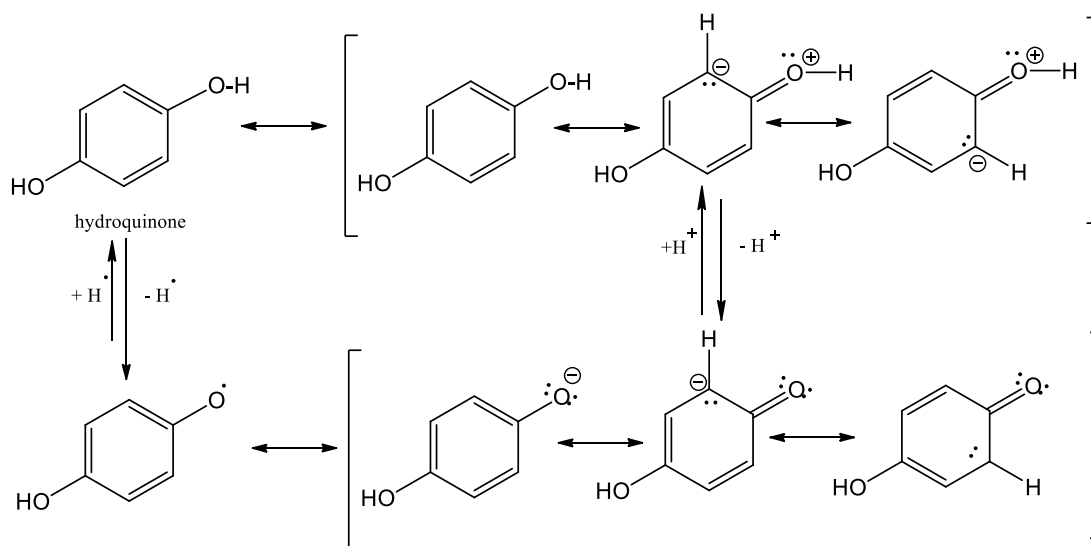
4.1.3 Health implications of phenolic compounds in khat

These resultant phenols produced from the pyrolysis of khat, particularly substituted phenols are well established to be exceedingly poisonous given that they have electron contributing substituents, primarily the methyl groups. Furthermore, the conjugation between the oxygen atom electron pair with the aromatic system leads to augmented polarity due to the transfer of negative charge from the oxygen atom to the aromatic ring and consequently charge delocalization therefore making these phenolic compounds to be very much reactive with biological systems once they gain entry into the consumer's' body systems (Panja et al., 2016). During the thermal degradation reactions, hydroquinone breaks down into environmentally active radicals as illustrated in scheme 4.1.



Scheme 4.1: hydroquinone thermal degradation to radicals

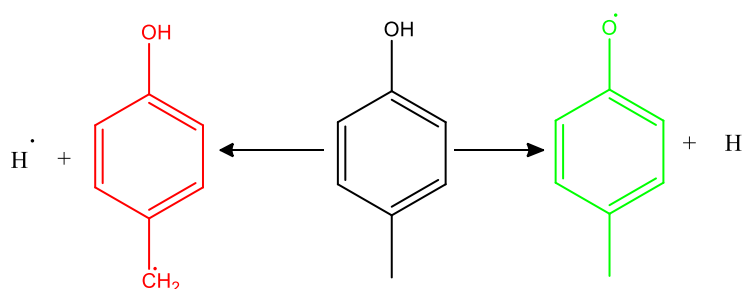
On the other hand, when khat is chewed, hydroquinone develops polarization in saliva and as a result acquires the acidic properties by establishing hydroxyphenolate ion whose negative charge distribution around the molecule can be illustrated by the resonance hybrids represented in scheme 4.2. This demonstrated features for hydroquinone contributes more towards its specific physical and chemical properties with much reinforcement made by the presence of substituent groups that are attached to the aromatic ring contingent on its ability to withdraw or donate electrons and applies to most phenolic compounds (Sobiesiak, 2017).



Scheme 4.2: Probable resonance stabilized structures for hydroquinone in saliva

It can be witnessed from scheme 4.2 that the achievement of resonance equilibrium for the phenolic chemical compounds is conceivably due to the separation in the charges which eventually result to the compound stabilization. For that reason, given

that the resonance stabilization of hydroxyphenolate ion is much greater than the stabilization of hydroquinone, it is more likely that it is extremely polar than its mother molecule, hydroquinone. Similarly, comparable reaction configurations are more likely to be noted in various phenolic chemical compounds. The low polar properties of hydroquinone is probably because of its high capacity to form hydrogen bonds that enhances strengthened structural symmetry of the hydroquinone molecules. Therefore, it is more likely for the hydroquinone molecule to result to the formation of a strong structure which is extremely hydrophobic and consequently viewed to be the insoluble in the human biological systems. For that reason, it can arguably be stated that hydroquinone can be less toxic once it gains entry into human body system. On the contrary, its transformation to hydroxyphenolate ion makes it more lethal.



Scheme 4.3: *P*-cresol thermal degradation to radicals

On the other hand, the detection of *p*-cresol in khat smoke should be worrying given that *p*-cresol has been scientifically informed to be exceedingly toxic by a number of scientific studies specifically when their chief entry route into the human body system is through the oral, subcutaneous, and intravenous or intraperitoneal where it is more probable to effect tissue corrosion alongside the associated body parts and probably result to cardiovascular infections and diseases, and consequently *p*-cresol is acknowledged as a protein bound uremic contaminant (Guerrero et al., 2020;

Tisserand & Young, 2014). In the course of thermal degradation reactions, the *p*-cresol chemical compound gets converted into radicals some of which are known to be very reactive to human biological systems and therefore they are more probable in initiating further distressing reactions on the human body tissues. Scheme 4.3 exhibits how the radicals can form from *p*-cresol as a result of thermal degradation.

4.1.4 Molecular modelling of phenolic compounds and selected khat alkaloids generated from khat pyrolysis

The energies, molecular structures and vibrational frequencies of some of the selected khat alkaloids and phenolic compounds that are generated from the pyrolysis of khat were determined by using the Gaussian 09 computational package. These resulted to the generation of the optimized geometries of the chemical compounds as illustrated in Figure 4.6. The obtained energies, thermodynamic properties, geometry optimizations and frequencies were theoretically calculated using DFT and 6-311G++ basis set under the Becke's three parameter Lee-Yang-Parr (B3LYP) hybrid function as described by (Smith et al., 2016). In order to calculate the associated energy change in the formation of free radicals from phenols, Equation 4.1 was employed in this study (Mosonik et al., 2019).

$$\Delta_r H^\circ = \sum(\varepsilon_0 - H_{\text{corr}})_{\text{products}} - \sum(\varepsilon_0 - H_{\text{corr}})_{\text{Reactants}}$$

Equation 4.1

where, $\Delta_r H^\circ$ is change in enthalpy of the reaction, H_{corr} is correction to the thermal enthalpy and ε_0 is the sum of electronic and thermal enthalpies.

The associated energy changes as theoretically computed using Gaussian 09 computational package for selected phenols from khat pyrolysis and the corresponding formed radicals were plotted in Figure 4.7.

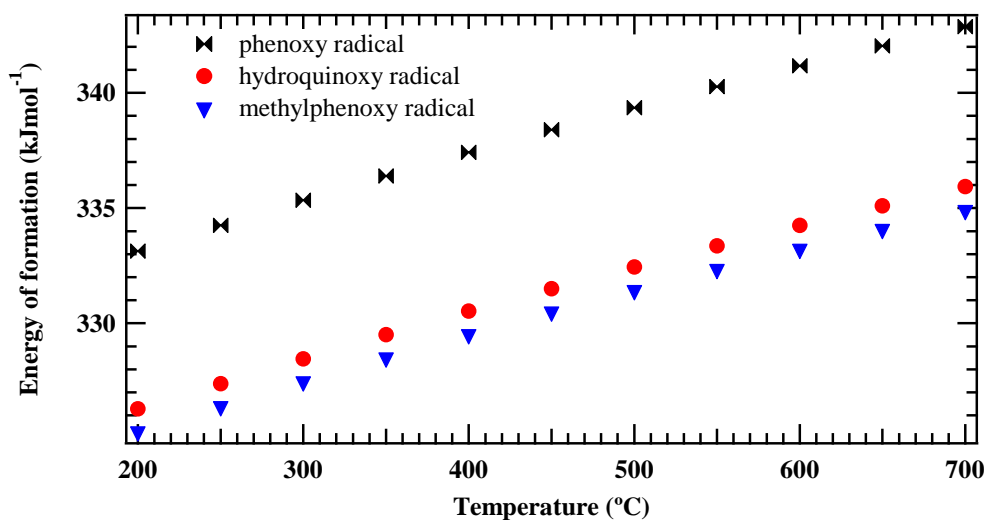
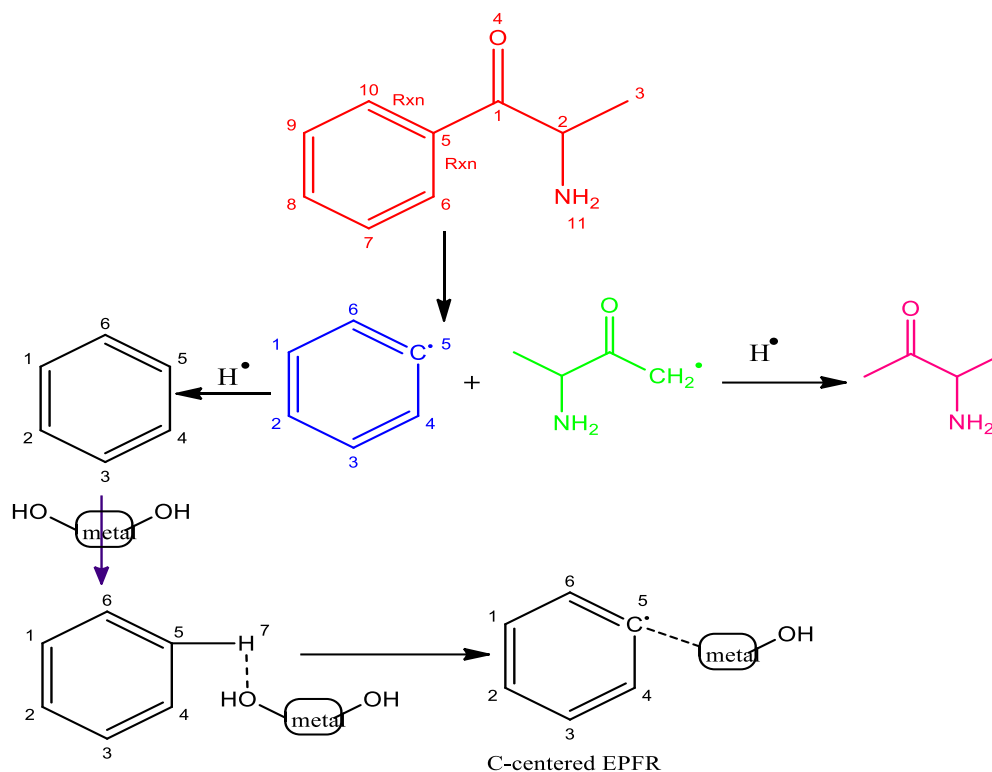


Figure 4.7: Energy change plots for the formation of radicals from phenolic compounds

It can be observed from Figure 4.7 above that all through the thermal degradation of phenols, the endothermicity of the reaction that involves the creation of radicals' increases with an increase in the temperature up to temperatures of 700 °C throughout the whole temperature range. Interestingly, phenol conversion to its radicals such as phenoxy was accompanied by the greatest energy changes, followed by hydroquinone and p-cresol respectively. In addition, khat pyrolysis breaks down the components of khat biomass into a series of other chemical compounds and radicals that are potentially toxic. A mechanistic pathway by which selected khat alkaloids thermally degrade to yield a set of radicals and eventually convert to other chemical compounds is as illustrated in scheme 4.4.



Scheme 4.4: Proposed mechanistic pathway for the formation of C-centered EPFR from cathinone

Accordingly, cathinone continuously breaks down to produce benzenyl and 3-aminobutan-2-one radicals that consequently react with hydride ions to form benzene and 3-aminobutan-2-one molecules respectively. Benzene molecule has been scientifically informed by a number of scientific studies as a great risk factor for exposure to human health and therefore an notorious initiator for human cell carcinogenesis (Harati et al., 2016). Extensive term contact to these benzene molecules induces damaging effects on the human bone marrow and a potential cause of decreased red blood cells and consequently leads to anemia in addition to becomes injurious to the human immune systems by starting blood antibody variation (CDCP, 2018). The benzene molecule is known to react with some of the

environmental trace metals such as copper thereby leading to the development of the C-centered environmentally persistent free radicals as illustrated in scheme 4.4.

Nevertheless, the formed subsequent 3-aminobutan-2-one chemical molecule can undergo more thermal degradation which lead to the formation of environmentally persistent free radicals which potentially have adversative effects on the human health when heated at temperatures of about 453 to 513K (Gao et al., 2018). Precisely, these, environmentally persistent free radicals can spawn from human undertakings especially when smoking or as a result of the failure of the biological activity of the catalase enzyme which normally initiates the biological eradication of the additional free radicals from the human body systems which leads to oxidative stress that has been associated to respiratory and cardiovascular infections, and at times intercellular mutilation (D'Arienzo et al., 2017; Pan et al., 2019).

Even though some informed scientific studies have identified and reported that some of the formed minute molecular free radicals to environmentally exist for smaller lifetimes (-10^{-9} s for OH^{\cdot} radical), it is imperative to note that these elements get unswervingly confined into the smoker's body system through the pulmonary track in the course of smoking as a result of incomplete incineration, and as such, because they are known to be highly reactive in nature, consequential oxidation reactions and pulmonary dysfunction have been reported to occurs (D'Arienzo et al., 2017). Consequently, Zhu et al. (2019) in their study have informed the half-life of oxygen centered and carbon centered environmentally persistent free radicals to be 160.45 and 401.10 days respectively, and therefore, the formed carbon centered environmentally persistent free radicals from the smoked khat alkaloids, once they gain entry into the smokers body/ biological systems, they are likely to stay in the

biological systems for periods long enough and consequently ignite biological processes that can lead to devastating bio-conditions. Similarly, the aromatism which is exhibited by these alkaloids present in khat can most likely lead to the development of benzene molecules whose reaction mechanism in the course of thermal degradation leads to the production of environmentally persistent free radicals thereby increasing their concentration levels in the smoked effluent and therefore, arguably depicting khat biomass pyrolysis and thermal degradation as a potential source of toxins into the environment.

4.1.5 Molecular geometries for phenolic and selected alkaloid compounds and their corresponding potential energy surfaces

The generated molecular structures for the selected chemical compounds can be well-defined by geometric parameters which include bond lengths and bond angles that solely help in determining the bond strengths of any given molecule. Figure 4.8 provides a brief summary of the geometric parameters for hydroquinone, p-cresol and phenol molecules and the comparisons made between the Gaussian input structure and the optimized structure. Even though much of the bonds in these phenolic compounds had the same lengths and angles as listed in Figure 4.8, it is important to note that phenol displayed the highest energy changes throughout the selected temperature range as illustrated in Figure 4.7, followed by hydroquinone and p-cresol respectively. This can be explained by the phenomenon of hydrogen bonding.

Since hydroquinone and phenol possesses relatively more hydrogen-oxygen bonds, these molecules require more energy to be absorbed in order to break the O-H bonds that leads to the formation of their corresponding radicals compared to p-cresol.

Therefore, p-cresol can freely go through chemical reactions that afterwards lead to the creation of radicals, a number of which form partial amounts of the smoked emissions from khat which gain admittance into the human biological system where they are expected to induce injurious biological conditions such as cardiac arrest and oxidative stress not forgetting that the exhibited aromatism by these organic compounds possibly undergo reactions that can lead to the formation of benzene molecules that further reacts to yield environmentally persistent free radicals.

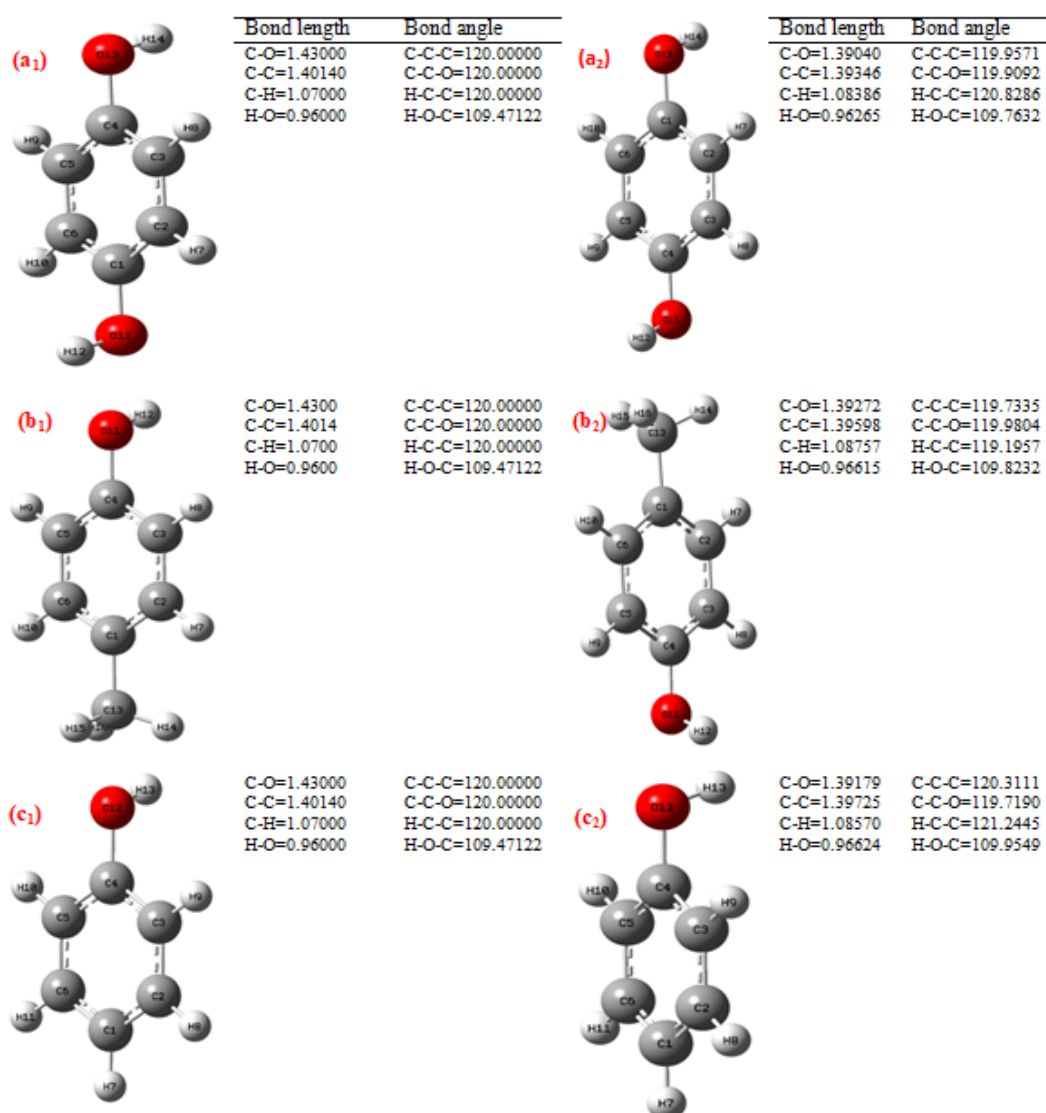


Figure 4.8: Input (1) and optimized (2) geometries and geometric parameters for hydroquinone (a) p-cresol (b) phenol (c)

4.1.6 Geometry optimization of phenolic compounds and selected alkaloids of khat

Optimization steps number that is taken by the molecules in achieving the utmost stable structural conformation at its minimum energy discloses more information as regards to the molecule stability. It displays the number of steps that are taken by a molecule so as to achieve its most stable molecular structure and the net inter-atomic forces that exist amidst the molecule atoms (Omare et al., 2020). The most unstable structures have the highest optimization step numbers. Figures 4.9-4.10 illustrate steps embarked on towards attaining structural optimization for cathinone and cathine respectively.

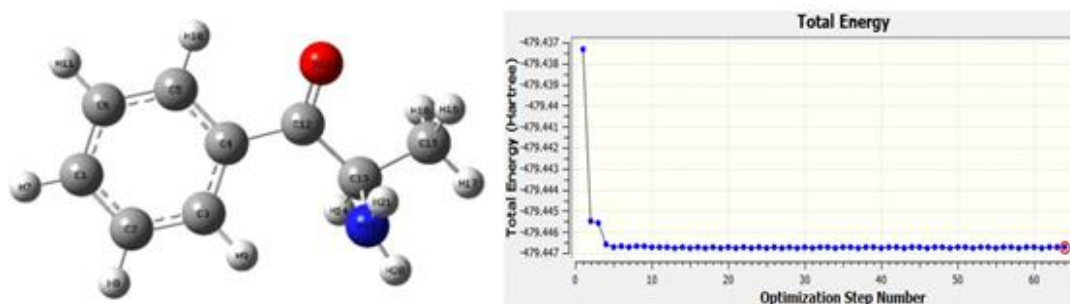


Figure 4.9: Cathinone optimized structure and its optimization steps plot

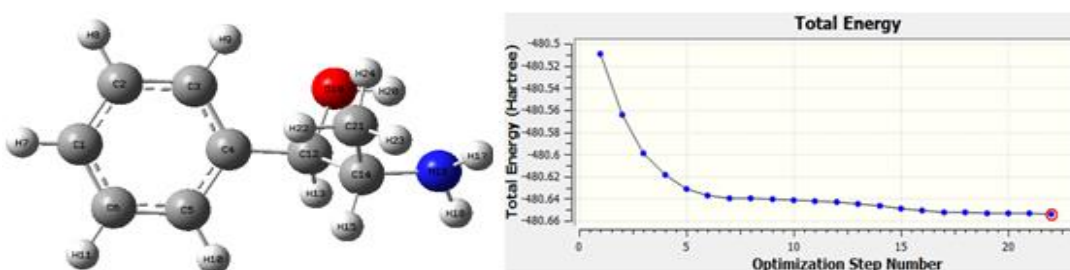


Figure 4.10: Cathine optimized structure and its optimization steps plot

It is important to note that cathinone optimization is achieved after 64 successful optimization steps at a total energy of -479.4467 Hartrees. On the other hand, cathine optimization successfully took 22 optimization step number with a total energy of -480.6537 Hartrees. Accordingly, phenol and hydroquinone had 5 optimization step numbers identified, with their most stable conformations being achieved at a total energy of -307.5531 and -382.7942 hartrees respectively while p-cresol exhibited 7 optimization step numbers at energy of -346.2437 hartrees. This information confirms to our earlier proposition that p-cresol is more lethal amongst the khat released phenols.

Benzenyl and 3-aminobuytanyl-2-one are some of the formed free radicals resulting from the thermolytic degradation of cathinone and had their overall energy minimization projected at -231.5201 and -247.7814 Hartrees, respectively as illustrated in Figure 4.11 and 4.12. Since the lengthier the time it takes for a chemical compound to have its geometry optimized, the further the unstable the compound becomes, and hence the more reactive the compound is in biological environments. The resulting radical, 3-aminobuytanyl-2-one with 28 optimization step numbers can be considered to be more venomous compared to benzenyl radical whose stability can be associated with its ability to exhibit structural resonance.

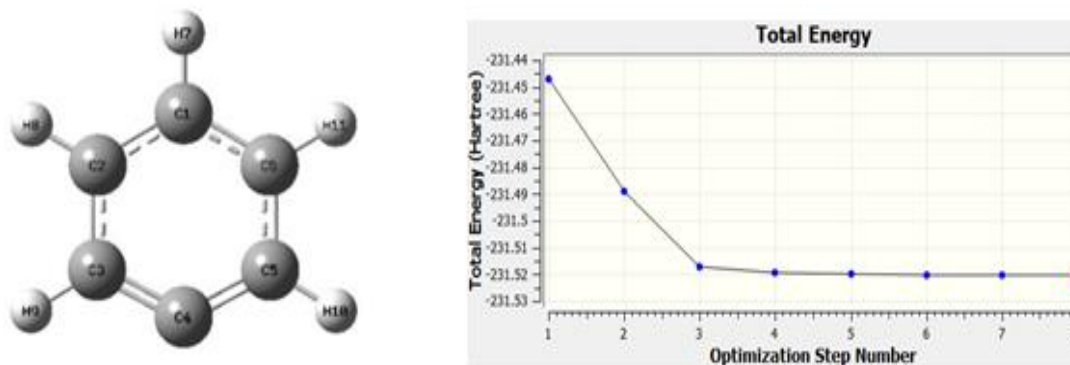


Figure 4.11 Benzenyl radical optimized structure and its optimization steps plot

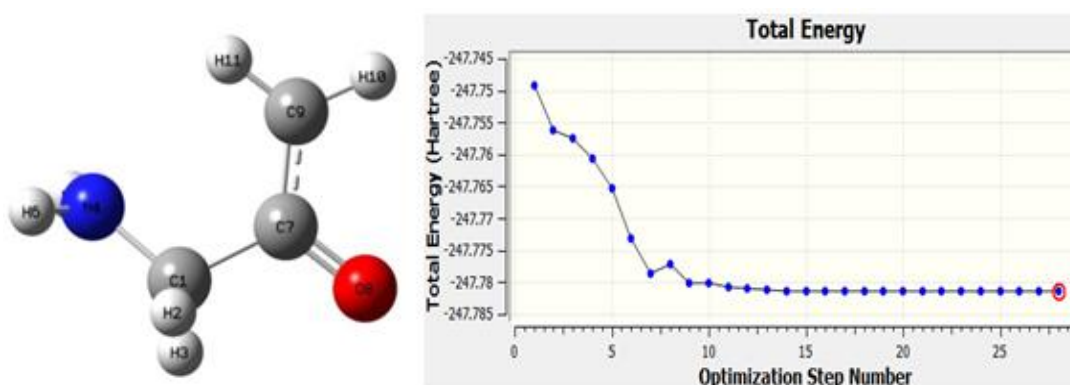


Figure 4.12: 3-aminobutanyl-2-one radical optimized structure and optimization steps plot

In reference to these outcomes therefore, it can be construed that cathine which has 22 optimization step numbers is more stable than cathinone with 64 optimization step numbers and therefore cathinone can be regarded as more lethal unlike cathine. Moreover, the subsequent free radicals, benzenyl and 3-aminobutanyl-2-one, had 8 and 28 optimization step numbers, respectively. In addition, the number of optimization steps, i.e. the minimization of energy of a molecule, reveals the net inter-atomic forces which act on every single atom of a particular molecule which is reasonably close to zero. The HOMO-LUMO energy profiles for hydroquinone, and p-cresol is as presented in Figure 4.13.

4.1.7 Molecular orbitals and Electronic properties for phenols and selected khat alkaloids

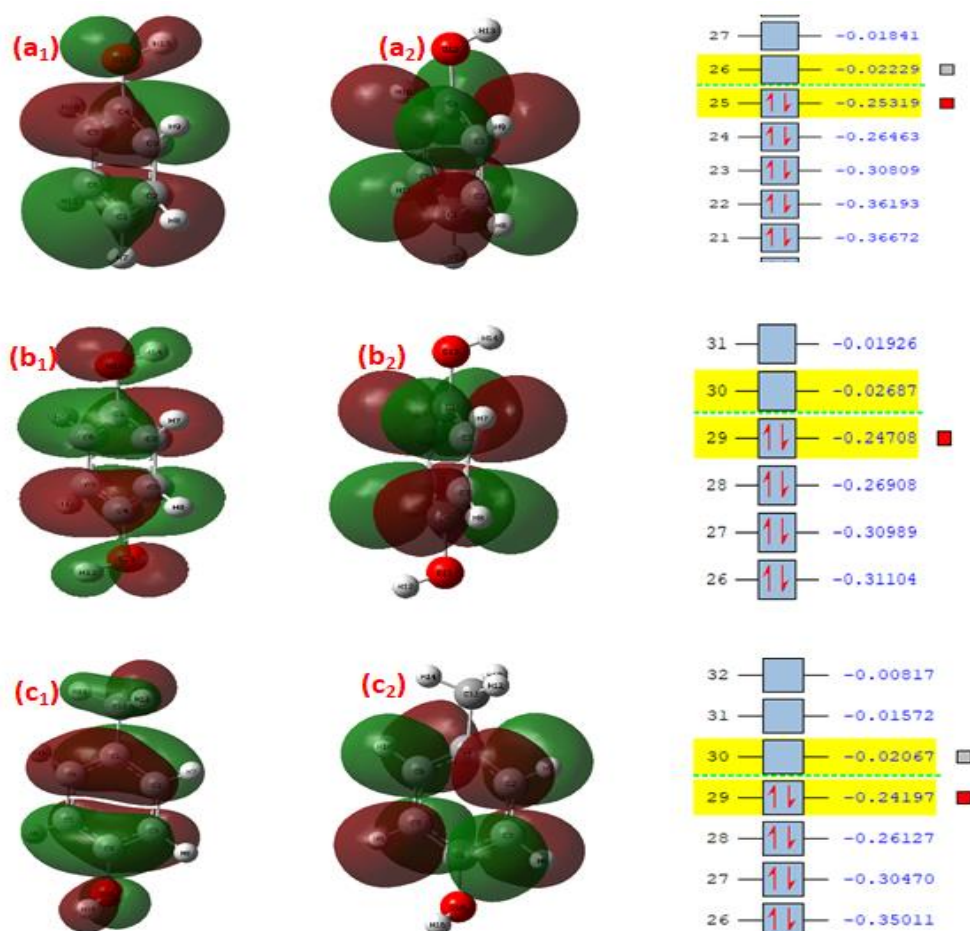


Figure 4.13: HOMO (1) LUMO (2) energies for hydroquinone (a) phenol (b) and *p*-cresol (c)

The highest occupied molecular orbital (HOMO)-lowest unoccupied molecular orbital (LUMO) energy band gap can similarly be used to predict the expected strength and stability of molecules and as a result the reactivity of molecules (Bartocci & Lió, 2016; Omare et al., 2020). Evidently, it can be inferred from the obtained energy profiles that the HOMO for hydroquinone, *p*-cresol and phenol is 29, 29 and 25 at energies of -0.24708, -0.24197 and -0.25319 eV correspondingly at an iso value of 0.02 and singlet spins under alpha occupancy. Similarly, the LUMO were 30, 30 and 26 at -0.02687, -0.02067 and -0.02480 eV respectively. This gives

rise to HOMO-LUMO band gap energy of -0.17838, -0.22021 and -0.02229 eV respectively.

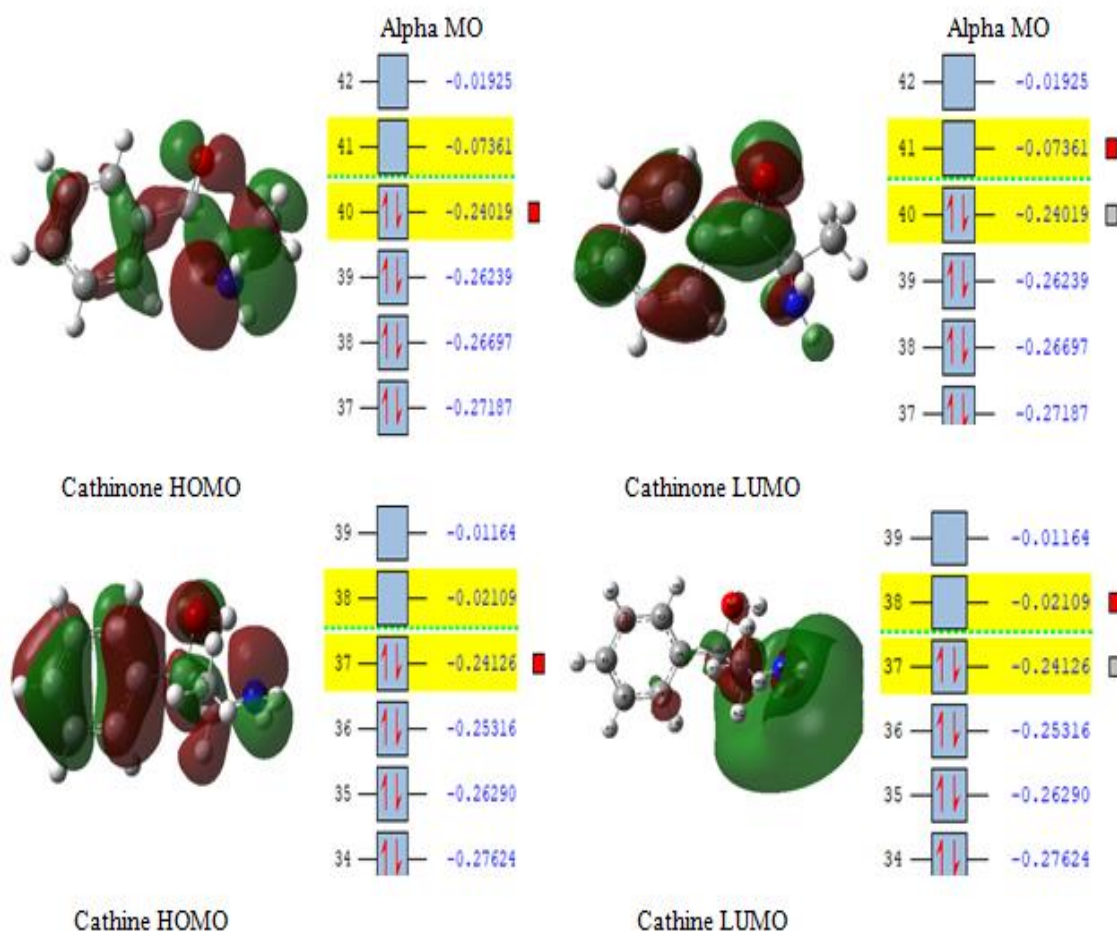


Figure 4.14: HOMO and LUMO structures for cathinone and cathine molecules

Phenol displayed the least band gap energy whereas p-cresol the largest band gap energy suggestive of p-cresol as the most unstable phenol and therefore more reactive since it an electron requires very little excitation energy for it to jump from HOMO to LUMO. This is in agreement to our earlier suggestion that p-cresol is the most lethal compound given that it can be perceived to be highly reactive to human body cells and prompt a series of cell damaging reactions that in all probability can lead to carcinogenesis. Accordingly, the highest occupied molecular orbital (HOMO) in addition to the lowest occupied molecular orbital (LUMO) energy profiles for

cathinone and cathine molecules together with benzenyl radical and 3-aminobutyryl-2-one radical obtained from their optimized geometry diagrams which relates to their ionization potentials and electron affinities are presented in Figures 4.14 and 4.15 respectively.

The attained results point out that cathinone has orbital 40 as the HOMO and orbital 41 as the LUMO at energies -0.24019 eV and -0.07361eV in that order with a band gap energy difference of 0.16658eV. In the same way, cathine displays orbital 37 as the highest occupied and orbital 38 as the lowest unoccupied orbital at energies of -0.24126 eV and -0.0219 eV with a band gap energy difference of 0.22017 eV both at singlet spin, 0 charge, isovalue 0.02 and alpha occupancy. On the other hand, the subsequent radicals' revealed alpha and beta molecular orbital occupancies with duplet spins at 0 charges and an isovalue of 0.02 as demonstrated in Figure 4.15. To be precise, benzenyl radical partakes orbital 21 to be the highest occupied alpha MO and orbital 22 to be the lowest unoccupied at energies -0.24985 eV and -0.02265 eV correspondingly with a band gap energy difference of 0.2272 eV.

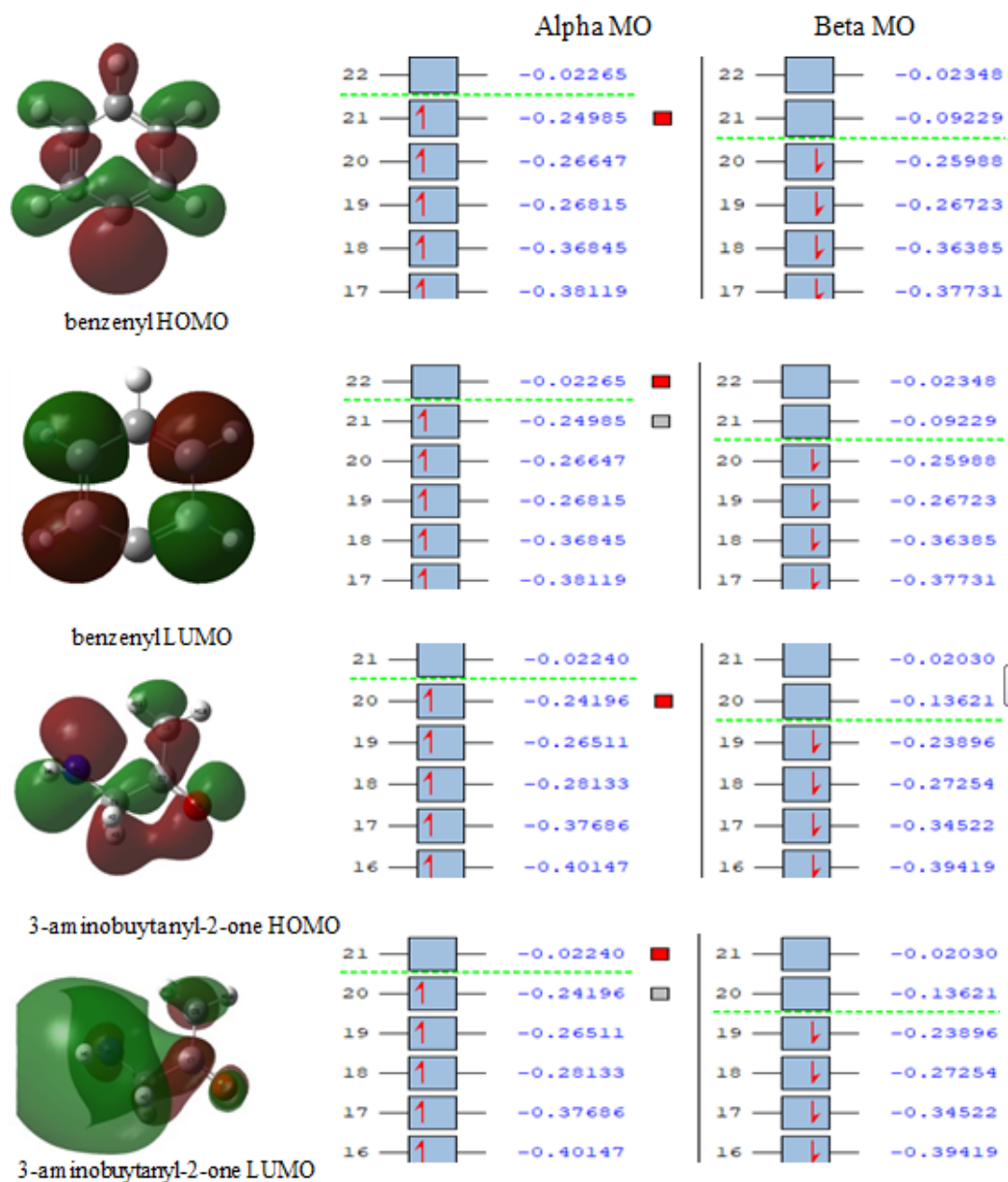


Figure 4.15: HOMO and LUMO structures for benzenyl and 3-aminobutyryl-2-one radicals

Similarly, 3-aminobutyryl-2-one displays orbital 20 as the highest occupied at an energy level of -0.24196 eV and orbital 21 as the lowest unoccupied at energy level -0.0224 eV which gave rise to a band gap energy difference of 0.21956 eV. In doing a comparison between the band gap energies of the chemical compounds and together with their corresponding radical band gap energies, it is apparent that cathinone

partook the smallest energy band gap, supposing that electrons get excited more freely in a cathinone molecule and readily absorb less energy for the electrons to jump from HOMO to LUMO compared to cathine and the formed radicals (Bouzzine et al., 2015). Since the less the energy required to cause electron excitement, the more reactive the molecule is, we can deduce that cathinone can readily react with biological systems where it is likely to cause more fatal reactions that may lead to gene alterations and consequently induced carcinogenesis (Adole et al., 2021).

Given that these compounds are known to have a high degree of unsaturation, hydroquinone and phenol cannot be considered safer because as soon as they have the ability to gain entry into the human system, undergo cyclic transition reactions at the region of double bonds “diene” where there exists as conjugated double pi-bonds with the single pi-bond sites “dienophile” which comprises of conjugated π -electron system in unsaturated molecules that include body fats and lipids (Omare et al., 2020). These active sites can be highlighted using electron density and contour maps as shown in Figure 4.16 and Figure 4.17. The electrostatic potential values are usually assigned coded colors with green color indicative of sites with high positive values where the excitation states are greatest while red color indicates points or regions where electrophilic attack is likely to occur (Medimagh et al., 2021).

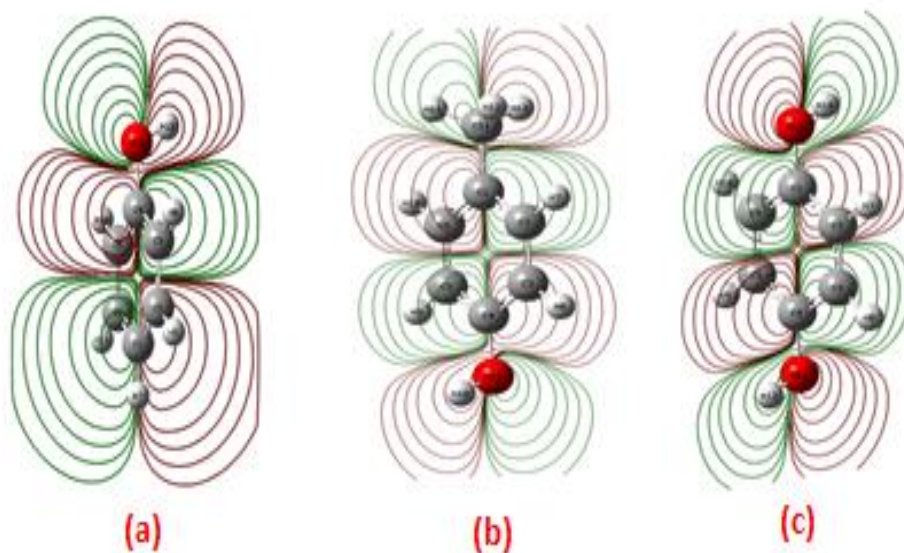


Figure 4.16: Contour maps for (a) phenol (b) *p*-cresol (c) hydroquinone

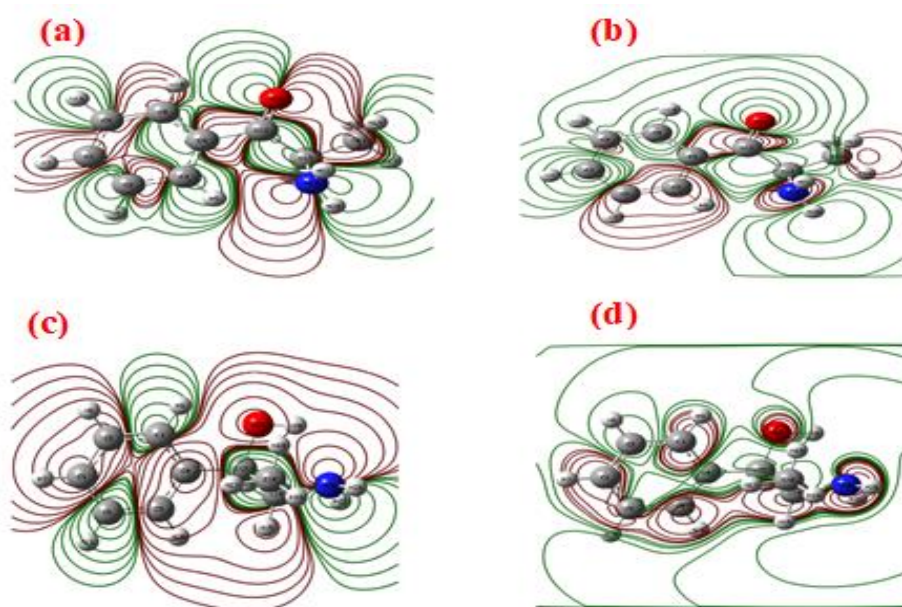


Figure 4.17 Contour maps for HOMO cathinone and cathine (a and c), respectively and LUMO (b and d) for cathinone and cathine, respectively

4.2 Molecular products released from thermal degradation of Marijuana

The pyrolysis of marijuana is accompanied with a release of a number of molecular products as illustrated by the GC-MS results in Figure 4.18.

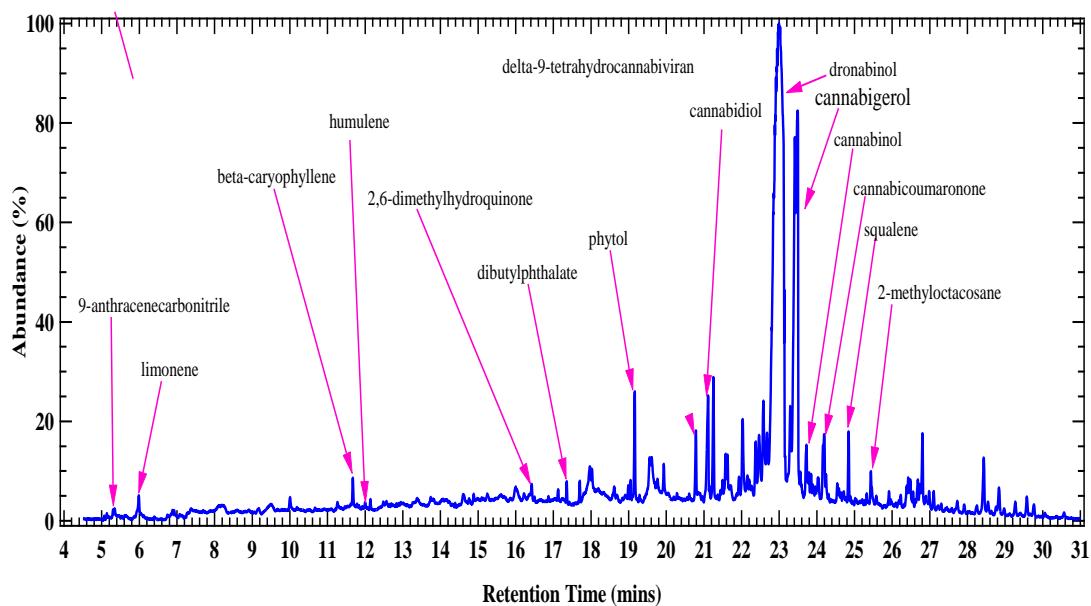


Figure 4.18: GC-MS chromatogram of products from marijuana pyrolysis at 500 °C

The identified constituent molecules released from marijuana pyrolysis include acyclic diterpenes such as phytol, and other classes of organic compounds including 9-anthracenitrile, cannabidiol, tetrahydrocannabinol, delta-9-tetrahydrocannabivarin, cannabigerol, and 2,6-dimethylhydroquinone. It is interesting to note that the release of these compounds displayed variations in concentration with increase in temperature within the selected temperature range as illustrated in Figures 4.19 (a) and (b).

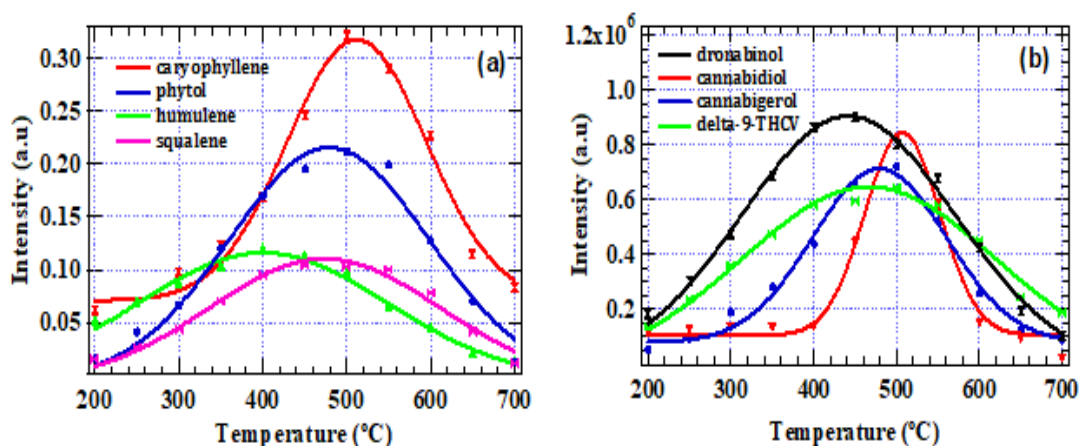


Figure 4.19: Terpenes (a) and cannabinoids (b) released from marijuana pyrolysis

For instance, terpenes including cyclic and alicyclic diterpenes, triterpenes and sesquiterpenes like phytol, squalene, β -caryophyllene and humulene respectively had their yield increase with increase in temperature up to temperatures between 400 °C and 600 °C, where the concentration is highest as indicated in Figure 4.19 (a). Similarly, cannabinoids present in marijuana pyrolysisate exhibited variation in concentration at various pyrolysis temperatures with maximum concentration yields being achieved between 400 °C to 600 °C as illustrated in Figure 4.19 (b).

It is important to note that amongst the identified terpenes, β -caryophyllene displayed the highest yields of 45.86 wt % throughout the selected pyrolysis temperature range and subsequently followed by phytol whose maximum yield of 30.22 wt % was attained at around temperatures of 500 °C. Interestingly, β -caryophyllene has been reported to be a potent anti-inflammatory antimicrobial, antibacterial and antioxidant agent with some scientific studies reporting it as a major aid in suppressing neurodegenerative diseases and cancers given that it has a higher ability to bind to CB2 receptors which make β -caryophyllene a potential in offering medical benefits (Francomano et al., 2019; Sitarek et al., 2017).

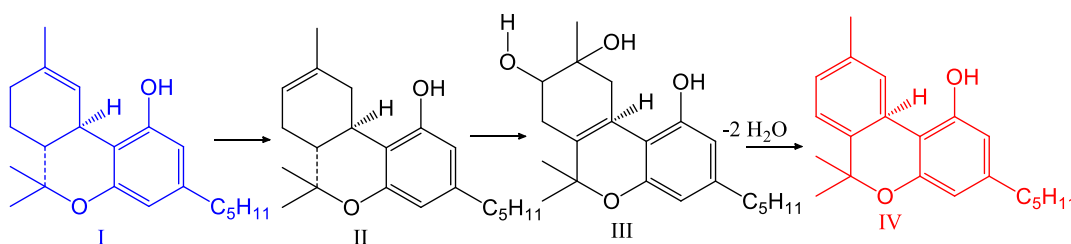
On the other hand, in a study carried out by de Alencar et al. (2019), the authors have demonstrated that phytol can offer antitumor properties and therefore a good candidate for developing treatments of oxidative stress induced diseases. Humulene and squalene displayed fairly low release concentrations throughout the pyrolysis period and scientific studies have reported humulene to be having a potential to help in terminating cancer cells when in combination with other phytocannabinoids and terpenes (Fidyt et al., 2016). Dronabinol (delta-9-tetrahydrocannabinol) had the highest concentration release throughout the pyrolysis temperature range amongst the identified phytocannabinoids.

Interestingly, cannabidiol had low concentrations in the low temperature zones and presented an increase in release concentration, hitting a maximum yield of 17.37 wt % at around temperatures of 500 °C. Cannabidiol, even though reported in low levels, it is known to biologically activate CB2 receptors and consequently minimizes body pains, seizures and irritations in patients (Archie & Cucullo, 2019) and therefore sometimes it is assimilated in the management of medical conditions such as epilepsy, schizophrenia and post-traumatic stress problems (Beale et al., 2018).

On the other hand, delta-9-tetrahydrocannabivarin and cannabinol had moderately high concentrations release throughout the pyrolysis temperature but their maximum yields were 22.86 wt % and 17.37 wt % respectively attained at temperatures of 450 °C. Cannabinol is known to be a rare cannabinoid found in low concentration in old cannabis plant and in most cases, it results from the degradation of tetrahydrocannabinol. Interestingly, cannabigerol was detected in high concentration levels at low temperature zones and these concentrations decreased tremendously

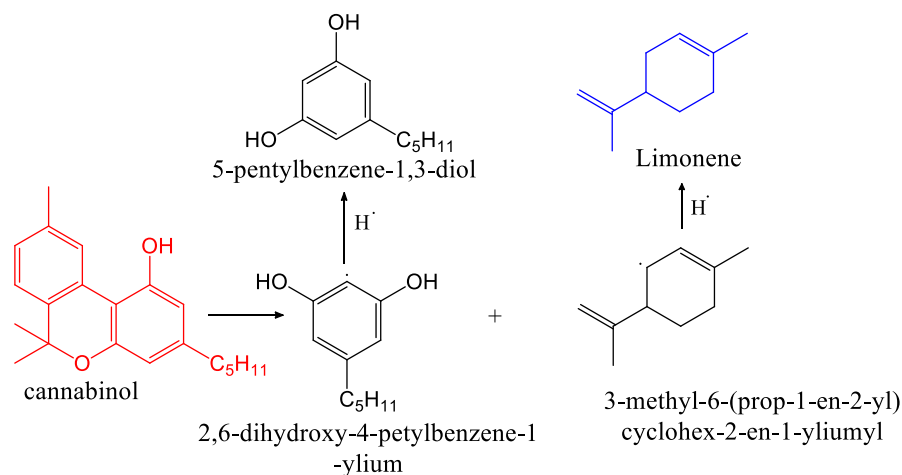
with increase in temperatures. This trend is expected given that even though present in low concentrations, it is a derivative of cannabigerolic acid, the precursor to tetrahydrocannabinolic acid and cannabidiolic acid which thermal degrades to tetrahydrocannabinol and cannabidiol.

Therefore, the concentration of cannabigerol decreases with increase in tetrahydrocannabinol and cannabidiol concentrations. Accordingly, the low concentrations of cannabinol reported in this study could be linked to the thermal degradation of tetrahydrocannabinol as illustrated in scheme 4.5. During pyrolysis, Δ -9-tetrahydrocannabinol (I) decomposes to form Δ -8-THC (II) which further converts by migrating the double bond of (I) to position 8,9 to form a binary mixture of 8,9-dihydroxy Δ -6a(10a)-THC (III) which is a more thermodynamically stable isomer.



Scheme 4.5: Proposed mechanism for thermal degradation of THC to CBN

Further heating may yield cannabinol (IV) as predicted by scheme 4.5. This proposition is in agreement with results in Figure 4.19 (b) which show that as the percentage yields of THC increased, it is encountered by a corresponding increase in CBN yields at various pyrolysis temperatures. The formed cannabinol further undergoes thermal degradation to yield other molecular products such as limonene that was also detected in marijuana pyrolysate as shown in scheme 4.6.



Scheme 4.6: Cannabinol proposed degradation pathway

Limonene has been identified as a potential renal toxic effluent responsible for hyaline droplet nephropathy and renal tubular tumors in rats raising alarm to chronic human limonene exposure alert (NCBI, 2020b). Nonetheless, even though 5-pentylbenzene-1,3-diol whose common name is olivetol, has not been reported as a harmful compound through ingestion, it is known to cause eye irritation and damage, skin inflammation accentuating pre-existing dermatitis conditions, respiratory irritation and suspected carcinogen due to long term and chronic exposure to respiratory system.

Other organic compounds that were identified to be present in marijuana pyrolysate include cannabicyclic acid and dibutylphthalate which belong to benzopyran and benzoic acid esters classes of organic compounds respectively, which displayed variations in percentage yields at various temperatures as illustrated in Figure 4.20. For instance, the yield of cannabicyclic acid was 2 times higher than that of dibutylphthalate. The yield of cannabicyclic acid derived from marijuana pyrolysis in this work was 59.79 wt % while that of dibutylphthalate was 30.44 wt %.

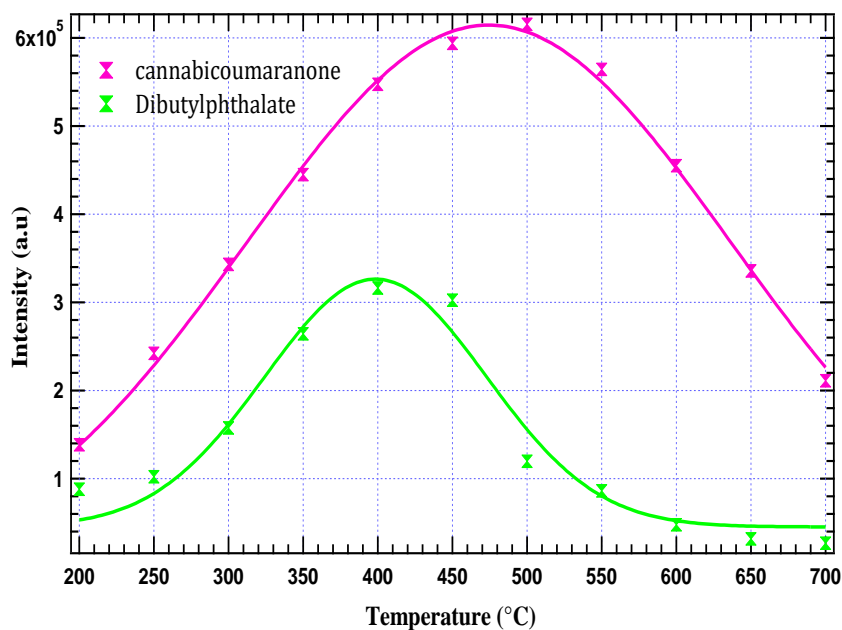


Figure 4.20: Coumaranone and phthalate from marijuana pyrolysis

4.2.1 Molecular geometries of cannabinoid derivatives generated from marijuana pyrolysis

This study analyzed the optimized geometries of CBD and THC under the DFT at B3LYP and 6-311++G d, p diffuse basis set shown in Figure 4.21. The structures were well selected and their optimization achieved when potential energy surfaces of the molecules attained lowest energy enabling us to predict the chemical kinetics, spectroscopy and thermodynamic properties of the selected compounds. During CBD and THC molecule geometrization, the wave functions and the energy of the input/starting CBD and THC molecules geometry were computed and progressed in series of steps aimed at establishing their lowest energy geometries.

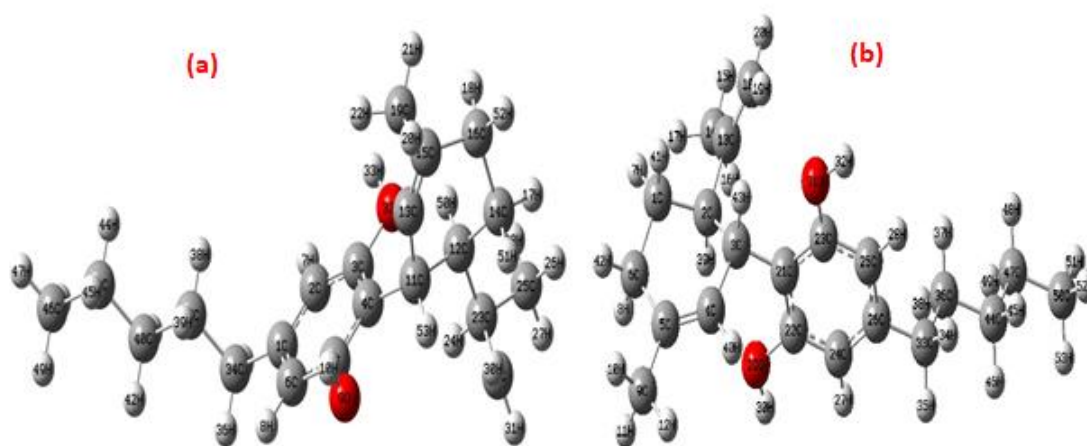


Figure 4.21: CBD input structure (a) and (b) CBD optimized structure

For CBD, from the input structure to the point where its optimized structure was attained, 40 optimization steps were involved which occur with an energy decrease from -968.408 Hartree at optimization step number of 0.924092, to the optimized geometry of lowest energy of -968.519 Hartree at optimization step number 40 as indicated in optimization plot in Figure 4.22. On the other hand, THC had 68 optimization steps whose energy decreased from -968.624 Hartree at optimization step number 1 to -968.727 Hartree at optimization plot number 68. Evidently, there are more optimization steps in THC than in CBD.

Arguably, the number of optimization steps reveals how long it takes for a molecule to attain its most stable geometry configuration which in turn assists in estimating and predicting the behaviour of the molecule inside biological systems (Larijani et al., 2017). Stable configurations remain less reactive compared to unstable molecules once they enter the human biological system (Qi et al., 2019). For instance, THC with more optimization steps is predicted to be more reactive than CBD which proceeds to minimum energy via slightly lower steps. This suggests that THC is likely to induce serious health consequences than CBD in humans.

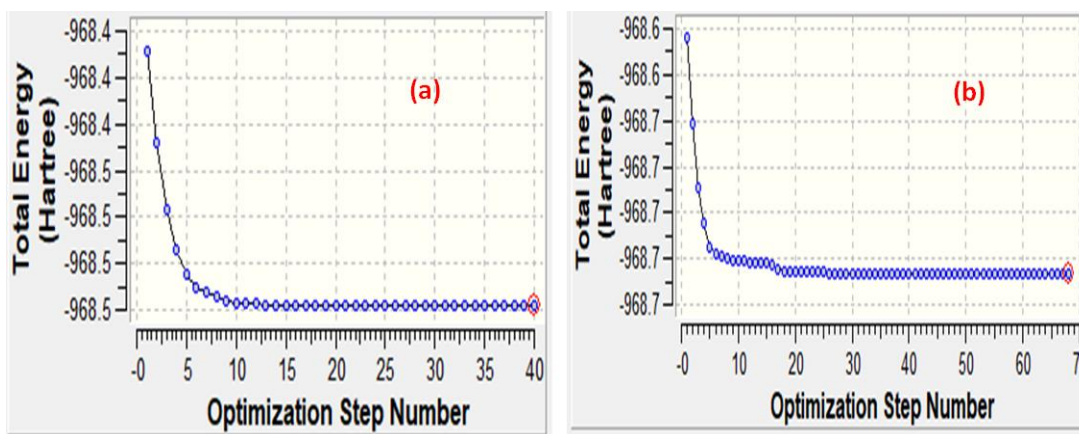


Figure 4.22: CBD optimization plot (a) and (b) THC optimization plot

4.2.2 Molecular orbitals and electronic properties of selected phytocannabinoids

In order to determine the molecular reactivity of a compound together with its probable reaction mechanism, the identification of orbital structure is significant (Kibet, 2016). Accordingly, the highest occupied molecular orbital (HOMO) and lowest occupied molecular orbital (LUMO) energy profiles for CBD and THC optimized geometry diagrams which relate to their ionization potentials and electron affinities are presented in Figure 4.23 and Figure 4.24, respectively. From the obtained results, for CBD, there were two sets of molecular orbital (MO) that were the highest occupied by electron, orbital 86 alpha and 86 beta both with same energy values of -0.340 eV. Two alpha and beta MO with same energies of -0.183 eV were the lowest unoccupied orbitals. The energy difference between the band gap is 0.157 eV, implying that very little energy is required for an electron to be excited and jump from the HOMO to the LUMO.

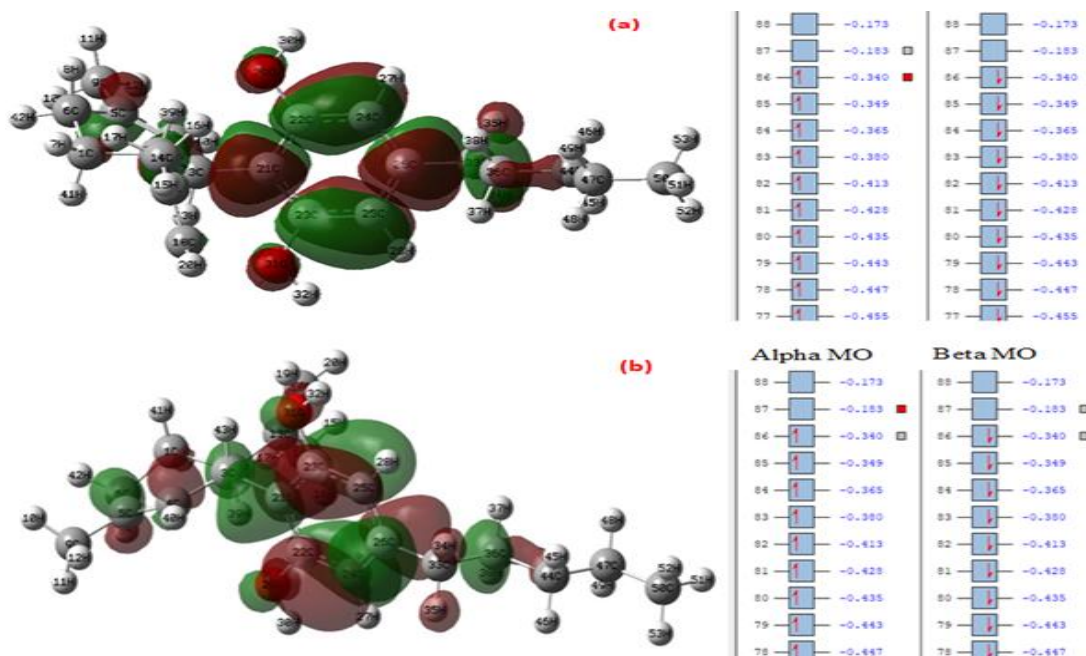


Figure 4.23: CBD HOMO (a) and (b) CBD LUMO

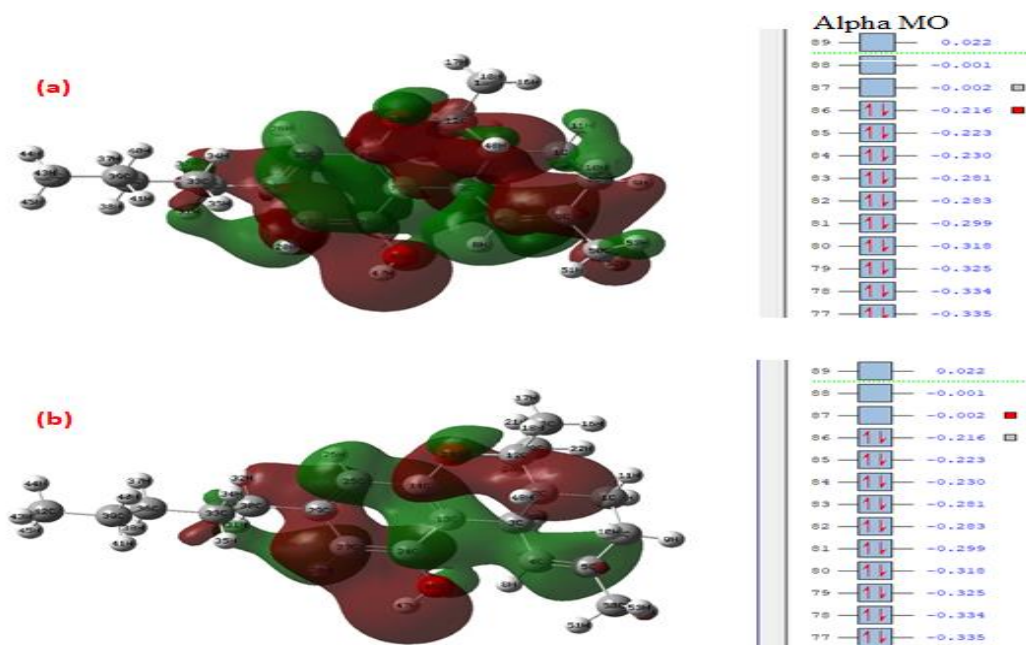


Figure 4.24: THC HOMO (a) and (b) THC LUMO

On the other hand, THC had only alpha MO, with an electron occupying orbital at level 86 as the highest with energy of -0.216 eV. Similarly, the lowest unoccupied orbital at level 87 had an energy of -0.002 eV. Therefore, the energy required by an excited electron to jump from HOMO to the LUMO is 0.214 eV. The band gap energy between THC HOMO-LUMO is larger than that of CBD HOMO-LUMO

and therefore suggesting that it is easier for an excited electron to jump from HOMO to LUMO in CBD unlike in THC and hence considered less reactive.

4.2.3 Electron density and contour maps of selected phytocannabinoids

In order to describe the effects of electron connotation to theoretical calculations, DFT methods provide a computationally viable means that essentially and accurately describes carbon and hydrogen bonds formed within molecules playing a major role in the stability of molecule complexes (Silva et al., 2019). With computational tools, the chemical structures and their distinct sites of interactions that can possibly form hydrogen bonds are presented as electrostatic density maps indicating the regions of high affinity interactions and corresponding electrostatic charge distribution of the optimized geometry. This is important in the fundamentals of describing the chemical properties of molecules in terms of its reactivity.

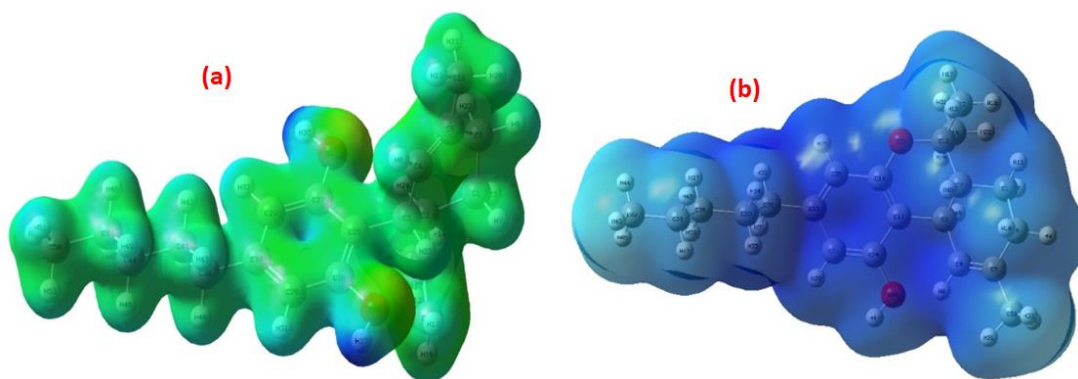


Figure 4.25: CBD electrostatic potential (a) and THC electrostatic potential (b)

Gaussian generated mapped electron density surfaces appear with color codings which indicate the values of the electrostatic potentials. The density surfaces display the differences in densities between the first excited state and the ground state by using a generated excited state electron density cube. Accordingly, the electrostatic potential for THC and CBD were as illustrated in Figure 4.25 (a) and (b). The blue

regions map the sites with positive values having different densities where the excited state is larger than the ground state density. On the other hand, red regions are indicative of sites with negative values where the excited state is smaller than the ground state density. Blue regions are prone to nucleophilic attack and red regions electrophilic attack. Therefore, for CBD molecule, electron density moves from the regions of the two hydroxide sites towards the central benzene ring as it transitions from the ground state to the first excited state.

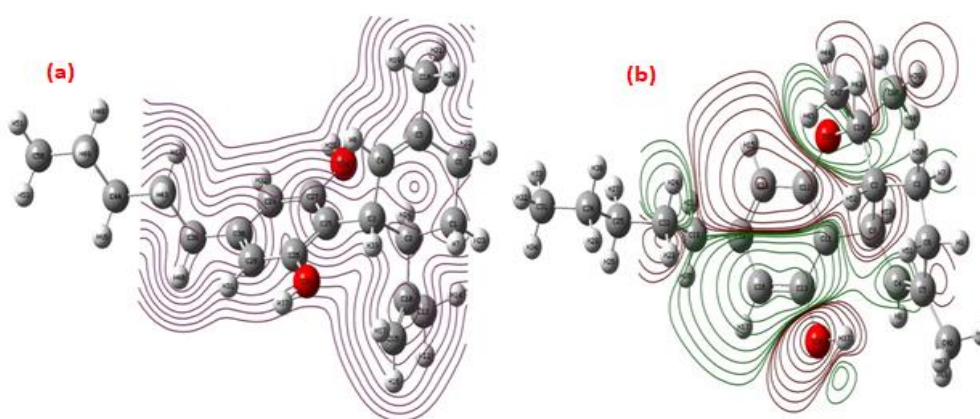


Figure 4.26: CBD contour map (a) and THC contour map (b)

Accordingly, THC has the benzene ring bonded to hydroxyl group area as a positive value site and hence more excited than at the ground state, therefore its electron density moves outwards to the two adjacent benzene ring and alkyl regions it transitions from the ground state to its first excited state. These trends lead to the generation of electron density contour maps in Figure 4.26, which contribute to the understanding of molecular charge distribution (Mosonik et al., 2019).

4.3 Molecular products released from thermal degradation of Marijuana-Khat biomass

The aim of this pyrolysis experiment was to evaluate the effects of biomass co-pyrolysis on the concentration (yields) of compounds released. During the

copyrolysis of an equimassic mixture of khat and marijuana, arrays of molecular compounds are released as reported in Figure 4.27. It is important to note that new products were detected in the pyrolysis of mixtures. The new compounds included tetradecanamide, pregnan-3-one, (Z)-9-tricosene, tetratetracontane and gamma-sitosterol.

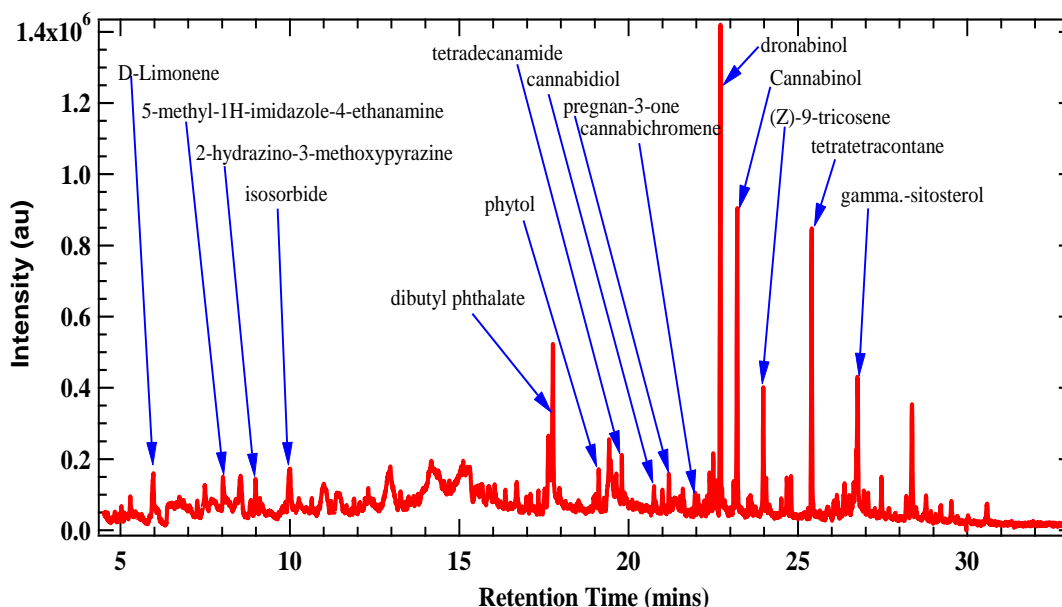


Figure 4.27: GC-MS chromatogram of products from marijuana-khat pyrolysis (500 °C)

4.3.1 Effects of Khat on concentration of Marijuana pyrolysis products

Qualitative comparison on the concentrations of the molecular products released from a mixture of khat-marijuana biomass to that of pure marijuana biomass pyrolysis showed a variation in concentration of various compounds within the selected temperature range as illustrated in Figure 4.28.

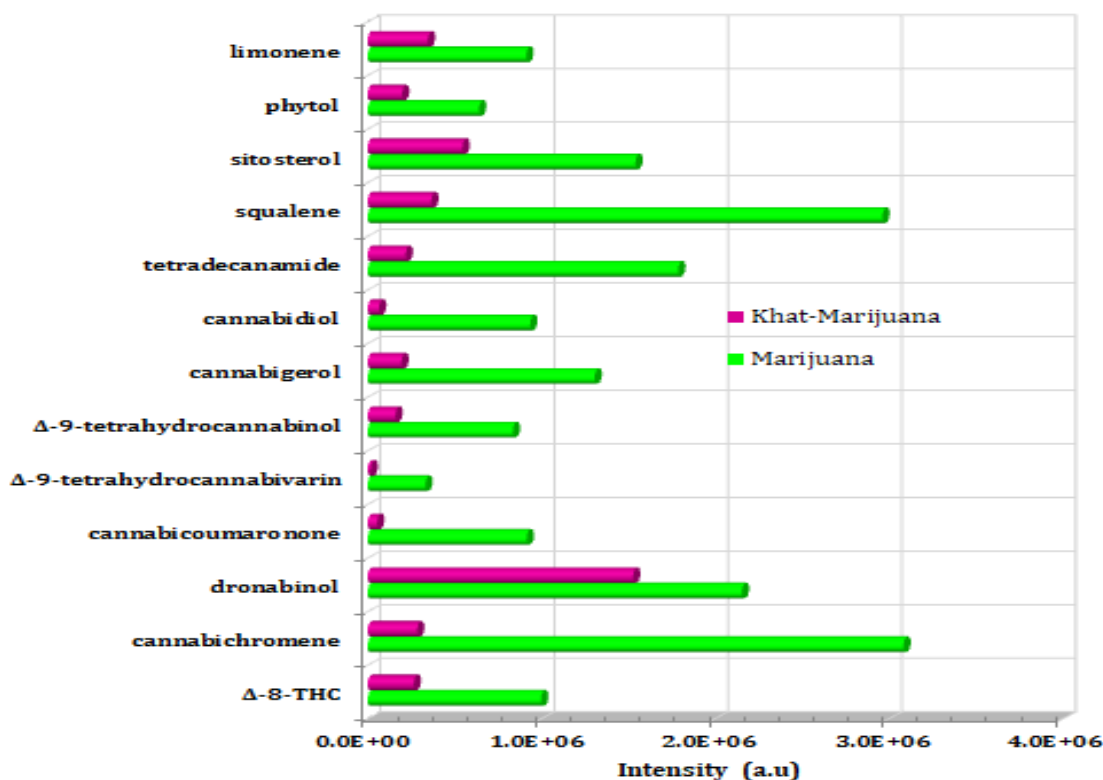


Figure 4.28: Comparison of GC-MS intensities of the molecular products released from the pyrolysis of equimassic mixture of khat and marijuana and pure marijuana

It is evident that khat has a noticeable effect on most of the released marijuana pyrolysis products. Many of the evolved products exhibited a tremendous decrease in concentration for the mixed biomass pyrolysis at a temperature of 500 °C. Interestingly, most of the cannabinoids displayed a decrease in concentration by almost twice the initial concentration in marijuana pure sample. Precisely, cannabichromene, cannabicooumarone, Δ-9-tetrahydrocannabivarin, cannabigerol, and cannabinol had their yields as 4.60, 0.89, 0.29, 3.15, and 2.58 wt %, respectively when marijuana pyrolysis was conducted in 50% khat. This translates to 10.81, 16.85, 18.80, 6.69 and 5.23 times lower, respectively compared to the yield during pure marijuana pyrolysis. On the other hand, dronabinol, cannabidiol, and delta-8-tetrahydrocannabinol, which are predominantly present in marijuana smoke, reported

a decrease in their yields by 14.25, 1.41 and 3.76 times lower respectively of the amounts present in the pyrolysis of pure marijuana. The comparisons in the sample means obtained are compared in Table 4.5 and Table 4.6.

Table 4.5: Paired samples statistics for the molecular compounds generated from Marijuana and Marijuana-khat mixture pyrolysis

	Mean	N	Std. Deviation	Std. Error Mean
Marijuana	3.1005×10^6	13	3.86964×10^6	1.07324×10^6
Marijuana-khat	3.2672×10^5	13	3.88078×10^5	1.07634×10^5

The mean composition of the molecular products in marijuana was 3.1005×10^6 whereas the mean composition of the molecular products in marijuana mixed with khat was 3.2672×10^5 respectively.

Table 4.6: Paired samples t-test

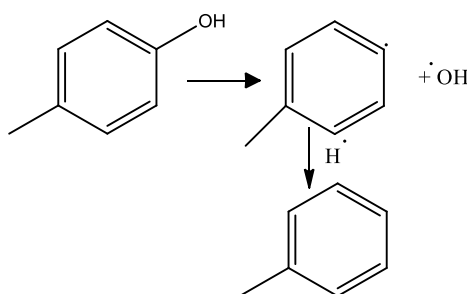
	Mean	Std. Deviation	Std. Error Mean	95% Confidence Interval of the Difference		t	df	Sig. (2-tailed)
				Lower	Upper			
Pair 1 Marijuana-khat	2.77376×10^6	3.52922×10^6	9.78830×10^5	6.41070×10^5	4.90645×10^6	2.834	12	0.015

According to the findings, the mean difference of the molecular products generated from the pyrolysis of marijuana and marijuana mixed with khat was 2.77376×10^6 which is statistically significant as per the p value ($0.015 < 0.05$). This implies that mixing marijuana with khat significantly reduces the elemental compounds.

4.3.2 The unique variations in yields of phytocannabinoids from the pyrolysis of marijuana in khat regime

To explain the surprisingly decrease in yield of phytocannabinoids from the thermal degradation of marijuana in khat regime; we consider the formation of the intermediate products from the main phytocannabinoids including Δ -9-

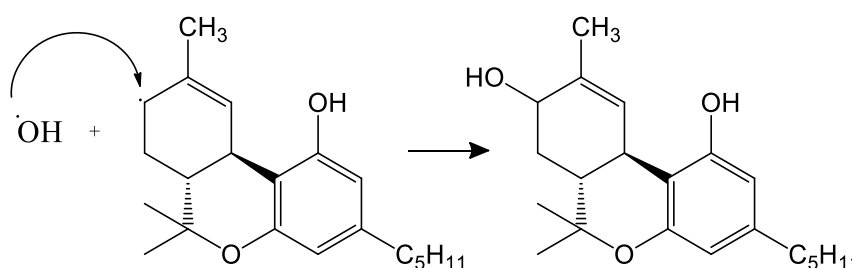
tetrahydrocannabinol, cannabinol and cannabidiol. Δ -9-THC, converts to cannabinol as illustrated earlier in Scheme 4.5. In addition, the formation of hydroxyl-delta-9-tetrahydrocannabinol, Δ -9-tetrahydrocannabinolic acid and hexahydrocannabinol-1,10-betadiol that were reported fairly low concentration yields of 10.16, 12.78 and 8.48 wt % respectively in pure marijuana pyrolysis imply that in khat regime, the conversion of the phytocannabinoids to these compounds is highly probable. This can be solely because khat pyrolysis leads to the generation of free radicals majorly comprising of hydroxyl radicals that arise from the conversion of phenolic compounds as previously illustrated in scheme 4.1 and scheme 4.3. These conversions of phytocannabinoids can be as illustrated in scheme 4.7.



Scheme 4.7: Formation of hydroxyl radical, and toluene from p-cresol

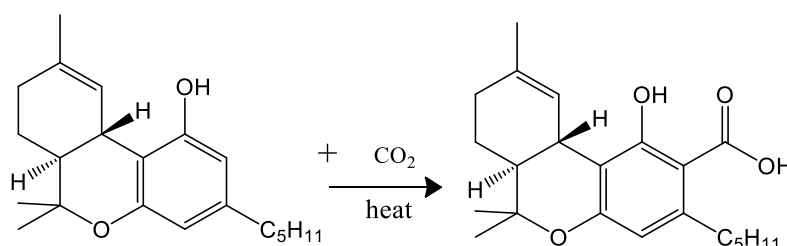
The subsequent hydroxyl radicals, mostly form as a result of easy cleavage of the carbon-oxygen (C-O) bond of *p*-cresol, phenol, hydroquinone and other aromatic compounds including methoxy phenols that are important toxicological khat pyrolysis products and responsible for yield of toluene, p-xylene a methyl benzene molecules. The methoxyl substituents heighten homolysis reaction of the β -O-4 linkage and the methoxyl-substituted phenoxy radicals subsequently go through multifarious reactions that involve abstraction of intermolecular hydrogen, rearrangement and β -scission reactions (Jakab, 2015). Therefore, one of the sources of hydroxyl radicals in the pyrolysis of khat-marijuana biomass is from the thermal

degradation of phenolic compounds which are dominantly present in khat. The generated hydroxyl radicals subsequently react with cannabinoids, for instant, THC to yield hydroxyl- Δ -9-tetrahydrocannabinol and hexahydrocannabi-1, 10-betadiol as shown in scheme 4.8 (Guy & Flint, 2004).



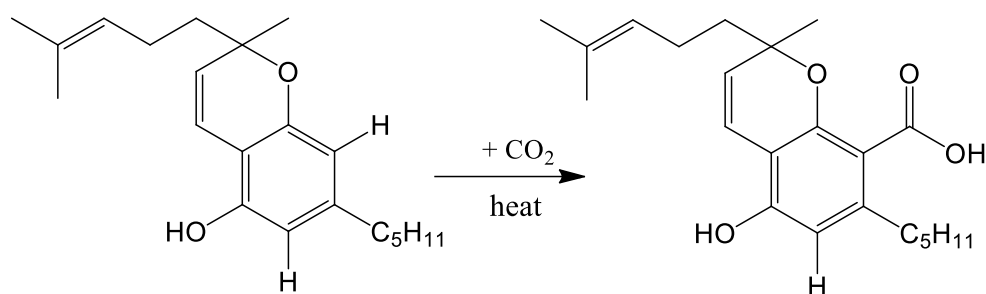
Scheme 4.8: Oxidation of delta-9-tetrahydrocannabinol to 11-hydroxyl-delta-9-tetrahydrocannabinol

The formed 11-hydroxyl- Δ -9-tetrahydrocannabinol exhibits high affinity to CB₁ and CB₂ receptor cells and has easier penetration to the brain, suggesting that the effects of marijuana can be highly experienced by the smoker if smoked in a mixture of khat even though most of the cannabinoids were reported in low amounts (Blunt et al., 2016). Moreover, the possible release of high amounts of carbon (IV) oxide from khat pyrolysis contributes to carboxylation of 11-hydroxy analogue to Δ -9-tetrahydrocannabinolic acid which was reported in high concentrations in khat-marijuana biomass pyrolysis compared to pure marijuana pyrolysis as shown in Scheme 4.9.



Scheme 4.9: Carboxylation of Δ -9-THC to THCA

The concentration decrease of about 10.81 lower were reported in cannabichromene which is one of the most abundant non-psychoactive phytocannabinoid with a potential to offer anti-inflammatory in human beings (Marcu, 2016). This observed decrease in concentration of cannabichromene can be associated with the carboxylation of cannabichromene to cannabichromenic acid (CBCA) during pyrolysis as illustrated in scheme 4.10. Therefore, it can be construed that the decrease in concentration of most of the phytocannabinoids during marijuana pyrolysis in khat regime can be linked to oxidative and carboxylation reactions.



Scheme 4.10: Carboxylation of CBC to CBCA

4.4 Molecular products released from thermal degradation of Tobacco–khat biomass

A representative GC-MS spectrum of the principle products generated from the thermal degradation of tobacco in khat regime at a temperature of 700 °C was as indicated in Figure 4.29.

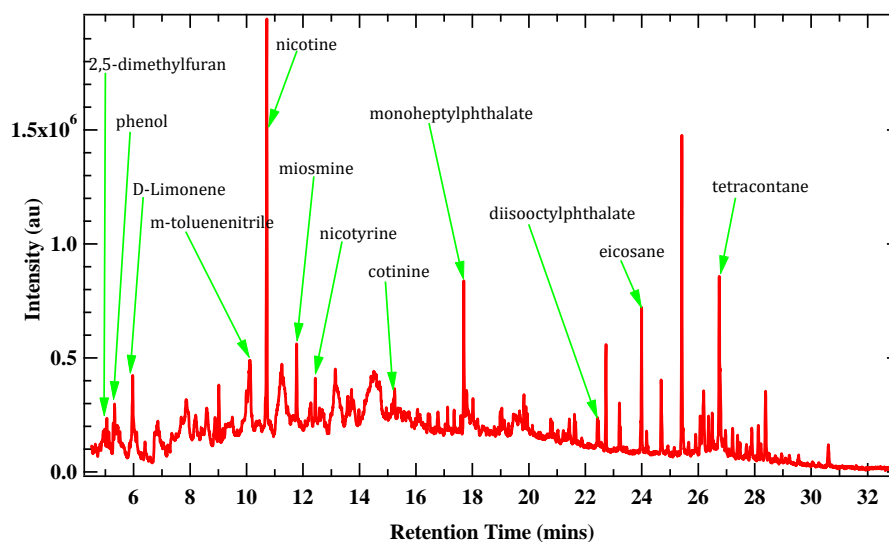


Figure 4.29: GC-MS chromatogram of products from tobacco pyrolysis in khat regime at 500 °C

The primary compounds and their relative distribution from the pyrolysis of the binary mixture of khat and tobacco exhibited variations in their abundance with nicotine, monoheptylphthalate, eicosane and tetracontane being the most abundant pyrolysis products. The second most abundant products included 2,5-dimethyl furan, phenol, D-limonene, m-toluenitrile, miosmine cotinine, and nicotyrine. Nicotine, monoheptylphthalate and tetracontane achieved maximum yields of 23.42, 32.27 and 20.85 wt % at 500 °C while eicosane achieved its maximum yield of 26.32 wt % at temperatures of 450 °C as illustrated in Figure 4.30a. This resulted into a two zoned decomposition regime within the temperature range of 300 °C and 700 °C. To this regard, the first decomposition zone for the high concentration pyrolysis products occurred between 300 °C and 450 °C while the second decomposition zone occurred above 450 °C (between 450 °C and 700 °C).

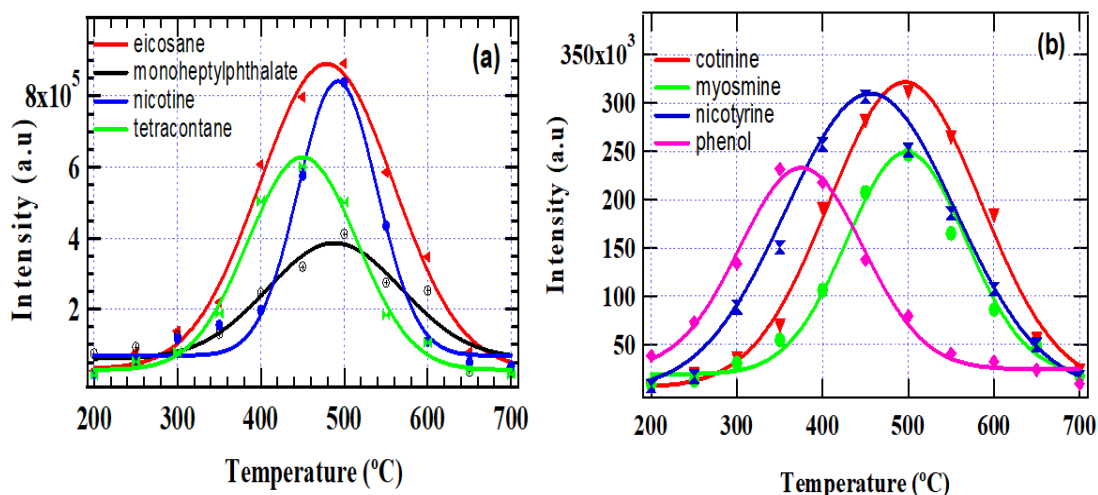


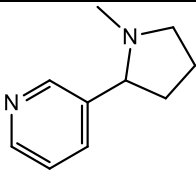
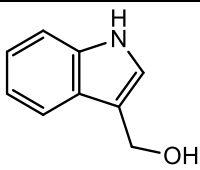
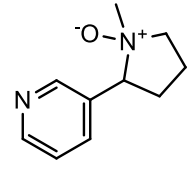
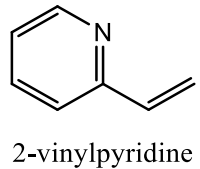
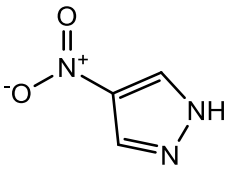
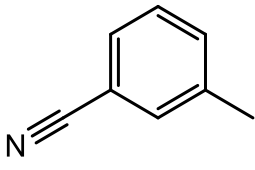
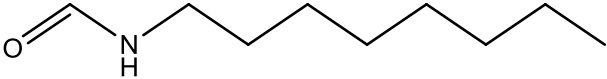
Figure 4.30: High concentration pyrolysis products (a) and low concentration pyrolysis product (b) from khat-tobacco binary mixture

Notably, throughout the pyrolysis temperatures it can be seen from Figure 4.30 (a) that nicotine exhibited the highest release concentrations compared to the other pyrolysis products. Remarkably, a majority of compounds that were categorized as low concentration pyrolysis products were produced at relatively low temperatures, precisely at 250 °C and reached a maximum yield at temperatures of about 350 °C and 500 °C as illustrated in Figure 4.30 (b). For instance, phenol had its decomposition regime beginning at 250 °C and end at 550 °C, with a maximum yield of 22.75 wt % attained at 350 °C. Likewise, myosmine, cotinine and nicotyrine had maximum wt % yields of 25.54, 21.43 and 20.89 at 500 °C, respectively.

Aromatic hydrocarbons such as benzene and its derivatives such as m-toluenitrile comprised of the category of these products. On the contrary to other studies that have focused on tobacco products release, common PAHs such as anthracene were not detected. This could be due to precursor oxidation to smaller compounds such as H₂O, CO and CO₂ during pyrolysis which is in agreement with Sharma and colleagues who have suggested that during biomass pyrolysis, the yields of pyrolysis

products may vary as a result of reactive species and their precursors getting oxidized before their formation (Sharma & Hajaligol, 2003). In addition, the analyzed khat-tobacco mixture samples revealed the presence of alkanes, pyridine derivatives, fatty acid esters and amides as listed in Table 4.7.

Table 4.7: Chemical formula and structure of some toxic/ carcinogenic components identified from pyrolysis of khat-tobacco binary mixture

S/No.	Component	S/No	Component
1.	 3-(1-Methyl-2-pyrrolidinyl) pyridine	2.	 indole-3-carbinol
3.	 (1s,2s)-Nicotine-N-oxide	4.	 2-vinylpyridine
5.	 4-nitropyrazole	6.	 m-toluenitrile
7.	 N-Octylformamide		

Some of these molecular products especially pyridine and its derivatives are known to damage the liver and kidneys, and cause severe effects to the brain (Bourget et al., 2014). Accordingly, the National Toxicology Program (2000) has tabled evidence on

pyridine and its derivatives as a potential carcinogen. Furthermore, the carcinogenic potential of octylformamide (an amide derivative) detected in khat-tobacco mixture has been reported in literature (Silva et al. (2020)). The carcinogenic activity of these class of compounds has been linked to occurrence of cleavage of a C-N bond in which the carbon fragment gets transferred to some nucleophilic atom, causing the amides to function as an alkylating agent (Wei et al., 2017). Once these amide compounds gain entry into the human biological system, the nucleophilic sites along the polymeric proteins are alkylated, disrupting the normal cell growth patterns (More et al., 2019).

4.4.1 Synergetic effects of khat on concentration of molecular products released during tobacco pyrolysis in khat regime

A GC-MS spectrum for the pyrolysis products generated from tobacco at a temperature of 500 °C is shown in Figure 4.31.

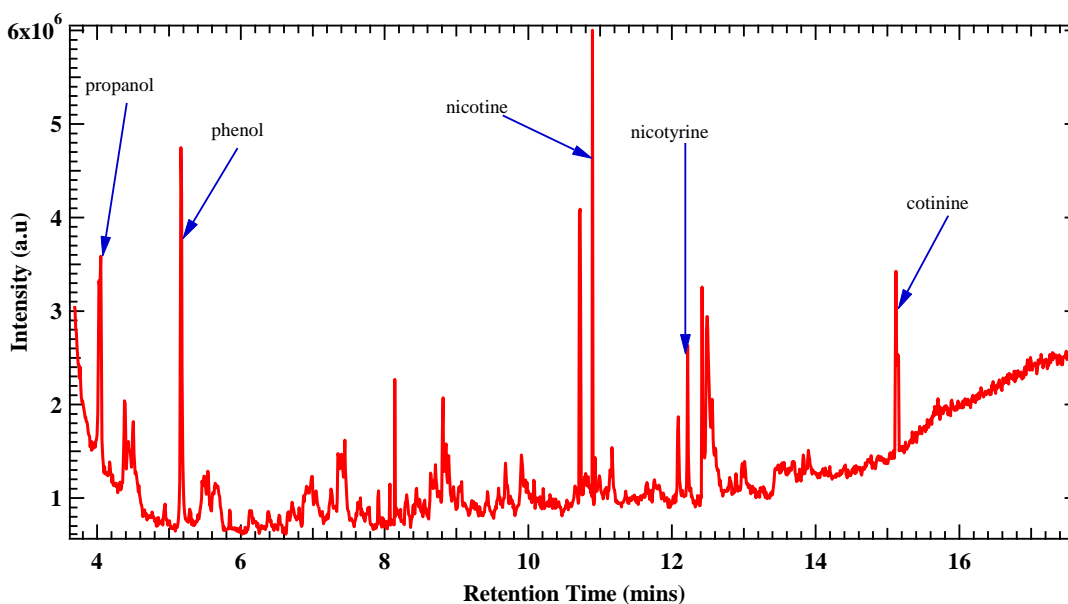


Figure 4.31: GC-MS chromatogram of products from tobacco pyrolysis at 500 °C

It can be noted that a number of compounds that were observed in tobacco-khat mixture pyrolysis were absent in the analyzed pure tobacco pyrolysis smoke. The interest of this study was to investigate the effects induced on nicotine concentration when tobacco is smoked in khat regime. It is important to note that nicotine, nicotyrine, and cotinine were some of the molecular products that were detected in both pure tobacco and tobacco-khat. A comparison in the concentration levels of these alkaloids partitioned in tobacco revealed a decrease in concentration throughout the pyrolysis temperature range. For instance, at a temperature of 500 °C, the variations were as illustrated as shown in Figure 4.32.

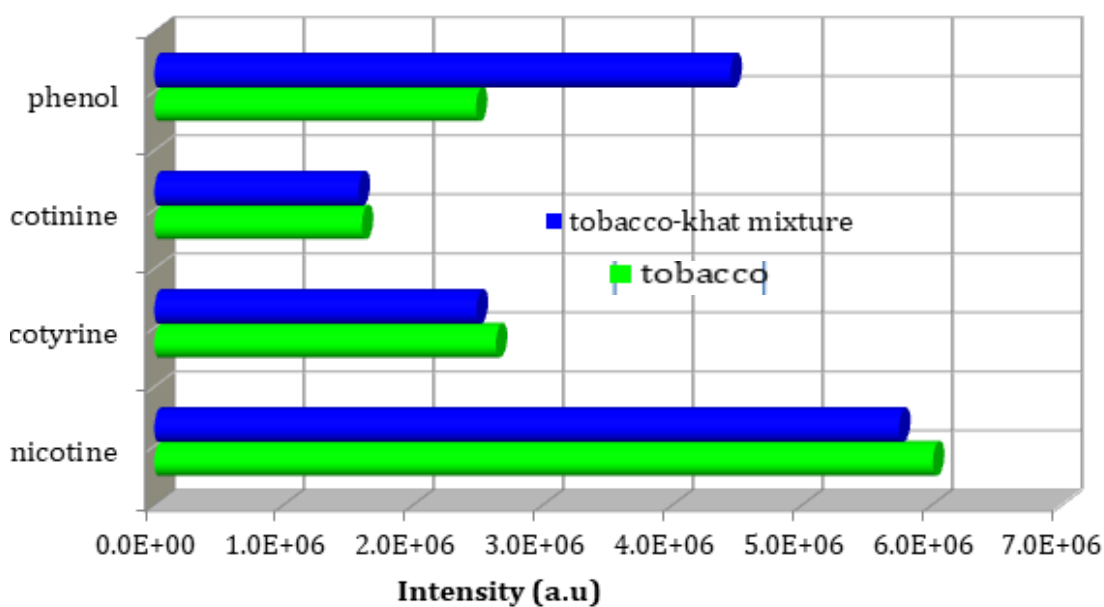


Figure 4.32: Comparison in concentration of molecular products released during pure tobacco pyrolysis and tobacco pyrolysis in khat regime at 500 °C.

It is evident that most of the alkaloids partitioned in khat displayed a minimal decrease in concentration levels when the pyrolysis was conducted in khat regime. For instance, nicotine, nicotyrine and cotinine had their concentration levels decrease by 4.34, 5.63 and 1.60 percent respectively. Phenol had its concentration increased by about 79.17 wt % when tobacco was heated in presence of 50 % khat. This

observation can be explained by the fact that khat pyrolysis is accompanied with the generation of phenol as discussed earlier. The mean comparisons are listed in Table 4.8 and Table 4.9.

Table 4.8: Paired samples statistics for tobacco and tobacco khat pyrolysis

		Mean	N	Std. Deviation	Std. Error Mean
Pair 1	Tobacco	3.1795 x10 ⁶	4	1.93695 x10 ⁶	9.68473 x10 ⁶
	Tobacco-khat	3.5617 x10 ⁶	4	1.88342 x10 ⁶	9.41712 x10 ⁵

The mean elemental composition of the molecular products generated from tobacco pyrolysis was 3.1795 x10⁶ whereas the mean concentration of the molecular compounds from marijuana mixed with khat was 3.5617 x 10⁶ respectively.

Table 4.9: Paired samples t-test for tobacco and tobacco khat pyrolysis

	Mean	Std. Deviation	Std. Error Mean	95% Confidence Interval of the Difference		t	df	Sig. (2- tailed)
				Lower	Upper			
Tobacco – Tobacco- khat	-3.82238 x10 ⁵	1.05856 x 10 ⁶	5.29281 x10 ⁵	-2.06665 x 10 ⁶	1.30217 x 10 ⁶	-0.722	3	0.522

The findings revealed that the mean difference between the molecular compounds generated from tobacco and tobacco mixed with khat was 3.82238E5 which is not statistically significant as per the p value (0.522 > 0.05). This implies that mixing tobacco with khat does not have any statistical significant effect in reducing the elemental compounds.

4.4.2 Synergetic effects of khat on concentration of molecular products released during tobacco pyrolysis in Marijuana

A GC-MS spectrum for the pyrolysis products generated from tobacco in marijuana regime at a temperature of 500 °C is shown in Figure 4.33.

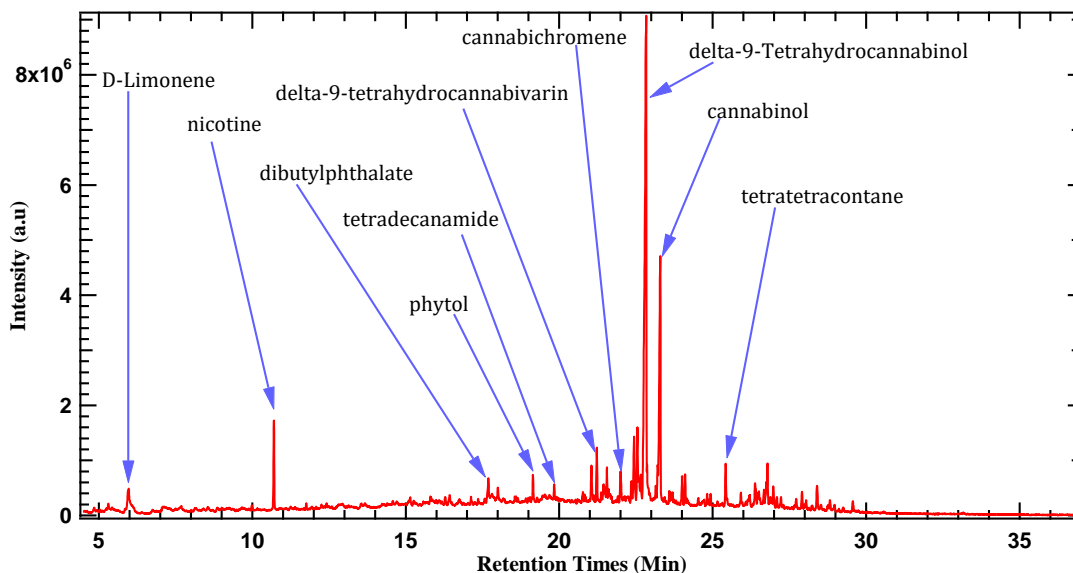


Figure 4.33: GC-MS chromatogram of products released from tobacco-marijuana mixture pyrolysis at 500 °C

It is evident from Figure 4.33 that a number of molecular products evolved during pure tobacco pyrolysis were not detected when tobacco pyrolysis was conducted in marijuana regime. For instance, compounds such as phenol, nicotyrine, and cotinine were not detected. Similarly, molecular compounds that were detected in pure marijuana pyrolysis such as caryophyllene and humulene were not detected. On the other hand, a decrease in phytocannabinoid levels was noted. For example, dronabinol, cannabinol and delta-9-tetrahydrocannabivarin recorded a decrease in their intensity levels by 45.59%, 63.89% and 81.02% respectively. A comparison of the level of intensities of the compounds released in marijuana pyrolysis to a racemic mixture of marijuana and tobacco is as illustrated in Figure 4.34.

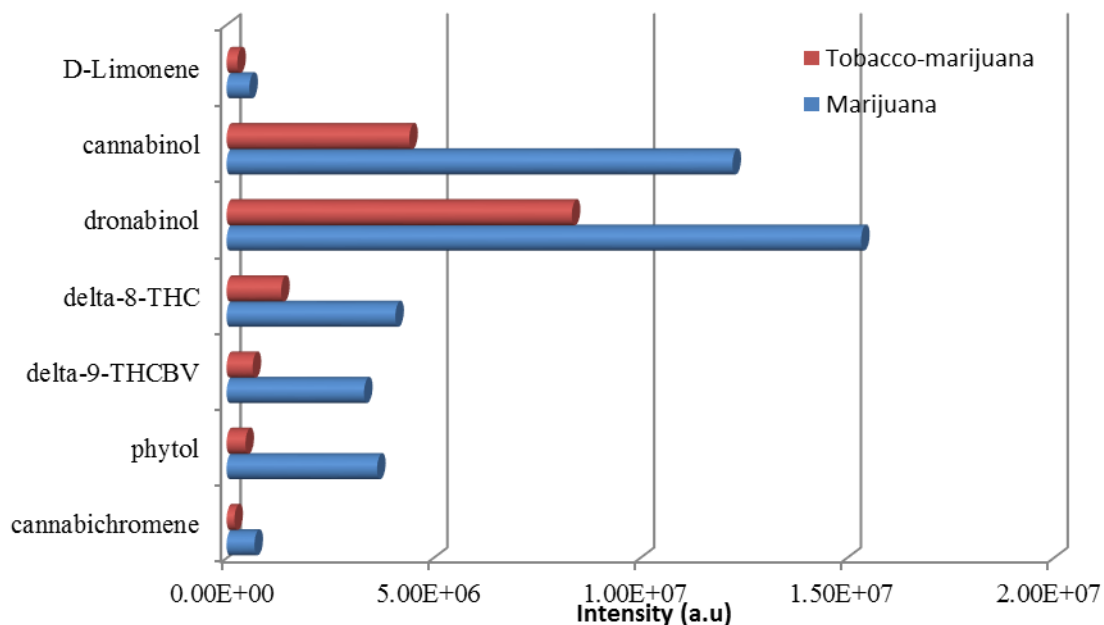


Figure 4.34: Level of intensities of the compounds released in marijuana pyrolysis to a racemic mixture of marijuana and tobacco

Interestingly, most of the compounds reported present in tobacco such as nicotine and cotinine were not detected. Even though nicotine was detected, the concentration levels were decreased by almost 40.03% of the levels reported in pure tobacco pyrolysis.

4.4.3 Synergetic effects of khat on the concentration of molecular products released during the co-pyrolysis of tobacco, khat and marijuana

A GC-MS spectrum for the pyrolysis products generated from tobacco in khat and marijuana at a temperature of 500 °C is shown in Figure 4.35. It is clear from Figure 4.35 that a number of compounds that were observed in the pyrolysis of tobacco-khat-marijuana combination were lacking in pure tobacco pyrolysis smoke. Our interest in this study was to explore the effects induced on nicotine concentration when tobacco is smoked in marijuana-khat regime. The results indicate that most of the molecular compounds dominantly present in tobacco smoke and marijuana

smoke are released during the pyrolysis of racemic mixture of tobacco, marijuana and khat.

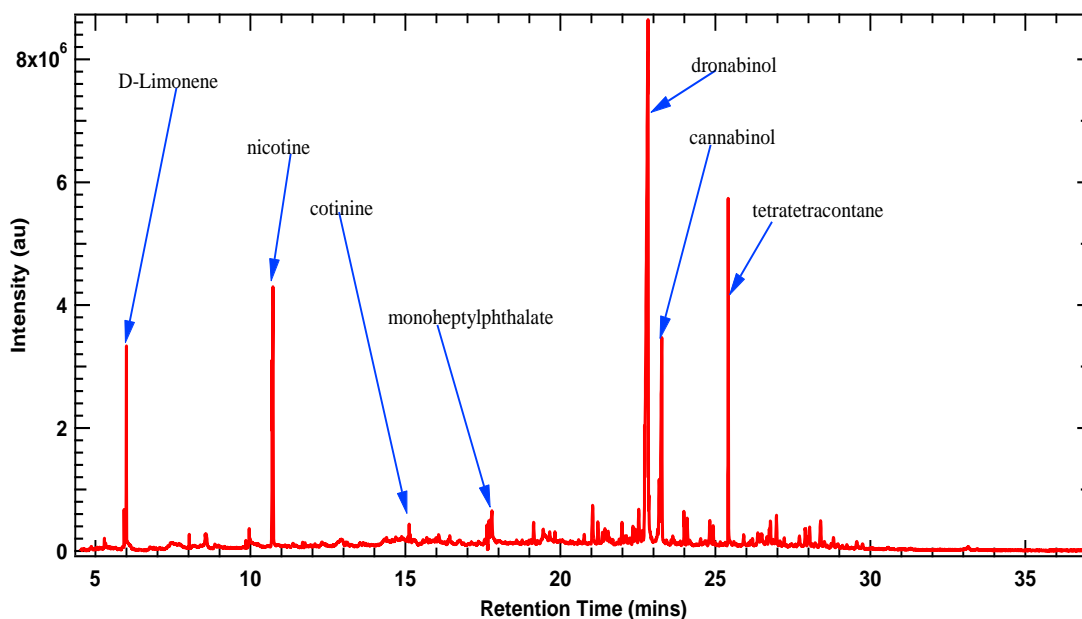


Figure 4.35: GC-MS chromatogram of products released from tobacco-marijuana-khat mixture pyrolysis at 700 °C

For instance, nicotine and cotinine found in tobacco smoke were detected but they showed variations in concentration, whereby lower intensities were noted in a racemic mixture of tobacco-marijuana-khat compared to the amounts that were recorded in pure tobacco and racemic mixture of tobacco-khat and tobacco-marijuana. Even though minimal levels of nicotine, a tobacco toxin, were recorded in this racemic mixture, it does not render it safe method of cigarette smoking given that the reaction is accompanied with high production of other environmentally toxic compounds such as tetratetracontane and D-limonene that have been identified to be potential carcinogens. Figure 4.36 gives a summary of the comparison in intensities of the compounds released from the racemic mixture of tobacco-marijuana-khat pyrolysis. Interestingly, phenols that were produced in higher concentration during

khat, tobacco and khat-tobacco racemic mixture pyrolysis were recorded in very low amounts.

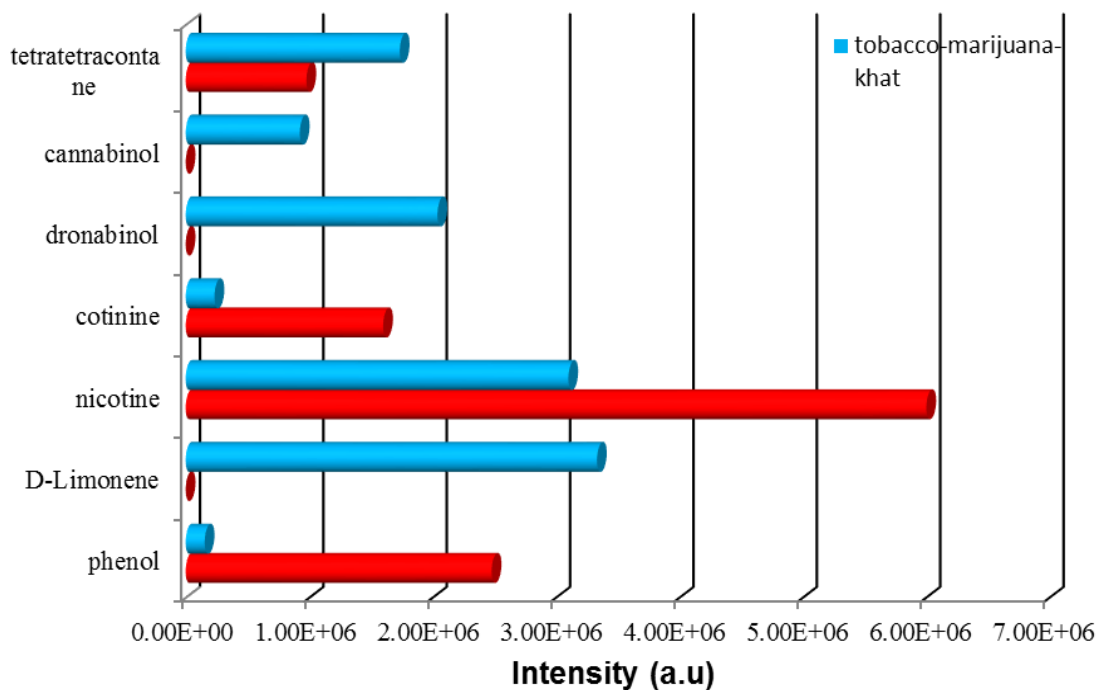


Figure 4.36: Comparison in intensity of molecular compounds released from tobacco-marijuana-khat racemic mixture with pure tobacco.

The quantities of the common phytocannabinoids present in marijuana such as tetrahydrocannabinol did not show much variation in their concentration release. This suggests that the smoker is likely to inhale much of these phytocannabinoids when smoking the racemic mixture of the three drugs just like in the case of pure marijuana, only that the individual is likely to ingest more toxic compounds such as tetratetracontane and D-limonene which have been identified as carcinogens.

Table 4.10: Paired samples statistics for molecular products generated from the pyrolysis of tobacco and tobacco marijuana pyrolysis

		Mean	N	Std. Deviation	Std. Error Mean
Pair 1	Tobacco	5.6931×10^6	7	5.77338×10^6	2.18213×10^6
	Tobacco-marijuana	2.2327×10^6	7	3.07670×10^6	1.16288×10^6

The mean molecular concentrations in tobacco were 5.6931×10^6 whereas the mean molecular concentrations in tobacco mixed marijuana was 2.2327×10^6 respectively.

Table 4.11: Paired samples t-test

	Mean	Std. Deviation	Std. Error Mean	95% Confidence Interval of the Difference		t	df	Sig. (2-tailed)
				Lower	Upper			
Pair 1 Tobacco – Tobacco-marijuana	3.46045 x 10 ⁶	2.93076 x 10 ⁶	1.10772 x 10 ⁶	7.49952 x 10 ⁵	6.17095 x 10 ⁶	3.124	6	0.020

Table 4.10 and Table 4.11 give a summary of the mean significances. The findings indicate that the mean difference of the molecular compounds generated from the pyrolysis of tobacco and tobacco mixed with marijuana was 3.46045×10^6 which is statistically significant as per the p value ($0.020 < 0.05$). This implies that mixing tobacco with marijuana significantly reduces the elemental compounds.

4.5 Thermogravimetric analysis and differential scanning calorimetry results

There are three decomposition regimes as in thermogravimetric analysis of tobacco-khat binary mixture. The first mass loss of 19.98% (3.40 mg) takes place between 148.28 ° C and 276.89 ° C whereas the second decomposition regime occurs between 284.67 ° C and 419.52 ° C accompanied by a mass loss of 21.46% (3.66 mg). The final decomposition regime begins from 419.52 ° C and ends at 700 ° C, corresponding to a mass loss of 22.96% (3.91 mg). Above 700 ° C, there is no significant mass loss because the substance is largely carbonaceous and remains constant at □ 15.68%. The copyrolysis behaviour of tobacco and khat binary mixture was investigated in this study using thermogravimetric analysis and the corresponding TGA curve was plotted as shown in Figure 4.37.

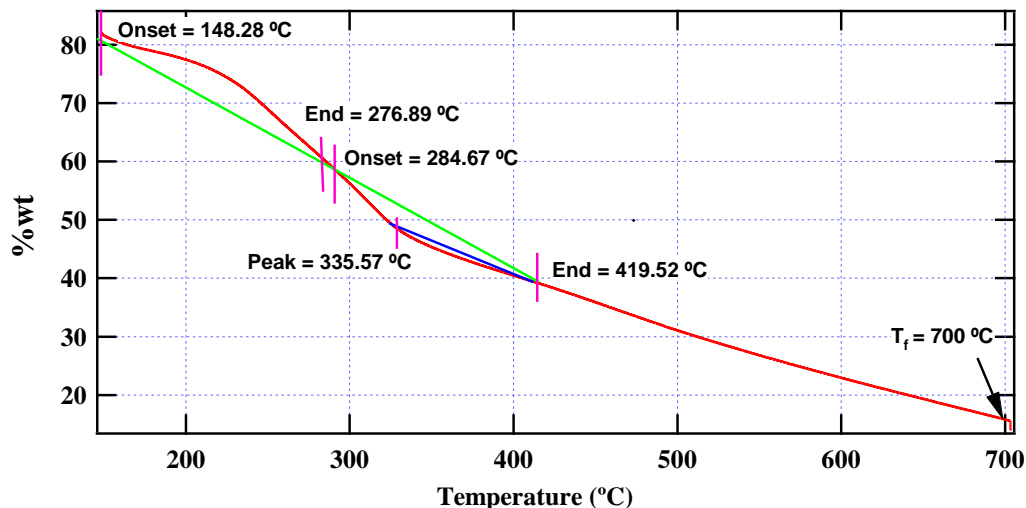


Figure 4.37: Tobacco-khat binary mixture weight loss at a heating rate of 5 °C/min

This implies that the char at the final decomposition temperature is approximately 2.67 mg. It is important to note that at the initial temperature of 148.28 °C, there was an initial mass loss of 17.86% (3.04 mg) mainly attributed to the loss of volatiles such as water vapour, CO₂, and methane. The mass balance from TGA is approximately 98% indicating a good thermal analysis of tobacco-khat binary mixture. On the other hand, the final mass loss during the decomposition of khat alone using the laboratory designed reactor (section 4.2) was 11.0% at 700 °C. This observation suggests that addition of tobacco to the pyrolysis of khat gives a high yield of thermal char possibly because of the high level of lignin content in tobacco (Kibet et al., 2012).

The differential scanning calorimetry curve, Figure 4.38, revealed that tobacco-khat reaction pathway during the biomass pyrolysis occurs in the exothermic zone. The reaction begins from a temperature of 148.31 °C. The first peak appears at about 269.14 °C and 397.98 °C where the enthalpy change was recorded as -246.01 J/g. The second peak was registered between 414.97 °C and 506.06 °C with an enthalpy

change of -131.66 J/g followed by an endothermic reaction that ends at $696.81 \text{ }^\circ\text{C}$. The enthalpy change recorded within the first zone was higher than the one recorded in the second peak. This is because at these temperatures, most thermo reactions lead to the formation of new reaction products and therefore more energy is given out for new bond formation.

At temperatures of $500 \text{ }^\circ\text{C}$ and above, the concentration of most pyrolysis products sharply decreased as observed in GC-MS results previously discussed in this study (section 4.11). The DSC curves at these temperatures reveal the endothermicity of reaction of biomass conversion to carbonaceous products. The TGA and DSC results agree GC-MS findings that revealed the yield of most molecular products occurs between $350 \text{ }^\circ\text{C}$ to $500 \text{ }^\circ\text{C}$ during the pyrolysis experiments.

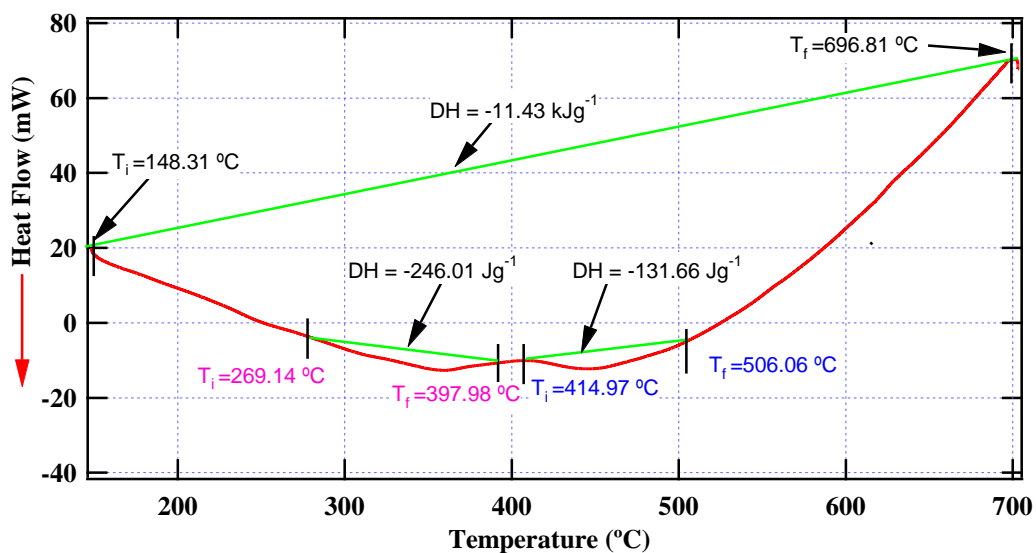


Figure 4.38: DSC curve for tobacco-khat binary mixture pyrolysis

4.6 Rejection or acceptance of hypotheses

This study was based on four formulated hypotheses; molecular products from the individual pyrolysis of tobacco, marijuana and khat will not be different from those evolved during the co-pyrolysis of tobacco, marijuana and khat, thermal char from the co-pyrolysis of tobacco and khat will not contain nitrogen as the major element, the thermal degradation data obtained from the pyrolysis of khat and tobacco binary mixtures using thermal analysis (TGA and DSC) will not be similar to the data obtained from the co-pyrolysis of tobacco and khat using laboratory designed thermal reactor and Gaussian '09 computational code cannot generate all the optimized geometries of the selected molecular compounds. The results obtained have revealed that the pyrolysis of the selected biomass materials under conditions that are simulative of cigarette smoking conditions within the smoking temperature range lead to the release of a number of molecular compounds in varying concentrations. Even though a slight similarity in released class of organic compounds was observed, it is important to note that the compounds released from the selected biomass materials were different. For instance, both khat and tobacco reported the release of alkaloids but there was no similarity in molecular structures and formula of the released alkaloids. The co-pyrolysis experiments on the other hand lead to the release of a number of molecular compounds whose molecular structures and formula were similar to those identified in the pyrolysis of pure biomass components. These observations lead to the acceptance of the first hypothesis, H1, which proposed that the molecular products from the individual pyrolysis of tobacco, marijuana and khat will not be different from those evolved during the co-pyrolysis of tobacco, marijuana and khat.

The second postulate, H2, inferred that thermal char from the co-pyrolysis of tobacco and khat will not contain nitrogen as the major element. The findings showed that the elemental components in tobacco-khat char samples had C, H, N, O and S. As discussed in section 4.3, it is evident that the most abundant element present in tobacco-khat char was C and O reported at 58.65% and 17.00% respectively. H, N and S reported fairly low concentrations ranges of 1.5% – 6.2%, 1.80% - 2.80%, and 0.10% - 0.45% respectively. These findings therefore lead to the nullification of the second hypothesis.

The third hypothesis, H3, suggested that the thermal degradation data obtained from the pyrolysis of khat and tobacco binary mixtures using thermal analysis (TGA and DSC) will not be similar to the data obtained from the co-pyrolysis of tobacco and khat using laboratory designed thermal reactor. The results obtained in this work were similar to pyrolysis data obtained by other studies performed elsewhere and therefore we reject the hypothesis.

The fourth hypothesis, H4, proposed that the optimized geometries of the selected molecular compounds cannot be generated. The computational data and the geometry structures for the molecules under study were generated using Gaussian '09 computational code. The data enabled us to analyse the geometric parameters such as bond lengths, bond angles and torsional strengths of the selected molecules. Further, the electronic properties including the HOMO and LUMO of the molecules were well investigated using Gaussian '09 computational code. To this regard therefore, hypothesis H4 is rejected.

CHAPTER FIVE

CONCLUSION AND RECOMMENDATION

5.1 Conclusion

This study has successfully analyzed the pyrolytic and thermal behaviour of khat, tobacco and marijuana in addition to selected binary mixtures under conditions that representative of cigarette smoking. This forms the basis towards understanding the pyrolytic characteristics of biomass, for selection of cigarette designs. The pyrolysis results from GCMS indicate that during the thermal degradation of khat, tobacco and marijuana biomass, numerous toxic molecular products that generate environmentally persistent free radicals are released throughout the pyrolysis temperature (200 °C -700 °C).

The pyrolysis of khat displayed the release of most phenolic compounds such as *p*-cresol, catechol, hydroquinone and other substituted methoxy phenols including 3-methoxy phenol in temperatures ranging between 300 °C and 500 °C. Remarkably, the findings indicate that most of the phenolic compounds are produced when the pyrolysis reaction is undertaken at high temperatures of about >300 °C. Of the phenolic compounds reported in khat pyrolysis, it was noted that hydroquinone and *p*-cresol registered high levels. Hydroquinone was released in high yields throughout the pyrolysis temperature.

Similarly, the evolution of *p*-cresol in khat smoke is of significant concern because of its association with human and environmental toxicological consequences given that it is a protein bound uremic toxin and readily converts into highly reactive radicals that are likely to initiate reactive oxygen species that are deleterious to human tissues. Numerous nitrogen containing compounds were generated in high yields in the temperature range 450 °C – 550 °C. This included 2, 4, 5-

trimetyloxazole, 1-methyl-2,5-pyrrolidinedione and 2- amino-1-naphthalenol N-phenoxyacetamide, indole and 4-methoxypyridine-N-oxide. Most of these nitrogen containing compounds in khat exhibit ring aromatism and are likely to break down at high temperatures to yield hydrogen cyanide which is responsible for cancer and death in humans. This study has therefore has demonstrated that these toxins are produced in higher concentration at temperatures between 350 °C to 700 °C.

The pyrolysis of marijuana biomass gave rise to molecular compounds such as phytol, and other class of organic compounds including 9-athracarbonitrile, cannabidiol, tetrahydrocannabinol, Δ -9- tetrahydrocannabivarin, cannabigerol, and 2,6-dimethylhydroquinone whose concentrations varied with temperature. More importantly, most of the compounds detected in marijuana smoke such a phytol are known to offer antitumor properties and therefore has medicinal properties for the treatment of oxidative stress induced diseases. Additionally, humulene has a potential to help in terminating cancer cells when in combination with other phytocannabinoids and terpenes. On the other hand, cannabidiol which was released in high concentration at high temperature can be used as an opioid to minimize body pains, seizures and irritations in patients. Therefore, most products released from the thermal degradation of marijuana were found to be of significant health values as reported by other researchers in literature, and therefore marijuana can be or has beneficial medicinal properties if used appropriately.

The co-pyrolysis experiments exhibited remarkable results given that some mixtures of biomass involved induced effects on each other by either causing a decrease or increasing the yield of the molecular products released. For instance, the pyrolysis of marijuana in khat regime reported a decrease in the concentration of most of the

phytocannabinoids such as cannabichromene, cannabicycoumaronone, delta-9-tetrahydrocannabivarin, cannabigerol, and cannabiol. Similar effects were noted when tobacco was pyrolysed in khat regime. For instance, nicotine, nicotyrine and cotinine had their concentration levels decrease by 4.34%, 5.63% and 1.60%, respectively. Although an increase in yield was observed in the evolution of phenols. The same observations were made when tobacco was thermally degraded in marijuana-khat regime. Therefore, the pyrolysis of tobacco in khat can lower nicotine levels in tobacco. This is very important in the introduction of khat additive for the manufacture of less toxic cigarettes.

The use of TGA and DSC data has successfully enabled an overview of the thermal decomposition behaviour of tobacco and khat biomass and revealed that much of the biomass weight is lost between 250 °C and 500 °C the second decomposition regime. For instance, tobacco-khat mixture had the regime occur between 284.67 ° C and 419.52 ° C and was accompanied by a mass loss of 21.46% (3.66 mg), the same temperature range where most organic toxins are released. This is a replication of the thermal degradation patterns of most biomass materials.

The molecular geometry properties such as bond lengths and bond angles were analyzed using Gaussian '09 computational platform. From the bond strengths derived theoretically, phenolic compounds such as *p*-cresol readily undergo reactions that lead to the formation of radicals, and well-established carcinogens in the human biosystem. This was further confirmed by the electronic properties that revealed *p*-cresol to have the lowest and gap energy suggesting that *p*-cresol is the most unstable phenol and hence more reactive since it requires very little excitation energy for it to be excited from the HOMO to the LUMO.

5.2 Recommendation

This study aimed at determining the molecular products released from the pyrolysis of tobacco, marijuana, and khat and their binary mixtures, and explored the elemental composition of the thermal char from the pyrolysis of tobacco-khat binary mixture using elemental analyzer and thermal analysis techniques. Furthermore, geometrical optimization and the reactivity coefficients (band-gap energies) for selected products were performed. By examining the findings of this study, the following recommendations are proposed.

1. Most toxic reaction products are evolved above 300 ° C hence there is need to design cigarettes that can be smoked below 300 ° C by use of catalytic inhibitors such as khat or marijuana additives. This can also be achieved by designing advanced smoking pipes fitted with thermal controllers for monitoring the temperatures during smoking. Besides, the use of fine pored filters can help in regulating the rate of air flow during smoke puffing and probably aid in lowering temperatures.
2. The smoking of khat was confirmed to be a possible route through which more toxic phenolic compounds are produced. These findings of this study should form the basis under which smoking of khat should be highly discouraged.
3. The analysis of the molecular products released during the pyrolysis of marijuana resulted in the yield of molecular compounds such as phytol, and other classes of organic compounds including 9-athracarbonitrile, cannabidiol, tetrahydrocannabinol, delta-9- tetrahydrocannabivarin, cannabigerol, and 2,6-dimethylhydroquinone. Most of these organic compounds have been reported to be of medicinal value and therefore

recommended for pyrosynthesis to help in the medical field possible as opioids or for the treatment of viral diseases.

4. This study was limited to laboratory experiments on the release of toxic molecular products from the pyrolysis of tobacco, khat and marijuana and therefore, future research should be extended to bioassays to ascertain their possible biological impact on animal and human health.

REFERENCES

- Abdel-Shafy HI, Mansour MS (2016) A review on polycyclic aromatic hydrocarbons: source, environmental impact, effect on human health and remediation. *Egyptian Journal of Petroleum*, 25(1); 107-123. doi: 10.1016/j.ejpe.2015.03.011
- Abebe M, Kindie S, Adane K (2015) Adverse health effects of khat: a review. *Family Medicine & Medical Science Research*, 4(1); 2-5. doi: 10.4172/2327-4972.1000154
- Abrams DB, Glasser AM, Pearson JL, Villanti AC, Collins LK, Niaura RS (2018) Harm minimization and tobacco control: reframing societal views of nicotine use to rapidly save lives. *Annual review of public health*, 39; 193-213. doi: 10.1146/annurev-publhealth-040617-013849
- Ademe BW, Brimer L, Dalsgaard A, Belachew T (2020) Chemical and microbiological hazards of Khat (*Catha edulis*) from field to chewing in Ethiopia. *GSC Biological and Pharmaceutical Sciences*, 11(1); 024-035. doi: 10.30574/gscbps.2020.11.1.0038
- Adole VA, Pawar TB, Jagdale BS (2021) DFT computational insights into structural, electronic and spectroscopic parameters of 2-(2-Hydrazineyl) thiazole derivatives: a concise theoretical and experimental approach. *Journal of Sulfur Chemistry*, 42(2); 131-148.
- Al- Maweri SA, Warnakulasuriya S, Samran A (2018) Khat (*Catha edulis*) and its oral health effects: An updated review. *Journal of Investigative and Clinical Dentistry*, 9(1); e12288. doi: 10.1111/jicd.12288
- Alshagga MA, Alshawsh MA, Seyedan A, Alsalahi A, Pan Y, Mohankumar SK et al. (2016) Khat (*Catha edulis*) and obesity: A scoping review of animal and human studies. *Annals of Nutrition and Metabolism*, 69(3-4); 200-211. doi: 10.1159/000452895
- Anderson GD, Chan L-N (2016) Pharmacokinetic drug interactions with tobacco, cannabinoids and smoking cessation products. *Clinical pharmacokinetics*, 55(11); 1353-1368. doi: 10.1007/s40262-016-0400-9
- Apelberg BJ, Feirman SP, Salazar E, Corey CG, Ambrose BK, Paredes A et al. (2018) Potential public health effects of reducing nicotine levels in cigarettes in the United States. *New England Journal of Medicine*, 378(18); 1725-1733.
- Archie SR, Cucullo L (2019) Harmful Effects of Smoking Cannabis: A Cerebrovascular and Neurological Perspective. *Frontiers in pharmacology*, 10; 1481-1481. doi: 10.3389/fphar.2019.01481
- Armendáriz-Castillo I, Guerrero S, Vera-Guapi A, Cevallos-Vilatuña T, García-Cárdenas JM, Guevara-Ramírez P et al. (2019) Genotoxic and Carcinogenic Potential of Compounds Associated with Electronic Cigarettes: A Systematic Review. *Hindawi*, 2019. doi: 10.1155/2019/1386710
- Arora HC, Fascelli M, Zhang JH, Isharwal S, Campbell SC (2018) Kidney, ureteral, and bladder cancer: a primer for the internist. *Medical Clinics*, 102(2); 231-249. doi: 10.1016/j.mcna.2017.10.002

- Ashok M, Girish R, Varsha N (2017) Know Your Cough: A New Index to Assess Effects of Cough Severity on Patient's Health and Overall Symptoms—An Indian Survey Report. *Primary Health Care*, 7(277); 2167-1079.1000277. doi: 10.4172/2167-1079.1000277
- Assaf NW, Altarawneh M, Oluwoye I, Radny M, Lomnicki SM, Dlugogorski BZ (2016) Formation of environmentally persistent free radicals on α -Al₂O₃. *Environmental science & technology*, 50(20); 11094-11102. doi: 10.1021/acs.est.6b02601
- Atakan Z (2012) Cannabis, a complex plant: different compounds and different effects on individuals. *Therapeutic advances in psychopharmacology*, 2(6); 241-254. doi: 10.1177/2045125312457586
- Atlabachew M, Chandravanshi BS, Redi-Abshiro M (2017) Preparative HPLC for large scale isolation, and salting-out assisted liquid-liquid extraction based method for HPLC-DAD determination of khat (*Catha edulis* Forsk) alkaloids. *Chemistry Central Journal*, 11(1); 107-107. doi: 10.1186/s13065-017-0337-6
- Atlabachew M, Chandravanshi BS, Redi M (2014) Selected Secondary Metabolites and Antioxidant Activity of Khat (*Catha edulis* Forsk) Chewing Leaves Extract. *International Journal of Food Properties*, 17(1); 45-64. doi: 10.1080/10942912.2011.614367
- Auer R, Concha-Lozano N, Jacot-Sadowski I, Cornuz J, Berthet A (2017) Heat-not-burn tobacco cigarettes: smoke by any other name. *JAMA internal medicine*, 177(7); 1050-1052. doi: 10.1001/jamainternmed.2017.1419
- Baali A, Yahyaoui A (2019) Polycyclic Aromatic Hydrocarbons (PAHs) and Their Influence to Some Aquatic Species Organic Pollutants: IntechOpen doi: 10.5772/intechopen.86213
- Babalik M, Topaloğlu İ, Saltürk Z, Berkiten G, Atar Y, Tutar B et al. (2018) The Effects of Exposure to Environmental Cigarette Smoke on the Vocal Folds of Rats. *Journal of Voice*, 32(6); 652-654. doi: 10.1016/j.jvoice.2017.09.006
- Baer R, Kronik L (2018) Time-dependent generalized Kohn–Sham theory. *The European Physical Journal B*, 91(7); 1-9.
- Baker RR (2006) Smoke generation inside a burning cigarette: modifying combustion to develop cigarettes that may be less hazardous to health. *Progress in Energy and Combustion Science*, 32(4); 373-385.
- Bakshi S, Banik C, Laird DA (2020) Estimating the organic oxygen content of biochar. *Scientific Reports*, 10(1); 13082. doi: 10.1038/s41598-020-69798-y
- Baldwin J. (2020). Healthiest Ways To Consume Weed: Better Than Smoking. <https://www.weednews.co/healthiest-ways-to-consume-cannabis/>
- Bartocci E, Lió P (2016) Computational Modeling, Formal Analysis, and Tools for Systems Biology. *PLOS Computational Biology*, 12(1); e1004591. doi: 10.1371/journal.pcbi.1004591
- Barzegar F, Kamankesh M, Mohammadi A (2019) Heterocyclic aromatic amines in cooked food: A review on formation, health risk-toxicology and their analytical techniques. *Food chemistry*, 280; 240-254. doi: 10.1016/j.foodchem.2018.12.058

- Bauld L, MacKintosh AM, Eastwood B, Ford A, Moore G, Dockrell M et al. (2017) Young people's use of e-cigarettes across the United Kingdom: findings from five surveys 2015–2017. *International journal of environmental research and public health*, 14(9); 973.
- Baumung C, Rehm J, Franke H, Lachenmeier DW (2016) Comparative risk assessment of tobacco smoke constituents using the margin of exposure approach: the neglected contribution of nicotine. *Scientific Reports*, 6; 35577.
- Beale C, Broyd SJ, Chye Y, Suo C, Schira M, Galettis P et al. (2018) Prolonged Cannabidiol Treatment Effects on Hippocampal Subfield Volumes in Current Cannabis Users. *Cannabis and cannabinoid research*, 3(1); 94-107. doi: 10.1089/can.2017.0047
- Beckwith A (2021) *The Tunneling Hamiltonian in Functional Quantum Field Theory*
- Benowitz NL, Burbank AD (2016) Cardiovascular toxicity of nicotine: implications for electronic cigarette use. *Trends Cardiovasc Med*, 26(6); 515-523. doi: 10.1016/j.tcm.2016.03.001
- Benowitz NL, Henningfield JE (2018) Nicotine Reduction Strategy: State of the science and challenges to tobacco control policy and FDA tobacco product regulation. *Preventive medicine*, 117; 5-7.
- Bevilacqua L, Goldman D (2009) Genes and addictions. *Clinical pharmacology and therapeutics*, 85(4); 359. doi: 10.1038/clpt.2009.6
- Binkley JS, Pople JA, Hehre WJ (1980). *America Chemical Society*, 102; 939.
- Bisallah¹ CI, Rampal¹ L, Sidik SM, Iliyasu Z, Lye M-S, Onyilo MO (2018) Knowledge, Attitude and Preventive Practices Regarding Tuberculosis and Its Predictors among HIV Patients in General Hospital, Minna, North-Central, Nigeria. *Malaysian Journal of Medicine and Health Sciences*, 14(1).
- Bjurlin MA, Matulewicz RS, Roberts TR, Dearing BA, Schatz D, Sherman S et al. (2020) Carcinogen Biomarkers in the Urine of Electronic Cigarette Users and Implications for the Development of Bladder Cancer: A Systematic Review. *European Urology Oncology*. doi: 10.1016/j.euo.2020.02.004
- Bloomfield MAP, Ashok AH, Volkow ND, Howes OD (2016) The effects of $\Delta(9)$ -tetrahydrocannabinol on the dopamine system. *Nature*, 539(7629); 369-377. doi: 10.1038/nature20153
- Blunt JW, Copp BR, Keyzers RA, Munroa M, Prinsep MR (2016) Natural product reports. *Natural Products Report*, 33; 382-431.
- Borgan F, Beck K, Butler E, McCutcheon R, Veronese M, Vernon A et al. (2019) The effects of cannabinoid 1 receptor compounds on memory: a meta-analysis and systematic review across species. *Psychopharmacology*, 236(11); 3257-3270. doi: 10.1007/s00213-019-05283-3
- Bourget P, Amin A, Dupont C, Abely M, Desmazes-Dufeu N, Dubus J et al. (2014) How to minimize toxic exposure to pyridine during continuous infusion of ceftazidime in patients with cystic fibrosis? *Antimicrobial agents and chemotherapy*, 58(5); 2849-2855.

- Bouzzine SM, Salgado-Morán G, Hamidi M, Bouachrine M, Pacheco AG, Glossman-Mitnik D (2015) DFT Study of Polythiophene Energy Band Gap and Substitution Effects. *Journal of Chemistry*, 2015; 296386. doi: 10.1155/2015/296386
- Bray F, Ferlay J, Soerjomataram I, Siegel RL, Torre LA, Jemal A (2018) Global cancer statistics 2018: GLOBOCAN estimates of incidence and mortality worldwide for 36 cancers in 185 countries. *CA: a cancer journal for clinicians*, 68(6); 394-424. doi: 10.3322/caac.21492
- Bruni N, Della Pepa C, Oliaro-Bosso S, Pessione E, Gastaldi D, Dosio F (2018) Cannabinoid Delivery Systems for Pain and Inflammation Treatment. *Molecules (Basel, Switzerland)*, 23(10); 2478. doi: 10.3390/molecules23102478
- Byers C (2017) *Marijuana Smoking and the Risk of Developing COPD, Lung Cancer, And/or Chronic Respiratory Symptoms: A Systematic Review*. The University of Arizona. Retrieved from <https://repository.arizona.edu/bitstream/handle/10150/623758/ByersC%20Poster.pdf?sequence=1&isAllowed=y>
- Cai B, Ji H, Fannin FF, Bush LP (2016) Contribution of nicotine and nor nicotine toward the production of N'-Nitrosonor nicotine in air-cured tobacco (*Nicotiana tabacum*). *Journal of natural products*, 79(4); 754-759. doi: 10.1021/acs.jnatprod.5b00678
- Callaghan RC, Allebeck P, Akre O, McGlynn KA, Sidorchuk A (2017) Cannabis use and incidence of testicular cancer: a 42-year follow-up of Swedish men between 1970 and 2011. *Cancer Epidemiology and Prevention Biomarkers*, 26(11); 1644-1652. doi: 10.1158/1055-9965
- Capelle K (2006) A bird's-eye view of density-functional theory. *Brazilian Journal of Physics*, 36(4A); 1318-1343.
- Carlsen KCL, Skjerven HO, Carlsen K-H (2018) The toxicity of E-cigarettes and children's respiratory health. *Paediatric respiratory reviews*, 28; 63-67.
- CDCP (2010a) Chemistry and Toxicology of Cigarette Smoke and Biomarkers of Exposure and Harm *How Tobacco Smoke Causes Disease: The Biology and Behavioral Basis for Smoking-Attributable Disease: A Report of the Surgeon General: Centers for Disease Control and Prevention (US)*
- CDCP (2010b) Publications and Reports of the Surgeon General., In Office of the Surgeon General (Ed.), *How Tobacco Smoke Causes Disease: The Biology and Behavioral Basis for Smoking-Attributable Disease: A Report of the Surgeon General*, . Atlanta (GA): Centers for Disease Control and Prevention (US) Retrieved from <https://www.ncbi.nlm.nih.gov/pubmed/21452462>
- CDCP (2018) Facts about Benzene [Press release]. Retrieved from [https://emergency.cdc.gov/agent/benzene/basics/facts.asp#:~:text=\(Long%2Dterm%20exposure%20means%20exposure,increasing%20the%20chance%20for%20infection.](https://emergency.cdc.gov/agent/benzene/basics/facts.asp#:~:text=(Long%2Dterm%20exposure%20means%20exposure,increasing%20the%20chance%20for%20infection.)
- Chen C-H (2020) Foreign Compounds: Foods, Drugs, and Other Chemicals Xenobiotic Metabolic Enzymes: Bioactivation and Antioxidant Defense (pp. 11-22): Springer doi: 10.1007/978-3-030-41679-9_2

- Clatici VG, Racoceanu D, Dalle C, Voicu C, Tomas-Aragones L, Marron SE et al. (2017) Perceived Age and Life Style. The Specific Contributions of Seven Factors Involved in Health and Beauty. *Maedica*, 12(3); 191-201.
- Coddington H. (2017). Dabbing, Terpenes, and the Possibility of Carcinogens. <https://gopurepressure.com/blogs/rosin-education/dabbing-terpenes-and-the-possibility-of-carcinogens>
- Cohen K, Kapitány-Fövény M, Mama Y, Arieli M, Rosca P, Demetrovics Z et al. (2017) The effects of synthetic cannabinoids on executive function. *Psychopharmacology*, 234(7); 1121-1134.
- Cohen K, Weizman A, Weinstein A (2019) Positive and negative effects of cannabis and cannabinoids on health. *American Society for Clinical Pharmacology and Therapeutics*, 105(5); 1139-1147. doi: 10.1002/cpt.1381
- Coleman HG, Xie S-H, Lagergren J (2018) The epidemiology of esophageal adenocarcinoma. *Gastroenterology*, 154(2); 390-405. doi: 10.1053/j.gastro.2017.07.046
- Craig B, Skylaris C-K, Schoetz T, de León CP (2020) A computational chemistry approach to modelling conducting polymers in ionic liquids for next generation batteries. *Energy Reports*, 6; 198-208.
- Crombie K, Mašek O, Sohi SP, Brownsort P, Cross A (2013) The effect of pyrolysis conditions on biochar stability as determined by three methods. *Gcb Bioenergy*, 5(2); 122-131.
- Curtiss LA, Raghavachari K, Redfern PC, Pople JA (2000) Assessment of Gaussian-3 and density functional theories for a larger experimental test set. *The Journal of chemical physics*, 112(17); 7374-7383.
- Czajczyńska D, Anguilano L, Ghazal H, Krzyżyńska R, Reynolds A, Spencer N et al. (2017) Potential of pyrolysis processes in the waste management sector. *Thermal Science and Engineering Progress*, 3; 171-197.
- D'Arienzo M, Gamba L, Morazzoni F, Cosentino U, Greco C, Lasagni M et al. (2017) Experimental and Theoretical Investigation on the Catalytic Generation of Environmentally Persistent Free Radicals from Benzene. *The Journal of Physical Chemistry C*, 121(17); 9381-9393. doi: 10.1021/acs.jpcc.7b01449
- d'Ettore G, Criscuolo M, Mazzotta M (2017) Managing formaldehyde indoor pollution in anatomy pathology departments. *IOS Press*, 56(3); 397-402. doi: 10.3233/WOR-172505
- Dasgupta A, Klein K (2014) Oxidative Stress Caused by Cigarette Smoking, Alcohol Abuse, and Drug Abuse (pp. 59-75)
- de Alencar MVOB, Islam MT, de Lima RMT, Paz MFCJ, Dos Reis AC, da Mata AMOF et al. (2019) Phytol as an anticarcinogenic and antitumoral agent: An in vivo study in swiss mice with DMBA- Induced breast cancer. *IUBMB life*, 71(2); 200-212.

- De Flora S, Ganchev G, Iltcheva M, La Maestra S, Micale RT, Steele VE et al. (2016) Pharmacological modulation of lung carcinogenesis in smokers: preclinical and clinical evidence. *Trends in pharmacological sciences*, 37(2); 120-142. doi: 10.1016/j.tips.2015.11.003
- de Godoy Lusso MF, Hayes AJ, Lion K, Davis G, Hart III RF, Morris JW (2019) Methods of reducing tobacco-specific nitrosamines (TSNAs) and/or improving leaf quality in tobacco. Retrieved from <https://patents.google.com/patent/US10390556B2/en>
- De Las Heras I, Dufour J, Coto B (2021) A novel method to obtain solid–liquid equilibrium and eutectic points for hydrocarbon mixtures by using differential scanning calorimetry and numerical integration. *Fuel*, 297; 120788.
- DEA (2019) Khat [Press release]. Retrieved from https://www.deadiversion.usdoj.gov/drug_chem_info/khat.pdf
- Deng N, Jing X, Cai R, Gao J, Shen C, Zhang Y et al. (2019) Molecular simulation and experimental investigation for thermodynamic properties of new refrigerant NBY-1 for high temperature heat pump. *Energy Conversion and Management*, 179; 339-348.
- DeVito EE, Krishnan-Sarin S (2018) E-cigarettes: impact of E-liquid components and device characteristics on nicotine exposure. *Current neuropharmacology*, 16(4); 438-459. doi: 10.2174/1570159X15666171016164430
- Dhabbah AM (2020) Determination of chiral cathinone in fresh samples of *Catha edulis*. *Forensic Science International*, 307; 110105. doi: 10.1016/j.forsciint.2019.110105
- Dong H, Xian Y, Li H, Bai W, Zeng X (2020) Potential carcinogenic heterocyclic aromatic amines (HAAs) in foodstuffs: Formation, extraction, analytical methods, and mitigation strategies. *Comprehensive Reviews in Food Science and Food Safety*, 19(2); 365-404. doi: 10.1111/1541-4337.12527
- Drazen JM, Morrissey S, Champion EW (2019) The dangerous flavors of e-cigarettes. *the New England Journal of Medicine*. doi: 10.1056/NEJMe1900484
- Drugs.com (2019) khat [Press release]. Retrieved from <https://www.drugs.com/npp/khat.html>
- Drzeżdżon J, Jacewicz D, Chmurzyński L (2018) The impact of environmental contamination on the generation of reactive oxygen and nitrogen species—Consequences for plants and humans. *Environment international*, 119; 133-151.
- Dunne FJ, Jaffar K, Hashmi S (2015) Legal Highs-Not so new and still growing in popularity. *British Journal of Medical Practitioners*, 8(1).
- DWAF (2013) Protected trees. Republic of South Africa [Press release]. Retrieved from <http://www2.dwaf.gov.za/dwaf/cmsdocs/4116poster%20protected%20trees.pdf>

- Eaton D, Jakaj B, Forster M, Nicol J, Mavropoulou E, Scott K et al. (2018) Assessment of tobacco heating product THP1. 0. Part 2: Product design, operation and thermophysical characterisation. *Regulatory Toxicology and Pharmacology*, 93; 4-13.
- Edwards SH, Rossiter LM, Taylor KM, Holman MR, Zhang L, Ding YS et al. (2017) Tobacco-specific nitrosamines in the tobacco and mainstream smoke of US commercial cigarettes. *Chemical research in toxicology*, 30(2); 540-551. doi: 10.1021/acs.chemrestox.6b00268
- El-Hellani A, El-Hage R, Baalbaki R, Salman R, Talih S, Shihadeh A et al. (2015) Free-base and protonated nicotine in electronic cigarette liquids and aerosols. *Chemical research in toxicology*, 28(8); 1532-1537. doi: 10.1021/acs.chemrestox.5b00107
- El Foujji L, El Bourakadi K, Mekhzoum MEM, Essassi EM, Boéré RT, Bouhfid R (2020) Synthesis, crystal structure, spectroscopic, thermal properties and DFT calculation of a novel ethyl 2-(2-(thiazol-4-yl)-1H-benzimidazol-1-yl) acetate. *Journal of Molecular Structure*, 1209; 127939.
- EMCDDA (2015) Khat Drug Profile [Press release]. Retrieved from <https://www.emcdda.europa.eu/publications/drug>
- EMCDDA (2020) synthetic cathinones drug profile [Press release]. Retrieved from https://www.emcdda.europa.eu/publications/drug-profiles/synthetic-cathinones_en
- Etemadi A, Poustchi H, Chang CM, Blount BC, Calafat AM, Wang L et al. (2019) Urinary biomarkers of carcinogenic exposure among cigarette, waterpipe, and smokeless tobacco users and never users of tobacco in the Golestan Cohort Study. *Cancer Epidemiology Biomarkers and Prevention*, 28(2); 337-347. doi: 10.1158/1055-9965.EPI-18-0743
- Evers F, Korytár R, Tewari S, van Ruitenbeek JM (2020) Advances and challenges in single-molecule electron transport. *Reviews of Modern Physics*, 92(3); 035001.
- Fatani AZ, Alshamrani HM, Alshehri KA, Almaghrabi AY, Alzahrani YA, Abduljabbar MH (2020) Awareness on the association between skin aging and smoking: Impact on smoking quitting. *Imam Journal of Applied Sciences*, 5(1); 33. doi: 10.4103/ijas.ijas_17_19
- Feng L-Y, Battulga A, Han E, Chung H, Li J-H (2017) New psychoactive substances of natural origin: A brief review. *Journal of Food and Drug Analysis*, 25(3); 461-471. doi: <https://doi.org/10.1016/j.jfda.2017.04.001>
- Ferrante M, Conti GO (2017) Environment and neurodegenerative diseases: an update on miRNA role. *Microna*, 6(3); 157-165. doi: 10.2174/2211536606666170811151503
- Ferreira IM, Pinho O, Petisca C (2019) Potential Effects of Furan and Related Compounds on HealthCoffee (pp. 520-540) doi: 10.1039/9781788015028-00520

- Fidyk K, Fiedorowicz A, Strzdała L, Szumny A (2016) β - caryophyllene and β - caryophyllene oxide—natural compounds of anticancer and analgesic properties. *Cancer medicine*, 5(10); 3007-3017.
- Fitzgerald KT, Bronstein AC, Newquist KL (2013) Marijuana poisoning. *Topics in companion animal medicine*, 28(1); 8-12.
- Foresman J, Frisch A (1996) Exploring chemistry with electronic structure methods.
- Francomano F, Caruso A, Barbarossa A, Fazio A, La Torre C, Ceramella J et al. (2019) β -Caryophyllene: a sesquiterpene with countless biological properties. *Applied Sciences*, 9(24); 5420.
- Frandsen M, Thorpe M, Shiffman S, Ferguson S (2017) A clinical overview of nicotine dependence and withdrawal Negative affective states and cognitive impairments in nicotine dependence (pp. 205-215): Elsevier doi: 10.1016/B978-0-12-802574-1.00012-0
- Franklin RM, Rosenthal E, Franklin RM (2019) Method for conducting concentrated cannabis oil to be stable, emulsifiable and flavorless for use in hot beverages and resulting powderized cannabis oil. Retrieved from <https://patents.google.com/patent/US9629886B2/en>
- Fuster V, Kelly BB, Vedanthan R (2011) Promoting global cardiovascular health: moving forward. *Circulation*, 123(15); 1671-1678.
- Gao P, Yao D, Qian Y, Zhong S, Zhang L, Xue G et al. (2018) Factors controlling the formation of persistent free radicals in hydrochar during hydrothermal conversion of rice straw. *Environmental Chemistry Letters*, 16(4); 1463-1468. doi: 10.1007/s10311-018-0757-0
- Gashawa A, Getachew T (2014) The chemistry of khat and adverse effect of khat chewing. *American Scientific Research Journal for Engineering, Technology and Sciences*, 9(1); 35-46.
- Ghasemiesfe M, Barrow B, Leonard S, Keyhani S, Korenstein D (2019) Association Between Marijuana Use and Risk of Cancer: A Systematic Review and Meta-analysis. *JAMA network open*, 2(11); e1916318-e1916318. doi: 10.1001/jamanetworkopen.2019.16318
- Ghosh A, Choudhury A, Das A, Chatterjee NS, Das T, Chowdhury R et al. (2012) Cigarette smoke induces p-benzoquinone–albumin adduct in blood serum: implications on structure and ligand binding properties. *Toxicology*, 292(2-3); 78-89.
- Gianturco FA, Huo WM (2013) *Computational Methods for Electron—Molecule Collisions*: Springer Science & Business Media
- Giles ML, Gartner C, Boyd MA (2018) Smoking and HIV: what are the risks and what harm reduction strategies do we have at our disposal? *AIDS Research Therapy*, 15(1); 26. doi: 10.1186/s12981-018-0213-z
- Girma T, Mossie A, Getu Y (2015) Association between body composition and khat chewing in Ethiopian adults. *BMC Research Notes*, 8(1); 680. doi: 10.1186/s13104-015-1601-2

- Glennon RA (2014) Bath salts, mephedrone, and methylenedioxypropylone as emerging illicit drugs that will need targeted therapeutic intervention *Advances in Pharmacology*. (Vol. 69, pp. 581-620): Elsevier
- Global Force Reggae. (2017). Ganja/ Marijuana/ Cannabis. <https://globalforcereggae.com/ganja-marijuana-cannabis/>
- Goldstein JI, Newbury DE, Michael JR, Ritchie NW, Scott JHJ, Joy DC (2017) *Scanning electron microscopy and X-ray microanalysis*: Springer
- Graves BM, Johnson TJ, Nishida RT, Dias RP, Savareear B, Harynuik JJ et al. (2020) Comprehensive characterization of mainstream marijuana and tobacco smoke. *Scientific Reports*, 10(1); 1-12. Retrieved from <https://www.nature.com/articles/s41598-020-63120-6>
- Griscik GJ, Miller CG (2019) Smokeless tobacco article. Retrieved from <https://patents.google.com/patent/US10271572B2/en>
- Grossi J, Kooi DP, Giesbertz KJ, Seidl M, Cohen AJ, Mori-Sánchez P et al. (2017) Fermionic statistics in the strongly correlated limit of Density Functional Theory. *Journal of chemical theory and computation*, 13(12); 6089-6100.
- Gudata ZG, Cochrane L, Imana G (2019) An assessment of khat consumption habit and its linkage to household economies and work culture: The case of Harar city. *PloS one*, 14(11); e0224606. doi: 10.1371/journal.pone.0224606
- Guerrero F, Carmona A, Obrero T, Jiménez MJ, Soriano S, Moreno JA et al. (2020) Role of endothelial microvesicles released by p-cresol on endothelial dysfunction. *Scientific Reports*, 10(1); 1-10.
- Gunduz I, Kondylis A, Jaccard G, Renaud JM, Hofer R, Ruffieux L et al. (2016) Tobacco-specific N-nitrosamines NNN and NNK levels in cigarette brands between 2000 and 2014. *Regulatory Toxicology and Pharmacology*, 76; 113-120. doi: 10.1016/j.yrtph.2016.01.012
- Guy GW, Flint ME (2004) A Single Centre, Placebo-Controlled, Four Period, Crossover, Tolerability Study Assessing, Pharmacodynamic Effects, Pharmacokinetic Characteristics and Cognitive Profiles of a Single Dose of Three Formulations of Cannabis Based Medicine Extracts (CBMEs) (GWPD9901), Plus a Two Period Tolerability Study Comparing Pharmacodynamic Effects and Pharmacokinetic Characteristics of a Single Dose of a Cannabis Based Medicine Extract Given via Two Administration Routes (GWPD9901 EXT). *Journal of Cannabis Therapeutics*, 3(3); 35-77. doi: 10.1300/J175v03n03_03
- Hajek P, Phillips-Waller A, Przulj D, Pesola F, Myers Smith K, Bisal N et al. (2019) E-cigarettes compared with nicotine replacement therapy within the UK Stop Smoking Services: the TEC RCT. *Health technology assessment*. doi: 10.3310/hta23430
- Hang B, Wang Y, Huang Y, Wang P, Langley SA, Bi L et al. (2018) Short-term early exposure to thirdhand cigarette smoke increases lung cancer incidence in mice. *Clinical Science*, 132(4); 475-488. doi: 10.1042/CS20171521
- Harati B, Shahtaheri SJ, Karimi A, Azam K, Ahmadi A, Rad MA et al. (2016) Cancer risk analysis of benzene and ethyl benzene in painters. *Basic & Clinical Cancer Research*, 8(4); 22-28.

- Harrison XA, Donaldson L, Correa-Cano ME, Evans J, Fisher DN, Goodwin CE et al. (2018) A brief introduction to mixed effects modelling and multi-model inference in ecology. *PeerJ*, 6; e4794.
- Hartman RL, Huestis MA (2013) Cannabis effects on driving skills. *Clinical chemistry*, 59(3); 478-492.
- Hassan AA, Hobani YH, Mosbah N, Abdalla SE, Zaino M, Mohan S et al. (2020) Chronic khat (*Catha edulis*) chewing and genotoxicity: The role of antioxidant defense system and oxidative damage of DNA. *Pharmacognosy Magazine*, 16(68); 168. doi: 10.4103/pm.pm_455_19
- Hassan SZ, Saberian C, Khan SK, Salam O (2019) Paternal Smoking May be Associated with Increased Risk of Miscarriage. *Internal Medicine and Medical Investigation Journal*, 4(1). doi: 10.24200/imminv.v3i4.8
- Hatzinikolaou DG, Lagesson V, Stavridou AJ, Pouli AE, Lagesson-Andrasko L, Stavrides JC (2006) Analysis of the gas phase of cigarette smoke by gas chromatography coupled with UV-diode array detection. *Analytical chemistry*, 78(13); 4509-4516.
- Haydock S (2012) Drug dependence *Clinical Pharmacology* (pp. 136-159): Elsevier
- Hecht SS (2016) Biomarkers for Assessment of Chemical Exposures From e-Cigarette Emissions Analytical Assessment of e-Cigarettes: From Contents to Chemical and Particle Exposure Profiles (pp. 59-73): Elsevier Inc. doi: 10.1016/B978-0-12-811241-0.00004-8
- Hecht SS (2018) DNA Damage by Tobacco Carcinogens Carcinogens, Dna Damage And Cancer Risk: Mechanisms Of Chemical Carcinogenesis (pp. 69)
- Hecht SS, Stepanov I, Carmella SG (2016) Exposure and metabolic activation biomarkers of carcinogenic tobacco-specific nitrosamines. *Accounts of chemical research*, 49(1); 106-114. doi: 10.1021/acs.accounts.5b00472
- Hilton S, Weishaar H, Sweeting H, Trevisan F, Katikireddi SV (2016) E-cigarettes, a safer alternative for teenagers? A UK focus group study of teenagers' views. *BMJ open*, 6(11); e013271. doi: 10.1136/bmjopen-2016-013271
- Hindocha C, Freeman TP, Winstock AR, Lynskey MT (2016) Vaping cannabis (marijuana) has the potential to reduce tobacco smoking in cannabis users.
- Holitzki H, Dowsett LE, Spackman E, Noseworthy T, Clement F (2017) Health effects of exposure to second- and third-hand marijuana smoke: a systematic review. *CMAJ open*, 5(4); E814. doi: 10.9778/cmajo.20170112
- Hossain A (2004) Introduction to density functional theory.
- Huang B, von Lilienfeld OA (2021) Ab initio machine learning in chemical compound space. *Chemical reviews*, 121(16); 10001-10036.
- Huang J-R, Li P, Wen J-H, Hu X, Chen Y-J, Yin D-H et al. (2018) Determination of arsenic species in mainstream cigarette smoke based on inductively coupled plasma mass spectrometry. *Spectroscopy Letters*, 51(6); 252-256.

- Hussain K, Hoque RR, Balachandran S, Medhi S, Idris MG, Rahman M et al. (2018) Monitoring and risk analysis of PAHs in the environment Handbook of Environmental Materials Management (pp. 1-35) Retrieved from sci-hub.tw/10.1007/978-3-319-58538-3_29-2 doi: 10.1007/978-3-319-58538-3_29-2
- IARC (2019) IARC monographs on the identification of carcinogenic hazards to humans List Classif. Agents Classif. by IARC Monogr (Vol. 1). Lyon, France Retrieved from <https://monographs.iarc.fr/agents-classified-by-the-iarc/>
- Ifegwu OC, Anyakora C (2015) Polycyclic aromatic hydrocarbons: part I. Exposure Advances in clinical chemistry (Vol. 72; pp. 277-304): Elsevier doi: 10.1016/bs.acc.2015.08.001
- International Agency for Research on Cancer (2010) Some non-heterocyclic polycyclic aromatic hydrocarbons and some related exposures IARC Monographs on the evaluation of carcinogenic risks to humans (Vol. 92; pp. 1) Retrieved from <https://www.ncbi.nlm.nih.gov/books/NBK321712/>
- International Agency for Research on Cancer (2013) Air Pollution and Cancer *IARC Scientific Publication No. 161*. Retrieved from <https://publications.iarc.fr/Book-And-Report-Series/Iarc-Scientific-Publications/Air-Pollution-And-Cancer-2013>
- Iserles A, Webb M (2020) A family of orthogonal rational functions and other orthogonal systems with a skew-Hermitian differentiation matrix. *Journal of Fourier Analysis and Applications*, 26(1); 19.
- Ivashynka A, D'Alfonso S, Copetti M, Naldi P, Fontana A, Cucovici A et al. (2019) Effects of cigarette smoking and smoking cessation on Multiple Sclerosis severity: a cross-sectional study (P4. 6-008). *AAN*.
- Jain A, Shin Y (2016) Computational predictions of energy materials using density functional theory. *Nature Reviews Materials*, 1; 15004.
- Jakab E (2015) Chapter 3 - Analytical Techniques as a Tool to Understand the Reaction Mechanism In A. Pandey, T. Bhaskar, M. Stöcker & R. K. Sukumaran (Eds.), *Recent Advances in Thermo-Chemical Conversion of Biomass* (pp. 75-108) Boston: Elsevier
- Jebet A, Kibet J, Ombaka L, Kinyanjui T (2017) Surface bound radicals, char yield and particulate size from the burning of tobacco cigarette. *Chemistry Central Journal*, 11(1); 79. doi: 10.1186/s13065-017-0311-3
- Jerah A, Bidwai AK, Alam MS (2017) A review of the history, cultivation, chemistry, pharmacology and adverse health effects of Khat. *International Journal of Applied and Natural Sciences*, 6(3).
- Jha P (2020) The hazards of smoking and the benefits of cessation: a critical summation of the epidemiological evidence in high-income countries. *Elife*, 9; e49979. doi: 10.7554/eLife.49979

- Ji M, Zhang Y, Li N, Wang C, Xia R, Zhang Z et al. (2017) Nicotine component of cigarette smoke extract (cse) decreases the cytotoxicity of CSE in BEAS-2B cells stably expressing human cytochrome P450 2A13. *International Journal of Environmental Research and Public Health*, 14(10); 1221. doi: 10.3390/ijerph14101221
- Jonnie W (2018) Alkaloid Composition for E-Cigarette. Retrieved from <https://patents.google.com/patent/US20120325228A1/en>
- Jun W, Yang H, Shi H, Zhou J, Bai R, Zhang M et al. (2017) Nitrate and nitrite promote formation of tobacco-specific nitrosamines via nitrogen oxides intermediates during postcured storage under warm temperature. *Hindawi*, 2017. doi: 10.1155/2017/6135215
- Kapar A, Ibrahimov A, Sergazina M, Alimzhanova M, Abilev M (2018) Analysis of tobacco products by chromatography methods. *International Journal of Biology and Chemistry*, 11(1); 133-141.
- Karlström G, Lindh R, Malmqvist P-Å, Roos BO, Ryde U, Veryazov V et al. (2003) MOLCAS: a program package for computational chemistry. *Computational Materials Science*, 28(2); 222-239.
- Kaur G, Muthumalage T, Rahman I (2018) Mechanisms of toxicity and biomarkers of flavoring and flavor enhancing chemicals in emerging tobacco and non-tobacco products. *Toxicology letters*, 288; 143-155.
- Keith JA, Vassilev-Galindo V, Cheng B, Chmiela S, Gastegger M, Müller K-R et al. (2021) Combining Machine Learning and Computational Chemistry for Predictive Insights Into Chemical Systems. *Chemical reviews*, 121(16); 9816-9872. doi: 10.1021/acs.chemrev.1c00107
- Khan Z, Suliankatchi RA, Heise TL, Dreger S (2019) Naswar (Smokeless Tobacco) Use and the Risk of Oral Cancer in Pakistan: A Systematic Review With Meta-Analysis. *Nicotine & Tobacco Research*, 21(1); 32-40. doi: 10.1093/ntr/ntx281
- Kibet J (2016) Computational Modeling of 2-Monochlorophenol and 2-Monochlorothiophenol. *Kabarak Journal of Research & Innovation*, 4(1); 49-61.
- Kibet J, Khachatryan L, Dellinger B (2012) Molecular products and radicals from pyrolysis of lignin. *Environmental science & technology*, 46(23); 12994-13001.
- Kibet J, Mathenge AB, Limo SC, Omare MO (2015) Theoretical modeling and experimental investigation of propanol and phenol in mainstream cigarette smoking. *The African Review of Physics*, 9.
- Kibet J, Mosonik BC, Nyamori VO, Ngari SM (2018) Free radicals and ultrafine particulate emissions from the co-pyrolysis of Croton megalocarpus biodiesel and fossil diesel. *Chemistry Central Journal*, 12(1); 1-9.
- Kibet J, Rono N, Mutumba M (2017) Particulate emissions from high temperature pyrolysis of cashew nuts. *Eurasian Journal Analytical Chemistry*, 12(3); 237-243.

- Kim K-H, Jahan SA, Kabir E, Brown RJ (2013) A review of airborne polycyclic aromatic hydrocarbons (PAHs) and their human health effects. *Environment international*, 60; 71-80.
- Kindvall M, Jonsson L, Schyberg M (2019) Freeze dried oral smokeless tobacco snuff or non-tobacco snuff product and method of manufacturing thereof. Retrieved from <https://patents.google.com/patent/US10278416B2/en>
- Kögel CC, López-Pelayo H, Balcells-Olivero M, Colom J, Gual A (2018) Psychoactive constituents of cannabis and their clinical implications: a systematic review Constituyentes psicoactivos del cannabis y sus implicaciones clínicas: una revisión sistemática. *Adicciones*, 30(2); 140-152.
- Konstantinou E, Fotopoulou F, Drosos A, Dimakopoulou N, Zagoriti Z, Niarchos A et al. (2018) Tobacco-specific nitrosamines: A literature review. *Food and chemical toxicology*, 118; 198-203. doi: 10.1016/j.fct.2018.05.008
- Koren G, Cohen R (2020) Medicinal Use of Cannabis in Children and Pregnant Women. *Rambam Maimonides medical journal*, 11(1); e0005. doi: 10.5041/RMMJ.10382
- Kratzer P, Neugebauer J (2019) The basics of electronic structure theory for periodic systems. *Frontiers in chemistry*, 7; 106.
- Kristjansson AL, Thomas S, Lilly CL, Thorisdottir IE, Allegrante JP, Sigfusdottir ID (2018a) Maternal smoking during pregnancy and academic achievement of offspring over time: a Registry data-based cohort study. *Preventive medicine*, 113; 74-79.
- Kristjansson AL, Thomas S, Lilly CL, Thorisdottir IE, Allegrante JP, Sigfusdottir ID (2018b) Maternal smoking during pregnancy and academic achievement of offspring over time: a Registry data-based cohort study. *Prev Med*, 113; 74-79. doi: 10.1016/j.ypmed.2018.05.017
- Kuo T, Kuo A, Roy S, Friederichsen PG, Whelan P (2019) Addressing the Dangers of Increased E-Cigarette Use Among Youth: A Call to Action for Clinicians.
- Kurgat C, Kibet J, Cheplogoi P, Omari O, Adika C (2015) Molecular Characterization of Nicotine in Mainstream Cigarette Smoking. *Research Journal of Chemical Sciences*, 2231; 606X.
- Lachenmeier DW, Anderson P, Rehm J (2018) Heat-not-burn tobacco products: the devil in disguise or a considerable risk reduction? *International Journal of Alcohol and Drug Research*, 7(2); 8-11. doi: 10.7895/ijadr.250
- Lammert PE (2018) In search of the Hohenberg-Kohn theorem. *Journal of Mathematical Physics*, 59(4); 042110.
- Langley TE (2019) Tobacco harm reduction: Making sure no one gets left behind. *National Tobacco Research*, 21(1). doi: 10.1093/ntr/nty186
- Larijani HT, Jahanshahi M, Ganji MD, Kiani M (2017) Computational studies on the interactions of glycine amino acid with graphene, h-BN and h-SiC monolayers. *Physical Chemistry Chemical Physics*, 19(3); 1896-1908. doi: 10.1039/C6CP06672K
- Laura C, Scot T, Ryan K, Sophie S, Nitara O, Kristina A (2019) what are the effects of khat? *Sunrise House; American Addiction Centers Treatment Facility*.

- Law Tech Publishing Group (2016) *2016 California Penal Code Unabridged*, : Ebooks2go Incorporated
- Lawin H, Fanou LA, Hinson V, Wanjiku J, Ukwaja NK, Gordon SB et al. (2017) Exhaled carbon monoxide: a non-invasive biomarker of short-term exposure to outdoor air pollution. *BMC public health*, *17*(1); 320. doi: 10.1186/s12889-017-4243-6
- Lee DC, Crosier BS, Borodovsky JT, Sargent JD, Budney AJ (2016) Online survey characterizing vaporizer use among cannabis users. *Drug and alcohol dependence*, *159*; 227-233. doi: 10.1016/j.drugalcdep.2015.12.020
- Lejaeghere K, Bihlmayer G, Björkman T, Blaha P, Blügel S, Blum V et al. (2016) Reproducibility in density functional theory calculations of solids. *Science*, *351*(6280).
- Leon ME, Assefa M, Kassa E, Bane A, Gemechu T, Tilahun Y et al. (2017) Qat use and esophageal cancer in Ethiopia: A pilot case-control study. *PloS one*, *12*(6); 0178911-0178911. doi: 10.1371/journal.pone.0178911
- Li MD (2018) Contribution of Variants in DRD2/ANKK1 on Chromosome 11 with Smoking and Other Addictions Tobacco Smoking Addiction: Epidemiology, Genetics, Mechanisms, and Treatment (pp. 107-142): Springer doi: 10.1007/978-981-10-7530-8_8
- Li MD, Burmeister M (2009) New insights into the genetics of addiction. *Nature Reviews Genetics*, *10*(4); 225-231. doi: 10.1038/nrg2536
- Liao Y-T, Tseng H-D, Chang PM-H, Chu P-Y, Kuo Y-J, Liu C-Y (2018) Second Primary Spindle Cell Carcinoma of Oral Cavity and Oropharynx: A Case Report and Literature Review. *Reports—Medical Cases, Images and Videos*, *1*(2); 16. doi: 10.3390/reports1020016
- Loomis D, Guyton KZ, Grosse Y, El Ghissassi F, Bouvard V, Benbrahim-Tallaa L et al. (2017) Carcinogenicity of benzene. *Lancet Oncology*, *18*(12); 1574-1575. doi: 10.1016/S1470-2045(17)30832-X
- Lu Y, Li Y, Xiang M, Zhou J, Chen J (2017) Khat promotes human breast cancer MDA-MB-231 cell apoptosis via mitochondria and MAPK-associated pathways. *Oncology letters*, *14*(4); 3947-3952. doi: 10.3892/ol.2017.6708
- Lukandu OM, Koech LS, Kiarie PN (2015) Oral lesions induced by chronic khat use consist essentially of thickened hyperkeratinized epithelium. *International Journal of Dentistry*, *2015*. doi: 10.1155/2015/104812
- MacNee W, Rabinovich RA, Choudhury G (2014) Ageing and the border between health and disease. *European Respiratory Journal*. doi: 10.1183/09031936.00134014
- Mahmud T (2019) Who runs the Khat smuggling ring in Bangladesh [Press release]. Retrieved from <https://www.dhakatribune.com/bangladesh/crime/2018/09/24/who-runs-the-khat-smuggling-ring-in-bangladesh>

- Mallock N, Böss L, Burk R, Danziger M, Welsch T, Hahn H et al. (2018) Levels of selected analytes in the emissions of “heat not burn” tobacco products that are relevant to assess human health risks. *Archives of toxicology*, 92(6); 2145-2149. doi: 10.1007/s00204-018-2215-y
- Marcu JP (2016) Chapter 62 - An Overview of Major and Minor Phytocannabinoids In V. R. Preedy (Ed.), *Neuropathology of Drug Addictions and Substance Misuse* (pp. 672-678) San Diego: Academic Press
- Mathews LM, Krishnan M (2019) Oral cancer and smokeless tobacco—A review. *Journal of Pharmacy Research*, 12(6). doi: 10.1177/154411130401500502
- Matt GE, Quintana PJ, Zakarian JM, Hoh E, Hovell MF, Mahabee-Gittens M et al. (2017) When smokers quit: exposure to nicotine and carcinogens persists from thirdhand smoke pollution. *Tobacco Control*, 26(5); 548-556.
- McAdam K, Faizi A, Kimpton H, Porter A, Rodu B (2013) Polycyclic aromatic hydrocarbons in US and Swedish smokeless tobacco products. *Chemistry Central Journal*, 7(1); 151. doi: 10.1186/1752-153X-7-151
- McAdam K, Murphy J, Eldridge A, Meredith C, Proctor C (2018) Integrating chemical, toxicological and clinical research to assess the potential of reducing health risks associated with cigarette smoking through reducing toxicant emissions. *Regulatory Toxicology and Pharmacology*, 95; 102-114. doi: 10.1016/j.yrtph.2018.03.005
- McKinney DL, Vansickel AR (2016) Nicotine chemistry, pharmacology, and pharmacokinetics *Neuropathology of Drug Addictions and Substance Misuse* (pp. 93-103): Elsevier doi: 10.1016/B978-0-12-800213-1.00009-2
- Mebel A, Morokuma K, Lin M-C (1995) Modification of the gaussian- 2 theoretical model: The use of coupled- cluster energies, density- functional geometries, and frequencies. *The Journal of chemical physics*, 103(17); 7414-7421.
- MedicineNet (2020) Khat [Press release]. Retrieved from https://www.medicinenet.com/khat/article.htm#what_are_the_health_side_effects_of_khat_use
- Medimagh M, Issaoui N, Gatfaoui S, Antonia Brandán S, Al-Dossary O, Marouani H et al. (2021) Impact of non-covalent interactions on FT-IR spectrum and properties of 4-methylbenzylammonium nitrate. A DFT and molecular docking study. *Heliyon*, 7(10); e08204. doi: <https://doi.org/10.1016/j.heliyon.2021.e08204>
- Medvedev MG, Bushmarinov IS, Sun J, Perdew JP, Lyssenko KA (2017) Density functional theory is straying from the path toward the exact functional. *Science*, 355(6320); 49-52.
- Mihretu A, Teferra S, Fekadu A (2017) What constitutes problematic khat use? An exploratory mixed methods study in Ethiopia. *Substance abuse treatment, prevention, and policy*, 12(1); 17. doi: 10.1186/s13011-017-0100-y
- Mishra S, Joseph RA, Gupta PC, Pezzack B, Ram F, Sinha DN et al. (2016) Trends in bidi and cigarette smoking in India from 1998 to 2015, by age, gender and education. *BMJ global health*, 1(1); e000005. doi: 10.1136/bmjgh-2015-000005

- Mohapatra T (2019) Gutkha and causative factors of gutkha addiction: A sociological study in “Twin City” of Odisha. *International Journal of Social and Economic Research*, 9(3); 476-513. doi: 10.5958/2249-6270.2019.00056.4
- More GS, Thomas AB, Chitlange SS, Nanda RK, Gajbhiye RL (2019) Nitrogen mustards as alkylating agents: a review on chemistry, mechanism of action and current USFDA status of drugs. *Anti-Cancer Agents in Medicinal Chemistry (Formerly Current Medicinal Chemistry-Anti-Cancer Agents)*, 19(9); 1080-1102.
- Morgan JC, Byron MJ, Baig SA, Stepanov I, Brewer NT (2017) How people think about the chemicals in cigarette smoke: a systematic review. *Journal of behavioral medicine*, 40(4); 553-564. doi: 10.1007/s10865-017-9823-5
- Mosonik BC, Ngari SM, Kibet JK (2019) Molecular Modelling of Selected Combustion By-Products from the Thermal Degradation of Croton megalocarpus Biodiesel. *Open Access Library Journal*, 6(10); 1. doi: 10.4236/oalib.1105840
- Muema EK (2015) *Biochemical, hormonal and toxicological effects of catha edulis (khat) on pregnancy and fetal development in olive Baboons (papio anubis)*. University of Nairobi, Nairobi, Kenya.
- Nakajima D, Yagishita M (2018) Carcinogenicity/Mutagenicity Polycyclic Aromatic Hydrocarbons (pp. 235-244): Springer doi: 10.1007/978-981-10-6775-4_18
- National Academies of Sciences Engineering and Medicine (2017) The health effects of cannabis and cannabinoids: The current state of evidence and recommendations for research: National Academies Press Retrieved from <https://www.ncbi.nlm.nih.gov/books/NBK425753/>
- National Toxicology Program (2000) NTP toxicology and carcinogenesis studies of pyridine (CAS No. 110-86-1) in F344/N rats, wistar rats, and B6C3F1 mice (drinking water studies). *National Toxicology Program technical report series*, 470; 1-330.
- NCBI. (2020a). Isobutylene, . Retrieved June 19, 2020, from PubChem Database <https://pubchem.ncbi.nlm.nih.gov/compound/Isobutylene>
- NCBI. (2020b). (-)-Limonene, CID=439250, . Retrieved 25, June 2020, from PubChem Database https://pubchem.ncbi.nlm.nih.gov/compound/4S_-1-methyl-4-prop-1-en-2-ylcyclohexene
- NIDA. (2019). Marijuana as Medicine. Retrieved 2020, May 29 <https://www.drugabuse.gov/publications/drugfacts/marijuana-medicine>
- NIDA. (2020a). Marijuana. Retrieved 2020, June 10 <https://www.drugabuse.gov/publications/research-reports/marijuana/there-link-between-marijuana-use-psychiatric-disorders>
- NIDA. (2020b). Marijuana DrugFacts. <https://www.drugabuse.gov/publications/drugfacts/marijuana>
- NIDA (2020c) Trends & Statistics. Retrieved from <https://www.drugabuse.gov/related-topics/trends-statistics>

- Nigussie T, Gobena T, Mossie A (2013) Association between khat chewing and gastrointestinal disorders: a cross sectional study. *Ethiopian journal of health sciences*, 23(2); 123-130.
- Nikolaou K (2021) Density functional theory based MD.
- Nlemedim ON (2017) *Organic Chemical Compounds in Different Brands of Cigarette Smoke*. Texas Southern University. Retrieved from <https://search.proquest.com/openview/f5b1a77567157706f78c65bc80ed37d/1?pq-origsite=gscholar&cbl=18750&diss=y>
- Nordholm S (2021) From Electronegativity towards Reactivity-Searching for a Measure of Atomic Reactivity. *Molecules (Basel, Switzerland)*, 26(12); 3680. doi: 10.3390/molecules26123680
- Nyshadham C, Oses C, Hansen JE, Takeuchi I, Curtarolo S, Hart GL (2017) A computational high-throughput search for new ternary superalloys. *Acta Materialia*, 122; 438-447. doi: 10.1016/j.actamat.2016.09.017
- O'Brien JL, Langlois PH, Lawson CC, Scheuerle A, Rocheleau CM, Waters MA et al. (2016) Maternal occupational exposure to polycyclic aromatic hydrocarbons and craniosynostosis among offspring in the national birth defects prevention study. *Birth Defects Research Part A: Clinical and Molecular Teratology*, 106(1); 55-60. doi: 10.1002/bdra.23389
- O'Connor R, Watson CH, Swan GE, Nettles DS, Geisler RC, Hendershot TP (2020) PhenX: agent measures for tobacco regulatory research. *BMJ Journal*, 29(Suppl 1); 20-26. doi: 10.1136/tobaccocontrol-2019-054976
- Omare MO (2015) *Determination of toxic molecular products and heavy metals from combustion of unprocessed and processed commercial cigarettes sold in Kenya: computational modeling and experimental studies*. Moi University.
- Omare MO, Kibet JK, Cherutoi JK, Kengara FO (2020) Contemporary Trends in the Use of Khat for Recreational Purposes and Its Possible Health Implications. *Open Access Library Journal*, 7(12); 1-22. doi: 10.4236/oalib.1106985
- Omari M, Kibet J, Cherutoi J, Bosire J, Rono N (2015) Heavy Metal Content in Mainstream Cigarette Smoke of Common Cigarettes Sold in Kenya, and their Toxicological Consequences. *International Research Journal of Environmental Science*, 4(6); 75-79.
- Omnes R (2018) *The interpretation of quantum mechanics* (Vol. 102): Princeton University Press
- Orlien SMS, Sandven I, Berhe NB, Ismael NY, Ahmed TA, Stene-Johansen K et al. (2018) Khat chewing increases the risk for developing chronic liver disease: A hospital-based case-control study. *Hepatology*, 68(1); 248-257. doi: 10.1002/hep.29809
- Osman G, Galal M, Abul-Ezz A, Mohammed A, Abul-Ela M, Hegazy AM (2017) Polycyclic aromatic hydrocarbons(PAHS) accumulation and histopathological biomarkers in gills and mantle of *Lanistes carinatus*(Molluscs, Ampullariidae) to assess crude oil toxicity. *Punjab University Journal of Zoology*, 32(1); 39-50.

- Osman OF, Elbashir RMI, Abbass IE, Kendrick C, Goyal M, Yap MH (2017) *Automated assessment of facial wrinkling: A case study on the effect of smoking*. Paper presented at the 2017 IEEE International Conference on Systems, Man, and Cybernetics (SMC).
- Pan B, Li H, Lang D, Xing B (2019) Environmentally persistent free radicals: occurrence, formation mechanisms and implications. *Environmental Pollution*, 248; 320-331. doi: 10.1016/j.envpol.2019.02.032
- Panja SK, Dwivedi N, Saha S (2016) Tuning the intramolecular charge transfer (ICT) process in push-pull systems: effect of nitro groups. *RSC advances*, 6(107); 105786-105794.
- Panth N, Paudel KR, Parajuli K (2016) Reactive oxygen species: a key hallmark of cardiovascular disease. *Advances in medicine*, 2016. doi: 10.1155/2016/9152732
- Parker S (2019) E-cigarettes-Tobacco Prevention and Control-Minnesota Department of Health. Retrieved from <https://www.health.state.mn.us/ecigarettes>
- Parks HL, McGaughey AJ, Viswanathan V (2019) Uncertainty quantification in first-principles predictions of harmonic vibrational frequencies of molecules and molecular complexes. *The Journal of Physical Chemistry C*, 123(7); 4072-4084.
- Peterson GA, Bennett A, Tensfeldt TG, Al-Laham MA, Shirley WJ, Mantzaris J (1988). *Chemistry and Physics*, 89; 5639.
- Petruzielo FR, Toulouse J, Umrigar C (2011) Basis set construction for molecular electronic structure theory: Natural orbital and Gauss-Slater basis for smooth pseudopotentials. *The Journal of chemical physics*, 134(6); 064104.
- Phaniendra A, Jestadi DB, Periyasamy L (2015) Free radicals: properties, sources, targets, and their implication in various diseases. *Indian journal of clinical biochemistry*, 30(1); 11-26. doi: 10.1007/s12291-014-0446-0
- Pillitteri JL, Shiffman S, Sembower MA, Polster MR, Curtin GM (2020) Assessing comprehension and perceptions of modified-risk information for snus among adult current cigarette smokers, former tobacco users, and never tobacco users. *Addictive Behaviors Reports*; 100254. doi: 10.1016/j.abrep.2020.100254. Retrieved from <https://www.sciencedirect.com/science/article/pii/S2352853219301993>
- Pires AF, Pais A, Faria T, Pinhal H, Silva S, Nogueira A (2018, 24-26 October 2018) *Occupational Exposure to formaldehyde in pathology laboratories*. Paper presented at the ICOETOX 2018-4th International Congress on Occupational & Environmental Toxicology.
- Polini A, Yang F (2017) Physicochemical characterization of nanofiber composites *Nanofiber composites for biomedical applications* (pp. 97-115): Elsevier
- Popova L, Lempert LK, Glantz SA (2018) Light and mild redux: heated tobacco products' reduced exposure claims are likely to be misunderstood as reduced risk claims. *BMJ Journal*, 27(Suppl 1); s87-s95. doi: 10.1136/tobaccocontrol-2018-054324

- Prosser JM, Nelson LS (2012) The Toxicology of Bath Salts: A Review of Synthetic Cathinones. *Journal of Medical Toxicology*, 8(1); 33-42. doi: 10.1007/s13181-011-0193-z
- Prueitt RL, Lynch HN, Zu K, Shi L, Goodman JE (2017) Dermal exposure to toluene diisocyanate and respiratory cancer risk. *Environment international*, 109; 181-192. doi: 10.1016/j.envint.2017.09.017
- Qi L, Luo Q, Zhang Y, Jia F, Zhao Y, Wang F (2019) Advances in toxicological research of the anticancer drug cisplatin. *Chemical research in toxicology*, 32(8); 1469-1486.
- Radhakrishnan R, Wilkinson ST, D'Souza DC (2014) Gone to Pot - A Review of the Association between Cannabis and Psychosis. *Frontiers in psychiatry*, 5; 54-54. doi: 10.3389/fpsy.2014.00054
- Rehman H, Jahan S, Ullah I, Winberg S (2019) Toxicological effects of furan on the reproductive system of male rats: An “in vitro” and “in vivo”-based endocrinological and spermatogonial study. *Chemosphere*, 230; 327-336. doi: 10.1016/j.chemosphere.2019.05.063
- Rehman H, Ullah I, David M, Ullah A, Jahan S (2019) Neonatal exposure to furan alters the development of reproductive systems in adult male Sprague Dawley rats. *Food and chemical toxicology*, 130; 231-241. doi: 10.1016/j.fct.2019.05.020
- Rengarajan T, Rajendran P, Nandakumar N, Lokeshkumar B, Rajendran P, Nishigaki I (2015) Exposure to polycyclic aromatic hydrocarbons with special focus on cancer. *Asian Pacific Journal of Tropical Biomedicine*, 5(3); 182-189. doi: 10.1016/S2221-1691(15)30003-4
- Reza MS, Islam SN, Afroze S, Bakar MSA, Taweekun J, Azad AK (2020) Data on FTIR, TGA–DTG, DSC of invasive pennisetum purpureum grass. *Data in brief*, 30; 105536.
- Ribeiro LI, Ind PW (2016) Effect of cannabis smoking on lung function and respiratory symptoms: a structured literature review. *NPJ primary care respiratory medicine*, 26; 16071-16071. doi: 10.1038/npjpcrm.2016.71
- Rodgman A, Perfetti TA (2013) *The chemical components of tobacco and tobacco smoke*: CRC press
- Roemer E, Meisgen T, Diekmann J, Conroy L, Stabbert R (2016) Heterocyclic aromatic amines and their contribution to the bacterial mutagenicity of the particulate phase of cigarette smoke. *Toxicology letters*, 243; 40-47. doi: 10.1016/j.toxlet.2015.12.008
- Romano L, Hazekamp A (2018) An Overview of Galenic Preparation Methods for Medicinal Cannabis. *Current Bioactive Compounds*, 14. doi: 10.2174/1573407214666180612080412
- Romano L, Hazekamp A (2019) An Overview of Galenic Preparation Methods for Medicinal Cannabis. *Current Bioactive Compounds*, 15(2); 174-195. doi: 10.2174/1573407214666180612080412

- Rubey WA, Carnes RA (1985) Design of a tubular reactor instrumentation assembly for conducting thermal decomposition studies. *Review of scientific instruments*, 56(9); 1795-1798.
- Russo C, Ferik F, Mišik M, Ropek N, Nersesyan A, Mejri D et al. (2019) Low doses of widely consumed cannabinoids (cannabidiol and cannabidiol) cause DNA damage and chromosomal aberrations in human-derived cells. *Archives of toxicology*, 93(1); 179-188. doi: 10.1007/s00204-018-2322-9
- Santonicola S, Albrizio S, Murru N, Ferrante MC, Mercogliano R (2017) Study on the occurrence of polycyclic aromatic hydrocarbons in milk and meat/fish based baby food available in Italy. *Chemosphere*, 184; 467-472. doi: 10.1016/j.chemosphere.2017.06.017
- Sapkota M, Wyatt TA (2015) Alcohol, aldehydes, adducts and airways. *Biomolecules*, 5(4); 2987-3008. doi: 10.3390/biom5042987
- SAPTA (2012) Substances of Abuse. [Press release]. Retrieved from <http://www.sapta.or.ke/alcoholdrug-information>
- Sarfraz A, Raza AH, Mirzaeian M, Abbas Q, Raza R (2020) Electrode materials for fuel cells *Reference Module in Materials Science and Materials Engineering*: Elsevier BV
- Sawicka B, Otekunrin OA, Skiba D, Bienia B, Ćwintal M (2020) Plant-derived stimulants and psychoactive substances—social and economic aspects. *Medical & Clinical Research*.
- Schaefer H (2012) *Applications of electronic structure theory* (Vol. 4): Springer Science & Business Media
- Sharma RK, Hajaligol MR (2003) Effect of pyrolysis conditions on the formation of polycyclic aromatic hydrocarbons (PAHs) from polyphenolic compounds. *Journal of Analytical and Applied Pyrolysis*, 66(1-2); 123-144.
- Shi X, Yang X (2017) Tobacco flavor extract with reduced tsnas. Retrieved from <https://patents.google.com/patent/US20170231267A1/en>
- Shihadeh A, Schubert J, Klaiany J, El Sabban M, Luch A, Saliba NA (2015) Toxicant content, physical properties and biological activity of waterpipe tobacco smoke and its tobacco-free alternatives. *BMJ*, 24(1); 22-30. doi: 10.1136/tobaccocontrol-2014-051907
- Silva CF, Borges KB, Nascimento CS (2019) Computational study on acetamiprid-molecular imprinted polymer. *Journal of molecular modeling*, 25(4); 104. doi: 10.1007/s00894-019-3990-y
- Silva V, Silva C, Soares P, Garrido EM, Borges F, Garrido J (2020) Isothiazolinone biocides: Chemistry, biological, and toxicity profiles. *Molecules (Basel, Switzerland)*, 25(4); 991.
- Singhavi H, Ahluwalia JS, Stepanov I, Gupta PC, Gota V, Chaturvedi P et al. (2018) Tobacco carcinogen research to aid understanding of cancer risk and influence policy. *Laryngoscope Investig Otolaryngol*, 3(5); 372-376. doi: 10.1002/lio2.204

- Sitarek P, Rijo P, Garcia C, Skala E, Kalembe D, Białas AJ et al. (2017) Antibacterial, Anti-Inflammatory, Antioxidant, and Antiproliferative Properties of Essential Oils from Hairy and Normal Roots of *Leonurus sibiricus* L. and Their Chemical Composition. *Oxidative Medicine and Cellular Longevity*, 2017; 7384061. doi: 10.1155/2017/7384061
- Skjodt N, Mamoshina P, Kochetov K, Cortese F, Kovalchuk A, Aliper A et al. (2018) Smoking causes early biological aging: a deep neural network analysis of common blood test results. *European Respiratory Journal*, 52(62). doi: 10.1183/13993003.congress-2018.OA3809
- Smith MW, Dallmeyer I, Johnson TJ, Brauer CS, McEwen J-S, Espinal JF et al. (2016) Structural analysis of char by Raman spectroscopy: Improving band assignments through computational calculations from first principles. *Carbon*, 100; 678-692.
- Sobiesiak M (2017) Chemical Structure of Phenols and Its Consequence for Sorption Processes
- Soi C, Muriithi N, Keriko J, Kurgat C, Kibet J (2015) The ash content from the thermal degradation of selected biomass waste from Githurai market, Nairobi, Kenya. *International Multidisciplinary Research Journal*, 1(4); 194-196.
- Sokolowski JA, Banks CM (2011) *Principles of modeling and simulation: a multidisciplinary approach*: John Wiley & Sons
- Soliman M (2018) Cancer Causing Chemicals, Cancer Causing Substances: IntechOpen doi: 10.5772/intechopen.71560
- Spahr S, Cirpka OA, Von Gunten U, Hofstetter TB (2017) Formation of N-nitrosodimethylamine during chloramination of secondary and tertiary amines: Role of molecular oxygen and radical intermediates. *Environmental Science and Technology*, 51(1); 280-290. doi: 10.1021/acs.est.6b04780
- Spindle TR, Cone EJ, Schlien NJ, Mitchell JM, Bigelow GE, Flegel R et al. (2020) Urinary Excretion Profile of 11-Nor-9-Carboxy- Δ^9 -Tetrahydrocannabinol (THCCOOH) Following Smoked and Vaporized Cannabis Administration in Infrequent Cannabis Users. *Journal of analytical toxicology*, 44(1); 1-14. doi: 10.1093/jat/bkz038
- Spokas KA (2010) Review of the stability of biochar in soils: predictability of O: C molar ratios. *Carbon Management*, 1(2); 289-303.
- Stanfill SB (2020) Reducing carcinogen levels in smokeless tobacco products Smokeless Tobacco Products (pp. 167-187): Elsevier doi: 10.1016/B978-0-12-818158-4.00008-X
- Stein CJ, Pantazis DA, Krewald V (2019) Orbital Entanglement Analysis of Exchange-Coupled Systems. *The journal of physical chemistry letters*, 10(21); 6762-6770.
- Stepanov I, Biener L, Yershova K, Nyman AL, Bliss R, Parascandola M et al. (2014) Monitoring tobacco-specific N-nitrosamines and nicotine in novel smokeless tobacco products: findings from round II of the new product watch. *National Tobacco Research*, 16(8); 1070-1078. doi: 10.1093/ntr/ntu026

- Stephen SH (2018) DNA Damage by Tobacco Carcinogens. *Carcinogens, Dna Damage And Cancer Risk: Mechanisms Of Chemical Carcinogenesis* (pp. 69-85) Retrieved from https://www.worldscientific.com/doi/abs/10.1142/9789813237209_0003 doi: 10.1142/9789813237209_0003
- Sun J, Remsing RC, Zhang Y, Sun Z, Ruzsinszky A, Peng H et al. (2016) Accurate first-principles structures and energies of diversely bonded systems from an efficient density functional. *Nature chemistry*, 8(9); 831.
- Swenberg JA, Moeller BC, Lu K, Rager JE, Fry RC, Starr TB (2013) Formaldehyde carcinogenicity research: 30 years and counting for mode of action, epidemiology, and cancer risk assessment. *Toxicologic pathology*, 41(2); 181-189. doi: 10.1177/0192623312466459
- Tan SLW, Chadha S, Liu Y, Gabasova E, Perera D, Ahmed K et al. (2017) A class of environmental and endogenous toxins induces BRCA2 haploinsufficiency and genome instability. *Cell*, 169(6); 1105-1118. e1115. doi: 10.1016/j.cell.2017.05.010
- Tashkin DP (2013) Effects of marijuana smoking on the lung. *Annals of the American Thoracic Society*, 10(3); 239-247.
- Tchernook D-CI (2016) Strategies for Computational Investigation of Reaction Mechanisms in Organic and Polymer Chemistry Using Static Quantum Mechanics.
- Tentscher PR, Lee M, von Gunten U (2019) Micropollutant oxidation studied by quantum chemical computations: methodology and applications to thermodynamics, kinetics, and reaction mechanisms. *Accounts of chemical research*, 52(3); 605-614.
- Theobaldo JD, Vieira-Junior WF, Catelan A, Maria do Carmo AM, Ysnaga OA, Rodrigues-Filho UP et al. (2018) Effect of Heavy Metals Contamination from Cigarette Smoke on Sound and Caries-Like Enamel. *Microscopy and Microanalysis*, 24(6); 762-767.
- Tisserand R, Young R (2014) 13 - Essential oil profiles In R. Tisserand & R. Young (Eds.), *Essential Oil Safety (Second Edition)* (pp. 187-482) St. Louis: Churchill Livingstone
- Tkatchenko A (2020) Machine learning for chemical discovery. *Nature Communications*, 11(1); 1-4.
- Tsai J, Homa DM, Gentzke AS, Mahoney M, Sharapova SR, Sosnoff CS et al. (2018) Exposure to secondhand smoke among nonsmokers—United States, 1988–2014. *MMWR. Morbidity and mortality weekly report*, 67(48); 1342. doi: 10.15585/mmwr.mm6748a3
- U.S Department of Health and Human Services (2006) The Health Consequences of Involuntary Exposure General, to Tobacco Smoke: A Report of the Surgeon General: . 1–2.
- Varandas AJ (2021) Canonical versus explicitly correlated coupled cluster: Post- complete- basis- set extrapolation and the quest of the complete- basis- set limit. *International Journal of Quantum Chemistry*, 121(9); e26598.

- Vellios N, Ross H, Perucic A-M (2018) Trends in cigarette demand and supply in Africa. *PloS one*, 13(8); e0202467-e0202467. doi: 10.1371/journal.pone.0202467
- Vicent-Luna JM, Apergi S, Tao S (2021) Efficient Computation of Structural and Electronic Properties of Halide Perovskites Using Density Functional Tight Binding: GFN1-xTB Method. *Journal of chemical information and modeling*, 61(9); 4415-4424.
- Volkow ND, Baler RD, Compton WM, Weiss SR (2014) Adverse health effects of marijuana use. *New England Journal of Medicine*, 370(23); 2219-2227.
- von Lilienfeld OA, Müller K-R, Tkatchenko A (2020) Exploring chemical compound space with quantum-based machine learning. *Nature Reviews Chemistry*, 4(7); 347-358.
- Vu AT, Taylor KM, Holman MR, Ding YS, Hearn B, Watson CH (2015) Polycyclic aromatic hydrocarbons in the mainstream smoke of popular US cigarettes. *Chemical research in toxicology*, 28(8); 1616-1626. doi: 10.1021/acs.chemrestox.5b00190
- Wang A, Cai B, Fu L, Liang M, Shi X, Wang B et al. (2021) Analysis of Pyrolysis Characteristics and Kinetics of Cigar Tobacco and Flue-Cured Tobacco by TG-FTIR. *Contributions to Tobacco and Nicotine Research*, 30(1). doi: 10.2478/cttr-2021-0003
- Wang X, Derakhshandeh R, Liu J, Narayan S, Nabavizadeh P, Le S et al. (2016) One minute of marijuana secondhand smoke exposure substantially impairs vascular endothelial function. *Journal of the American Heart Association*, 5(8); e003858. doi: 10.1161/JAHA.116.003858
- Warden H, Richardson H, Richardson L, Siemiatycki J, Ho V (2018) Associations between occupational exposure to benzene, toluene and xylene and risk of lung cancer in Montréal. *Occupational Environmental Medicine*, 75(10); 696-702. doi: 10.1136/oemed-2017-104987
- Warnakulasuriya S, Straif K (2018) Carcinogenicity of smokeless tobacco: Evidence from studies in humans & experimental animals. *Journal of behavioral medicine*, 148(6); 681. doi: 10.4103/ijmr.IJMR_149_18
- Wei Z, Xu C, Wang J, Lu F, Bie X, Lu Z (2017) Identification and characterization of *Streptomyces flavogriseus* NJ-4 as a novel producer of actinomycin D and holomycin. *PeerJ*, 5; e3601.
- WHO (2008) WHO report on the global tobacco epidemic, 2008: the MPOWER package. *Research for International Tobacco Control*.
- WHO (2018) Delta-9-tetrahydrocannabinol *WHO Expert Committee on Drug Dependence Critical Review*. Retrieved from <https://www.who.int/medicines/access/controlled-substances/THCv1.pdf?ua=1>
- WHO (2019) WHO report on the global tobacco epidemic 2019: Offer help to quit tobacco use. Retrieved from <https://escholarship.org/content/qt1g16k8b9/qt1g16k8b9.pdf>

- Williams JR (2012) Alkaloid composition for e-cigarette. Retrieved from <https://patents.google.com/patent/US20120325228A1/en>
- Williams K (2014) *The different ways to smoke and consume cannabis* Retrieved from <https://www.leafly.com/news/cannabis-101/the-complete-list-of-cannabis-delivery-methods>
- Wolff V, Jouanjus E (2017) Strokes are possible complications of cannabinoids use. *Epilepsy & Behavior*, 70; 355-363. doi: 10.1016/j.yebeh.2017.01.031
- Wolff V., Armspach J, Lauer V (Eds.). (2018). *Street Drugs II: Amphetamine Derivatives and Hallucinogens*.
- Wolff Valérie, Lauer V, Rouyer O, Sellal F, Meyer N, Raul JS et al. (2011) Cannabis use, ischemic stroke, and multifocal intracranial vasoconstriction: a prospective study in 48 consecutive young patients. *Stroke*, 42(6); 1778-1780. doi: 10.1161/STROKEAHA.110.610915
- Worku A (2018) Khat and synthetic cathinones: Emerging drugs of abuse with dental implications. *Oral Surgery, Oral Medicine, Oral Pathology and Oral Radiology*, 125(2); 140-146. doi: 10.1016/j.oooo.2017.11.015
- Xue J, Yang S, Seng S (2014) Mechanisms of cancer induction by tobacco-specific NNK and NNN. *Cancers*, 6(2); 1138-1156. doi: 10.3390/cancers6021138
- Yershova K, Yuan JM, Wang R, Valentin L, Watson C, Gao YT et al. (2016) Tobacco-specific N-nitrosamines and polycyclic aromatic hydrocarbons in cigarettes smoked by the participants of the Shanghai cohort study. *International journal of cancer*, 139(6); 1261-1269.
- Yu Y, Wang P, Cui Y, Wang Y (2018) Chemical analysis of DNA damage. *Analytical chemistry*, 90(1); 556-576. doi: 10.1021/acs.analchem.7b04247
- Zamora R, Hidalgo FJ (2020) Formation of heterocyclic aromatic amines with the structure of aminoimidazoazarenes in food products. *Food chemistry*, 313; 126128. doi: 10.1016/j.foodchem.2019.126128
- Zhu Y, Wei J, Liu Y, Liu X, Li J, Zhang J (2019) Assessing the effect on the generation of environmentally persistent free radicals in hydrothermal carbonization of sewage sludge. *Scientific Reports*, 9(1); 1-10.
- Zinicovscaia I, Culicov OA, Dului OG, Yushin NS, Gundorina SF (2018) Major-and trace-element distribution in cigarette tobacco, ash and filters. *Journal of Radioanalytical and Nuclear Chemistry*, 316(2); 629-634.

APPENDICES**Appendix 1: Sample GC-MS data for marijuana**

Sample Information

Analyzed by : Neal
Analyzed : 2020-02-12 08:50:05 PM
Sample Type : Unknown
Level # : 1
Sample Name : M7
Sample ID : M7
IS Amount : [1]=1
Sample Amount : 1
Dilution Factor : 1
Vial # : 8
Injection Volume : 8.00
Data File : C:\GCMSsolution\Data\2020 Joshua Kenya\12 02 2020\M7.qgd
Org Data File : C:\GCMSsolution\Data\2020 Joshua Kenya\12 02 2020\M7.qgd
Method File : C:\GCMSsolution\Methods\SCAN 310C splitless 37 mins
NEW.qgm
Org Method File : C:\GCMSsolution\Methods\SCAN 310C splitless 37 mins
NEW.qgm
Report File :
Tuning File : C:\GCMSsolution\System\Tune1\2020 Tuning Files\21-01-
2020.qgt
Modified by : Neal
Modified : 2020-02-12 09:27:05 PM

17	24.193	24.085	24.225	8044004	1.86	2167902	2.82
18	24.841	24.770	24.890	3451854	0.80	2261164	2.95
19	26.387	26.365	26.405	642525	0.15	397905	0.52
20	26.426	26.405	26.445	623859	0.14	517526	0.67
21	26.483	26.465	26.505	832304	0.19	598027	0.78
22	26.808	26.765	26.850	4544534	1.05	2345389	3.06
23	28.432	28.335	28.480	5409869	1.25	1871621	2.44
24	28.839	28.800	28.875	1989993	0.46	796758	1.04
25	29.269	29.185	29.310	1285752	0.30	472063	0.62
26	29.578	29.515	29.625	1749491	0.41	645319	0.84
27	29.769	29.730	29.810	1095155	0.25	399494	0.52
				431681656	100.00	76749518	100.00

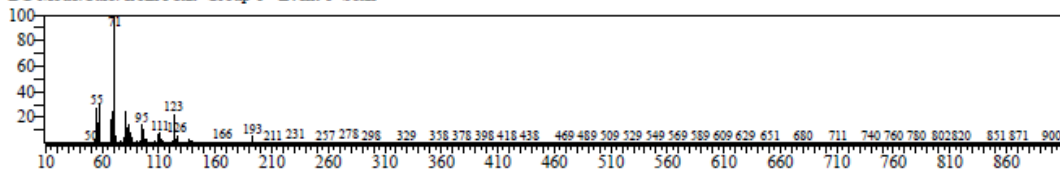
Library

<< Target >>

Line#: 1 R.Time: 19.165(Scan#: 2934) MassPeaks: 525

RawMode: Averaged 19.160-19.170(2933-2935) BasePeak: 71.10(741662)

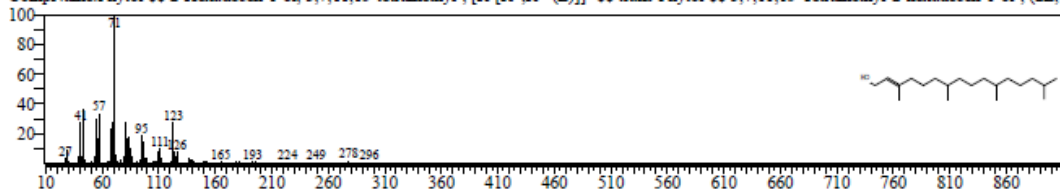
BG Mode: Calc. from Peak Group 1 - Event 1 Scan



Hit#1 Entry: 115516 Library: NIST11.lib

SI: 95 Formula: C₂₀H₄₀O CAS: 150-86-7 MolWeight: 296 RetIndex: 2045

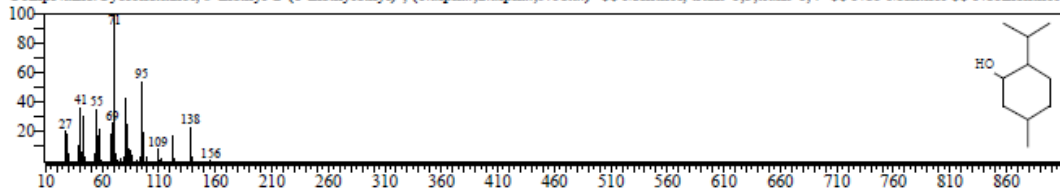
CompName: Phytol \$\$ 2-Hexadecen-1-ol, 3,7,11,15-tetramethyl-, [R-[R*,R*(E)]]- \$\$ trans-Phytol \$\$ 3,7,11,15-Tetramethyl-2-hexadecen-1-ol-, (2E,7E,11E,15E)-



Hit#2 Entry: 18678 Library: NIST11.lib

SI: 86 Formula: C₁₀H₂₀O CAS: 491-01-0 MolWeight: 156 RetIndex: 1164

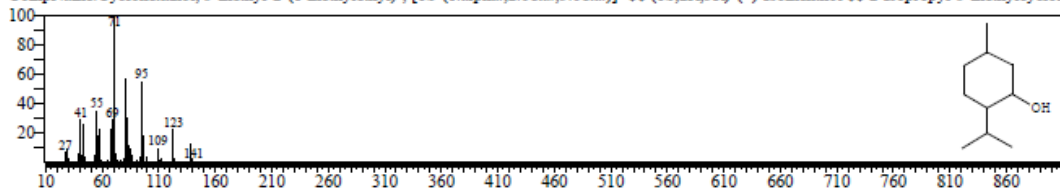
CompName: Cyclohexanol, 5-methyl-2-(1-methylethyl)-, (1.alpha.,2.alpha.,5.beta.)- \$\$ Menthol, trans-1,3,trans-1,4- \$\$ Neo-Menthol \$\$ Neomenthol



Hit#3 Entry: 18670 Library: NIST11.lib

SI: 86 Formula: C₁₀H₂₀O CAS: 23283-97-8 MolWeight: 156 RetIndex: 1164

CompName: Cyclohexanol, 5-methyl-2-(1-methylethyl)-, [1S-(1.alpha.,2.beta.,5.beta.)]- \$\$ (1S,2R,5R)-(+)-Isomenthol \$\$ 2-Isopropyl-5-methylcyclohexanol



Appendix 2: Sample GC-MS data for khat

Sample Information

Analyzed by : Neal

Analyzed : 2020-02-11 09:36:13 PM

Sample Type : Unknown

Level # : 1

Sample Name : K4

Sample ID : K4

IS Amount : [1]=1

Sample Amoun : 1

Dilution Factor : 1

Vial # : 4

Injection Volume : 8.00

Data File : C:\GCMSsolution\Data\2020 Joshua Kenya\11 02 2020\K4.qgd

Org Data File : C:\GCMSsolution\Data\2020 Joshua Kenya\11 02 2020\K4.qgd

Method File : C:\GCMSsolution\Methods\SCAN 310C splitless 37 mins
NEW.qgm

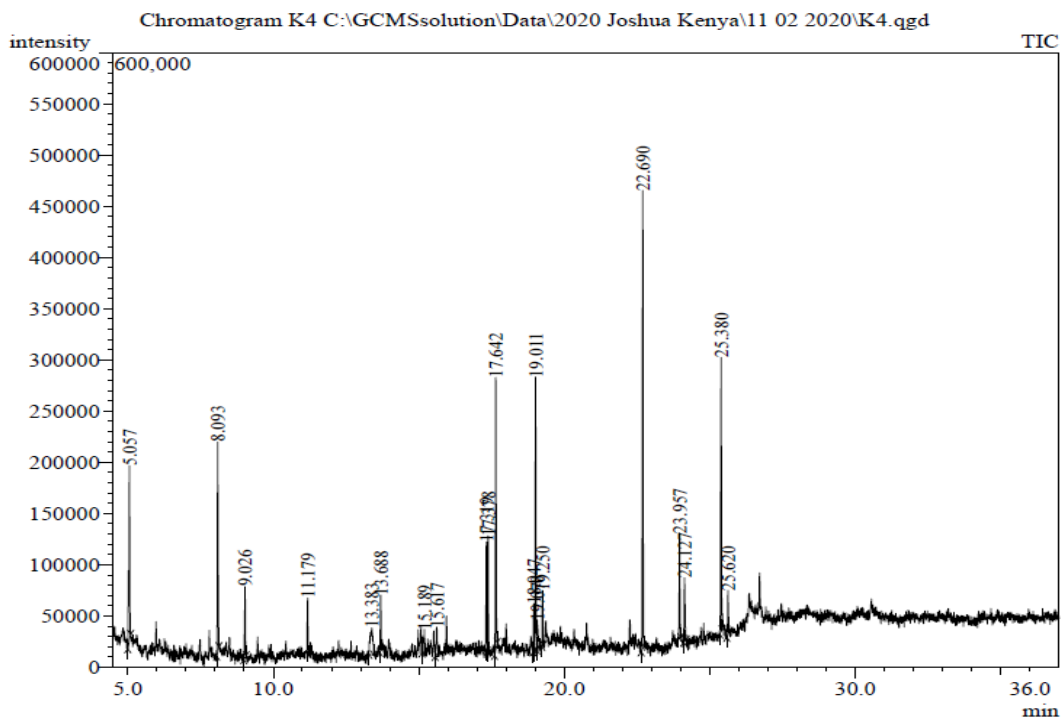
Org Method File : C:\GCMSsolution\Methods\SCAN 310C splitless 37 mins
NEW.qgm

Report File :

Tuning File : C:\GCMSsolution\System\Tune1\2020 Tuning Files\21-01-
2020.qgt

Modified by : Neal

Modified : 2020-02-11 10:13:13 PM



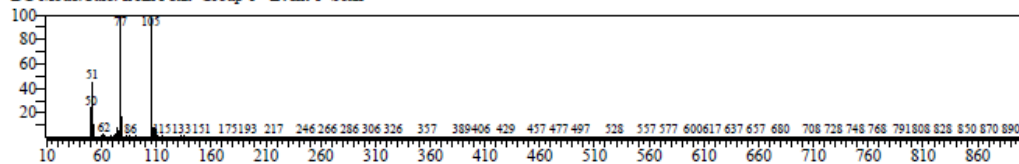
Peak Report TIC

Peak#	R.Time	I.Time	F.Time	Area	Area%	Height	Height%
1	5.057	5.000	5.100	380735	8.84	170680	7.01
2	8.093	8.055	8.135	337207	7.83	204746	8.40
3	9.026	8.985	9.070	113581	2.64	69635	2.86
4	11.179	11.150	11.220	81083	1.88	53777	2.21
5	13.383	13.285	13.445	156096	3.62	26272	1.08
6	13.688	13.650	13.720	88838	2.06	54473	2.24
7	15.189	15.100	15.220	81204	1.88	24397	1.00
8	15.617	15.560	15.655	79730	1.85	28577	1.17
9	17.319	17.290	17.345	167022	3.88	106150	4.36
10	17.378	17.345	17.415	174344	4.05	113593	4.66
11	17.642	17.600	17.695	453617	10.53	265702	10.91
12	18.947	18.925	18.970	73729	1.71	46851	1.92
13	19.011	18.970	19.045	418335	9.71	266846	10.95
14	19.070	19.045	19.140	81347	1.89	28880	1.19
15	19.250	19.225	19.280	86540	2.01	54094	2.22
16	22.690	22.635	22.730	701932	16.29	446986	18.35
17	23.957	23.915	24.000	172467	4.00	101871	4.18
18	24.127	24.095	24.175	124346	2.89	61993	2.54
19	25.380	25.335	25.420	449103	10.42	267670	10.99
20	25.620	25.580	25.665	87497	2.03	43010	1.77
				4308753	100.00	2436203	100.00

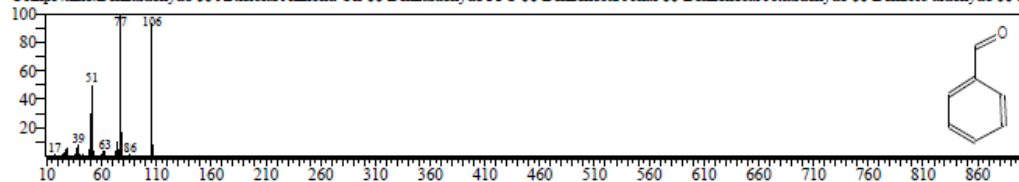
Library

<< Target >>

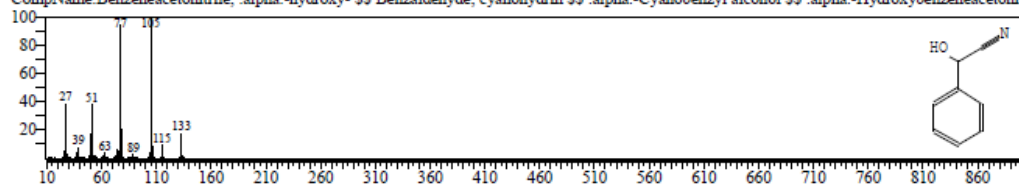
Line# 1 R.Time: 5.055(Scan#: 112) MassPeaks: 529
 RawMode: Averaged 5.050-5.060(111-113) BasePeak: 77.05(34856)
 BG Mode: Calc. from Peak Group 1 - Event 1 Scan



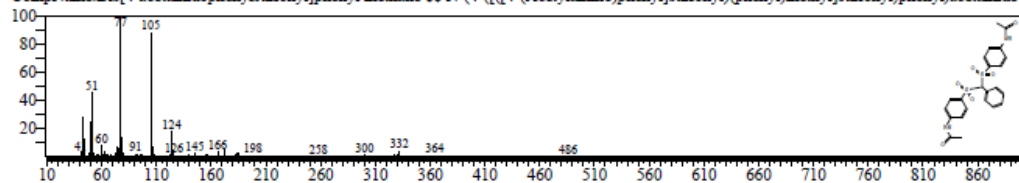
Hit# 1 Entry: 2661 Library: NIST11.lib
 SI: 93 Formula: C₇H₆O CAS: 100-52-7 MolWeight: 106 RefIndex: 982
 CompName: Benzaldehyde \$\$ Artificial Almond Oil \$\$ Benzaldehyde FFC \$\$ Benzenecarbonal \$\$ Benzenecarboxaldehyde \$\$ Benzoic aldehyde \$\$ I



Hit# 2 Entry: 8722 Library: NIST11.lib
 SI: 89 Formula: C₈H₇NO CAS: 532-28-5 MolWeight: 133 RefIndex: 1301
 CompName: Benzeneacetonitrile, .alpha.-hydroxy- \$\$ Benzaldehyde, cyanohydrin \$\$.alpha.-Cyanobenzyl alcohol \$\$.alpha.-Hydroxybenzeneacetoni



Hit# 3 Entry: 202973 Library: NIST11.lib
 SI: 89 Formula: C₂₃H₂₂N₂O₆S₂ CAS: 81269-03-6 MolWeight: 486 RefIndex: 4315
 CompName: Bis[4-(acetamidophenyl)sulfonyl]phenyl methane \$\$ N-(4-([(4-(Acetylamino)phenyl)sulfonyl](phenyl)methyl)sulfonyl]phenyl)acetamide



Appendix 3: Sample GC-MS data for tobacco-khat

Sample Information

Analyzed by : Neal

Analyzed : 2020-03-02 12:04:29 PM

Sample Type : Unknown

Level # : 1

Sample Name : TK 3

Sample ID : TK 3

IS Amount : [1]=1

Sample Amount : 1

Dilution Factor : 1

Vial # : 4

Injection Volume : 7.00

Data File : C:\GCMSsolution\Data\2020 Joshua Kenya\Repeats\TK 3.qgd

Org Data File : C:\GCMSsolution\Data\2020 Joshua Kenya\Repeats\TK 3.qgd

Method File : C:\GCMSsolution\Methods\SCAN 310C splitless 37 mins
NEW.qgm

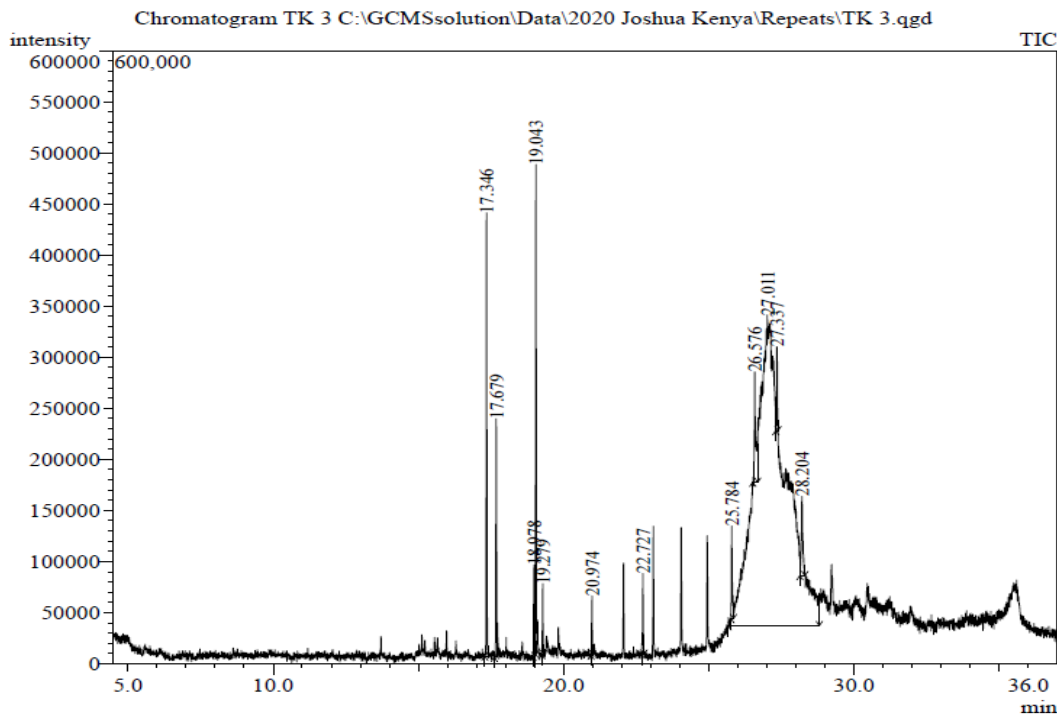
Org Method File : C:\GCMSsolution\Methods\SCAN 310C splitless 37 mins
NEW.qgm

Report File : C:\GCMSsolution\Report Formats\Full report TIC peak area &
library.qgr

Tuning File : C:\GCMSsolution\System\Tune1\2020 Tuning Files\21-01-
2020.qgt

Modified by : Neal

Modified : 2020-03-02 12:41:29 PM



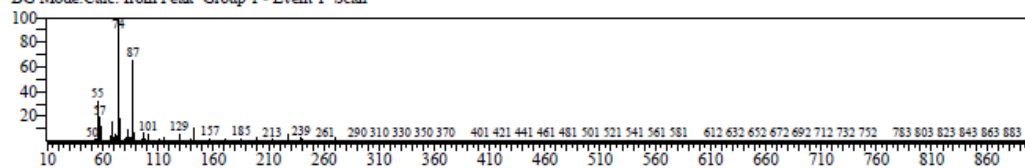
Peak Report TIC

Peak#	R.Time	I.Time	F.Time	Area	Area%	Height	Height%
1	17.346	17.285	17.430	667621	2.57	433832	20.62
2	17.679	17.610	17.715	365925	1.41	233514	11.10
3	18.978	18.950	19.005	132274	0.51	89426	4.25
4	19.043	19.005	19.075	725585	2.80	478151	22.73
5	19.279	19.245	19.310	96900	0.37	69427	3.30
6	20.974	20.940	21.010	84684	0.33	57841	2.75
7	22.727	22.680	22.770	137507	0.53	79031	3.76
8	25.784	25.755	25.845	186850	0.72	90507	4.30
9	26.576	26.505	26.675	375733	1.45	108048	5.14
10	27.011	25.655	28.800	22718798	87.57	304144	14.46
11	27.337	27.300	27.375	161921	0.62	82140	3.90
12	28.204	28.130	28.305	290619	1.12	77559	3.69
				25944417	100.00	2103620	100.00

Library

<< Target >>

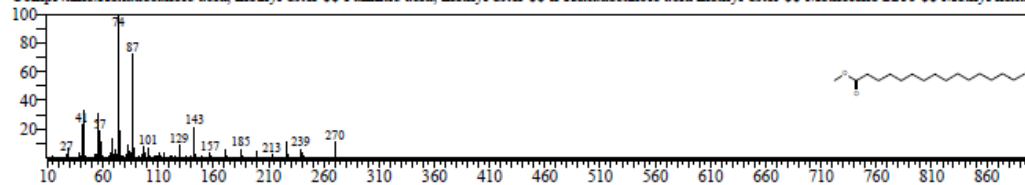
Line# 1 R.Time:17.345(Scan#:2570) MassPeaks:375
 RawMode:Averaged 17.340-17.350(2569-2571) BasePeak:74.10(107990)
 BG Mode:Calc. from Peak Group 1 - Event 1 Scan



Hit# 1 Entry:95188 Library:NIST11.lib

SI:94 Formula:C17H34O2 CAS:112-39-0 MolWeight:270 RetIndex:1878

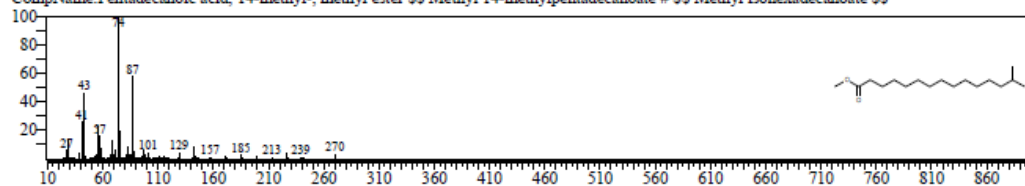
CompName:Hexadecanoic acid, methyl ester \$\$ Palmitic acid, methyl ester \$\$ n-Hexadecanoic acid methyl ester \$\$ Metholene 2216 \$\$ Methyl hexadecanoate



Hit# 2 Entry:95189 Library:NIST11.lib

SI:94 Formula:C17H34O2 CAS:5129-60-2 MolWeight:270 RetIndex:1814

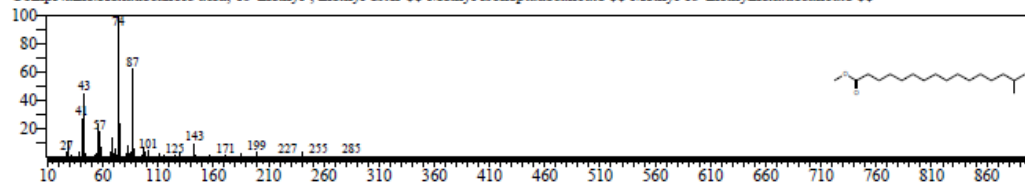
CompName:Hexadecanoic acid, 14-methyl-, methyl ester \$\$ Methyl 14-methylpentadecanoate # \$\$ Methyl isohexadecanoate \$\$



Hit# 3 Entry:106180 Library:NIST11.lib

SI:93 Formula:C18H36O2 CAS:6929-04-0 MolWeight:284 RetIndex:1914

CompName:Hexadecanoic acid, 15-methyl-, methyl ester \$\$ Methyl isoheptadecanoate \$\$ Methyl 15-methylhexadecanoate \$\$

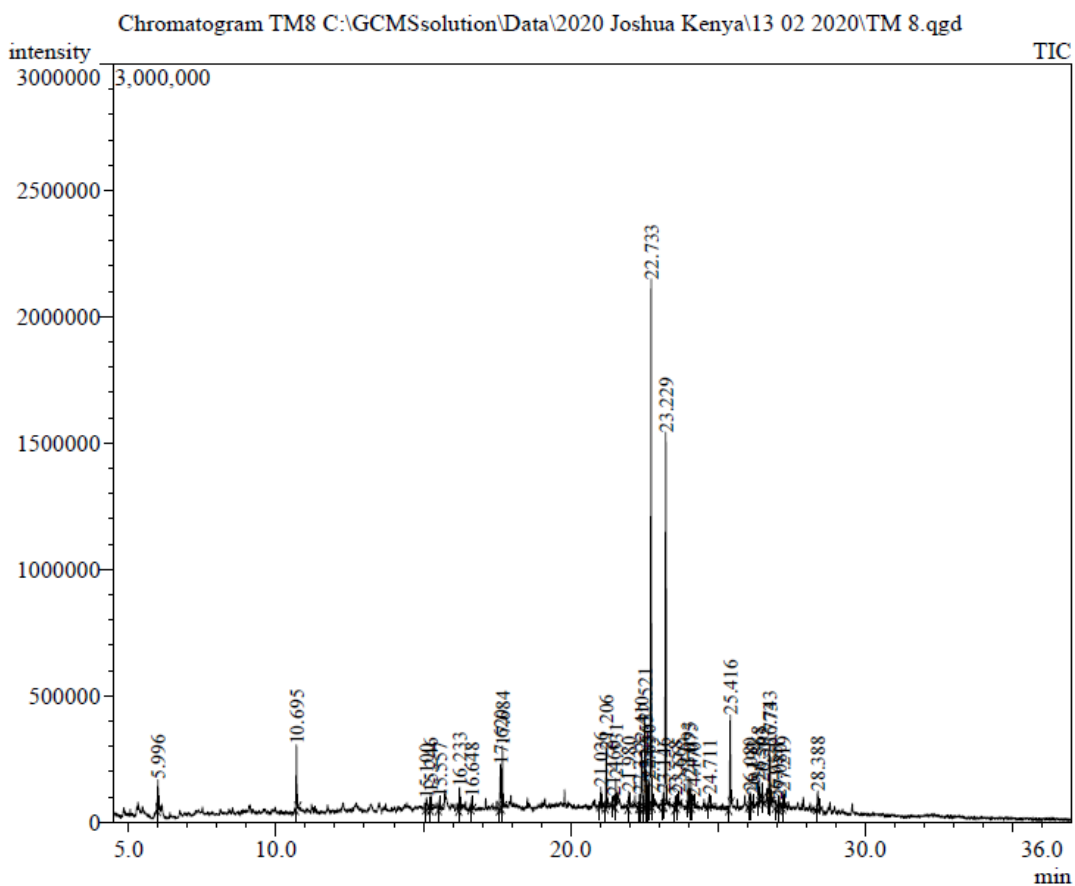


Hit# 4 Entry:73852 Library:NIST11.lib

Appendix 4: Sample GC-MS data for tobacco-khat

Sample Information

Analyzed by : Neal
Analyzed : 2020-02-13 02:22:53 PM
Sample Type : Unknown
Level # : 1
Sample Name : TM8
Sample ID : TM8
IS Amount : [1]=1
Sample Amount : 1
Dilution Factor : 1
Vial # : 9
Injection Volume : 8.00
Data File : C:\GCMSsolution\Data\2020 Joshua Kenya\13 02
2020\TM 8.qgd
Org Data File : C:\GCMSsolution\Data\2020 Joshua Kenya\13 02
2020\TM 8.qgd
Method File : C:\GCMSsolution\Methods\SCAN 310C splitless 37 mins
NEW.qgm
Org Method File : C:\GCMSsolution\Methods\SCAN 310C splitless 37 mins
NEW.qgm
Report File :
Tuning File : C:\GCMSsolution\System\Tune1\2020 Tuning Files\21-
01-2020.qgt
Modified by : Neal
Modified : 2020-02-14 06:59:28 AM



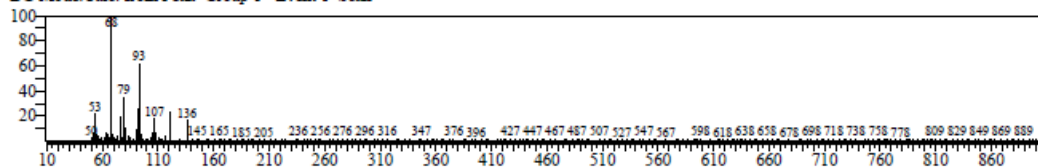
Peak#	R.Time	I.Time	F.Time	Area	Area%	Height	Height%
1	5.996	5.975	6.035	187596	1.27	119046	1.52
2	10.695	10.660	10.745	414540	2.81	252267	3.23
3	15.100	15.080	15.230	159969	1.08	40120	0.51
4	15.246	15.230	15.290	120525	0.82	65391	0.84
5	15.557	15.510	15.585	109702	0.74	46388	0.59
6	16.233	16.200	16.265	164065	1.11	89292	1.14
7	16.648	16.615	16.685	90557	0.61	45988	0.59
8	17.620	17.580	17.650	358517	2.43	178173	2.28
9	17.684	17.650	17.725	405502	2.75	244392	3.13
10	21.026	20.985	21.060	126518	0.86	77176	0.99
11	21.206	21.175	21.235	387710	2.63	231466	2.97
12	21.460	21.400	21.500	131579	0.89	41808	0.54
13	21.531	21.500	21.560	171268	1.16	108746	1.39
14	21.980	21.940	22.015	130588	0.88	64006	0.82
15	22.333	22.300	22.355	87871	0.59	52356	0.67
16	22.410	22.355	22.480	610426	4.13	225846	2.89

17	22.521	22.480	22.545	620352	4.20	339932	4.35
18	22.555	22.545	22.605	240326	1.63	153257	1.96
19	22.630	22.605	22.665	191349	1.30	112799	1.44
20	22.733	22.675	22.760	3701550	25.06	2089424	26.76
21	22.775	22.760	22.805	91818	0.62	56245	0.72
22	23.146	23.130	23.165	80192	0.54	54335	0.70
23	23.229	23.165	23.280	2872203	19.45	1472166	18.86
24	23.558	23.530	23.590	93652	0.63	48671	0.62
25	23.665	23.590	23.680	145385	0.98	49849	0.64
26	23.993	23.950	24.020	195344	1.32	114989	1.47
27	24.075	24.040	24.100	184609	1.25	116581	1.49
28	24.170	24.100	24.210	162095	1.10	43114	0.55
29	24.711	24.665	24.745	117876	0.80	52949	0.68
30	25.416	25.365	25.445	573959	3.89	357355	4.58
31	26.080	26.035	26.115	157398	1.07	58824	0.75
32	26.192	26.115	26.225	151919	1.03	45148	0.58
33	26.368	26.335	26.425	241254	1.63	85072	1.09
34	26.503	26.485	26.525	90105	0.61	65572	0.84
35	26.743	26.690	26.760	457706	3.10	222213	2.85
36	26.773	26.760	26.805	259387	1.76	175859	2.25
37	26.955	26.940	27.060	96123	0.65	28538	0.37
38	27.080	27.060	27.195	112797	0.76	41531	0.53
39	27.219	27.195	27.245	109426	0.74	64665	0.83
40	28.388	28.350	28.435	165740	1.12	75024	0.96
				14769498	100.00	7806573	100.00

Library

<< Target >>

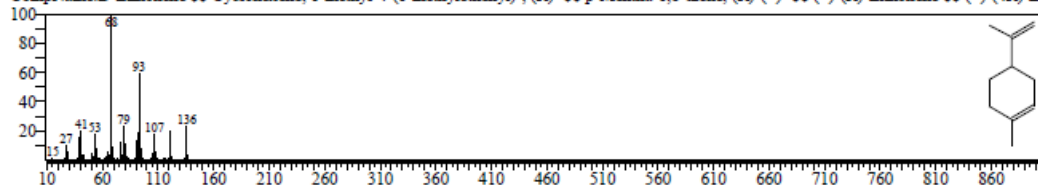
Line# 1 R.Time: 5.995 (Scan#: 300) MassPeaks: 530
 RawMode: Averaged 5.990-6.000 (299-301) BasePeak: 68.10 (15623)
 BG Mode: Calc. from Peak Group 1 - Event 1 Scan



Hit# 1 Entry: 9748 Library: NIST11.lib

SI: 89 Formula: C10H16 CAS: 5989-27-5 MolWeight: 136 RefIndex: 1018

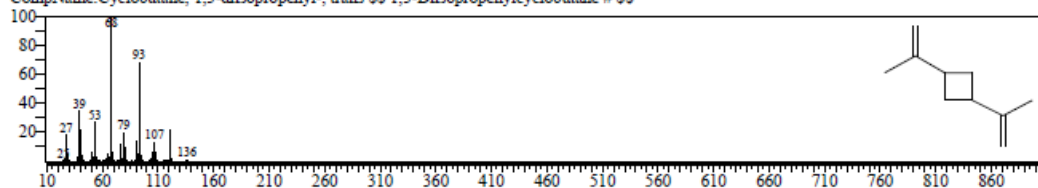
CompName: D-Limonene \$\$ Cyclohexene, 1-methyl-4-(1-methylethenyl)-, (R)- \$\$ p-Mentha-1,8-diene, (R)-(+)- \$\$ (+)-Limonene \$\$ (+)-(4R)-Li



Hit# 2 Entry: 9744 Library: NIST11.lib

SI: 88 Formula: C10H16 CAS: 0-00-0 MolWeight: 136 RefIndex: 934

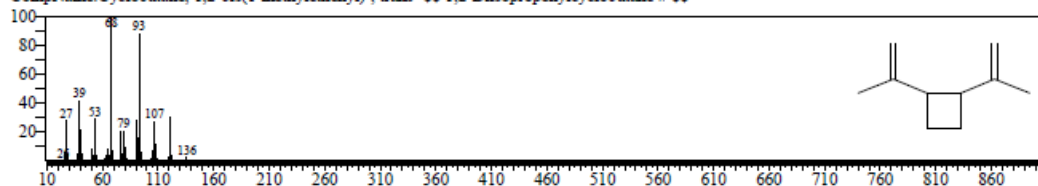
CompName: Cyclobutane, 1,3-diisopropenyl-, trans \$\$ 1,3-Diisopropenylcyclobutane # \$\$



Hit# 3 Entry: 9746 Library: NIST11.lib

SI: 88 Formula: C10H16 CAS: 19465-02-2 MolWeight: 136 RefIndex: 934

CompName: Cyclobutane, 1,2-bis(1-methylethenyl)-, trans \$\$ 1,2-Diisopropenylcyclobutane # \$\$



Appendix 5: Sample GC-MS data for marijuana-khat

Sample Information

Analyzed by : Neal

Analyzed : 2020-02-17 06:32:33 AM

Sample Type : Unknown

Level # : 1

Sample Name : MK 8

Sample ID : MK 8

IS Amount : [1]=1

Sample Amount : 1

Dilution Factor : 1

Vial # : 9

Injection Volume : 8.00

Data File : C:\GCMSsolution\Data\2020 Joshua Kenya\15 02 2020\MK 8.qgd

Org Data File : C:\GCMSsolution\Data\2020 Joshua Kenya\15 02 2020\MK 8.qgd

Method File : C:\GCMSsolution\Methods\SCAN 310C splitless 37 mins
NEW.qgm

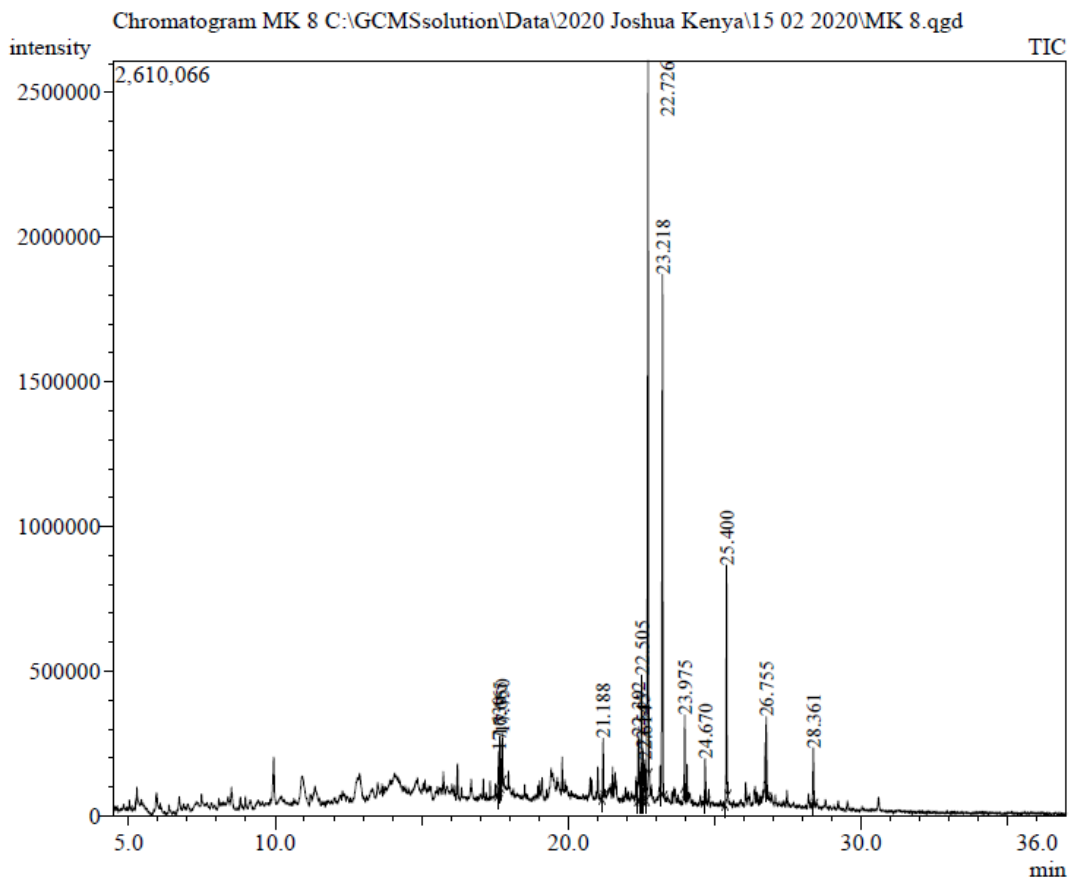
Org Method File : C:\GCMSsolution\Methods\SCAN 310C splitless 37 mins
NEW.qgm

Report File :

Tuning File : C:\GCMSsolution\System\Tune1\2020 Tuning Files\21-01-
2020.qgt

Modified by : Neal

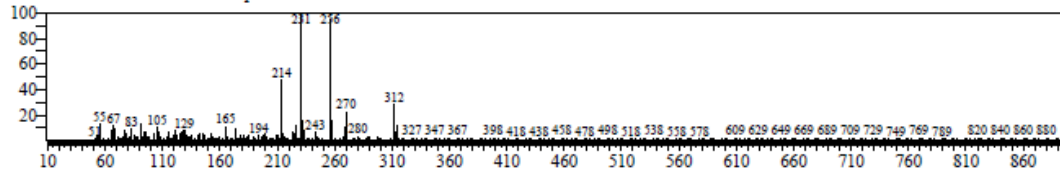
Modified : 2020-02-17 07:09:33 AM



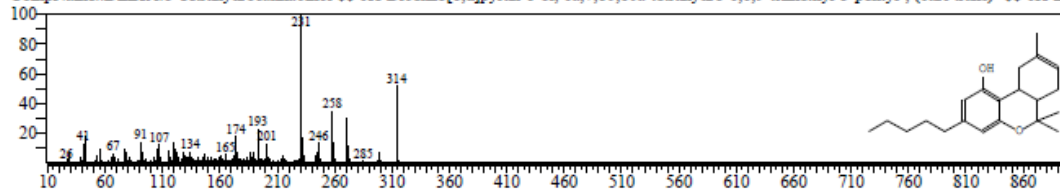
Peak#	R.Time	I.Time	F.Time	Area	Area%	Height	Height%
1	17.630	17.590	17.650	314871	2.11	143693	1.88
2	17.665	17.650	17.695	286796	1.92	186027	2.43
3	17.750	17.695	17.780	384918	2.58	173079	2.26
4	21.188	21.155	21.220	341453	2.29	203966	2.67
5	22.392	22.370	22.435	559817	3.75	222937	2.91
6	22.505	22.435	22.525	883307	5.91	433526	5.67
7	22.545	22.525	22.575	292649	1.96	178038	2.33
8	22.614	22.575	22.660	282020	1.89	141015	1.84
9	22.726	22.660	22.755	5235574	35.04	2492477	32.58
10	23.218	23.160	23.270	3506095	23.47	1798156	23.50
11	23.975	23.940	24.010	386941	2.59	274241	3.58
12	24.670	24.645	24.725	287804	1.93	146183	1.91
13	25.400	25.350	25.445	1325277	8.87	811559	10.61
14	26.755	26.740	26.815	439152	2.94	253612	3.31
15	28.361	28.320	28.410	413806	2.77	192158	2.51
				4940480	100.00	7650667	100.00

<< Target >>

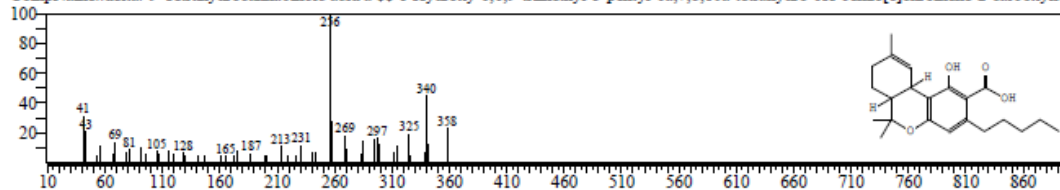
Line# 4 R.Time: 21.190 (Scan# 3339) MassPeaks: 462
 RawMode: Averaged 21.185-21.195 (3338-3340) BasePeak: 231.00 (23683)
 BG Mode: Calc. from Peak Group 1 - Event 1 Scan



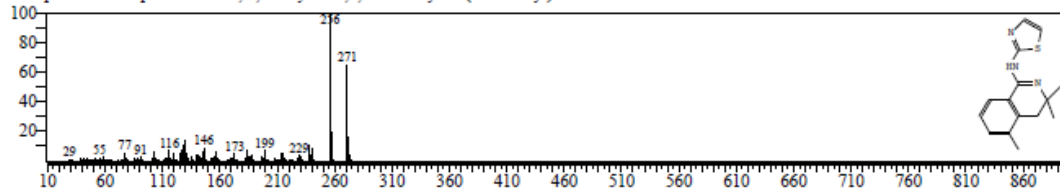
Hit# 1 Entry: 129839 Library: NIST11.lib
 SI: 50 Formula: C₂₁H₃₀O₂ CAS: 5957-75-5 MolWeight: 314 RefIndex: 2475
 CompName: DELTA-8-Tetrahydrocannabinol



Hit# 2 Entry: 160863 Library: NIST11.lib
 SI: 50 Formula: C₂₂H₃₀O₄ CAS: 23978-85-0 MolWeight: 358 RefIndex: 2945
 CompName: delta-9-Tetrahydrocannabinolic acid



Hit# 3 Entry: 95757 Library: NIST11.lib
 SI: 49 Formula: C₁₅H₁₇N₃S CAS: 0-00-0 MolWeight: 271 RefIndex: 2335
 CompName: 1-Isoquinolinamine, 3,4-dihydro-3,5-trimethyl-N-(2-thiazolyl)-

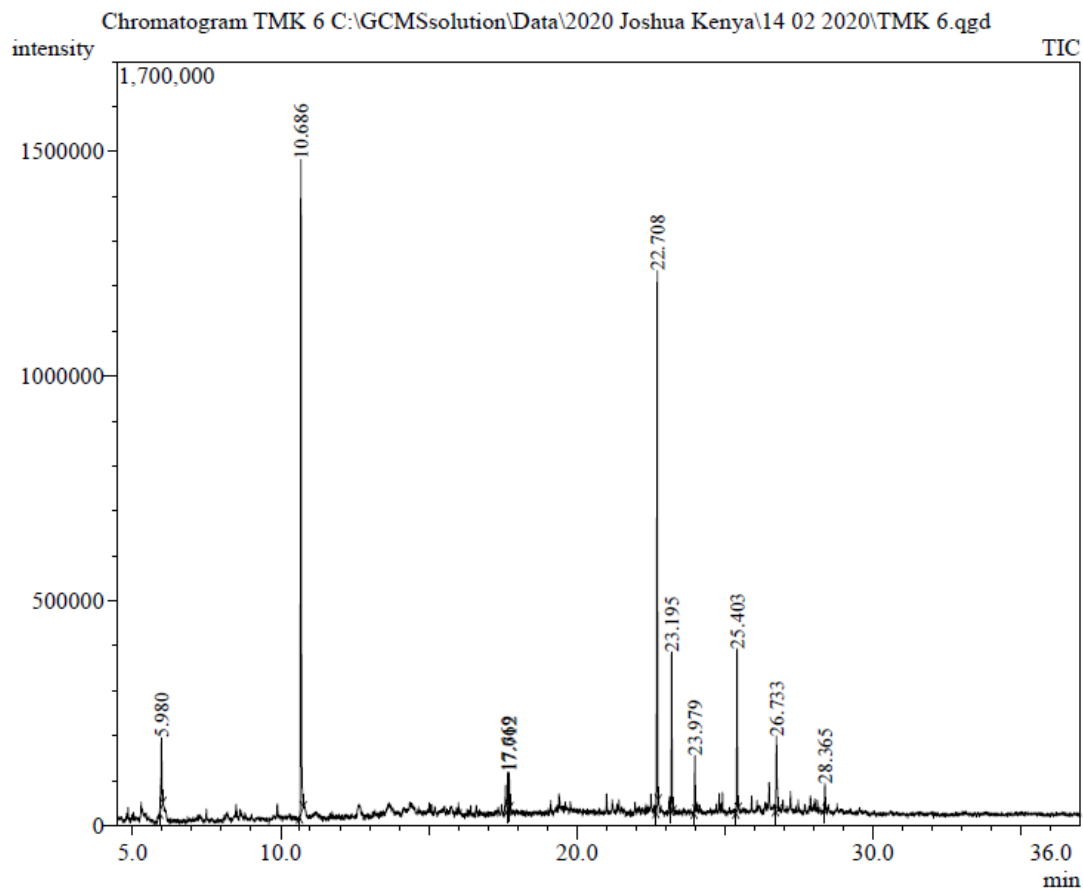


Hit# 4 Entry: 128246 Library: NIST11.lib

Appendix 6: Sample GC-MS data for Tobacco-marijuana-khat

Sample Information

Analyzed by : Neal
Analyzed : 2020-02-14 09:32:54 PM
Sample Type : Unknown
Level # : 1
Sample Name : TMK 6
Sample ID : TMK 6
IS Amount : [1]=1
Sample Amount : 1
Dilution Factor : 1
Vial # : 19
Injection Volume : 8.00
Data File : C:\GCMSsolution\Data\2020 Joshua Kenya\14 02 2020\TMK
6.qgd
Org Data File : C:\GCMSsolution\Data\2020 Joshua Kenya\14 02 2020\TMK
6.qgd
Method File : C:\GCMSsolution\Methods\SCAN 310C splitless 37 mins
NEW.qgm
Org Method File : C:\GCMSsolution\Methods\SCAN 310C splitless 37 mins
NEW.qgm
Report File :
Tuning File : C:\GCMSsolution\System\Tune1\2020 Tuning Files\21-01-
2020.qgt
Modified by : Neal
Modified : 2020-02-14 10:09:54 PM

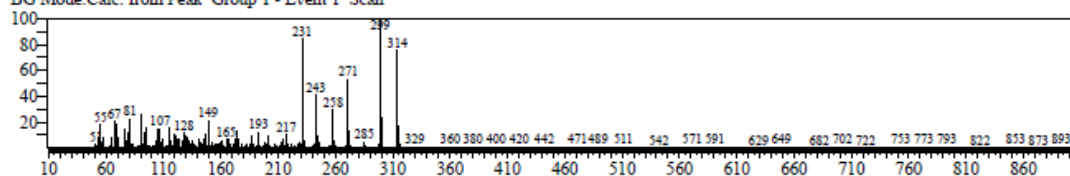


Peak Report TIC

Peak#	R.Time	I.Time	F.Time	Area	Area%	Height	Height%
1	5.980	5.920	6.025	345210	4.98	153860	3.82
2	10.686	10.640	10.765	2583868	37.31	1455739	36.17
3	17.669	17.650	17.690	114470	1.65	83750	2.08
4	17.712	17.690	17.740	121106	1.75	79560	1.98
5	22.708	22.665	22.740	1990387	28.74	1189075	29.54
6	23.195	23.155	23.245	543779	7.85	352662	8.76
7	23.979	23.950	24.015	195206	2.82	125588	3.12
8	25.403	25.360	25.440	549244	7.93	360429	8.95
9	26.733	26.700	26.800	367511	5.31	165935	4.12
10	28.365	28.335	28.405	115524	1.67	58328	1.45
				6926305	100.00	4024926	100.00

<< Target >>

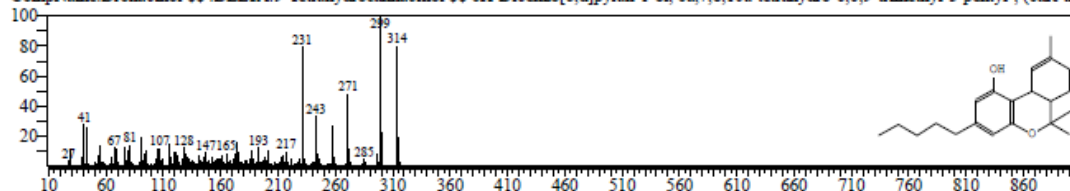
Line# 5 R-Time: 22.710 (Scan# 3643) MassPeaks: 578
 RawMode: Averaged 22.705-22.715 (3642-3644) BasePeak: 299.05 (87042)
 BG Mode: Calc. from Peak Group 1 - Event 1 Scan



Hit# 1 Entry: 129845 Library: NIST11.lib

SI: 91 Formula: C₂₁H₃₀O₂ CAS: 1972-08-3 MolWeight: 314 RefIndex: 2475

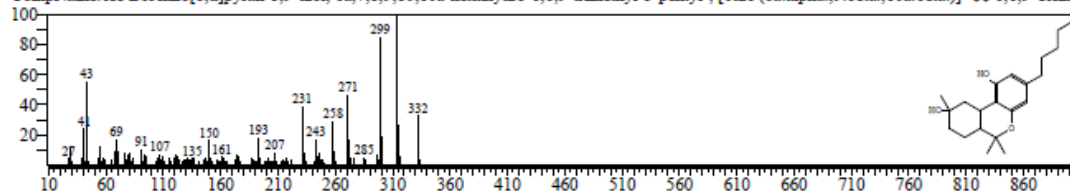
CompName: Dronabinol \$\$ DELTA-9-Tetrahydrocannabinol \$\$ 6H-Dibenzo[b,d]pyran-1-ol, 6a,7,8,10a-tetrahydro-6,6,9-trimethyl-3-pentyl-, (6aR-tra



Hit# 2 Entry: 143303 Library: NIST11.lib

SI: 76 Formula: C₂₁H₃₂O₃ CAS: 52522-56-2 MolWeight: 332 RefIndex: 2615

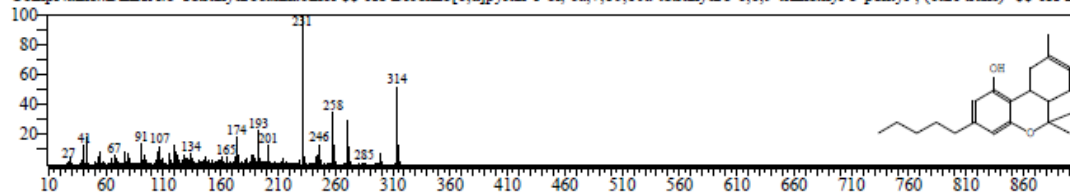
CompName: 6H-Dibenzo[b,d]pyran-1,9-diol, 6a,7,8,9,10,10a-hexahydro-6,6,9-trimethyl-3-pentyl-, [6aR-(6a.alpha.,9.beta.,10a.beta.)]- \$\$ 6,6,9-Trimer



Hit# 3 Entry: 129839 Library: NIST11.lib

SI: 74 Formula: C₂₁H₃₀O₂ CAS: 5957-75-5 MolWeight: 314 RefIndex: 2475

CompName: DELTA-8-Tetrahydrocannabinol \$\$ 6H-Dibenzo[b,d]pyran-1-ol, 6a,7,10,10a-tetrahydro-6,6,9-trimethyl-3-pentyl-, (6aR-trans)- \$\$ 6H-Di



Hit# 4 Entry: 143297 Library: NIST11.lib

Appendix 8: Gaussian raw geometric data for benzenyl radical at 673 °C

Gaussian 09: IA32W-G03RevC.01 3-Apr-2010

13-Sep-2020

%chk=C:\Users\hp\Desktop\gauss\THC computation\benzenyl 673.chk

Default route: MaxDisk=2000MB

opt freq b3lyp/6-311++g geom=connectivity freq=ReadIsotopes

Symbolic Z-matrix:

Charge = 0 Multiplicity = 2

C	-0.07935	-1.32358	0.
C	1.35579	-0.59041	0.
C	1.36975	0.76739	0.
C	-0.03845	1.16813	0.
C	-1.28727	0.90065	0.
C	-1.32563	-0.63504	0.
H	-0.0967	-2.39344	0.
H	2.26552	-1.15368	0.
H	2.22695	1.40778	0.
H	-2.11088	1.5837	0.
H	-2.2539	-1.16721	0.

GradGradGradGradGradGradGradGradGradGradGradGradGradGradGradGradGrad

Input orientation:

Center Number	Atomic Number	Atomic Type	Coordinates (Angstroms)		
			X	Y	Z
1	6	0	-0.079352	-1.323576	0.000000
2	6	0	1.355786	-0.590406	0.000000
3	6	0	1.369754	0.767388	0.000000
4	6	0	-0.038450	1.168132	0.000000
5	6	0	-1.287275	0.900646	0.000000
6	6	0	-1.325627	-0.635044	0.000000
7	1	0	-0.096702	-2.393436	0.000000
8	1	0	2.265524	-1.153679	0.000000
9	1	0	2.226953	1.407785	0.000000
10	1	0	-2.110883	1.583705	0.000000
11	1	0	-2.253905	-1.167211	0.000000

Distance matrix (angstroms):

	1	2	3	4	5
1 C	0.000000				
2 C	1.611570	0.000000			
3 C	2.544020	1.357866	0.000000		
4 C	2.492044	2.244181	1.464115	0.000000	
5 C	2.531056	3.034634	2.660368	1.277150	0.000000
6 C	1.423826	2.681784	3.038403	2.215461	1.536169
7 H	1.070000	2.315305	3.484436	3.562044	3.502633
8 H	2.351022	1.070000	2.119646	3.270948	4.103977

```

9 H 3.574825 2.179840 1.070000 2.278044 3.550632
10 H 3.546746 4.092011 3.575082 2.113689 1.070000
11 H 2.180168 3.655484 4.107745 3.219016 2.282631
      6      7      8      9      10
6 C 0.000000
7 H 2.145274 0.000000
8 H 3.628409 2.667791 0.000000
9 H 4.098046 4.455183 2.561754 0.000000
10 H 2.353608 4.458091 5.161997 4.341403 0.000000
11 H 1.070000 2.481360 4.519448 5.168045 2.754631
      11
11 H 0.000000

```

Stoichiometry C6H5(2)

Framework group CS[SG(C6H5)]

Deg. of freedom 19

Full point group CS NOp 2

Largest Abelian subgroup CS NOp 2

Largest concise Abelian subgroup C1 NOp 1

Standard orientation:

```

-----
Center  Atomic  Atomic      Coordinates (Angstroms)
Number  Number  Type        X      Y      Z
-----
1      6      0  -0.122851 -1.320250 0.000000
2      6      0   1.335629 -0.634689 0.000000
3      6      0   1.394257 0.721910 0.000000
4      6      0   0.000000 1.168765 0.000000
5      6      0  -1.256949 0.942507 0.000000
6      6      0  -1.345801 -0.591090 0.000000
7      1      0  -0.175389 -2.388959 0.000000
8      1      0   2.226344 -1.227585 0.000000
9      1      0   2.272061 1.333761 0.000000
10     1      0  -2.057641 1.652291 0.000000
11     1      0  -2.291083 -1.092431 0.000000
-----

```

Rotational constants (GHZ): 6.6327528 4.7935432 2.7825629

Standard basis: 6-31++G (6D, 7F)

There are 75 symmetry adapted basis functions of A' symmetry.

There are 18 symmetry adapted basis functions of A'' symmetry.

Integral buffers will be 262144 words long.

Raffenetti 2 integral format.

Two-electron integral symmetry is turned on.

93 basis functions, 181 primitive gaussians, 93 cartesian basis functions

21 alpha electrons 20 beta electrons

nuclear repulsion energy 189.7681468805 Hartrees.

NAtoms= 11 NActive= 11 NUniq= 11 SFac= 1.00D+00 NAtFMM= 60 Big=F

One-electron integrals computed using PRISM.

NBasis= 93 RedAO= T NBF= 75 18

NBUse= 93 1.00D-06 NBFU= 75 18

Harris functional with IExCor= 402 diagonalized for initial guess.

ExpMin= 3.60D-02 ExpMax= 3.05D+03 ExpMxC= 4.57D+02 IAcc=3 IRadAn= 5 AccDes= 0.00D+00

HarFok: IExCor= 402 AccDes= 0.00D+00 IRadAn= 5 IDoV=1

ScaDFX= 1.000000 1.000000 1.000000 1.000000

Initial guess orbital symmetries:

Alpha Orbitals:

Occupied (A')
(A') (A') (A') (A') (A') (A') (A') (A'') (A'') (A'')
(A')

Virtual (A'') (A'') (A') (A'') (A') (A') (A') (A') (A') (A'')
(A') (A') (A'') (A'') (A') (A') (A') (A') (A') (A')
(A'') (A'') (A') (A') (A') (A') (A') (A'') (A') (A')
(A') (A') (A') (A') (A') (A') (A') (A') (A') (A')
(A') (A') (A') (A'') (A') (A') (A'') (A'') (A') (A'')
(A'') (A') (A') (A') (A'') (A') (A') (A') (A') (A')
(A') (A') (A') (A') (A') (A') (A') (A') (A') (A')
(A') (A')

Beta Orbitals:

Occupied (A')
(A') (A') (A') (A') (A') (A') (A') (A'') (A'') (A'')

Virtual (A') (A'') (A'') (A') (A'') (A') (A') (A') (A') (A')
(A'') (A') (A') (A'') (A'') (A') (A') (A') (A') (A')
(A') (A'') (A'') (A') (A') (A') (A') (A') (A'') (A')
(A') (A') (A') (A') (A') (A') (A') (A') (A') (A')
(A') (A') (A') (A') (A'') (A') (A') (A'') (A'') (A')
(A'') (A'') (A') (A') (A') (A'') (A') (A') (A') (A')
(A') (A') (A') (A') (A') (A') (A') (A') (A') (A')
(A') (A') (A')

Population analysis using the SCF density.

Sum of Mulliken spin densities= 1.00000

Electronic spatial extent (au): <R**2>= 459.5848

Charge= 0.0000 electrons

Dipole moment (field-independent basis, Debye):

X= 0.1906 Y= -0.5883 Z= 0.0000 Tot= 0.6184

Quadrupole moment (field-independent basis, Debye-Ang):

XX= -29.5058 YY= -34.6938 ZZ= -40.1208

XY= -0.1608 XZ= 0.0000 YZ= 0.0000

Traceless Quadrupole moment (field-independent basis, Debye-Ang):

XX= 5.2676 YY= 0.0797 ZZ= -5.3473

XY= -0.1608 XZ= 0.0000 YZ= 0.0000

Octapole moment (field-independent basis, Debye-Ang**2):

XXX= 1.8042 YYY= -7.6944 ZZZ= 0.0000 XYY= -0.7450

XXY= 2.7770 XXZ= 0.0000 XZZ= 0.1823 YZZ= 0.3771

YYZ= 0.0000 XYZ= 0.0000

Hexadecapole moment (field-independent basis, Debye-Ang**3):

XXXX= -309.2368 YYYY= -265.0989 ZZZZ= -51.6309 XXXY= 2.3556

XXXZ= 0.0000 YYYYX= -1.3184 YYYZ= 0.0000 ZZZX= 0.0000

ZZZY= 0.0000 XXYY= -86.7819 XXZZ= -73.7974 YYZZ= -59.6631

XXYZ= 0.0000 YYXZ= 0.0000 ZZXY= 0.2130

N-N= 1.897681468805D+02 E-N=-9.153302543072D+02 KE= 2.298901785485D+02

Symmetry A' KE= 2.235484553534D+02

Symmetry A" KE= 6.341723195156D+00

Isotropic Fermi Contact Couplings

Atom	a.u.	MegaHertz	Gauss	10(-4) cm-1
1 C(13)	-0.00025	-0.27774	-0.09910	-0.09264
2 C(13)	0.04290	48.22279	17.20709	16.08539
3 C(13)	-0.02625	-29.50989	-10.52986	-9.84344
4 C(13)	0.16167	181.74429	64.85088	60.62337
5 C(13)	-0.03565	-40.07314	-14.29909	-13.36696
6 C(13)	0.10074	113.24617	40.40905	37.77485
7 H(1)	0.00056	2.51598	0.89777	0.83924
8 H(1)	0.00542	24.22565	8.64431	8.08081
9 H(1)	0.01160	51.85563	18.50338	17.29718
10 H(1)	0.02359	105.46301	37.63182	35.17867
11 H(1)	0.00691	30.87206	11.01592	10.29781

Center ---- Spin Dipole Couplings ----
3XX-RR 3YY-RR 3ZZ-RR

***** Axes restored to original set *****

Center Number	Atomic Number	Forces (Hartrees/Bohr)		
		X	Y	Z
1	6	0.028513628	0.045923824	0.000000000
2	6	-0.065068123	-0.047352465	0.000000000
3	6	-0.082008101	-0.006473819	0.000000000
4	6	0.127942174	0.104625042	0.000000000
5	6	-0.039041379	-0.095257225	0.000000000
6	6	0.036751244	0.024021498	0.000000000
7	1	0.003826707	-0.010879104	0.000000000
8	1	0.006151161	-0.014885635	0.000000000
9	1	0.004103293	0.007792078	0.000000000
10	1	-0.011293367	0.001134176	0.000000000
11	1	-0.009877239	-0.008648371	0.000000000

Cartesian Forces: Max 0.127942174 RMS 0.041479453

This molecule is an asymmetric top.

Rotational symmetry number 1.

Rotational temperatures (Kelvin) 0.29821 0.26676 0.14080

Rotational constants (GHZ): 6.21372 5.55829 2.93388

Zero-point vibrational energy 231973.2 (Joules/Mol)

55.44292 (Kcal/Mol)

Warning -- explicit consideration of 18 degrees of freedom as vibrations may cause significant error

Vibrational temperatures: 587.97 627.03 890.25 915.66 974.50

(Kelvin) 1064.98 1205.05 1322.67 1426.39 1457.17

1465.22 1469.16 1528.16 1565.36 1734.96

1744.10 1913.18 1951.20 2133.43 2147.19

2273.05 2350.55 4583.66 4595.06 4615.69

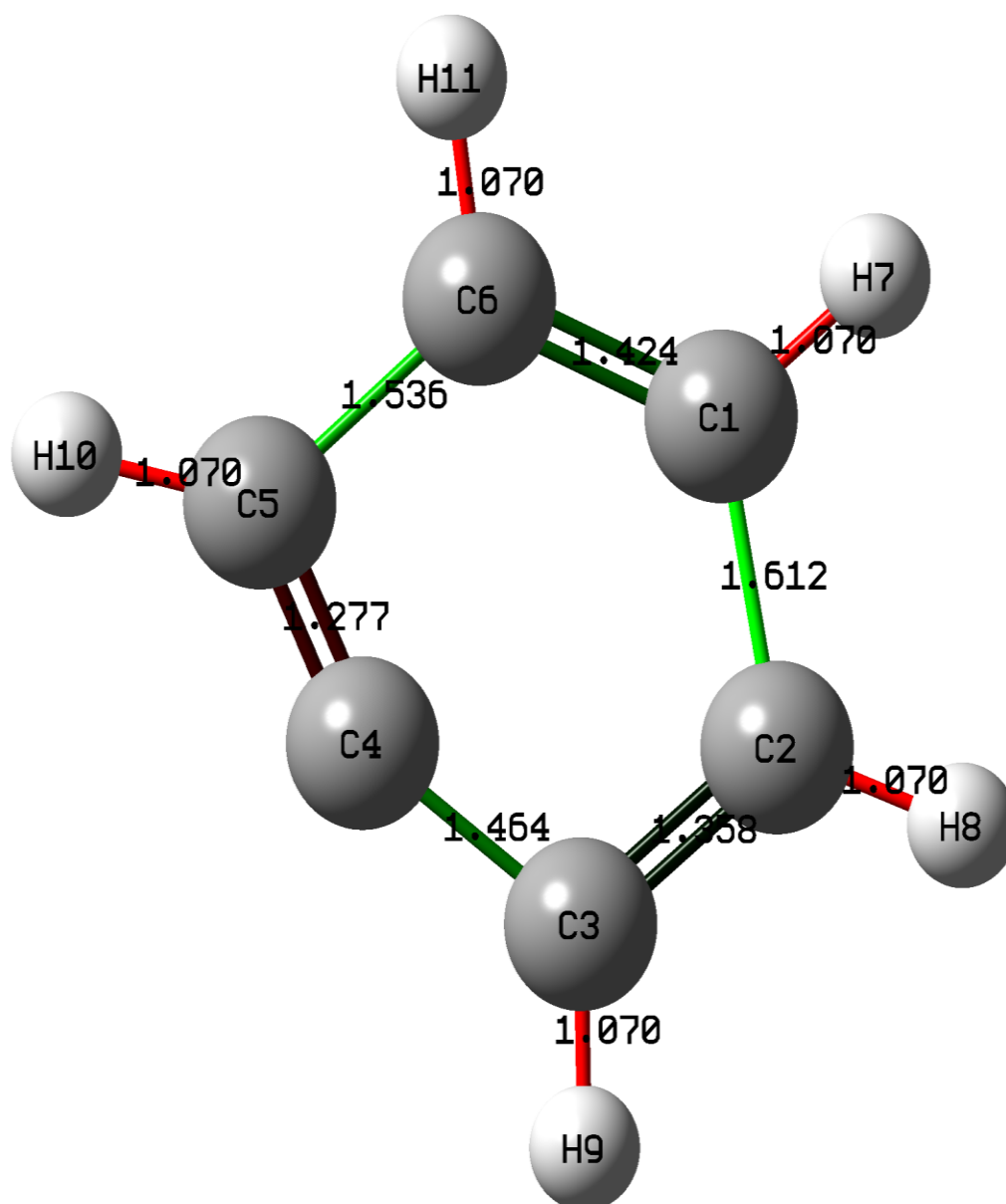
4622.63 4635.58

Zero-point correction= 0.088354 (Hartree/Particle)
 Thermal correction to Energy= 0.108943
 Thermal correction to Enthalpy= 0.111075
 Thermal correction to Gibbs Free Energy= 0.011587
 Sum of electronic and zero-point Energies= -231.431757
 Sum of electronic and thermal Energies= -231.411168
 Sum of electronic and thermal Enthalpies= -231.409036
 Sum of electronic and thermal Free Energies= -231.508524

	E (Thermal) KCal/Mol	CV Cal/Mol-Kelvin	S Cal/Mol-Kelvin
Total	68.363	35.808	92.763
Electronic	0.000	0.000	1.377
Translational	2.006	2.981	42.985
Rotational	2.006	2.981	27.992
Vibrational	64.351	29.846	20.409
Vibration 1	1.421	1.865	2.318
Vibration 2	1.433	1.849	2.198
Vibration 3	1.527	1.721	1.570
Vibration 4	1.538	1.707	1.522
Vibration 5	1.563	1.674	1.417
Vibration 6	1.605	1.620	1.270
Vibration 7	1.677	1.532	1.075
Vibration 8	1.742	1.454	0.936
Vibration 9	1.804	1.385	0.829
Vibration 10	1.823	1.364	0.800
Vibration 11	1.828	1.358	0.792
Vibration 12	1.831	1.356	0.789
Vibration 13	1.868	1.315	0.736
Vibration 14	1.892	1.290	0.705
Vibration 15	2.007	1.174	0.578
Vibration 16	2.014	1.168	0.572
Vibration 17	2.136	1.055	0.469
Vibration 18	2.165	1.030	0.448
	Q	Log10(Q)	Ln(Q)
Total Bot	0.435405D-02	-2.361106	-5.436648
Total V=0	0.439572D+16	15.643031	36.019409
Vib (Bot)	0.365948D-16	-16.436581	-37.846626
Vib (Bot) 1	0.110901D+01	0.044934	0.103464
Vib (Bot) 2	0.103545D+01	0.015130	0.034839
Vib (Bot) 3	0.703539D+00	-0.152712	-0.351631
Vib (Bot) 4	0.681213D+00	-0.166717	-0.383880
Vib (Bot) 5	0.633772D+00	-0.198067	-0.456066
Vib (Bot) 6	0.570520D+00	-0.243729	-0.561207
Vib (Bot) 7	0.490310D+00	-0.309529	-0.712718
Vib (Bot) 8	0.435302D+00	-0.361210	-0.831716
Vib (Bot) 9	0.393853D+00	-0.404666	-0.931778
Vib (Bot) 10	0.382611D+00	-0.417242	-0.960736
Vib (Bot) 11	0.379746D+00	-0.420507	-0.968254
Vib (Bot) 12	0.378355D+00	-0.422101	-0.971923
Vib (Bot) 13	0.358308D+00	-0.445744	-1.026363

Vib (Bot) 14	0.346395D+00	-0.460428	-1.060175
Vib (Bot) 15	0.298196D+00	-0.525498	-1.210004
Vib (Bot) 16	0.295850D+00	-0.528928	-1.217903
Vib (Bot) 17	0.256315D+00	-0.591227	-1.361350
Vib (Bot) 18	0.248331D+00	-0.604969	-1.392993
Vib (V=0)	0.369450D+02	1.567556	3.609431
Vib (V=0) 1	0.171651D+01	0.234646	0.540293
Vib (V=0) 2	0.164985D+01	0.217445	0.500686
Vib (V=0) 3	0.136312D+01	0.134533	0.309773
Vib (V=0) 4	0.134502D+01	0.128727	0.296406
Vib (V=0) 5	0.130726D+01	0.116362	0.267932
Vib (V=0) 6	0.125861D+01	0.099892	0.230010
Vib (V=0) 7	0.120029D+01	0.079286	0.182562
Vib (V=0) 8	0.116294D+01	0.065557	0.150950
Vib (V=0) 9	0.113649D+01	0.055566	0.127945
Vib (V=0) 10	0.112960D+01	0.052923	0.121860
Vib (V=0) 11	0.112786D+01	0.052255	0.120321
Vib (V=0) 12	0.112702D+01	0.051931	0.119576
Vib (V=0) 13	0.111513D+01	0.047325	0.108971
Vib (V=0) 14	0.110827D+01	0.044645	0.102798
Vib (V=0) 15	0.108217D+01	0.034295	0.078968
Vib (V=0) 16	0.108097D+01	0.033814	0.077860
Vib (V=0) 17	0.106187D+01	0.026071	0.060031
Vib (V=0) 18	0.105827D+01	0.024598	0.056638
Electronic	0.200000D+01	0.301030	0.693147
Translational	0.203457D+09	8.308473	19.130966
Rotational	0.292396D+06	5.465972	12.585865

***** Axes restored to original set *****

Appendix 9: Benzenyl bond parameter for output structure

Appendix 10: Gaussian raw geometric data for CBD at 623 °C

```
%chk=CBD 623.chk
%mem=6MW
%nproc=1
Will use up to 1 processors via shared memory.
Default route: MaxDisk=2000MB
Symbolic Z-matrix:
Charge = 0 Multiplicity = 1
C      -4.31136  0.49578 -0.02379
C      -2.78872  0.3848  0.09721
C      -2.16146  1.4929 -0.76744
C      -2.73155  2.8769 -0.39454
C      -3.97475  3.00946  0.14388
C      -4.74934  1.79008  0.68439
H      -4.78869 -0.33494  0.45262
H      -2.14242  3.75175 -0.57471
H      -4.53252  1.69592  1.72795
C      -4.61408  4.4078  0.23084
H      -5.67853  4.31773  0.16967
H      -4.34767  4.86458  1.16104
H      -4.26027  5.01265 -0.57778
C      -1.07422 -1.09437 -0.98334
H      -0.44349 -0.23423 -1.06842
H      -0.73575 -2.04365 -1.34279
C      -2.30174 -0.98146 -0.42027
C      -3.2096  -2.21935 -0.29786
H      -2.60509 -3.09632 -0.19585
H      -3.83788 -2.11723  0.56222
H      -3.81661 -2.30461 -1.17488
H      -5.80042  1.93479  0.54582
H      -4.58218  0.51235 -1.05883
C      -0.63288  1.48708 -0.58044
C      -0.02297  1.0534  0.76555
C      0.17561  1.86364 -1.60072
C      1.32236  1.0478  0.92938
C      1.7042  1.85734 -1.41455
C      2.24103  1.47521 -0.23042
H      1.74622  0.74639  1.86447
H      2.34249  2.15465 -2.2202
H      -2.50818  0.49338  1.12405
H      -2.40055  1.30047 -1.79249
O      -0.87613  0.65659  1.8424
H      -0.45458  0.8669  2.67886
O      -0.39071  2.26684 -2.85032
```

H	0.18588	2.9092	-3.27048
C	3.76978	1.46846	-0.04499
H	4.0888	2.42153	0.32212
H	4.04069	0.7072	0.65642
C	4.4494	1.18564	-1.39771
H	4.17837	1.94693	-2.09905
H	4.13033	0.23256	-1.76478
C	5.97823	1.17887	-1.21283
H	6.29735	2.13193	-0.84577
H	6.24934	0.41757	-0.51153
C	6.65755	0.89609	-2.56568
H	6.38639	1.65739	-3.26697
H	6.33841	-0.05698	-2.93271
C	8.18642	0.88931	-2.381
H	8.65835	0.69281	-3.32098
H	8.50558	1.84238	-2.014
H	8.45759	0.12802	-1.67971

Stoichiometry C₂₁H₃₀O₂

Framework group C₁[X(C₂₁H₃₀O₂)]

Deg. of freedom 153

Full point group C₁ NOp 1

Largest Abelian subgroup C₁ NOp 1

Largest concise Abelian subgroup C₁ NOp 1

Standard orientation:

Center Number	Atomic Number	Atomic Type	Coordinates (Angstroms)		
			X	Y	Z
1	6	0	-4.586451	0.635109	0.124764
2	6	0	-3.088353	0.927898	-0.190087
3	6	0	-2.234949	-0.138147	0.566668
4	6	0	-2.799675	-1.553151	0.393303
5	6	0	-4.058346	-1.842132	0.018325
6	6	0	-5.004623	-0.743117	-0.430709
7	1	0	-5.231765	1.406347	-0.313507
8	1	0	-2.109461	-2.368910	0.615000
9	1	0	-4.978345	-0.695471	-1.534150
10	6	0	-4.577703	-3.273184	-0.024320
11	1	0	-5.654392	-3.298331	0.192694
12	1	0	-4.435315	-3.735680	-1.015398
13	1	0	-4.064258	-3.898555	0.716292
14	6	0	-1.465924	2.641940	0.665430
15	1	0	-0.779737	1.803052	0.801168

16	1	0	-1.142353	3.651921	0.911196
17	6	0	-2.689559	2.373803	0.173620
18	6	0	-3.699405	3.492991	-0.043654
19	1	0	-3.177532	4.443854	-0.208898
20	1	0	-4.347899	3.310884	-0.910502
21	1	0	-4.351373	3.610894	0.835302
22	1	0	-6.038091	-0.989114	-0.141977
23	1	0	-4.735810	0.648611	1.216449
24	6	0	-0.744492	-0.181211	0.194004
25	6	0	-0.281413	-0.092235	-1.134341
26	6	0	0.228678	-0.453056	1.144109
27	6	0	1.060633	-0.179092	-1.459124
28	6	0	1.592639	-0.545275	0.843306
29	6	0	2.028426	-0.408551	-0.465877
30	1	0	1.389286	-0.077663	-2.492614
31	1	0	2.285374	-0.721253	1.662397
32	1	0	-2.876156	0.776163	-1.261660
33	1	0	-2.305038	0.121599	1.632328
34	8	0	-1.258714	0.100132	-2.133115
35	1	0	-0.945512	-0.224407	-3.002968
36	8	0	-0.189694	-0.571862	2.480572
37	1	0	0.433810	-1.103770	3.013709
38	6	0	3.487367	-0.512303	-0.906644
39	1	0	3.693840	-1.561136	-1.179952
40	1	0	3.602234	0.093070	-1.817561
41	6	0	4.553756	-0.057374	0.118165
42	1	0	4.478799	-0.663715	1.032807
43	1	0	4.363679	0.991741	0.392176
44	6	0	5.990667	-0.188149	-0.440410
45	1	0	6.176070	-1.239725	-0.715800
46	1	0	6.078204	0.418101	-1.357149
47	6	0	7.075079	0.265176	0.564616
48	1	0	6.988330	-0.339947	1.481180
49	1	0	6.890395	1.315648	0.840072
50	6	0	8.507840	0.131556	0.000015
51	1	0	9.258058	0.460331	0.732969
52	1	0	8.728024	-0.913118	-0.264356
53	1	0	8.629051	0.743441	-0.905851

Standard orientation:

Center Number	Atomic Number	Atomic Type	Coordinates (Angstroms)		
			X	Y	Z
1	6	0	-4.584166	0.624617	0.131023
2	6	0	-3.097141	0.923383	-0.189836

3	6	0	-2.215286	-0.101241	0.596295
4	6	0	-2.791114	-1.516024	0.543178
5	6	0	-4.031629	-1.846913	0.146559
6	6	0	-4.994518	-0.780800	-0.338239
7	1	0	-5.240125	1.368861	-0.335503
8	1	0	-2.108976	-2.298911	0.877985
9	1	0	-5.023090	-0.799951	-1.443761
10	6	0	-4.509069	-3.283135	0.100745
11	1	0	-5.571502	-3.354719	0.371065
12	1	0	-4.410407	-3.717076	-0.907565
13	1	0	-3.942192	-3.921069	0.790207
14	6	0	-1.554280	2.715985	0.657120
15	1	0	-0.867443	1.934017	0.969944
16	1	0	-1.255902	3.750392	0.805891
17	6	0	-2.718432	2.384275	0.069951
18	6	0	-3.685973	3.454684	-0.397466
19	1	0	-3.173639	4.417237	-0.515807
20	1	0	-4.150818	3.205140	-1.360301
21	1	0	-4.504744	3.601197	0.323138
22	1	0	-6.019031	-1.010614	-0.010028
23	1	0	-4.733222	0.703072	1.219973
24	6	0	-0.744513	-0.157533	0.191384
25	6	0	-0.301115	-0.239052	-1.139628
26	6	0	0.261800	-0.302286	1.165263
27	6	0	1.050923	-0.361304	-1.482203
28	6	0	1.622919	-0.433344	0.852165
29	6	0	2.038183	-0.472073	-0.487429
30	1	0	1.341642	-0.368062	-2.531130
31	1	0	2.345580	-0.499648	1.662272
32	1	0	-2.908519	0.723275	-1.256548
33	1	0	-2.226119	0.215246	1.649705
34	8	0	-1.277068	-0.147328	-2.150226
35	1	0	-0.938029	-0.457361	-3.012620
36	8	0	-0.162066	-0.248329	2.504981
37	1	0	0.511996	-0.591205	3.121641
38	6	0	3.494313	-0.648643	-0.888404
39	1	0	3.707372	-1.724204	-1.017273
40	1	0	3.637098	-0.196721	-1.880582
41	6	0	4.535638	-0.054476	0.078618
42	1	0	4.441227	-0.523418	1.070356
43	1	0	4.330146	1.018049	0.219329
44	6	0	5.981611	-0.239011	-0.420130
45	1	0	6.183771	-1.313555	-0.563557
46	1	0	6.086521	0.229575	-1.412545
47	6	0	7.040139	0.351951	0.530411

48	1	0	6.937024	-0.116324	1.522168
49	1	0	6.837413	1.424984	0.674085
50	6	0	8.480145	0.166583	0.023834
51	1	0	9.209856	0.597881	0.721616
52	1	0	8.723950	-0.898280	-0.098276
53	1	0	8.622638	0.653582	-0.951176

Harris functional with IExCor= 402 diagonalized for initial guess.

ExpMin= 4.38D-02 ExpMax= 5.48D+03 ExpMxC= 8.25D+02 IAcc=2 IRadAn= 4 AccDes= 0.00D+00

HarFok: IExCor= 402 AccDes= 0.00D+00 IRadAn= 4 IDoV=1

ScaDFX= 1.000000 1.000000 1.000000 1.000000

Requested convergence on RMS density matrix=1.00D-08 within 128 cycles.

Requested convergence on MAX density matrix=1.00D-06.

Requested convergence on energy=1.00D-06.

No special actions if energy rises.

SCF Done: E(RB+HF-LYP) = -968.517958960 A.U. after 19 cycles

Conv = 0.8610D-09 -V/T = 2.0059

S**2 = 0.0000

***** Axes restored to original set *****

Center Number	Atomic Number	Forces (Hartrees/Bohr)		
		X	Y	Z
1	6	-0.000226221	-0.000181003	-0.000115382
2	6	0.000352437	0.000097830	-0.000028812
3	6	-0.000106000	-0.000272567	0.000246140
4	6	-0.000194150	0.000222151	0.000117405
5	6	0.000251486	-0.000187922	-0.000014845
6	6	-0.000159836	0.000166313	0.000045767
7	1	-0.000006932	0.000022448	0.000049098
8	1	0.000048542	0.000014729	0.000110705
9	1	0.000094316	0.000026123	0.000009981
10	6	-0.000018066	0.000005936	0.000106871
11	1	-0.000051783	0.000040801	-0.000097960
12	1	-0.000026116	-0.000016962	-0.000081212
13	1	0.000007437	0.000053722	-0.000000736
14	6	-0.000036151	-0.000015044	-0.000017622
15	1	-0.000026375	-0.000137977	-0.000149008
16	1	0.000020015	-0.000057360	-0.000010797
17	6	-0.000292355	0.000055156	-0.000156066
18	6	0.000168439	-0.000060258	0.000165665
19	1	0.000028588	-0.000022493	-0.000035002
20	1	-0.000054065	-0.000026344	0.000015637
21	1	-0.000059952	-0.000043075	-0.000025861

22	1	-0.000031798	-0.000034962	-0.000000587
23	1	0.000061512	0.000034827	0.000009232
24	6	0.000336884	0.000148490	-0.000659728
25	6	0.000194922	-0.000187506	0.000148428
26	6	-0.000372701	-0.000208127	0.000443409
27	6	-0.000227981	-0.000081996	0.000105589
28	6	0.000426093	0.000110608	0.000182813
29	6	-0.000092113	0.000209966	-0.000178990
30	1	0.000036131	0.000090988	0.000001938
31	1	-0.000007284	-0.000087023	-0.000064764
32	1	0.000523158	0.000458760	0.000166780
33	1	-0.000029904	-0.000002954	0.000012185
34	8	-0.000566874	-0.000188844	-0.000340803
35	1	0.000060794	-0.000054125	0.000097436
36	8	-0.000137348	0.000318270	0.000005589
37	1	0.000055003	-0.000095126	-0.000051578
38	6	0.000062450	-0.000124814	-0.000020165
39	1	0.000017410	-0.000027725	-0.000036878
40	1	-0.000029116	-0.000000530	0.000036066
41	6	-0.000104249	0.000018317	-0.000015488
42	1	0.000013735	-0.000020393	-0.000042862
43	1	0.000012401	0.000051009	0.000022652
44	6	0.000085031	0.000141317	-0.000031304
45	1	-0.000048917	-0.000050290	-0.000019349
46	1	0.000028552	0.000000280	0.000025864
47	6	-0.000097643	-0.000121677	0.000085210
48	1	0.000006607	-0.000017436	-0.000043173
49	1	0.000015792	0.000050244	0.000011080
50	6	0.000085708	0.000013017	0.000036680
51	1	0.000016602	-0.000026689	-0.000027872
52	1	-0.000026502	0.000011175	-0.000008350
53	1	0.000020387	-0.000011256	0.000016972

Item	Value	Threshold	Converged?
Maximum Force	0.000228	0.000450	YES
RMS Force	0.000039	0.000300	YES
Maximum Displacement	0.102356	0.001800	NO
RMS Displacement	0.020263	0.001200	NO

Predicted change in Energy=-2.231162D-07

Grad

Stoichiometry C21H30O2
 Framework group C1[X(C21H30O2)]
 Deg. of freedom 153
 Full point group C1 NOp 1

Largest Abelian subgroup C1 NOp 1
 Largest concise Abelian subgroup C1 NOp 1
 Standard orientation:

Center	Atomic	Atomic	Coordinates (Angstroms)			
Number	Number	Type	X	Y	Z	

1	6	0	-4.305361	1.201705	-0.196101	
2	6	0	-2.758120	1.091736	-0.296544	
3	6	0	-2.292794	-0.114457	0.570578	
4	6	0	-3.146945	-1.348175	0.292408	
5	6	0	-4.353919	-1.339039	-0.299851	
6	6	0	-4.998149	-0.047436	-0.767650	
7	1	0	-4.654174	2.097783	-0.725258	
8	1	0	-2.719251	-2.296647	0.616683	
9	1	0	-4.982381	-0.015634	-1.870647	
10	6	0	-5.139146	-2.605442	-0.552062	
11	1	0	-6.102011	-2.589569	-0.020406	
12	1	0	-5.370354	-2.719352	-1.621647	
13	1	0	-4.587096	-3.494793	-0.229002	
14	6	0	-1.687519	2.786409	1.266438	
15	1	0	-1.736178	2.119191	2.120435	
16	1	0	-1.261542	3.770275	1.449587	
17	6	0	-2.103843	2.431398	0.037772	
18	6	0	-1.987312	3.384465	-1.135573	
19	1	0	-1.582007	4.354785	-0.829975	
20	1	0	-1.330031	2.965391	-1.910646	
21	1	0	-2.963530	3.558046	-1.609851	
22	1	0	-6.062360	-0.044761	-0.485163	
23	1	0	-4.577262	1.331276	0.861341	
24	6	0	-0.806164	-0.437018	0.439898	
25	6	0	-0.185546	-0.774980	-0.776394	
26	6	0	0.028749	-0.457342	1.570912	
27	6	0	1.176281	-1.088329	-0.868986	
28	6	0	1.392930	-0.766458	1.504931	
29	6	0	1.986689	-1.082021	0.275373	
30	1	0	1.606652	-1.340721	-1.836188	
31	1	0	1.992954	-0.766864	2.412472	
32	1	0	-2.515035	0.853707	-1.339694	
33	1	0	-2.448506	0.152075	1.623101	
34	8	0	-0.992092	-0.787660	-1.922481	
35	1	0	-0.497590	-1.080598	-2.710959	
36	8	0	-0.571479	-0.160709	2.804234	
37	1	0	0.071667	-0.181506	3.536933	
38	6	0	3.471682	-1.373115	0.178640	

39	1	0	3.820253	-1.823691	1.118279
40	1	0	3.651205	-2.116066	-0.611041
41	6	0	4.322953	-0.113890	-0.118071
42	1	0	4.139867	0.636052	0.665269
43	1	0	3.981756	0.335782	-1.062013
44	6	0	5.830315	-0.414214	-0.203825
45	1	0	6.170923	-0.847559	0.749803
46	1	0	6.007035	-1.182997	-0.972735
47	6	0	6.681687	0.828345	-0.527341
48	1	0	6.500929	1.598507	0.237452
49	1	0	6.344112	1.257273	-1.482644
50	6	0	8.187702	0.525066	-0.604150
51	1	0	8.766163	1.428345	-0.832574
52	1	0	8.557572	0.122215	0.347758
53	1	0	8.401766	-0.216236	-1.385101

 Rotational constants (GHZ): 0.4772034 0.1058553 0.0999357

Standard basis: 6-311++G (6D, 7F)

There are 359 symmetry adapted basis functions of A symmetry.

Integral buffers will be 262144 words long.

Raffenetti 2 integral format.

Two-electron integral symmetry is turned on.

359 basis functions, 718 primitive gaussians, 359 cartesian basis functions

86 alpha electrons 86 beta electrons

nuclear repulsion energy 1922.4881095799 Hartrees.

Stoichiometry C21H30O2

Framework group C1[X(C21H30O2)]

Deg. of freedom 153

Full point group C1 NOp 1

Largest Abelian subgroup C1 NOp 1

Largest concise Abelian subgroup C1 NOp 1

Standard orientation:

Center Number	Atomic Number	Atomic Type	Coordinates (Angstroms)		
			X	Y	Z
1	6	0	-4.305290	1.201909	-0.200519
2	6	0	-2.758599	1.090290	-0.305338
3	6	0	-2.290895	-0.107401	0.572203
4	6	0	-3.148345	-1.342812	0.312915
5	6	0	-4.357217	-1.339343	-0.275552
6	6	0	-5.000538	-0.052491	-0.757531
7	1	0	-4.655984	2.093085	-0.736701
8	1	0	-2.721731	-2.287668	0.649052
9	1	0	-4.986665	-0.032604	-1.860761

10	6	0	-5.143607	-2.608138	-0.511761
11	1	0	-6.111997	-2.579774	0.008931
12	1	0	-5.363647	-2.741780	-1.581585
13	1	0	-4.597285	-3.492637	-0.166454
14	6	0	-1.680989	2.797674	1.238513
15	1	0	-1.724350	2.136834	2.097808
16	1	0	-1.255711	3.783676	1.411761
17	6	0	-2.102598	2.432562	0.014696
18	6	0	-1.991974	3.375986	-1.167137
19	1	0	-1.604978	4.355678	-0.867851
20	1	0	-1.320727	2.960155	-1.932073
21	1	0	-2.966364	3.528779	-1.651938
22	1	0	-6.064278	-0.045620	-0.473106
23	1	0	-4.573590	1.341314	0.856593
24	6	0	-0.805050	-0.433605	0.438697
25	6	0	-0.190979	-0.795033	-0.773954
26	6	0	0.036099	-0.433296	1.565826
27	6	0	1.170263	-1.111834	-0.867389
28	6	0	1.399322	-0.744790	1.498662
29	6	0	1.986250	-1.085832	0.272389
30	1	0	1.595676	-1.380958	-1.832264
31	1	0	2.004628	-0.726530	2.402539
32	1	0	-2.519554	0.843540	-1.347488
33	1	0	-2.440430	0.171437	1.622308
34	8	0	-1.002562	-0.828118	-1.916046
35	1	0	-0.514249	-1.144974	-2.699096
36	8	0	-0.556718	-0.110571	2.796121
37	1	0	0.088230	-0.128301	3.527305
38	6	0	3.471075	-1.377477	0.173953
39	1	0	3.820743	-1.826083	1.114155
40	1	0	3.649610	-2.121858	-0.614454
41	6	0	4.322138	-0.118276	-0.125157
42	1	0	4.137922	0.633038	0.656558
43	1	0	3.981344	0.329402	-1.070155
44	6	0	5.829755	-0.417863	-0.208731
45	1	0	6.166645	-0.862117	0.741269
46	1	0	6.009076	-1.178000	-0.985591
47	6	0	6.682944	0.827886	-0.514427
48	1	0	6.501351	1.588196	0.259953
49	1	0	6.347942	1.269717	-1.464797
50	6	0	8.188871	0.524015	-0.592035
51	1	0	8.768555	1.429378	-0.808758
52	1	0	8.556715	0.109571	0.355684
53	1	0	8.403541	-0.208183	-1.381382

Rotational constants (GHZ): 0.4777444 0.1058812 0.0998688

Standard basis: 6-31+G (6D, 7F)

There are 359 symmetry adapted basis functions of A symmetry.

Integral buffers will be 262144 words long.

Raffenetti 2 integral format.

Two-electron integral symmetry is turned on.

359 basis functions, 718 primitive gaussians, 359 cartesian basis functions

86 alpha electrons 86 beta electrons

nuclear repulsion energy 1922.4475690292 Hartrees.

NAtoms= 53 NActive= 53 NUniq= 53 SFac= 1.00D+00 NATFMM= 60 Big=F

One-electron integrals computed using PRISM.

NBasis= 359 RedAO= T NBF= 359

NBsUse= 357 1.00D-06 NBFU= 357

Initial guess read from the read-write file:

Initial guess orbital symmetries:

Occupied (A)
(A) (A) (A) (A) (A) (A) (A) (A) (A) (A) (A) (A) (A)

(A) (A) (A) (A) (A) (A) (A) (A) (A) (A) (A) (A) (A)

(A) (A) (A) (A) (A) (A) (A) (A) (A) (A) (A) (A) (A)

(A) (A) (A) (A) (A) (A) (A) (A) (A) (A) (A) (A) (A)

(A) (A) (A) (A) (A) (A) (A) (A) (A) (A) (A) (A) (A)

(A) (A) (A) (A) (A) (A) (A) (A) (A) (A) (A) (A) (A)

(A) (A)

Virtual (A)
(A) (A) (A) (A) (A) (A) (A) (A) (A) (A) (A) (A) (A)

(A) (A) (A) (A) (A) (A) (A) (A) (A) (A) (A) (A) (A)

(A) (A) (A) (A) (A) (A) (A) (A) (A) (A) (A) (A) (A)

(A) (A) (A) (A) (A) (A) (A) (A) (A) (A) (A) (A) (A)

(A) (A) (A) (A) (A) (A) (A) (A) (A) (A) (A) (A) (A)

(A) (A) (A) (A) (A) (A) (A) (A) (A) (A) (A) (A) (A)

(A) (A) (A) (A) (A) (A) (A) (A) (A) (A) (A) (A) (A)

(A) (A) (A) (A) (A) (A) (A) (A) (A) (A) (A) (A) (A)

(A) (A) (A) (A) (A) (A) (A) (A) (A) (A) (A) (A) (A)

(A) (A) (A) (A) (A) (A) (A) (A) (A) (A) (A) (A) (A)

(A) (A) (A) (A) (A) (A) (A) (A) (A) (A) (A) (A) (A)

(A) (A) (A) (A) (A) (A) (A) (A) (A) (A) (A) (A) (A)

(A) (A) (A) (A) (A) (A) (A) (A) (A) (A) (A) (A) (A)

(A) (A) (A) (A) (A) (A) (A) (A) (A) (A) (A) (A) (A)

(A) (A) (A) (A) (A) (A) (A) (A) (A) (A) (A) (A) (A)

(A) (A) (A) (A) (A) (A) (A) (A) (A) (A) (A) (A) (A)

(A) (A) (A) (A) (A) (A) (A) (A) (A) (A) (A) (A) (A)

(A) (A) (A) (A) (A) (A) (A) (A) (A) (A) (A) (A) (A)

(A) (A) (A) (A) (A) (A) (A) (A) (A) (A) (A) (A) (A)

(A) (A) (A) (A) (A) (A) (A) (A) (A) (A) (A) (A) (A)

(A) (A) (A) (A) (A) (A) (A) (A) (A) (A) (A) (A) (A)

(A) (A) (A) (A) (A) (A) (A)

Harris functional with IExCor= 402 diagonalized for initial guess.

ExpMin= 4.38D-02 ExpMax= 5.48D+03 ExpMxC= 8.25D+02 IAcc=2 IRadAn= 4 AccDes= 0.00D+00

HarFok: IExCor= 402 AccDes= 0.00D+00 IRadAn= 4 IDoV=1

ScaDFX= 1.000000 1.000000 1.000000 1.000000

Requested convergence on RMS density matrix=1.00D-08 within 128 cycles.

Requested convergence on MAX density matrix=1.00D-06.

Requested convergence on energy=1.00D-06.

No special actions if energy rises.

SCF Done: E(RB+HF-LYP) = -968.518018492 A.U. after 15 cycles

Conv = 0.8906D-08 -V/T = 2.0059

S**2 = 0.0000

***** Axes restored to original set *****

Center Number	Atomic Number	Forces (Hartrees/Bohr)		
		X	Y	Z
1	6	-0.000099611	0.000089319	0.000068978
2	6	0.000095410	-0.000201872	0.000025281
3	6	0.000221872	0.000220616	-0.000018441
4	6	-0.000017958	-0.000010337	0.000033774
5	6	0.000074180	0.000006293	0.000104172
6	6	-0.000003359	-0.000039377	-0.000137995
7	1	0.000015329	-0.000021600	-0.000025305
8	1	-0.000028939	-0.000002024	-0.000003790
9	1	-0.000013087	0.000034621	0.000027867
10	6	0.000012945	-0.000040089	0.000028188
11	1	-0.000027036	0.000010735	0.000003269
12	1	0.000028645	0.000010950	-0.000052761
13	1	-0.000023871	0.000009673	-0.000023233
14	6	0.000020477	0.000022994	-0.000076976
15	1	0.000036510	-0.000057274	0.000012690
16	1	0.000005783	0.000029223	0.000013989
17	6	-0.000228014	-0.000120216	0.000022880
18	6	0.000147695	0.000067055	-0.000038557
19	1	-0.000033174	-0.000005466	0.000020832
20	1	-0.000032210	-0.000022214	0.000010853
21	1	-0.000022971	0.000027785	0.000024369
22	1	0.000021064	-0.000007106	0.000006623
23	1	0.000015801	-0.000023589	0.000004101
24	6	-0.000144555	-0.000050601	-0.000039141
25	6	0.000047183	-0.000117804	0.000004224
26	6	-0.000044242	-0.000077734	-0.000026680
27	6	-0.000052507	0.000039805	0.000063061

28	6	0.000104055	-0.000013830	-0.000022235
29	6	0.000062181	0.000035907	0.000072625
30	1	-0.000001416	0.000028539	-0.000007558
31	1	0.000023669	0.000007012	0.000007686
32	1	0.000083785	0.000173967	0.000032037
33	1	-0.000029134	-0.000004822	-0.000001759
34	8	-0.000111005	-0.000005495	-0.000031349
35	1	-0.000013917	-0.000027538	-0.000018087
36	8	-0.000017594	0.000091937	-0.000009217
37	1	-0.000010891	-0.000016128	0.000008411
38	6	-0.000031448	0.000031930	-0.000134086
39	1	0.000034215	-0.000030716	0.000027184
40	1	-0.000001557	0.000000556	-0.000001065
41	6	0.000030033	-0.000003730	0.000022212
42	1	-0.000025581	-0.000022775	-0.000027886
43	1	-0.000027530	0.000022553	0.000019319
44	6	-0.000040600	-0.000042408	-0.000025592
45	1	0.000001412	0.000009128	0.000016658
46	1	0.000004798	0.000007425	-0.000005836
47	6	0.000043247	0.000031776	0.000034917
48	1	-0.000000772	-0.000016626	0.000016559
49	1	-0.000000333	-0.000002824	-0.000017886
50	6	-0.000042304	-0.000042341	-0.000005264
51	1	0.000004822	0.000015517	0.000005831
52	1	-0.000005885	-0.000001339	0.000014245
53	1	-0.000003610	0.000002559	-0.000002136

 Cartesian Forces: Max 0.000228014 RMS 0.000057348

Grad
 - Thermochemistry -

Temperature 623.000 Kelvin. Pressure 1.00000 Atm.

Atom 1 has atomic number 6 and mass 12.00000

Atom 2 has atomic number 6 and mass 12.00000

Atom 3 has atomic number 6 and mass 12.00000

Atom 4 has atomic number 6 and mass 12.00000

Atom 5 has atomic number 6 and mass 12.00000

Atom 6 has atomic number 6 and mass 12.00000

Atom 7 has atomic number 1 and mass 1.00783

Atom 8 has atomic number 1 and mass 1.00783

Atom 9 has atomic number 1 and mass 1.00783

Atom 10 has atomic number 6 and mass 12.00000

Atom 11 has atomic number 1 and mass 1.00783

Atom 12 has atomic number 1 and mass 1.00783

Atom 13 has atomic number 1 and mass 1.00783

Atom 14 has atomic number 6 and mass 12.00000
 Atom 15 has atomic number 1 and mass 1.00783
 Atom 16 has atomic number 1 and mass 1.00783
 Atom 17 has atomic number 6 and mass 12.00000
 Atom 18 has atomic number 6 and mass 12.00000
 Atom 19 has atomic number 1 and mass 1.00783
 Atom 20 has atomic number 1 and mass 1.00783
 Atom 21 has atomic number 1 and mass 1.00783
 Atom 22 has atomic number 1 and mass 1.00783
 Atom 23 has atomic number 1 and mass 1.00783
 Atom 24 has atomic number 6 and mass 12.00000
 Atom 25 has atomic number 6 and mass 12.00000
 Atom 26 has atomic number 6 and mass 12.00000
 Atom 27 has atomic number 6 and mass 12.00000
 Atom 28 has atomic number 6 and mass 12.00000
 Atom 29 has atomic number 6 and mass 12.00000
 Atom 30 has atomic number 1 and mass 1.00783
 Atom 31 has atomic number 1 and mass 1.00783
 Atom 32 has atomic number 1 and mass 1.00783
 Atom 33 has atomic number 1 and mass 1.00783
 Atom 34 has atomic number 8 and mass 15.99491
 Atom 35 has atomic number 1 and mass 1.00783
 Atom 36 has atomic number 8 and mass 15.99491
 Atom 37 has atomic number 1 and mass 1.00783
 Atom 38 has atomic number 6 and mass 12.00000
 Atom 39 has atomic number 1 and mass 1.00783
 Atom 40 has atomic number 1 and mass 1.00783
 Atom 41 has atomic number 6 and mass 12.00000
 Atom 42 has atomic number 1 and mass 1.00783
 Atom 43 has atomic number 1 and mass 1.00783
 Atom 44 has atomic number 6 and mass 12.00000
 Atom 45 has atomic number 1 and mass 1.00783
 Atom 46 has atomic number 1 and mass 1.00783
 Atom 47 has atomic number 6 and mass 12.00000
 Atom 48 has atomic number 1 and mass 1.00783
 Atom 49 has atomic number 1 and mass 1.00783
 Atom 50 has atomic number 6 and mass 12.00000
 Atom 51 has atomic number 1 and mass 1.00783
 Atom 52 has atomic number 1 and mass 1.00783
 Atom 53 has atomic number 1 and mass 1.00783
 Molecular mass: 314.22458 amu.

Principal axes and moments of inertia in atomic units:

	1	2	3
EIGENVALUES --	3786.61749	*****	*****
X	1.00000	0.00244	0.00025

Y -0.00244 0.99997 -0.00777
 Z -0.00027 0.00777 0.99997

This molecule is an asymmetric top.

Rotational symmetry number 1.

Warning -- assumption of classical behavior for rotation
 may cause significant error

Rotational temperatures (Kelvin) 0.02287 0.00509 0.00480

Rotational constants (GHZ): 0.47661 0.10596 0.10001

Zero-point vibrational energy 1229503.2 (Joules/Mol)
 293.85831 (Kcal/Mol)

Warning -- explicit consideration of 85 degrees of freedom as
 vibrations may cause significant error

Vibrational temperatures: 28.12 33.59 60.18 70.17 76.06
 (Kelvin) 85.63 107.88 129.73 149.92 181.02

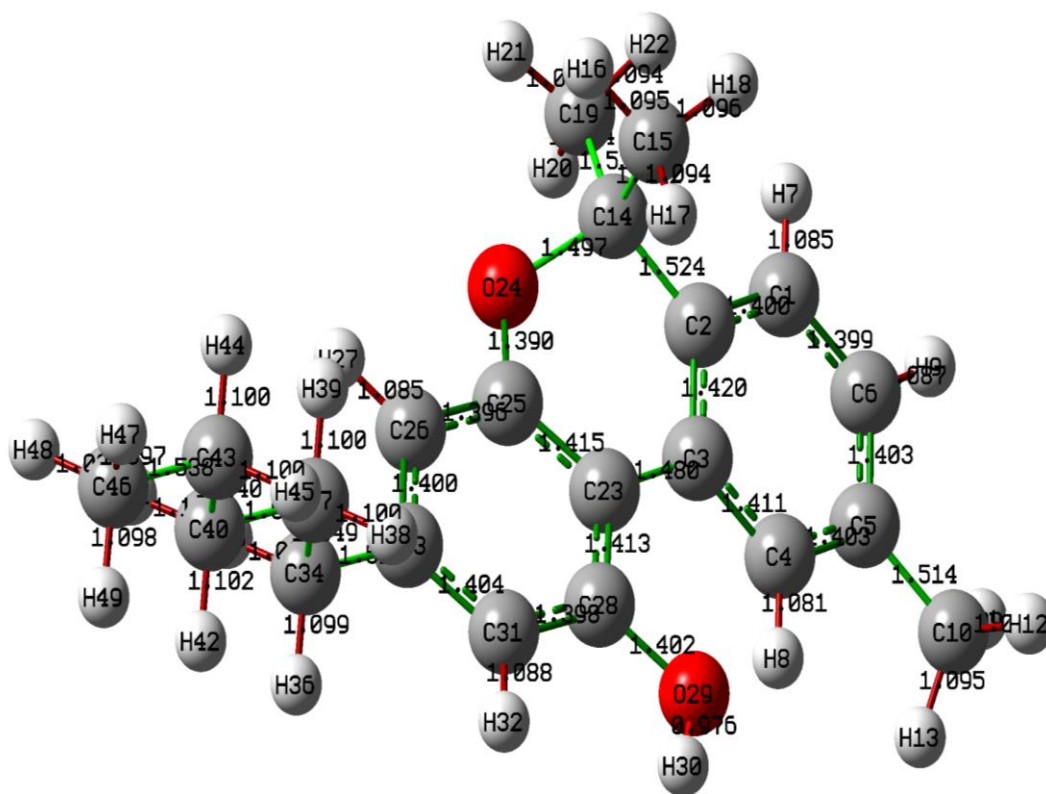
190.68 213.79 243.14 259.80 263.75
 289.26 330.41 343.26 345.57 348.29
 391.73 420.59 425.36 439.42 458.49
 486.43 497.76 514.67 558.08 611.44
 634.56 656.71 687.08 719.87 765.13
 774.69 809.12 819.32 869.41 885.23
 890.45 943.07 995.56 1049.10 1081.25
 1107.96 1126.33 1147.57 1166.53 1209.48
 1238.05 1239.24 1260.40 1296.05 1312.28
 1327.83 1375.50 1380.08 1415.53 1431.93
 1448.24 1456.10 1459.58 1475.56 1498.64
 1508.01 1508.73 1542.04 1551.96 1560.36
 1581.39 1608.40 1634.11 1640.41 1645.84
 1659.39 1717.34 1726.78 1741.39 1757.71
 1785.52 1801.89 1823.60 1837.16 1851.13
 1872.81 1885.97 1907.90 1927.41 1934.77
 1941.76 1953.93 1965.64 1971.08 1976.46
 1994.63 2007.48 2014.03 2022.93 2025.11
 2049.49 2088.10 2089.88 2090.53 2110.90
 2145.78 2180.25 2184.83 2187.00 2193.43
 2196.37 2198.40 2201.94 2206.13 2206.17
 2212.41 2217.67 2231.35 2250.69 2354.50
 2393.57 2464.86 2500.83 4300.74 4320.63
 4333.53 4339.47 4343.14 4346.31 4347.47
 4355.35 4360.23 4361.33 4367.96 4384.60
 4393.26 4399.08 4402.86 4411.17 4418.15
 4432.92 4434.67 4460.97 4466.52 4475.22
 4482.53 4533.71 4542.60 4557.46 4563.66
 4674.18 5290.07 5302.55

Zero-point correction= 0.468293 (Hartree/Particle)
 Thermal correction to Energy= 0.563965
 Thermal correction to Enthalpy= 0.565938
 Thermal correction to Gibbs Free Energy= 0.297660
 Sum of electronic and zero-point Energies= -968.049729
 Sum of electronic and thermal Energies= -967.954057
 Sum of electronic and thermal Enthalpies= -967.952084
 Sum of electronic and thermal Free Energies= -968.220362

	E (Thermal)	CV	S
	KCal/Mol	Cal/Mol-Kelvin	Cal/Mol-Kelvin
Total	353.893	173.833	270.220
Electronic	0.000	0.000	0.000
Translational	1.857	2.981	46.792
Rotational	1.857	2.981	37.605
Vibrational	350.179	167.871	185.823
Vibration 1	1.238	1.987	8.144
Vibration 2	1.238	1.987	7.791
Vibration 3	1.239	1.986	6.633
Vibration 4	1.239	1.985	6.328
Vibration 5	1.240	1.985	6.167
Vibration 6	1.240	1.984	5.933
Vibration 7	1.241	1.982	5.474
Vibration 8	1.242	1.980	5.109
Vibration 9	1.244	1.978	4.823
Vibration 10	1.247	1.973	4.450
Vibration 11	1.248	1.972	4.348
Vibration 12	1.250	1.968	4.122
Vibration 13	1.254	1.962	3.870
Vibration 14	1.256	1.959	3.740
Vibration 15	1.256	1.958	3.710
Vibration 16	1.260	1.952	3.530
Vibration 17	1.267	1.941	3.271
Vibration 18	1.269	1.938	3.197
Vibration 19	1.270	1.937	3.184
Vibration 20	1.270	1.936	3.168
Vibration 21	1.279	1.923	2.942
Vibration 22	1.285	1.913	2.805
Vibration 23	1.286	1.912	2.784
Vibration 24	1.289	1.907	2.722
Vibration 25	1.293	1.900	2.641
Vibration 26	1.300	1.889	2.529
Vibration 27	1.303	1.885	2.485
Vibration 28	1.308	1.878	2.422
Vibration 29	1.320	1.859	2.271

Vibration 30	1.336	1.835	2.102
Vibration 31	1.343	1.824	2.034
Vibration 32	1.351	1.813	1.972
Vibration 33	1.361	1.797	1.890
Vibration 34	1.373	1.780	1.807
Vibration 35	1.390	1.755	1.699
Vibration 36	1.394	1.750	1.677
Vibration 37	1.407	1.730	1.602
Vibration 38	1.412	1.724	1.580
Vibration 39	1.433	1.694	1.479
Vibration 40	1.440	1.684	1.448
Vibration 41	1.442	1.681	1.438
Vibration 42	1.466	1.648	1.343
Vibration 43	1.491	1.613	1.254
Vibration 44	1.518	1.577	1.171
Vibration 45	1.534	1.555	1.124
Vibration 46	1.548	1.537	1.086
Vibration 47	1.558	1.524	1.061
Vibration 48	1.570	1.509	1.032
Vibration 49	1.580	1.496	1.008
Vibration 50	1.604	1.465	0.954
Vibration 51	1.621	1.445	0.920
Vibration 52	1.622	1.444	0.919
Vibration 53	1.634	1.428	0.895
Vibration 54	1.655	1.403	0.855
Vibration 55	1.665	1.391	0.838
Vibration 56	1.675	1.379	0.821
Vibration 57	1.704	1.344	0.773
Vibration 58	1.707	1.341	0.769
Vibration 59	1.730	1.315	0.735
Vibration 60	1.740	1.303	0.720
Vibration 61	1.751	1.291	0.705
Vibration 62	1.756	1.285	0.698
Vibration 63	1.758	1.282	0.695
Vibration 64	1.769	1.270	0.682
Vibration 65	1.784	1.253	0.662
Vibration 66	1.791	1.246	0.654
Vibration 67	1.791	1.246	0.654
Vibration 68	1.814	1.221	0.627
Vibration 69	1.821	1.214	0.619
Vibration 70	1.826	1.208	0.612
Vibration 71	1.841	1.192	0.596
Vibration 72	1.860	1.173	0.576
Vibration 73	1.878	1.154	0.558
Vibration 74	1.882	1.149	0.553

Vibration 75	1.886	1.145	0.549
Vibration 76	1.896	1.135	0.540
Vibration 77	1.938	1.093	0.502
Vibration 78	1.945	1.087	0.496
Vibration 79	1.955	1.076	0.487
Vibration 80	1.968	1.065	0.477
Vibration 81	1.988	1.045	0.460
Vibration 82	2.001	1.033	0.451
Vibration 83	2.017	1.018	0.438
Vibration 84	2.027	1.008	0.431
Vibration 85	2.038	0.999	0.423
Q	Log10(Q)	Ln(Q)	

Appendix 11: THC bond parameter for output structure

Appendix 12: Rights to use information of published work in thesis by oalib journal

**OPEN ACCESS LIBRARY (OALib)
COPYRIGHT FORM**

This form is intended for original material submitted to Open Access Library Journal (OALib Journal) sponsored by Open Access Library (OALib) in California (US). The following transfer agreement must be signed and returned to OALib Journal Editorial Office before the manuscript can be published. Please read it carefully and keep a copy for your files.

Paper ID	1106985
Paper Title	Contemporary Trends in the Use of Khat for Recreational Purposes and Its Possible Health Implications
Paper Authors	Micah O. Omare, Joshua K. Kibet, Jackson K. Cherutoi, Fredick O. Kengara
Journal Title	Open Access Library Journal

COPYRIGHT TRANSFER

The undersigned hereby assigns to the OALib all rights under copyright that may exist in and to the above Work, and any revised or expanded derivative works submitted to the OALib by the undersigned based on the Work. The undersigned hereby warrants that the Work is original and that he/she is the author of the Work; to the extent the Work incorporates text passages, figures, data or other material from the works of others, the undersigned has obtained any necessary permission.

RETAINED RIGHTS/TERMS AND CONDITIONS

Authors/employers retain all proprietary rights in any process, procedure, or article of manufacture described in the Work. Authors/employers may reproduce or authorize others to reproduce The Work, material extracted verbatim from the Work, or derivative works to the extent permissible under US's law for works authored by US Government employees, and for the author's personal use or for company or organizational use, provided that the source and any OALib copyright notice are indicated, the copies are not used in any way that implies OALib endorsement of a product or service of any employer, and the copies themselves are not offered for sale.

Authors/employers may make limited distribution of all or portions of the Work prior to publication if they inform the OALib in advance of the nature and extent of such limited distribution.

In the case of a Work performed under a China Government contract or grant, the OALib recognizes that the China Government has royalty-free permission to reproduce all or portions of the Work, and to authorize others to do so, for official China Government purposes only, if the contract/grant so requires.

OALib Copyright Ownership

It is the formal policy of the OALib to own the copyrights to all copyrightable material in its technical publications and to the individual contributions contained therein, in order to protect the interests of the OALib, its authors and their employers, and, at the same time, to facilitate the appropriate re-use of this material by others. The OALib distributes its technical publications throughout the world and does so by various means such as hard copy, microfiche, microfilm, and electronic media. It also abstracts and may translate its publications, and articles contained therein, for inclusion in various compendiums, collective works, databases and similar publications.

Author/Employer Rights

If you are employed and prepared the Work on a subject within the scope of your employment, the copyright in the Work belongs to your employer as a work-for-hire. In that case, the OALib assumes that when you sign this Form, you are authorized to do so by your employer and that your employer has consented to the transfer of copyright, to the representation and warranty of publication rights, and to all other terms and conditions of this Form. If such authorization and consent has not been given to you, an authorized representative of your employer should sign this Form as the Author.

In the event the above work is not accepted and published by the OALib or is withdrawn by the author(s) before acceptance by the OALib, the foregoing copyright transfer shall become null and void and all materials embodying the Work submitted to the OALib Journal will be destroyed.

The author signs for and accepts responsibility for releasing this material on behalf of any and all co-authors.

Signature: Micah Omare



Author/Authorized Agent For Joint Authors
28, 2020

Date: November

Appendix 13: Rights to use information of published work in thesis by journal of public health

Re: copyright [JOPH][PU]  Inbox x



Soren Malpass <soren.malpass@springer.com>

May 19, 2021, 10:42 PM



to me, Josephine, Irish ▾

Dear Omari,

Thank you for your query. Author retains the right to use his/her article for his/her further scientific career by including the final published journal article in other publications such as dissertations and postdoctoral qualifications provided acknowledgement is given to the original source of publication.

You do not need permission to reuse your article in a thesis/dissertation.

Best regards,

Soren Malpass

he/him/his

Editorial Assistant, Journals

Behavioral + Health Sciences

Springer

1 New York Plaza, Suite 4600 | New York, NY 10004-1562

Activate Windows

Go to Settings to activate Window

Appendix 14: Rights to use information of published work in thesis by JANSET



ACA Publishing

to me ▾

Mon, May 17, 11:12 PM



The authors can use their printed manuscripts for their own usage, for non-commercial usage. You dont need any another copyrightform.

—
Regards

